

UC Irvine

UC Irvine Electronic Theses and Dissertations

Title

Marine Phytoplankton Responses to Scrubber Washwater Discharges

Permalink

<https://escholarship.org/uc/item/7n9312h2>

Author

Tavares-Reager, Joana Flor

Publication Date

2023

Peer reviewed|Thesis/dissertation

UNIVERSITY OF CALIFORNIA,  
IRVINE

Marine Phytoplankton Responses to Scrubber Washwater Discharges

DISSERTATION

submitted in partial satisfaction of the requirements  
for the degree of

DOCTOR OF PHILOSOPHY

in Earth System Science

by

Joana Flor Tavares-Reager

Dissertation Committee:

Professor Katherine R. M. Mackey, Chair

Professor Adam C. Martiny

Professor J. Keith Moore

Professor Eric Saltzman

2023



## DEDICATION

To

Tereza Navarro Ribeiro & Elena Tavares Reager

*"The future isn't something hidden in a corner.*

*The future is something we build in the present."*

Paulo Freire

## TABLE OF CONTENTS

	Page
LIST OF FIGURES	iv
LIST OF TABLES	vi
ACKNOWLEDGEMENTS	vii
VITA	viii
ABSTRACT OF THE DISSERTATION	xi
INTRODUCTION	1
DISSERTATION STRUCTURE AND ACCOMPLISHMENTS	11
CONCLUSION AND FUTURE DIRECTIONS	15
CHAPTER 1: Chemical characterization and model simulations	20
CHAPTER 2: Coastal Incubations	60
CHAPTER 3: Sargasso Sea Incubations	114
REFERENCES	150

## LIST OF FIGURES

	Page	
Figure 0.1	Typical structure of engine exhaust particles	5
Figure 0.2	Conceptual model of fuel combustion PM composition	5
Figure 0.3	Structure of open and closed-loop scrubbers	9
Figure 1.1	Experimental setup used during sampling Campaign 1	28
Figure 1.2	Photo of Boat A	31
Figure 1.3	N content in scrubber washwater from small engines, distilled fuels	38
Figure 1.4	Rate of discharge of N compounds by small engines, distilled fuels	39
Figure 1.5	Dissolved metals in scrubber water from small engines, distilled fuels	42
Figure 1.6	Metals discharged by open-loop scrubbers in the comparative analysis	45
Figure 1.7	Map of the Newport Bay Harbor (California, USA)	49
Figure 1.8	Assumptions used to simulate the range of DIN and trace metal concentrations in a hypothetical water parcel	51
Figure 1.9	Post-dilution dFe concentration in open-ocean seawater	53
Figure 2.1	Study Areas for coastal incubation experiments	65
Figure 2.2.	Concentration plots for N+N and NH <sub>4</sub> <sup>+</sup> for the 2019 KS experiment	78
Figure 2.3	Chlorophyll <i>a</i> concentrations for the 2019 KS experiment	79
Figure 2.4.	Concentrations of microplankton for the 2019 KS experiment	80
Figure 2.5	Micrographs of representative microplankton, 2019 KS experiment	81
Figure 2.6	Picoeukaryotes and <i>Synechococcus</i> sp. in the 2019 KS experiment	84
Figure 2.7	Concentration plots for N+N and NH <sub>4</sub> <sup>+</sup> for the 2020 SCB experiment	87
Figure 2.8	Chlorophyll <i>a</i> concentrations the 2020 SCB experiment	88
Figure 2.9	Picoeukaryotes and <i>Synechococcus</i> in the 2020 SCB experiment	89
Figure 2.10	Concentration plots for N+N and NH <sub>4</sub> <sup>+</sup> for the 2021 SCB experiment	91
Figure 2.11	Chlorophyll <i>a</i> concentrations the 2021 SCB experiment	92
Figure 2.12	Concentrations of microplankton for the 2021 SCB experiment	93

Figure 2.13	Micrographs of representative microplankton, 2021 SCB experiment	94
Figure 2.14	Picoeukaryotes and <i>Synechococcus</i> in the 2021 SCB experiment	97
Figure 3.1	Study Areas for Sargasso Sea incubation experiments	122
Figure 3.2	Initial conditions at Hydrostation S before for oceanic experiment	130
Figure 3.3	Initial and final N+N in oceanic and coastal experiments	133
Figure 3.4	Changes in chlorophyll <i>a</i> for oceanic and coastal experiments	135
Figure 3.5	<i>Synechococcus</i> abundance in oceanic and coastal experiments	136
Figure 3.6	<i>Prochlorococcus</i> abundance in oceanic experiment	138
Figure 3.7	Cytograms from pico- and nanophytoplankton analysis	139
Figure 3.8	Picoeukaryotes in oceanic and coastal experiments	140

## LIST OF TABLES

		Page
Table 1.1	Summary of sampling campaigns conducted during this study	27
Table 1.2	Summary of relevant aspects from literature review	44
Table 2.1	Fuel and engine types used to generate scrubber washwater spikes	67
Table 2.2	Water chemistry of incubation seawater and scrubber washwater spikes	76
Table 3.1	Water chemistry of incubation seawater and scrubber washwater spikes	132



## ACKNOWLEDGEMENTS

I extend my deepest gratitude to the individuals and organizations who have played pivotal roles in the completion of this doctoral journey.

I am profoundly grateful to my advisor, Professor Katherine Mackey, for her support, insightful guidance, and invaluable mentorship throughout this research endeavor. I also express my sincere appreciation to my committee members, Professors Keith Moore, Adam Martiny and Eric Salzman, whose constructive feedback have significantly enriched the quality of this dissertation.

I would like to acknowledge the exceptional faculty at UCI's Earth System Science Department, whose commitment to academic excellence have profoundly influenced my intellectual growth. Special thanks to Professor Claudia Czimczik for her exceptional support during the most challenging phases of my PhD journey. Her mentorship and encouragement have been a guiding light during moments of uncertainty. I extend my appreciation to the dedicated staff of the department whose administrative support and logistical assistance have been indispensable. A special thank you goes to Bao Vu and Cyril McCormick.

I would like to acknowledge the numerous researchers with whom I have collaborated. In particular, I would like to thank Dr. Christa Marandino and Dr. Dennis Booge (GEOMAR Helmholtz-Zentrum für Ozeanforschung Kiel, Germany), Dr. Liudimila Osipova (the International Council on Clean Transportation, ICCT), Dr. Octavio Marin-Enriquez (Germany's Federal Maritime and Hydrographic Agency), Dr. Shun-Chung Yang, and Professor Seth John (Dept of Earth Sciences, University of Southern California, USC), Professor Ida-Maja Hassellöv, Dr. Kent Salo, Dr. Amanda Nylund (Chalmers University, Sweden), Dr. Amy Mass and Paul Lethaby (Bermuda Institute of Ocean Sciences, BIOS), Professor Peter Bryant (UCI), and the staff from CA Fish and Wildlife's Back Bay Science Center, and from the Orange County Sanitation District. Their generosity in sharing data, expertise, and resources has enriched the depth and breadth of my research. This collaborative spirit exemplifies the collective pursuit of knowledge within the academic community. I also express my gratitude to the funding sources that have supported my research. NASA's FINESST Program, the University of California, Irvine, and the Bermuda Institute for Ocean Sciences (BIOS) have provided invaluable financial support, enabling me to conduct experiments, attend conferences, and disseminate my findings. This support has been essential to the successful completion of this dissertation.

A heartfelt thank you to my lab mates and classmates at the department: Rae, Jess, Chris, Ash, my first-year cohort, and the many other amazing people I had the honor to become friends with. The camaraderie and collaborative spirit within our academic community have made this journey not only intellectually stimulating but also immensely enjoyable. Your friendship and shared experiences have been a source of strength and resilience.

Finally, I could not have done this without the love and support of my family: my mom, Teka, my daughter, Elena, and my best friend, JT Reager. Obrigada por tudo. Amo vocês!

## VITA

**Joana Tavares**

### **EDUCATION**

2018, M.S. in Earth System Science, University of California, Irvine, CA, USA

2008, M.S. in Marine Studies and Marine Policy, University of Delaware, Newark, DE, USA

2005, B.S. in Oceanography, Federal University of Rio Grande, RS, Brazil

### **HONORS, FELLOWSHIPS, GRANTS, AND AWARDS**

2022 Margaret Atwood/DISCO Practical Utopias Founding Fellowship

2022 AAAS Mass Media Fellowship Award

2021 UCI's Public Impact Distinguished Fellowship Award

2020 UCI's Blum Center Small Change Better World Seed Grant/ Award

2019 Future Investigator in NASA Earth and Space Science and Technology (FINESST) Award

2017 UC Irvine Diversity Recruitment Fellowship, UC Irvine CA, U.S.

2017 Nevin Graduate Endowment Fellowship, UC Irvine CA, U.S.

2016 National Socio-environmental Synthesis Center (SESYNC) Travel Grant to "Teaching about Socio-Environmental Synthesis with Case Studies Course", Annapolis, MD, U.S.

2015 California Coastal Commission Whale Tail Public Education Grant to expand the FLOW Citizen Science Program, CA

2008 The Frances Severance Academic Council Award for best thesis in Marine Policy University of Delaware, DE, U.S.

2007 The Barbara Prosser Research Grant for Marine Policy College of Marine and Earth Studies, University of Delaware, DE, U.S.

2004 US - Brazil Consortium in Marine Policy Fellowship: Training Program and Exchange of Best Experiences on Integrated Ocean and Coastal Management CAPES/Univ. of Delaware

## **PUBLICATIONS**

Yañez, C., Hopkins, F.; Xu, X.; Tavares, J., Welch, A.; Czimczik, C., Reductions in California's urban fossil fuel CO2 emissions during the COVID-19 pandemic *open access peer-reviewed paper published in AGU Advances*, Vol. 3, Issue 6, December 2022

Williams, L. C., A. Wenczel, and J. F. Tavares (2017) Navigating Coastal Decision-Making: Using Shellfish Aquaculture as a Model for Socio-Ecological Knowledge Development. Teaching Case Study published by the National Socio-environmental Synthesis Center (SESYNC) and presented at the Coastal and Estuarine Research Federation (CERF) Conference in Providence, Rhode Island.

Lejano R., J. Tavares-Reager and F. Berkes (2013), Climate and narrative: Environmental knowledge in everyday life, peer-reviewed paper published in *Environmental Science and Policy*, vol. 31, pp. 61-70.

Tavares, J.F., L. Proença and C. Odebrecht (2009). Assessing the Harmful Microalgae Occurrence and Temporal Variation in a Coastal Aquaculture Area, Southern Brazil, *peer-reviewed paper published in Atlântica Rio Grande*, vol. 31(2), pp. 129-144.

Tavares-Reager, J.F. (2008). Chemical Toolbox for Aquatic Invasive Species Management in Hawaii: A Review of Methods, Opportunities and Risks. Technical report published by the Hawaii Department of Lands and Natural Resources. 245pp.

Loper C., M.C. Balgos, J. Brown B. Cicin-Sain, C. Jarvis, J. Lilley, I.T. Noronha, A. Skarke, and J.F. Tavares (2004). Small Islands, Large Ocean States: A Review of Ocean and Coastal Management in Small Island Developing States Since the 1994 Barbados Programme of Action for the Sustainable Development of Small Island Developing States (SIDS). Technical Paper Series No. 2003-3 Sponsored by: UNEP/GPA and the Global Forum on Oceans, Coasts, and Islands, Global Forum on Oceans, Coasts, and Islands toward Mauritius 2004 Series.

## **PROFESSIONAL EXPERIENCE**

2023 – present Director of the California Center for Climate Change Education at West Los Angeles College

2010 - 2017 Community College Adjunct Faculty (Lecturer and lab/ field instructor)

2010 - 2017 Community Education Program Coordinator and Curriculum Developer for Amigos de Bolsa Chica Foundation, Huntington Beach, CA.

2011 - 2013 Science Technology Engineering and Math (STEM) Program Coordinator for U.S. Department of Education Hispanic Serving Institutions STEM and Articulation Programs Cooperative, Fullerton College, Fullerton, CA.

2007 - 2009 Aquatic Invasive Species Research Specialist for the State of Hawaii's Department of Lands and Natural Resources, Division of Aquatic Resources, Research Corporation of the University of Hawaii.

2007 Principal Researcher in University of Delaware Sea Grant's Coastal Community Enhancement Initiative: An Approach for Addressing Growth, Land Use & Environmental Impacts in Southern Delaware.

2005 - 2007 Research Assistant in Consideration, assessment and modeling the introduction of non-native species from marine transportation ballast water. University of Delaware.

2004 Research Assistant in Small Islands, Large Ocean States: An Analysis of the Implementation of Barbados Programme of Action Related to Oceans and Coasts. Gerard J. Mangone Center for Marine Policy, University of Delaware.

2000 - 2003 Research Assistant in Harmful Algal Blooms in the South of Brazil. Federal University of Rio Grande, Brazil.

## **SERVICE AND COMMUNITY BUILDING**

2016 - 2022 Board member of Amigos de Bolsa Chica, Environmental Not-for-profit Organization in Huntington Beach, CA, USA.

2017- 2020 Board member and Science Committee Co-Chair of Newport Bay Conservancy, Environmental Not-for-profit organization in Newport Beach, CA, USA.

2020 Co-organizer and curriculum developer for *Educating for Sustainability in Times of Uncertainty*, Amigos de Bolsa Chica/ National Geographic Summer Institute for Educators hosted between July 13th- July 24th, 2020 (online workshop)

2019- 2020 Creator and lead organizer for the *Climate Solutions Conference*, hosted by UCI's Ridge to Reef Program and the Newport Bay Conservancy on February 1, 2020, at Orange Coast College, Costa Mesa, CA, USA.

2018- 2020 Diverse Educational Community and Doctoral Experience (DECADE) Graduate Student Representative for the Earth System Science Department, University of California, Irvine, CA, USA.

2018- 2019 UCI's Physical Sciences Undergraduate Mentoring Program Mentor

## **ABSTRACT OF THE DISSERTATION**

Marine Phytoplankton Responses to Scrubber Washwater Discharges  
by

Joana Tavares

Doctor of Philosophy in Earth System Science

University of California, Irvine, 2023

Professor Katherine Mackey, Chair

The combustion of fuels in the engines of ships releases inorganic compounds and metals that can promote phytoplankton growth (e.g. N, Fe, Mn, Zn) or decrease productivity (e.g. Cu). Many ship operators comply with air quality regulations by installing scrubber systems that clean emissions going into the air, but discharge washwater containing nutrients and contaminants directly into ocean water. This has the potential to change primary production rates and the structure of phytoplankton populations.

Chapter 1 of the dissertation analyzed scrubber washwater samples from small engines combusting distilled fuels. Results revealed consistent enrichment of washwater with nitrogen and dissolved trace metals, with variations in the specific metals enriched. I compared our results to those found in the literature for a distilled fuel that was combusted in a small engine, and for residual fuels combusted in large ship engines. Using diverse model simulations, Chapter 1 demonstrated that cumulative scrubber water discharges could fertilize phytoplankton in specific regions by providing essential nutrients like iron.

In Chapter 2, I presented results from mesocosm experiments simulating acute exposure of coastal phytoplankton to high concentrations (1%, 5%, and 10%) of scrubber

washwater from engines using both distilled and residual fuels. Growth responses varied across phytoplankton taxa and fuel types, providing insights into potential ecological consequences in heavily trafficked coastal regions.

Chapter 3 explored the impact of scrubber washwater discharges on natural phytoplankton communities in the Sargasso Sea. Both conventional heavy fuel oil (HFO) and alternative distilled fuel (HGO) exhibited mild fertilizing effects at a 2% concentration. This chapter emphasized co-limitation by multiple nutrients, with scrubber washwater at 2% adequately supplying nutrients compared to lower concentrations.

This dissertation highlights the complex interactions between ship emissions, scrubber washwater, and marine ecosystems, emphasizing the need for comprehensive assessments to inform sustainable maritime practices.

## **INTRODUCTION**

### **Overview**

Anthropogenic pollution significantly impacts marine ecosystems. Pollution in the ocean can be conspicuous, such as in the case of oil spills, or insidious, such as with air pollution produced by the combustion of certain fuels in marine engines (Walker et al., 2018). The combustion of fuels in marine engines produces toxic gases and particulate matter, which are emitted via marine vessels' smokestacks into the atmosphere as aerosols that may later deposit over the ocean surface, or that may be discharged into the ocean as the liquid waste produced by exhaust gas cleaning systems, also known as scrubbers (Agrawal et al., 2009; Celo et al., 2015; Eyring et al., 2010a, 2010b; Moldanová et al., 2009a; Popovicheva et al., 2012; Salo et al., 2016; Walker et al., 2018). The environmental consequences of these air emissions and liquid waste discharges may be substantial but scientific knowledge regarding impacts is lacking, particularly in what concerns the effects these components may have on marine phytoplankton (Jägerbrand et al., 2019; Turner et al., 2017; Ytreberg et al., 2019, 2022a; C. Zhang et al., 2021). The PhD research presented here addresses this specific knowledge gap.

### **Background**

Marine phytoplankton are responsible for half of all photosynthesis on Earth. They serve as the basis of most marine food webs and sequester carbon dioxide, affecting global fisheries and, in the long run, climate (Arrigo, 2005; Bunt, 1975; Field et al., 1998; Sarmiento & Gruber, 2006). Phytoplankton abundance in the ocean is naturally constrained by the

bioavailability of chemical components that serve as macro- and micronutrients for primary producers including nitrogen (N), phosphorus (P), and trace metals such as iron (Fe), and zinc (Zn) (Martin & Fitzwater, 1988; Mills & Arrigo, 2010; C. M. Moore et al., 2013a; Sunda & Huntaman, 1997). Some of these potentially fertilizing components are known to be emitted as byproducts from the combustion of commonly used marine fuels (Coufalík et al., 2019; Eyring et al., 2005, 2010b; Hardaway et al., 2004; Lack et al., 2009a; Moldanová et al., 2009a; Popovicheva et al., 2012; Raudsepp et al., 2019b; Viana et al., 2009). Toxic components such as polycyclic aromatic hydrocarbons (PAHs), and certain metals such as copper (Cu), and lead (Pb) are also known to be released as byproducts of fuel combustion, and depending on concentration and on the sensitivity of the microbial taxa present in the receiving ocean waters, may hinder phytoplankton growth in otherwise productive zones (Jordi et al., 2012; Lopez et al., 2019; B. H. Othman et al., 2018; Paytan et al., 2009a). Ultimately, the net effects that emissions from marine engines will have on marine primary productivity in any given region and time depends on the balance between positive and negative disturbances on different types of phytoplankton, combined to the influence of physical processes in the ocean, and to other effects that ship emissions may have on phytoplankton grazers. For example, closed-loop scrubber washwater has been shown to affect development and survival in single species of copepods, and at the community level, by causing both lethal and sublethal effects in marine zooplankton, due to contaminants, some of which are persistent in the marine environment (Koski et al., 2017; Thor et al., 2021).

Since the 1950s, most vessels that engage in global maritime transport and commercial fishing have relied on internal combustion diesel engines and on various types of hydrocarbon-based fossil fuels to power their propulsion (Andersson et al., 2016). Bunker



fuel, or heavy fuel oil (HFO) has historically dominated the maritime fuel market. HFO is a relatively cheap residual fuel that is known to produce more combustion byproducts than the distillate fuels used in other transportation sectors (Chu Van et al., 2018, 2019; Moldanová et al., 2013; Winnes et al., 2020; Zetterdahl et al., 2016).

The combustion of fossil fuels consists of a chemical reaction between hydrocarbon molecules and oxygen that produces heat, water, and carbon dioxide. Because marine fuels often contain impurities and combustion is rarely complete, the process also releases byproducts such carbon monoxide (CO), sulfur oxides (SO<sub>x</sub>), nitrous oxides (NO<sub>x</sub>), polycyclic aromatic hydrocarbons (PAHs), volatile organic compounds (VOCs), and particulate matter (PM) (Avakian et al., 2002; Koshland & Seeker, 2007; Stone, 2012). PM may include metals typically present as oxides, sulfates, or present as organometallic inclusions in soot and char (Celo et al., 2015; Corbin et al., 2018; Eyring et al., 2005; Moldanová et al., 2009b; Popovicheva et al., 2009; Sarvi et al., 2011).

The quantity, size, structure and chemical composition of the combustion byproducts emitted by marine vessels differs greatly (Figures 0.1 and 0.2) depending not only on the quality of fuels being combusted but also on engine size and type, the vessels' operation conditions and engine load, and on various factors that affect the evolution of the plume after the aerosols are emitted into the atmosphere or dissolved in water (Agrawal et al., 2008, 2009; Moldanová et al., 2009a). The amount of NO<sub>x</sub> produced by any given engine, for instance, is expected to be directly proportional to the engine's combustion temperature and, to a lesser extent, to the amount of nitrogen present as impurities in the fuel being combusted (Andersson et al., 2016; Fridell, 2019; Hebbar, 2014).

The term NO<sub>x</sub>, or nitrogen oxides, refers mainly to two gases: nitric oxide (NO) and nitrogen dioxide (NO<sub>2</sub>), which are combustion byproducts subject to rapid interconversion in the presence of oxygen. It has been estimated that, globally, ship emissions contribute to almost a quarter of all anthropogenic NO<sub>x</sub> input into the ocean (Cheng et al., 2017; Corbett et al., 1999a; Eyring et al., 2010b). Upon reacting with water, NO<sub>x</sub> generates nitrous and nitric acids that can serve as sources of nitrate (NO<sub>3</sub><sup>-</sup>), and nitrite (NO<sub>2</sub><sup>-</sup>). Once dissolved in seawater, these components may serve as macronutrients for primary producers in the form of dissolved inorganic nitrogen (DIN).

Combustion byproducts released by ship emissions into the air have been identified as a significant form of pollution that travels onshore and causes lung cancer, cardiovascular diseases, and ~400,000 premature human deaths per year (Corbett, 1997, 2003; Corbett et al., 2007; Sofiev et al., 2018). These findings have galvanized changes in policies aimed at controlling shipping air pollution at international and national levels.

Sulphur content in fuels serves as an indicator for how “polluting” the emissions from their combustion will be, not only in terms of SO<sub>x</sub> emissions but also in respect to the amount and nature of other combustion byproducts such as particulate matter, and metals (Agrawal et al., 2009; J. O. Anderson et al., 2012; Brook et al., 2010; Gangwar et al., 2012; Griffiths, 2011; J. P. Jalkanen et al., 2012; Moldanová et al., 2009a; Ntziachristos et al., 2016; Valavanidis et al., 2008; Viana et al., 2008). In response, the International Maritime Organization (IMO) has mandated sequential reductions of the content of sulfur (S) in air emission from ocean-going vessels over the past two decades.

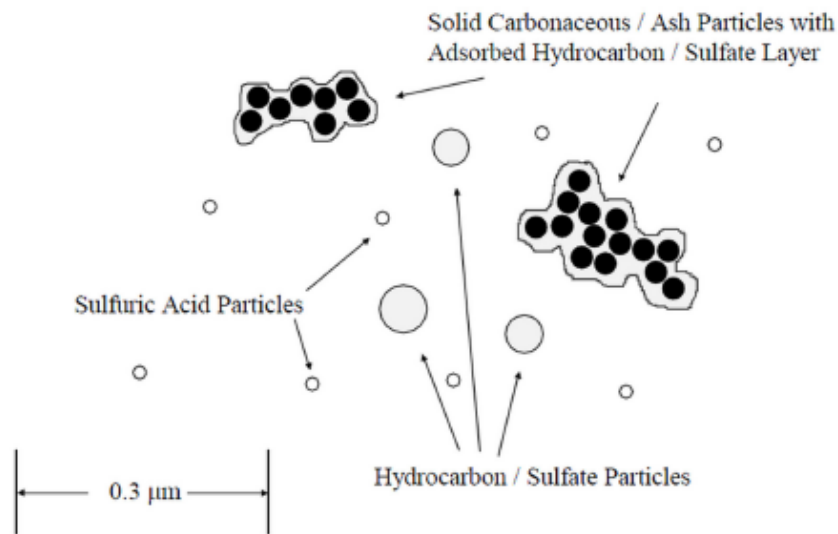


Figure 0.1. Typical structure of engine exhaust particles (Kittelson, 1998)

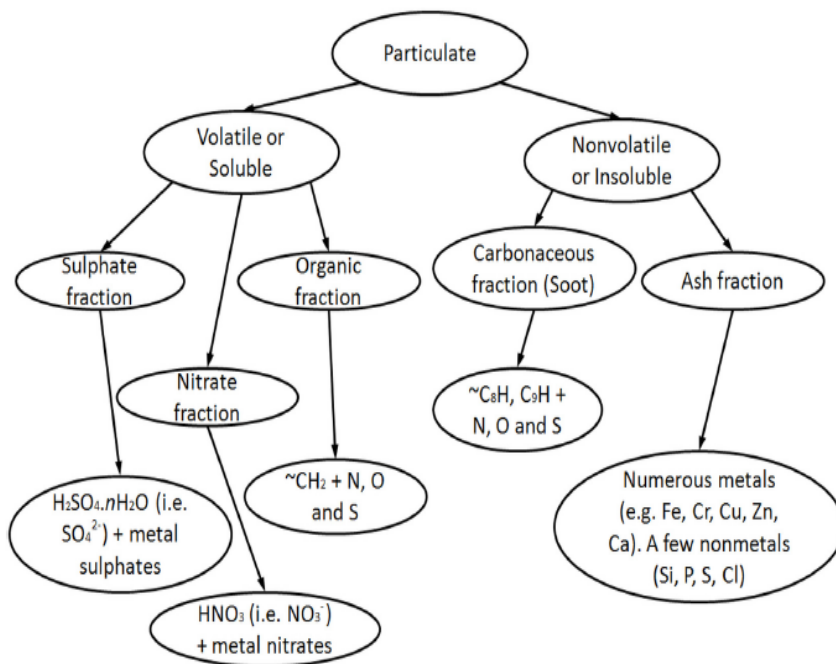


Figure 0.2. Conceptual model of fuel combustion PM composition, terminating in five distinct groups or fractions: sulphates, nitrates, organics, carbonaceous and ash (Eastwood, 2008)

According to IMO rules that took effect in January of 2020, all commercial ships operating in international waters must comply with standards that lower fuel sulfur content from the historical 3.5% S content (by mass) to 0.5% S. This policy is commonly referred to as the global sulfur cap. Inside ocean areas determined to be Sulfur Emission Control Areas (SECAs) the cap is 0.1% S, and the governments of many countries, provinces, and states have established specific emission and/or fuel standards for their territorial seas (i.e. the ocean area that extends seaward up to 12 nautical miles from its coastal baselines), and/or their contiguous zones (i.e. area within 24 nautical miles from the coast). In certain areas, provisions to control the amount of NO<sub>x</sub> released by ships have also been established through the creation of nitrogen emission control areas (NECAs). To comply with various emission and fuel standards, ship operators can either combust “cleaner” alternative fuels or, in some places, use scrubbers (Christodoulou et al., 2019; Comer et al., 2020; Kontovas, 2020).

Popular alternative fuels in the maritime sector consist of distillate fuels and blends of residual and distillate fuels (e.g. marine gas oils or MGO, heavy gas oil or HGO, and low- or ultra-low sulfur diesel fuels or ULSD) that vary greatly in composition but that will pass sulfur regulation enforcement (Khan et al., 2012; Lehtoranta et al., 2019; Viana et al., 2020). However, the cost of using alternative fuels is generally higher than that of installing and operating scrubbers. According to the IMO, ships operating scrubbers are allowed continue combusting cheaper, high-sulfur residual fuels (HFO) in international waters, and many nations allow for the use of scrubbers in their waters as well (ICCT, 2023). This loophole in the global sulfur cap has incentivized the adoption of scrubbers by the maritime industry (Kontovas, 2020; Zis et al., 2022). An estimated 50,000 merchant ships are currently

operating in the world ocean (International Chamber of Shipping, 2023) and scrubbers are currently used by 25% of the world merchant fleet as measured by deadweight tonnage (Marin-Enriquez et al., 2023). Scrubber installations ramped up considerably in 2019, in preparation for the IMO's 2020 global fuel sulfur cap. Between the year 2015 and 2020, the number of ships in the international shipping fleet fitted with scrubbers increased from 243 to more than 4,300 (Osipova et al., 2021) and projections are that the scrubber fleet is going to increase to ~5,060 scrubbers by 2025 (ICCT, 2023).

Approximately 80% of the scrubbers currently installed on ships work by pumping ambient seawater aboard and then spraying that seawater onto the exhaust smoke before it comes out from the vessel's smokestack, in systems called open-loop scrubbers (Fig. 0.3 a). In high seas, and in many coastal locations (e.g. most territorial waters of South, Central and North America, Europe, India and Australia), ship operators are allowed to use open-loop scrubbers (ICCT, 2023). This practice reduces air pollution but discharges untreated washwater directly into the ocean. The other form of scrubbing is called closed-loop, a system in which the washwater is treated with a base, usually a sodium hydroxide (NaOH) solution. Closed-loop scrubbers (Fig. 0.3 b) include the collection of contaminants as sludge that is later disposed in port reception facilities but the overflow water, also known as bleed-off, is periodically discharged overboard. Discharge washwater volumes from closed-loop systems are much smaller than that from open-loop systems. About 2% of the scrubbers currently in use are closed-loop units, and ~ 17% of the scrubber fleet have been equipped with hybrid scrubbers that can switch from operating as open- or closed-loop scrubbers (Lunde Hermansson et al., 2021).

Little is known about the effects of these air emissions and scrubber washwater discharges on marine phytoplankton. Some authors have speculated that ship emissions can increase the input of bioavailable nutrients such as nitrogen (N) and iron (Fe) in atmospheric deposition and potentially affect ocean biogeochemical processes, as other pyrogenic sources do (Hamilton, Moore, et al., 2020; Ito, 2013a, 2013b; Ito et al., 2021; Ito & Feng, 2010; Ito & Shi, 2016; T. D. Jickells, 2005; Rathod et al., 2020a; C. Zhang et al., 2021). In some ocean areas, NO<sub>x</sub> being released into the air from ships' smokestacks has been identified as a relatively important source of DIN for marine productivity (C. Zhang et al., 2021) and as a potential cause of eutrophication (Raudsepp et al., 2013, 2019a). Few have measured nitrogen content in scrubber washwater samples produced by ships, and the measurements that have been made used methods that may be suitable for general water quality enforcement in coastal regions, but not sensitive enough for the study marine biogeochemistry (Marin-Enriquez et al., 2023).

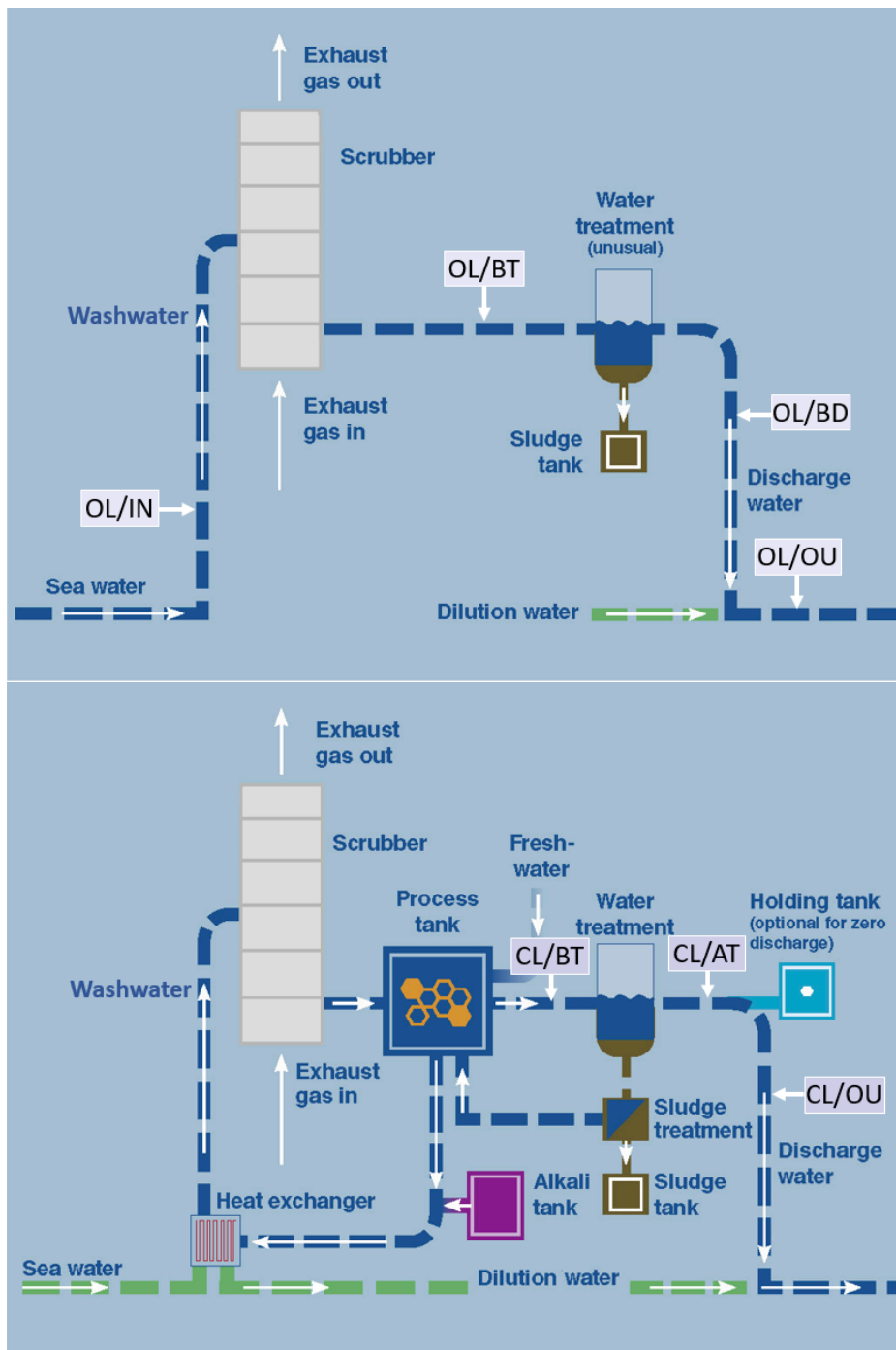


Figure 0.3: Diagram showing the overall structure of open (top panel) and closed-loop scrubbers (bottom panel) (Marin-Enriquez et al 2023).

One study has documented the artificial fertilization of phytoplankton in an incubation experiment after a 13-day exposure to relatively high (10%) scrubber washwater produced by a small engine combusting a distillate fuel in a testbed facility in Sweden (Ytreberg et al., 2019). These authors and others have alerted to the potentially toxic and inhibitory effects of scrubber washwater discharges on marine microbes (Picone et al., 2023a; Turner et al., 2017; Ytreberg et al., 2021).

About Fe in particular, one central impediment to understanding the relative importance of shipping emissions as a source of this metal for phytoplankton is the issue of solubility. Iron occurs in two main redox states in the environment: ferric iron (Fe(III)), which is poorly soluble at circumneutral pH, and ferrous iron (Fe(II)), which is typically more soluble and therefore more bioavailable. As other anthropogenic sources of Fe, shipping emissions are characterized by acidic conditions which are known to increase iron solubility (M. S. Johnson & Meskhidze, 2013; Myriokefalitakis et al., 2015; Solmon et al., 2009). In general, the solubility of iron associated to particles emitted by the combustion of fuels is assumed to be relatively high (77–81%) in comparison to the iron solubility of mineral aerosols (<1%) (Schroth, 2018; Schroth et al., 2009). Studies indicate that major sources of soluble iron deposition vary greatly from region to region and with seasons, and that anthropogenic activity is the main determinant of this variability in recent times (Hamilton, Scanza, et al., 2020; Ito et al., 2019; N. M. Mahowald et al., 2018). The few reports about metal composition of emissions from marine engines (Celo et al., 2015; Corbin et al., 2018; Moldanová et al., 2009a; Popovicheva et al., 2009, 2012) and scrubber washwater discharges (Marin-Enriquez et al., 2023; Ytreberg et al., 2022a) that exist show that maritime transport may also be a source of other trace metals of physiological importance to marine microbial



life such as cobalt (Co), Copper (Cu), lead (Pb), and zinc (Zn) (Lopez et al., 2019; K. R. M. Mackey, Buck, et al., 2012; N. M. Mahowald et al., 2018; Sunda & Huntsman, 1995a, 1998).

## **DISSERTATION STRUCTURE AND ACCOMPLISHMENTS**

The overarching goal of the present thesis is to quantify the effects of scrubber washwater discharges on the abundance and community composition of marine phytoplankton in different ocean areas via experiments and modeling. These efforts are presented in this thesis in three chapters, as described below:

**Chapter 1** In the first chapter we present the characterization of scrubber washwater samples produced by small and large engines combusting distillate and residual fuels in terms of their nitrogen and trace metals content. For that, we first measured the content of nitrate, nitrate, ammonium, and of some metals known to affect phytoplankton physiology in the washwater produced by scrubbing units that are used in small engines to combust distillate fuels. Next, we conducted a literature review that allowed us to account for the concentrations of metals and discharge flow rates of each scrubbing unit. We used this information to estimate the marine input of nutrients and toxicants associated to the typical operation of these vessels. We compared our measurements to those documented in the literature for large ships combusting residual fuels (HFO). Our results corroborate the notion that the amount of metals that serve as fertilizing agents for phytoplankton released by fossil fuel combustion in marine engines is affected by the quality of the fuels being combusted, but the influence of engine size and operation, which affects the temperature of the combustion, cannot be ruled out. This is in line with what is established in the literature about ship emissions (Moldanová et al., 2009a; Popovicheva et al., 2009; Raudsepp et al.,

2019b) and with the few published studies that have tested this effect empirically in the Baltic and in the Northwest Pacific regions (Ytreberg et al., 2019; C. Zhang et al., 2021). Once post-discharge dilution is considered, the amount of dissolved iron being discharged by marine vessels operating scrubbers and wet exhaust systems in semi-enclosed bodies of water can represent a significant source of nutrients for marine phytoplankton, if accumulation occurs. In the open ocean, the effect caused by discharges from individual ships may be minimal due to horizontal and vertical mixing that reduce exposure concentrations. However, it is possible that cumulative effects of scrubber washwater discharges in heavily-trafficked shipping lanes that cross over or near oligotrophic gyres, such as the South Atlantic gyre and the southern section of the Indian basin, may cause regional fertilization effects that lead to increases in net primary production, nitrogen fixation, carbon export, and the depletion of available nitrate in surface waters. These impacts could become more relevant in the future if the volume of scrubber washwater discharge increases in those areas and/or if dissolved iron content in scrubber washwater significantly increases. Increased upper ocean stratification due to climate change may also amplify the regional relevance of scrubber washwater discharges as a source of nutrients to marine phytoplankton (Li et al., 2020; Roch et al., 2023; Sallée et al., 2021; Yamaguchi & Suga, 2019).

**Chapter 2** In the second chapter we compile the results from three mesocosm incubation experiments conducted for the quantification of responses by natural microbial populations present in coastal seawater to acute, high exposure concentrations to scrubber washwater (1%, 5% and 10% for 48h). We measured fertilization effects of various scrubber washwater formulations on primary productivity, and on taxa composition of marine phytoplankton from two different study areas. One experiment was conducted in the

Kattegat Strait, a region adjacent to the Baltic Sea in the fall of 2019, and two experiments were conducted in the Southern California Bight, in the USA, in the summer of 2020 and early fall of 2021. These experiments were conducted following standard methods established in the literature for bottle experiments (K. R. M. Mackey et al., 2010a, 2017; K. R. M. Mackey, Mioni, et al., 2012; Paytan et al., 2009b) using samples of scrubber washwater characterized in this dissertation's Chapter 1 (i.e. scrubber washwater produced with HGO in a testbed facility, with Ultra Low Sulfur Diesel/ CARB fuel combusted in small boat engines, or with HFO combusted in engines of real commercial ferry). Changes in phytoplankton abundance and composition were monitored after exposure to various scrubber washwater concentrations. Chlorophyll *a* (chl *a*) was used as a proxy for phytoplankton biomass and productivity, and cell counts obtained via flowcytometry and, in some experiments, microscopy counts, were used to track changes in relative abundance amongst certain taxa. Auxiliary data on nutrients (i.e. nitrite and nitrate, ammonium, phosphate, water soluble trace metals) collected before (time zero) and after exposure (time 48hr) allowed for the interpretation of the relative importance of scrubber washwater discharges for biogeochemical processes taking place during the experiments. Chapter 2 results indicate that the response of microbial communities to acute exposure to scrubber washwater depended largely on the initial trophic status and composition of the receiving seawater, the final concentration exposure that was simulated by experimental treatments and the type of scrubber washwater used. Nitrogen enrichment was the most relevant process in all experiments conducted near coastal waters, with all treatments that were spiked with scrubber washwater increasing in biomass over 48hrs relative to non-addition controls. These results are in line with those reported in analogous studies (Marin-Enriquez et al.,

2023; Picone et al., 2023b; Ytreberg et al., 2019, 2021). In terms of exposure concentration, our experiments simulated extreme forms of contamination by scrubber water discharges, and revealed interesting responses that can help us better understand how coastal phytoplankton respond to broad ranges of anthropogenic disturbance levels. For example, in Chapter 2 I documented, for the first time, shifts in composition in the experimental treatments that simulated exposure to very high (10%) concentration of scrubber washwater produced with HFO. This effect on taxa composition was not observed in the one experiment conducted with scrubber washwater produced with ultra-distillate high-quality fuel (CARB diesel). I conjecture that shifts in taxa composition results from group-specific sensitivity to certain metals (e.g. Cu, V) that were present in the scrubber washwater produced with residual fuels (HFO) but not in the scrubber washwater produced with highly distillate fuels. The findings presented in Chapter 2 are particularly relevant for coastal policy considerations.

**Chapter 3** The objective of Chapter 3 was to test the hypothesis that in remote and naturally nutrient-poor ocean biomes, the addition of nitrogen, iron, and other metal components released from ship emissions as scrubber washwater would cause an artificial fertilization effect on picoplankton communities, thus simulating what may be happening along shipping lanes in open ocean. For this, one mesocosm incubation experiment was conducted using seawater from an offshore site located approximately 40 km from the Bermuda Atlantic Time-series Study, BATS station in September of 2021. For comparative purposes, another experiment was conducted in parallel, using seawater collected from the Hamilton Harbor, in Bermuda. Experimental treatments simulated acute exposure of phytoplankton communities to scrubber washwater from large ships combusting HFO and

using the testbed HGO scrubber wash water. Various exposure concentrations (i.e. 0.01%, 0.1% and 2%) were used in this experiment and parameters were measured after 24h (chl *a* only) and 48h (all other parameters). Chapter 3 results showed that after 48hr exposure, chl *a* increased relative to control in both high concentration exposure treatments (i.e. 2% final concentration of treatments spiked with SDW produced with HGO and HFO), but not in other treatments. As in Chapter 2, taxa-specific sensitivity to HFO scrubber washwater was documented.

## **CONCLUSION AND FUTURE DIRECTIONS**

Global emissions from shipping are expected to more than triple between 2020 and 2050 (Gössling et al., 2021). As the shipping industry continues to adjust to new regulations and to societal expectations regarding the sustainability of their operations, several technologies emerge- some will remain, others won't. Per usual, the reduction of costs is at the forefront of business decisions, and that can become a problem when public policies fail to identify and address economic externalities, such as environmental and human health impacts that are either not well understood or not discussed enough to spur public demands for change. That is the story of scrubbers.

The implementation of the global IMO 0.5% S fuel standard in 2020 is estimated to have reduced the number of deaths from cardiovascular diseases and lung cancer from 400,000 to 265,000 per year and to have reduced the annual number of new childhood asthma cases from 14 million to 6.4 million. As with most new regulations of global importance, the debate regarding pros and cons of the IMO sulfur cap, including the regulations' broader impacts on the earth system and climate are still ongoing (Hansen et al.,

2023). In some ways, the “scrubbers loophole” is a part of this debate. Clearly, this loophole was created without the full consideration of the environmental impacts these discharges may have on marine life and biogeochemistry. This dissertation adds to the growing body of research that shows that scrubbers may be altering natural processes. Our results indicate that under certain conditions, some formulations of scrubber washwater may fertilize marine phytoplankton, although at limited scales, thanks to the good old solution to pollution: dilution.

Thinking more broadly about the potential impacts of shipping to marine biogeochemistry and microbial ecology, I am compelled to return to the original question that motivated this research: are shipping air emissions contributing to significant amounts of fertilizing components, such as highly bioavailable iron and nitrogen? I spend the first two years of this PhD research trying to find a way to answer that broader question. Due to a series of impediments that included lack of access to proper sampling opportunities, methods, equipment, and expertise in the field of combustion aerosols from ships, and a global pandemic, I was unable to further pursue that investigation, but what I learned during this journey allows us to make some recommendations:

First, it seems like any effects that ship emissions may have, be them delivered to the ocean as liquid discharges of scrubber washwater or as aerosol deposition, will cause a chronic effect, and not an acute one. Thus, future studies should use strategies to evaluate the long-term cumulative effects of very small additions of metals and nitrogen near shipping lanes. I have attempted to do that using remote sensing and believe that this is a promising method to verify the annual changes in abundance that I predicted with the modeling study

presented in chapter 1. Modern ocean color remote sensing tools may allow for the investigation of some changes in composition as well. If resources are available, field research could also be used to validate model predictions and remote sensing observation by analyzing and comparing water samples collected from transects that cross well-defined shipping lanes in the South Atlantic and South Indian gyres.

Secondly, we need a better understanding of the processes that determine the quality and quantity of metals that are being added to ecosystems from ships, and particularly we need a better understanding of the original source of all the Fe. Limited evidence indicates that most of the Fe that has been measured in scrubber washwater samples (summarized in our literature review in chapter 1), as well as the Fe that others have found in smokestack emissions (Celo et al., 2015; Corbin et al., 2018) may not come from the fuels. As part of Germany's ImpEx project, Marin-Enriquez et al (2023) recently measured the amount of Fe in the original fuels and lubricants being used in the ships that generated the scrubber washwater samples that they later analyzed for dFe content, and the two data sets are not correlated. Many combustion and ship experts I spoke to said they think the Fe is probably coming from the ship and its parts, or maybe from additives, but none of them had concrete data to confirm their theories. This is important, because if it is true that the Fe is not coming from impurities in the fuel, it means that using alternative fuels – be them distillate fuels, blends, or liquified natural gas– will not necessarily alter the role of shipping as a possible fertilizing agent in the world ocean.

Thirdly, while our mesocosm incubations were very useful in documenting how diverse the marine phytoplankton responses can be to the addition of scrubber washwater

spikes, there were many results that could not be explained with the methods I used. For example, in both chapters 2 and 3, I observed greater growth of certain taxa when exposed to lower exposure concentrations of the scrubber washwater spikes being used. That was particularly the case with HFO, which I know had more metals in it, but I could not unequivocally determine the reason for the differences that I observed. To address these unanswered questions, I would recommend a series of monospecific essays to better understand taxa-specific sensitivities to individual components. Here, it is important to highlight that the exposure concentrations used in most of our experiments were much higher than what we would expect marine phytoplankton to ever experience in the real world, and so that needs to be taken into consideration when evaluating the motivations and settings for such toxicity essays.

Finally, if one wanted to further investigate the effects of scrubber washwater discharges may have on microbial community composition, including possible effects in the role of diazotrophs, I would recommend using omics to test the hypothesis that these additions are supplying enough nitrogen and metals to remote ocean areas, such as shipping lanes in the subtropical ocean gyres, as to alter the relative abundance of these organisms.

Thinking again more broadly about the initial motivations for this research, it is interesting to consider these topics in the bigger context of global climate change. Climate change will continue to alter virtually every aspect of the ways in which human and natural systems function, shipping included. The melting of ice caps is “creating” new shipping routes that are expanding faster than models projected (Cao et al., 2022). Changes in the distribution of arable lands, the displacement of people, and changes in production and



consumption patterns in the next decades, will likely alter shipping routes. And as mentioned before, climate change is affecting ocean stratification (Li et al., 2020; Roch et al., 2023; Sallée et al., 2021; Yamaguchi & Suga, 2019), which could concentrate external nutrient inputs in the euphotic zone. At the same time, there is mounting pressure (and need) for the shipping industry to reduce their greenhouse gas emissions. The shipping industry is known as a hard-to-decarbonize sector and many ideas for new technologies with unknown externalities are currently being discussed, such as the use of ammonia to fuel ships (Al-Aboosi et al., 2021; Machaj et al., 2022). Research that builds on the work presented in this dissertation- particularly models and projections- should take these emerging trends and unknowns related to the shipping industry and global changes into account.

## **CHAPTER 1**

# **ARE SCRUBBERS FERTILIZING THE OCEAN? ARTIFICIAL ENRICHMENT OF SEAWATER BY EXHAUST GAS CLEANING SYSTEMS USED WITH MARINE ENGINES COMBUSTING RESIDUAL AND DISTILLED FUELS**

### **ABSTRACT**

Air emissions from marine engines may be causing the artificial fertilization of ocean areas. This could lead to impacts on marine primary production, community composition, biodiversity, and carbon sequestration rates. I measured the concentration of dissolved nitrogen and trace metals of interest in samples of washwater generated from the scrubbing of exhaust gases emitted from the combustion of two types of distilled fuels, in three small engines. Our results show that scrubbing enriched the washwater with nitrogen and dissolved trace metals in all cases, but the level and types of metals that became enriched varied. I compared our dissolved metals results to those found in the literature for a distilled fuel that was combusted in a small engine, and for residual fuels combusted in large ship engines. Using metal concentrations and reported rates for scrubber water discharge, I consider the dilution of these metal inputs under variable oceanographic scenarios. Using various models, I show that in certain situations, the cumulative effects of scrubber water discharges could fertilize marine phytoplankton by providing iron for growth. Although small relative to other nutrient sources, nutrient additions from scrubber water discharges may cause the fertilization of certain marine phytoplankton in some parts of the world.

### **INTRODUCTION**

Phytoplankton are collectively responsible for about half of the net primary production on Earth. In the ocean, this form of primary productivity supports nearly all marine foodwebs, maintaining biodiversity and fisheries. On long time scales, marine phytoplankton also play a role in global climate through the biological pump (Arrigo et al., 2000; Basu et al., 2018; Gruber & Sarmiento, 1997; C. M. Moore et al., 2013b; Pierce et al., 2011; Sarmiento & Gruber, 2006).

Phytoplankton abundance in the ocean is naturally constrained by the bioavailability of chemical components that serve as macro- and micronutrients for primary producers

including nitrogen (N), phosphorus (P), and trace metals such as iron (Fe), and zinc (Zn). Near coastlines, the main sources of nutrients into the euphotic zone are land run-off and upwelling (Martin & Fitzwater, 1988; Mills & Arrigo, 2010; C. M. Moore et al., 2013a; Sunda & Huntaman, 1997). Further away from these sources, nutrient supplies are generally scarce and sporadic. Nitrogen fixation, a process that is carried out by a very specific group of microorganisms (i.e. diazotrophs) represents an importance source of new nitrogen into those remote ocean areas, and the main source of trace metals into the open ocean is the deposition of atmospheric aerosols onto the seawater surface (Duce & Tindale, 1991; Gruber & Sarmiento, 1997; T. Jickells & Moore, 2015; Kanakidou et al., 2016; K. R. M. Mackey et al., 2010b; Monteiro et al., 2011; Zehr & Kudela, 2011).

Natural aerosols, such as desert dust transported by wind, dominate atmospheric deposition by mass. However, anthropogenic combustion of fossil fuels and biomass burning have been shown to be significant sources of nutrients for primary producers in certain regions and seasons, particularly because, compared to mineral sources, combustion aerosols have higher fractional metal solubility, which appears to be correlated to higher bioavailability (Buck et al., 2013; Duce et al., 2008; Ito, 2015; Ito et al., 2019; Rathod et al., 2020a; Sedwick et al., 2007; Sholkovitz et al., 2012; Bonneville et al., 2004; Wozniak et al., 2015).

Potentially fertilizing components, including N, Fe, Zn, and other trace metals are known to be emitted as combustion byproducts of commonly used marine fuels (Coufalík et al., 2019; Eyring et al., 2005, 2010b; Hardaway et al., 2004; Lack et al., 2009a; Moldanová et al., 2009a; Popovicheva et al., 2012; Raudsepp et al., 2019b; Viana et al., 2009). Toxic

components such as polycyclic aromatic hydrocarbons (PAHs), and metals such as copper (Cu), and lead (Pb) are also known to be released as byproducts of fuel combustion and may hinder phytoplankton growth in otherwise productive zones (Jordi et al., 2012; Lopez et al., 2019; B. H. Othman et al., 2018; Paytan et al., 2009a), depending on concentration and on the sensitivity of the microbial taxa present in the receiving ocean waters. Ultimately, this balance between positive and negative disturbances on different types of phytoplankton, combined to other effects that emissions from marine engines may have on phytoplankton grazers (Koski et al., 2017; Thor et al., 2021), to physical factors, determines the net effects that emissions from ships and boats will have on marine primary productivity.

Combustion byproducts released by ships cause significant human health problems (Corbett, 1997, 2003; Corbett et al., 2007; Sofiev et al., 2018), and environmental disturbances (Jägerbrand et al., 2019; Neumann et al., 2020; Turner et al., 2017). In response, policies aimed at controlling air pollution from ship emissions in international waters have been put in place by many governments, and by the International Maritime Organization (IMO). Sulphur content in fuels serves as an indicator for how “polluting” the emissions from their combustion will be (Agrawal et al., 2009; Gangwar et al., 2012; J. P. Jalkanen et al., 2012; Moldanová et al., 2009a). Thus, the IMO has mandated that from January of 2020 forward, all commercial ships must reduce their air emissions from the historical 3.5% S content (by mass) to 0.5% S in international waters.

Inside ocean areas determined to be Sulfur Emission Control Areas (SECAs) the cap is 0.1% S, and many countries, provinces, and states have established specific emission standards for their territorial seas (i.e. the ocean area that extends seaward up to 12 nautical

miles from its coastal baselines), and/or contiguous zones (i.e. area within 24 nautical miles from the coast). In certain areas, rules that control the amount of NO<sub>x</sub> released by ships have also been set through the creation of nitrogen emission control areas (NECAs). To comply with emission standards that vary greatly from region to region, ship operators have two main options: they can combust alternative fuels that emit lower amounts of sulfur and other pollutants than what is released by the use of the historically popular residual fuel known as bunker fuel or heavy fuel oil (HFO), or in some places, they can use exhaust gas cleaning systems, also known as scrubbers (Christodoulou et al., 2019; Comer et al., 2020; Kontovas, 2020).

Generally, alternative marine fuels used by most in the maritime industry consist of distillate fuels (e.g. marine gas oils or MGO, heavy gas oil or HGO, and low- or ultra-low sulfur diesel fuels or ULSD) or blends of distillate and residual fuels that vary greatly in composition but that will pass air quality enforcement, whereas scrubbers work by spraying water onto exhaust smoke before it comes out from the vessel's smokestack, which reduces the amount of pollution that is emitted into the air and permits ship operators to continue using the relatively cheap HFO. Savings have incentivized the adoption of scrubbers by the maritime industry (Kontovas, 2020; Zis et al., 2022). An estimated 50,000 merchant ships are currently operating in the world ocean (International Chamber of Shipping, 2023). Between the year 2015 and 2020, the number of ships in the international shipping fleet fitted with scrubbers increased from 243 to more than 4,300 (Osipova et al., 2021) and currently, scrubbers are used by 25% of the world merchant fleet as measured by deadweight tonnage (Marin-Enriquez et al., 2023). In international waters, and in many coastal locations around the globe, ship operators are allowed to meet air quality standards by running scrubbers.

These devices reduce air pollution but discharge untreated slurry directly into the ocean. The effects of these liquid discharges for marine phytoplankton are understudied. A few incubation experiments have been conducted to investigate the acute impacts of scrubber washwater on certain phytoplankton assemblages (Picone et al., 2023a; Ytreberg et al., 2019, 2021), but large-scale questions remain unresolved, particularly in what concerns the potential fertilization of marine phytoplankton by scrubber discharges.

Models have been used to estimate how certain byproducts of fossil fuel combustion in marine engines may be altering marine chemistry and the possible consequences of these disturbances for ocean productivity (Hamilton, Moore, et al., 2020; Ito, 2013a; Raudsepp et al., 2019b; C. Zhang et al., 2021). Ito (2013) used a global chemical transport model to investigate the effect of aerosol emissions from ship plumes on iron solubility in particles from combustion and dust sources. Based on the results, the author predicted that “air emissions from shipping in 2100 would contribute 30–60% of the soluble iron deposition over the high-latitude North Pacific and North Atlantic” and speculated on the relevance of the findings for primary production in those ocean regions. Subsequent studies aimed at describing global and regional fluxes of iron have incorporated shipping air emissions in their inventories and modeling exercises (Hamilton et al., 2020b, 2020a; Liu et al., 2022; Rathod et al., 2020). All in all, these studies, much like the ones that alert for possible toxic effects of metals in ships scrubber washwater discharges (Lunde Hermansson et al., 2021; Ytreberg et al., 2022a), are inherently limited by how incomplete the current knowledge still is regarding the variability in concentration, composition, and bioavailability of the components of interest for phytoplankton ecophysiology that are released by the

combustion of different fuels, in various engines, ship types, and variable operating conditions.

In this study, I advance knowledge in this field by combining empirical and modeling methods to quantify the importance of scrubber washwater discharges as a source of fertilizing components for marine phytoplankton in coastal and open-ocean regions. Our overarching research questions were: 1) are there differences in nitrogen and/or trace metal enrichment levels when comparing scrubber washwater produced by various small engines combusting different distilled fuels to large ship engines combusting heavy fuel oil (HFO)? And 2) does the discharge of scrubber washwater into the ocean represent a significant source of nitrogen and/or trace metals of interest for phytoplankton ecophysiology?

To answer these questions, I first present the results from chemical analyses of scrubber washwater samples produced by three small engines using open-loop scrubbers to treat exhaust gases emitted from the combustion of two types of distilled fuels (i.e. HGO and CARB diesel, which is a type of ULSF). Open-loop systems draw in seawater, spray it into the exhaust, and discharge it overboard, often without treatment. Specifically, I quantify the enrichment of seawater with dissolved inorganic nitrogen (nitrate, nitrite and ammonium) and with dissolved trace metals of major interest for phytoplankton ecophysiology (dFe, dZn, dCu, dMn, dPb, dCo, dCd, dNi), after the seawater is passed through three scrubbing systems: one “traditional” open-loop scrubber that was installed in a laboratory testbed engine to reduce the resulting air emission enough so that it is in compliance with IMO environmental quality standards, and two small fishing boats equipped with wet exhaust systems that scrub 100% of their air emissions (i.e. these boats don’t have smokestacks). I also measured

dissolved Vanadium (dV), which is used as an indicator for the distillation quality of the fuels (Barwise, 1990; Corbin et al., 2018).

I then compare the dissolved metals results obtained from the above-described chemical analyses to metal concentration values documented in the literature for scrubber washwater samples that were produced using a distilled fuel combusted in a small engine, or using residual fuels combusted in large ship engines. By applying various modeling approaches, metal concentrations, and associated rates of scrubber washwater volumes being discharged, I considered the dilution of nitrogen species and selected metals under variable oceanographic scenarios and spatial scales, from coastal estuaries shipping lanes.

This study advances our collective understanding of the environmental impacts related to the use of scrubbers by boats and ships combusting different types of fuels and operating in coastal ecosystems and international waters. Our results serve to inform those working on policies and regulations aimed at reducing pollution from the maritime sector.

## **METHODS**

### **Sampling Campaigns**

Two sampling campaigns were conducted as part of this project and are summarized in Table 1. Samples of scrubber washwater were collected at the Chalmers Marine Engine Lab at the Division for Maritime Studies, a test bed lab facility that is owned and operated by the Department of Mechanics and Maritime Sciences, Chalmers University of Technology (Gothenburg, Sweden). This sampling campaign was conducted in June of 2019 as part of a broader study about the implications of fuel sulfur content regulations and wet scrubbing



for the physical properties of exhaust particles produced from the combustion of distilled fuels. The full experimental setup used, including a detailed description of the test-bed engine and laboratory scrubber unit, were presented in (Santos et al., 2022). A schematic depiction of the experimental system that was used to produce the samples used in the present study is shown in Fig. 1.1.

Table 1.1. Summary of sampling campaigns conducted during this study.

<b>Campaign</b>	<b>Vessel Type</b>	<b>Engine</b>	<b>Fuel types, S content (by mass)</b>	<b>Washwater flow rate(s) (L per min.)</b>	<b>Location of sample collection</b>
<b>1</b>	Test-bed facility	4-stroke Volvo Penta D3-110	HGO, 1%	~1	Chalmers University test-bed facility, Gothenburg, Sweden
<b>2 A and B</b>	Two fishing boats with wet-exhaust systems	Twin 400 (Boat A) and twin 450 HP (Boat B) John Deere marine engines	CARB fuel, <0.1%	~160 (Boat A, at 5 knots) and ~250 (Boat B, at 10 knots)	Shipboard sampling within Newport Harbor, Newport Beach, CA, USA

**Sampling Campaign 1: Scrubber discharge water produced from the combustion of heavy gas oil (HGO) in a small marine engine at Chalmers University's test-bed lab facility.**

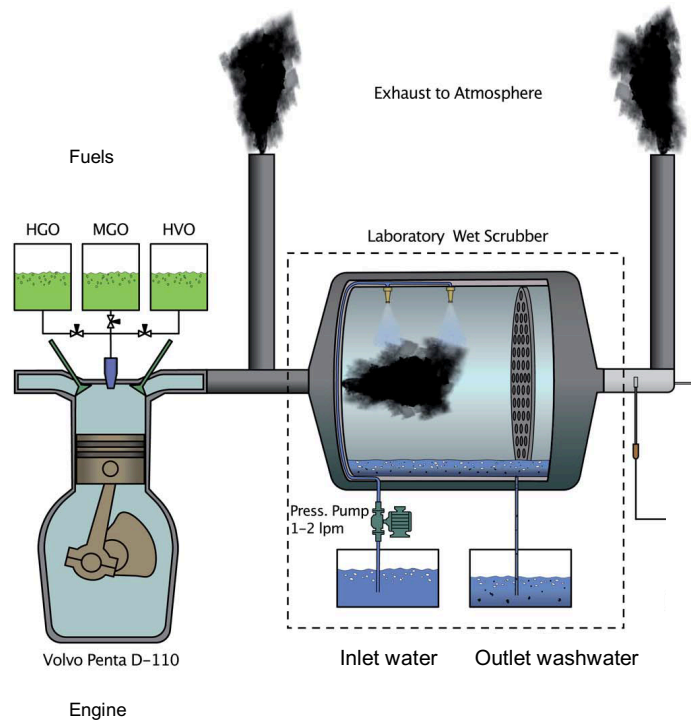


Figure 1.1.. Schematic description of the experimental setup used to produce the scrubber discharge water samples during sampling Campaign 1 of the present study (modified from Santos et al 2022). Note that in the present study only HGO fuel was used to produce scrubber washwater.

Scrubber washwater samples were produced from the combustion of a commercially available distilled fuel blend (i.e., HGO with 1 % sulfur content) using a four-stroke turbocharged Volvo Penta D3-110 marine diesel engine. The engine has five cylinders with a power of 81kW and is equipped with a common rail injection system and a hydraulic brake system that allows for experiments to be performed at different engine loads. Scrubber washwater samples collected for the present study were produced at an engine load of 30% and the discharge flow rate was of approximately 0.02 L per second. The scrubber unit is made of stainless steel and is 50 cm long and 40 cm in diameter. This is a relatively small

marine engine that would normally be found in small to medium-sized recreational motorboats. All the samples acquired during this campaign were collected at the Chalmers University testbed facility. Twelve replicates of scrubber washwater samples were taken from the scrubber system's outlet tap. Six replicate samples of seawater that was loaded into the scrubber system (inlet samples) were also collected. All samples were collected into 250 L acid-cleaned polycarbonate bottles, which were filled to that volume, sealed, frozen at -20 °C and shipped in ice from Gothenburg, Sweden to UCI/ Mackey Lab, USA, where three replicates of outlet samples and three replicates of inlet samples were randomly selected, defrosted overnight at 4 °C, and processed following the procedures described in the Chemical Analysis Section.

**Sampling Campaign 2: Scrubber discharge water sampled from wet exhaust systems of recreational fishing boats combusting CARB fuel.**

Samples of scrubber outlet washwater were collected from two recreational fishing boats (Boats A and B). Both boats were combusting a type of marine diesel oil with a maximum sulfur level of 0.1% that is approved for sale in the state of California and is commonly known as "CARB diesel", and comparable to federally approved ultralow sulfur diesel (ULSD). The use of this type of marine distillate grade fuel (i.e., ULSD marine gas oil or marine diesel oil) is required of all ships, boats, and other watercraft transiting within the State of California's contiguous zone, which extends 24 nautical miles from the coast, as mandated by the California Air Resources Board Ocean-going Vessel (OGV) Regulation of July 2008 (Fuel Sulfur and Other Operational Requirements for Ocean-Going Vessels within California Waters and 24 Nautical Miles of the California Baseline. Title 13, California Code of Regulations (CCR) §2299.2 and Title 17, CCR §93118.2., 2008).

Boat A is charter fishing boat that is 75-feet long with 22-feet of beam and is powered by twin 400 HP John Deere diesel engines. Boat A was sampled in October of 2020. Boat B is a charter boat that is 70-feet long with 20-feet of beam and powered by twin 450 HP John Deere diesel engines. Boat B was sampled in May of 2021. Both boats are equipped with wet exhaust systems that scrub 100% of their emissions (i.e., neither boat has smokestacks), an adaptation that is commonly found in recreational fishing boats because it decreases fumes and unpleasant odors inhaled by passengers on deck. Boat A was moving at approximately 5 knots inside the Newport Harbor ( $33^{\circ} 36' 7.3794''$  N,  $117^{\circ} 53' 16.3752''$  W). Boat B was cruising at approximately 10 knots in an area that was approximately 4 nautical miles away from the Newport Beach coast ( $33^{\circ} 34' 13.944''$  N,  $117^{\circ} 51' 37.5618''$  W). According to the boats' captains, both boats consume approximately the same amount of fuel on a regular basis, i.e., 1 gallon per hour per engine at 5 knots (800 rpm) and 6 gallons per hour per engine at 10 knots (1300 rpm). The wet exhaust systems in these boats discharges  $\sim 410$  L of seawater per minute when their engines are operating at full power (2100 rpm). Assuming a linear relationship between the system's seawater flow-through rate and the engines' operating power in rpm, we estimate that these boats discharge from all their exhaust outlets, approximately 2.6 L of washwater per second when sailing inside the harbor at  $\sim 5$  knots (at 800 rpm), and approximately 4.23 L of washwater per second when cruising offshore at  $\sim 10$  knots (at 1,300 rpm).

Six replicates of scrubber washwater samples were collected using an acid-cleaned plastic collection cup mounted on a long plastic handle which allowed access to the outlets that discharge scrubber washwater from the boats' wet exhaust system into the ocean (Fig. 1.2). Six replicates of ambient seawater (inlet) samples were collected near the bow of the

boats, from a position that was forward from the washwater outlets using the same trace clean metal collection, processing, and storage procedures used for outlet samples. Inlet and outlet scrubber washwater samples were immediately transferred into 1L acid cleaned polycarbonate bottles, which were sealed, stored cool during transport from the Newport Bay to UCI/ the Mackey Lab (~30 min. travel time). Three replicates of inlet and outlet SDW samples were randomly selected and immediately processed following the procedures described in the Chemical Analysis Section.



Figure 1.2. Photo of Boat A, a recreational fishing boat equipped with a wet exhaust system that scrubs 100% of all emissions produced by the boat's twin engines and discharges the scrubber washwater and byproducts from the combustion of the fuel being used (in this case, CARB diesel) continuously into the ocean through the outlet holes located on the boat's stern.

### **Analysis of Dissolved Nitrogen Components**

Samples collected during Campaigns 1 and 2 were analyzed as follows: 50 mL- aliquots were taken from each sample replicate bottle and filtered through 25 mm glass fiber filter GF/F (Whatman) using a peristaltic pump. The filtrates were collected in sterile Falcom tubes that were immediately frozen and kept at -20 °C until analysis. The combined

concentrations of nitrate ( $\text{NO}_3^-$ ) and nitrite ( $\text{NO}_2^-$ ), thereafter referred to as N+N, and ammonium ( $\text{NH}_4^+$ ) were measured on a flow injection autoanalyzer (FIA, Lachat Instruments, Zellweger Analytics, Inc., QuikChem 8500 Series 2) at the Marine Science Institute Analytical Laboratory at the University of California, Santa Barbara using standards prepared in Milli-Q water and blanks were prepared in aged, low nutrient seawater. The method minimum limit of quantification (LOQ) is the lowest concentration of an analyte that can be reliably measured and quantified with acceptable precision and accuracy. The LOQ for  $\text{NH}_4^+$  and N+ N was of  $0.20 \mu\text{M}$  for each analyte. For use in statistical tests, measurements below LOQ were treated as LOQ divided by 2.

### **Analysis of Water-soluble Dissolved Trace Metals**

For the analysis of water-soluble dissolved trace metals in samples collected during both campaigns, 30 mL aliquots of inlet and outlet samples were filtered through acid rinsed VWR  $0.2 \mu\text{m}$  PES sterile syringe filter cartridges in a laminar flow hood and stored in acid cleaned high-density polyethylene (HDPE) bottles until analysis. These aliquots were acidified using distilled HCl at sample to acid volume ratio of 1000:1 under a laminar flow hood. Acidified samples were allowed to sit for two weeks to allow labile and dissolved metals that may have been adsorbed onto the walls of the vials to be recovered.

Acidified samples were transported to a trace metal-clean room at the University of Southern California (John Lab) where they were preconcentrated using ten parallel PERIFIX resin columns and prepared according to the following steps, 1) Resin was cleaned by filling up columns twice with 3N  $\text{HNO}_3$  and conditioned using 3x 0.5 mL MilliQ water; 2) 15 mL aliquots from samples were transferred from HDPE bottles into acid cleaned VWR 15 mL

tubes; 3) Samples were analyzed in batches of 10, including two method blanks (i.e. 200  $\mu\text{L}$  of spike and buffer only); 4) Each VWR tube was spiked with 50  $\mu\text{L}$  of a multi element spike and 150  $\mu\text{L}$  of a buffer (6N ammonium acetate at pH 6, clean); 5) Contents were transferred from tubes into columns and when all the liquid had passed thru the columns, 2x 0.5 mL were used to wash away salts; 6) Samples were eluted into clean VWR tubes using 5 x 200  $\mu\text{L}$  3NHNO<sub>3</sub>. All these activities were carried out under a laminar flow hood, following the guidelines established by GEOTRACES (Cutter et al., 2017) to reduce metal contamination of samples.

The concentrations of water-soluble trace metals in preconcentrated scrubber washwater inlet and outlet samples were measured with a Thermo Element 2 ICPMS using a 100  $\mu\text{L min}^{-1}$  Teflon nebulizer, glass cyclonic spray chamber with a PC<sup>3</sup> Peltier cooled inlet system (ESI), standard Ni sampler and Ni 'H-type' skimmer cones at the Department of Earth Sciences of University of Southern California. The sensitivity and stability of the instrument was tuned to optimal conditions before analyses, which were conducted at sensitivity around  $10^6$  counts  $\text{s}^{-1}$  for 1 ppb Indium. Both the standard and samples were treated with 1 ppb In addition to correct for shifts in instrumental sensitivity and matrix. Elemental concentrations in samples were determined by their signal intensity compared to a 10 ppb multi-element standard, which was diluted from a certified standard (Santa Clarita). The method's LOQs were the following: dFe= 3.35 nM, dZn= 1.39 nM, dCu= 0.82 nM, dMn= 0.08 nM, dPb= 0.03 nM, dCo= 0.12 nM, dCd= 0.03 nM, dNi= 0.23 nM, dV= 0.34 nM. For use in statistical tests, measurements below LOQ were treated as LOQ divided by 2.

## Literature Review and Comparative Analysis for Dissolved Metals

To contextualize dissolved trace metal values, we 1) conducted a literature search to identify all previous studies that had quantified metals of interest in scrubber washwater; 2) selected data from these studies that included the concentration of metals measured in both inlet and outlet samples; 3) converted all concentration values found in the literature to a common unit (nM); 4) standardized these values by accounting for the rate of discharge associated to each scrubber system (i.e. volume of washwater being discharged by each scrubber per unit of time); 5) compared the results from the standardization (in nanomoles per second) to the results we found in the present study. Our focus was on metals (vs nitrogen) enrichment because the references we found for the chemical composition of scrubber washwater produced by real ships all reported the nitrogen enrichment as negligible.

To be included in the comparative analysis, references had to meet two criteria: a) must have measured the concentration of at least dFe, dZn, dCu and dV in samples produced from the combustion of any fuel by engines of any size and discharging scrubber washwater from open-loop systems, and b) must have measured the concentration of dissolved metals in both inlet and outlet samples. Many of the measurements included in the comparative analysis came from broad technical reports, produced by the German government to describe the chemical nature of scrubber washwater being discharged in the Baltic Sea. These reports did not have the investigation of components of interest to phytoplankton ecophysiology as their goal, and so we had to request the nitrogen and metal concentrations values mentioned in those reports from the authors.



## **Statistical analyses and model simulations**

Statistical analyses were conducted using GraphPad Prism Versions 9 and 10.1. Significant differences ( $P \leq 0.05$ ) were determined using unpaired t-tests with Welch's correction when comparing independent pairs of means (i.e., inlet vs. outlet samples for enrichment analysis) or ordinary one-way analysis of variance (ANOVA) followed and Tukey and Dunnett post-hoc test, when comparing multiple means. Values below the limit of quantification (LOQ) were substituted by  $\frac{1}{2}$  of the LOQ in all analyses and for all parameters.

To quantify the relative importance of scrubber washwater discharges from boats and ships transiting in coastal ocean areas in California as a source of nutrients for primary producers, we simulated various scenarios employing simple dilution calculations, variable mixed layer depths, and either the values of dissolved nitrogen species, and Fe (dFe) that we measured in our own chemical analyses, or that were documented by others in the literature.

## **RESULTS AND DISCUSSION**

### **Nitrogen Components**

To characterize the nitrogen enrichment of washwater by the open-loop scrubbing of exhaust gas produced by small engines combusting distilled fuels, we measured the concentrations of dissolved ammonium ( $\text{NH}_4^+$ ) and of nitrate ( $\text{NO}_3^-$ ) and nitrite ( $\text{NO}_2^-$ ), or N+N, in inlet water samples and scrubber washwater outlet samples collected during Campaigns 1 and 2 (Fig. 1.3).

Unpaired two-tailed t-tests with Welch's corrections were performed to compare  $\text{NH}_4^+$  and N+N concentrations in the three outlet samples that were generated by the

combustion of HGO in the test bed system, against three inlet samples taken from the seawater that was loaded into that scrubbing system (Campaign 1). Ammonium concentration in those outlet samples ( $M= 5.9$ ,  $SEM= 0.8 \mu\text{M}$ ) was significantly higher ( $p=0.05$ ) than in the corresponding inlet samples ( $M=2.5$ ,  $SEM= 0.1 \mu\text{M}$ ). Likewise, N+N concentration in those outlet samples ( $M= 19.7$ ,  $SEM= 0.6 \mu\text{M}$ ) was significantly higher ( $p=0.001$ ) than in inlet samples ( $M=1.2$ ,  $SEM= 0.04 \mu\text{M}$ ). The scrubbing process in the Chalmer's testbed system combusting HGO caused a significant nitrogen enrichment of the washwater that would be discharged into the ocean if this system were operated in a real vessel, with  $\text{NH}_4^+$  and N+N values becoming 2 times and 17 times higher than the original values in the inlet water samples, respectively (Fig. 1.4).

The concentration of a  $\text{NH}_4^+$  and N+N was measured in randomly selected replicates of inlet and outlet washwater samples produced by the wet exhaust systems of Boats A and B from Campaign 2 (Fig.1.3). The concentration of  $\text{NH}_4^+$  and N+ N in inlet samples for both boats were below the limit of quantification (LOQ) of  $0.20 \mu\text{M}$  for each analyte, except for one of four inlet samples collected in 2020 (Boat A), which contained  $0.21 \mu\text{M}$  N+N and one of three inlet samples collected in 2021 (Boat B), which contained  $0.34 \mu\text{M}$  of  $\text{NH}_4^+$ . These results indicate that the ambient seawater that was used to scrub emissions in the wet exhaust system of both boats was nitrogen depleted. In contrast, nitrogen values measured in all outlet samples (i.e., four replicates from Boat A and three replicates from Boat B) were between 2 and 4 times higher than the LOQ for  $\text{NH}_4^+$  and between 25 and 90 times higher than the LOQ for N+N, which indicates that nitrogen enrichment occurred due to the scrubbing process in these fishing boats' wet exhaust systems.

The results from unpaired t-tests with Welch's corrections showed that the mean value of ammonium concentrations in Boat A's outlet samples ( $M= 0.64$ ,  $SEM=0.04 \mu\text{M}$ ) was significantly higher ( $p =0.001$ ) than the mean for the corresponding inlet samples ( $M=0.10$ ,  $SEM= 0.00 \mu\text{M}$ ). Likewise, N+N concentrations in outlet samples from Boat A ( $M= 5.57$ ,  $SEM= 0.40 \mu\text{M}$ ) were significantly higher ( $p =0.001$ ) than the mean for corresponding inlet samples ( $M=0.13$ ,  $SEM= 0.03 \mu\text{M}$ ). Using the same statistical tests, the ammonium concentrations in Boat B's outlet samples ( $M= 0.59$ ,  $SEM=0.07\mu\text{M}$ ) were significantly higher ( $p =0.019$ ) than in corresponding inlet samples ( $M=0.01$ ,  $SEM= 0.00 \mu\text{M}$ ), and N+N concentrations in outlet samples from Boat B ( $M= 17.7$ ,  $SEM=0.1 \mu\text{M}$ ) were significantly higher ( $p <0.0001$ ) than in inlet samples ( $M=0.1$ ,  $SEM=0.00 \mu\text{M}$ ).

To compare the relative contribution of different small engines combusting distilled fuels as sources of dissolved inorganic nitrogen for phytoplankton in the receiving seawater where their scrubber washwater effluents would be (in the case of the testbed system) or are being discharged, we calculated the rate of discharge for  $\text{NH}_4^+$  and N+N by each vessel's scrubbing system into the ocean in micromoles per second. For this calculation, we subtracted the amount of nitrogen components measured in inlet water samples from Campaigns 1 and 2 from their corresponding outlet measurements, and then multiplied these values by the flow rates of each scrubbing unit (i.e. 0.02, 2.7, and 4.2 liters of scrubber washwater discharged per second by the Testbed system, Boat A, and Boat B, respectively). Fig. 1.4 summarizes the results, where the discharge rate for each engine and scrubbing system is presented in log-10 scale.

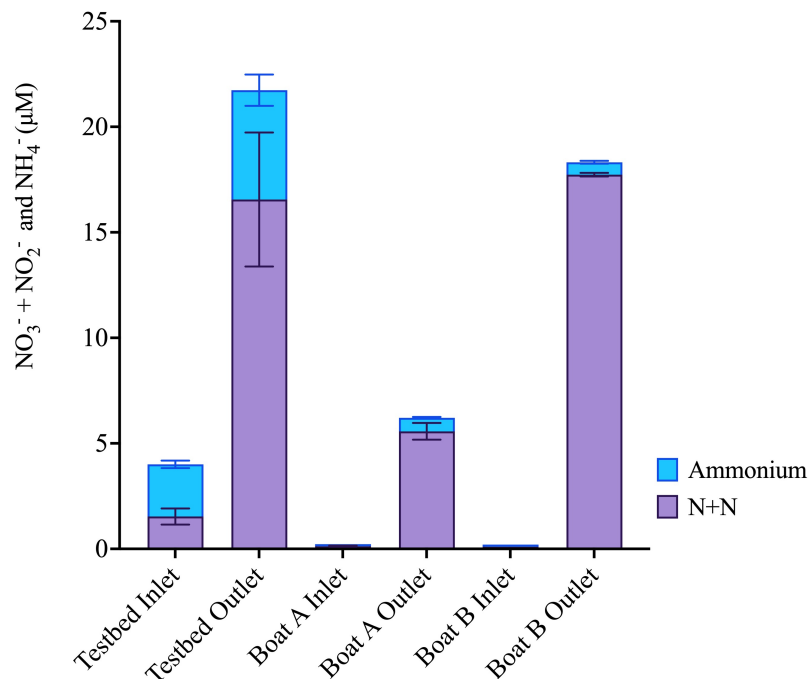


Figure 1.3. Nitrogen (ammonium and nitrate + nitrite) content in scrubber washwater produced by small engines combusting distilled fuels. Most nitrogen concentration values measured in inlet samples during Campaign 2 (i.e. Boat A and B Inlet) were below the methods' LOQ (0.2 µM). Error bars show standard error of mean.

Two independent one-way ANOVA followed by Tukey's HSD Tests for multiple comparisons tests confirmed that there were significant differences in both  $\text{NH}_4^+$  and N+N discharge rates for the three scrubbing systems included in this section of the study. The mean values for the rate of nitrogen discharge for both  $\text{NH}_4^+$  and N+N by all three vessels' scrubbing systems was significantly different for all comparisons (for  $\text{NH}_4^+$  comparisons,  $p=0.007$  for Test bed vs. Boat A,  $p < .0001$  for Test bed vs. Boat B and,  $p = .0179$  for Boat A vs Boat B; for N+ N comparisons,  $p < .0001$  for all compared pairs).

After normalizing the nitrogen discharges by the scrubbing systems' discharge rates as described above, we find that on a per hour basis, Boat B discharged ~30 times the amount

of  $\text{NH}_4^+$  that would have been discharged by the Testbed engine and its scrubbing system and  $\sim 1.5$  times the amount of  $\text{NH}_4^+$  discharged by Boat A. Using the same comparative approach, Boat B discharged  $\sim 200$  times the amount of N+N that would have been discharged by the Testbed engine and  $\sim 5$  times the amount of N+N discharged by Boat A (Fig. 1.4).

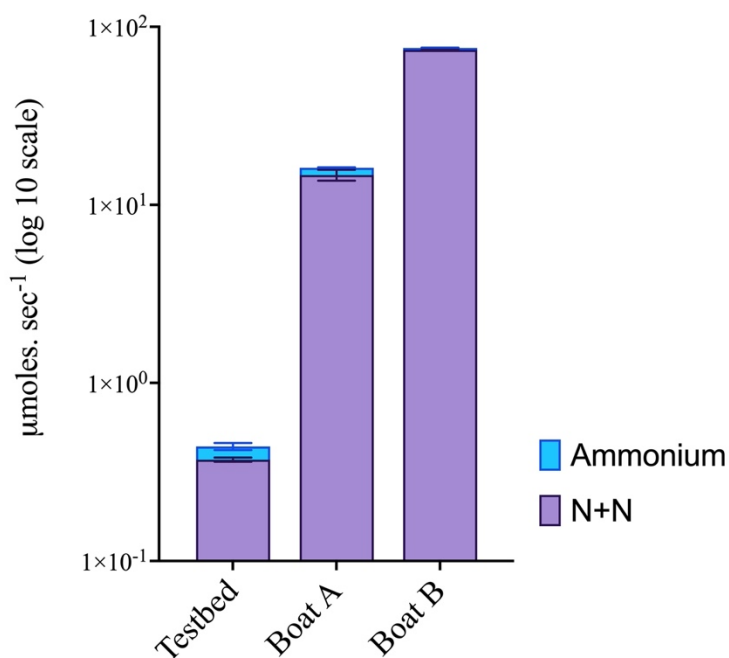


Figure 1.4. Rate of discharge of nitrogen compounds (ammonium and nitrate + nitrite) by small engines scrubbing exhaust gas from the combustion of distilled fuels in open-loop mode. Error bars show standard error of mean. Values are shown in log-10 scale.

### Dissolved Trace Metals

The concentrations of nine dissolved trace metals of interest (dFe, dZn, dCu, dMn, dPb, dCo, dCd, dNi, dV) were measured in inlet and outlet samples that were collected during Campaigns 1 and 2. All metal concentrations were found to be above the method's LOQs, except for dCo, dCd and dNi. The concentration of dCo was found to be below its LOQ of 0.12 nM in inlet samples from Boat B and from the Testbed, and dCd and dNi, were found to be

below their LOQs of 0.03 and 0.23 nM, respectively, in inlet samples from the Test Bed system.

All concentration values presented in this section refer to measurements converted into nanomolar (nM), including the difference between the means of outlet and their respective inlet samples ( $\Delta$ conc.), standard error of means (*SME*), and standard deviations (*SD*). The enrichment of trace metals due to scrubbing was determined based on a significant ( $p < 0.05$ ) and positive difference between the outlet and inlet means ( $\Delta$  conc.  $> 0$ ). A series of unpaired two-tailed t-tests with Welch's correction were conducted to assess the significance of those differences. The results from these tests are summarized in Figure 1.5 (a-c).

Our results show that the enrichment of metals occurred in all scrubber washwater outlet samples analyzed for this study, for all metals except for dPb and dV. In the case of the Testbed samples, four metals became enriched after scrubbing: dFe ( $\Delta$  conc.= 271.0 nM,  $p= 0.005$ ), dMn ( $\Delta$  conc.= 5.0 nM,  $p= 0.015$ ), dCo ( $\Delta$  conc.= 0.6 nM,  $p= 0.018$ ), dNi ( $\Delta$  conc.= 35.6 nM,  $p= 0.011$ ) (Figure 1.5 a).

In the case of Boat A samples, three dissolved trace metals were enriched due to scrubbing: dZn ( $\Delta$  conc.= 80.7 nM,  $p=0.001$ ), dCo ( $\Delta$  conc.=0.2 nM,  $p=0.001$ ), and dNi ( $\Delta$  conc.= 1.6 nM,  $p<0.001$ ) and the mean concentration for dCd significantly decreased ( $\Delta$  conc.= -0.2 nM,  $p=0.006$ ) in the outlet sample from Boat A compared to the corresponding inlet mean (Figure 1.5 b).

In the case of Boat B samples, seven metals were enriched: dFe ( $\Delta$  conc.= 11.6 nM,  $p=0.005$ ), dZn ( $\Delta$  conc.= 113.4 nM,  $p= 0.004$ ), dCu ( $\Delta$  conc.= 33.1 nM,  $p<0.001$ ), dMn ( $\Delta$  conc.=

16.8 nM,  $p=0.001$ ), dCo ( $\Delta$  conc.= 0.3 nM,  $p=0.003$ ), dCd ( $\Delta$  conc.= 0.19 nM,  $p< 0.0001$ ), dNi ( $\Delta$  conc.= 2.1 nM,  $p<0.0001$ ) (Figure 1.5 c). The mean concentration of dPb significantly decreased ( $\Delta$  conc.= -1.0 nM,  $p= 0.001$ ) in the outlet samples from Boat B compared to that boat's inlet mean.

Comparing the enrichment of various metals across the three engines and scrubbers' combos included in this study, we find that the largest enrichment of dFe happened in the outlet samples from the Testbed engine with partial scrubbing, which contained, on average, ~32 times more dFe than the corresponding inlet samples, while dFe in Boat B outlet samples were on average 3.4 times higher than the corresponding inlet samples. There was no enrichment of dFe in Boat A samples. Enrichment of dZn did not occur in Test Bed samples, and was somewhat similar for Boats A and B, with concentrations in outlet samples being ~1.5 and 1.8 times higher than in inlet samples, respectively. Enrichment of dCu was only observed in outlet samples from Boat B (~2 times that of inlet values), and dMn enrichment was observed in outlet samples from the Testbed and from Boat B (7 and 6 times that of inlet values, respectively). Enrichment of dCo occurred in outlet samples from all three engine and scrubber systems, with an approximate increase in concentration of 11.0, 1.2, and 5.8 times that of the inlet sample means for Testbed, Boat A and Boat B, respectively. Enrichment of dCd occurred only in Boat B (~4.5 times greater in outlet vs inlet samples) and the enrichment of dNi was observed in all systems, with an increase of 56.7, 1.3, and 1.5 times in outlet sample means, compared to inlet sample means of Testbed, Boat A and Boat B, respectively.

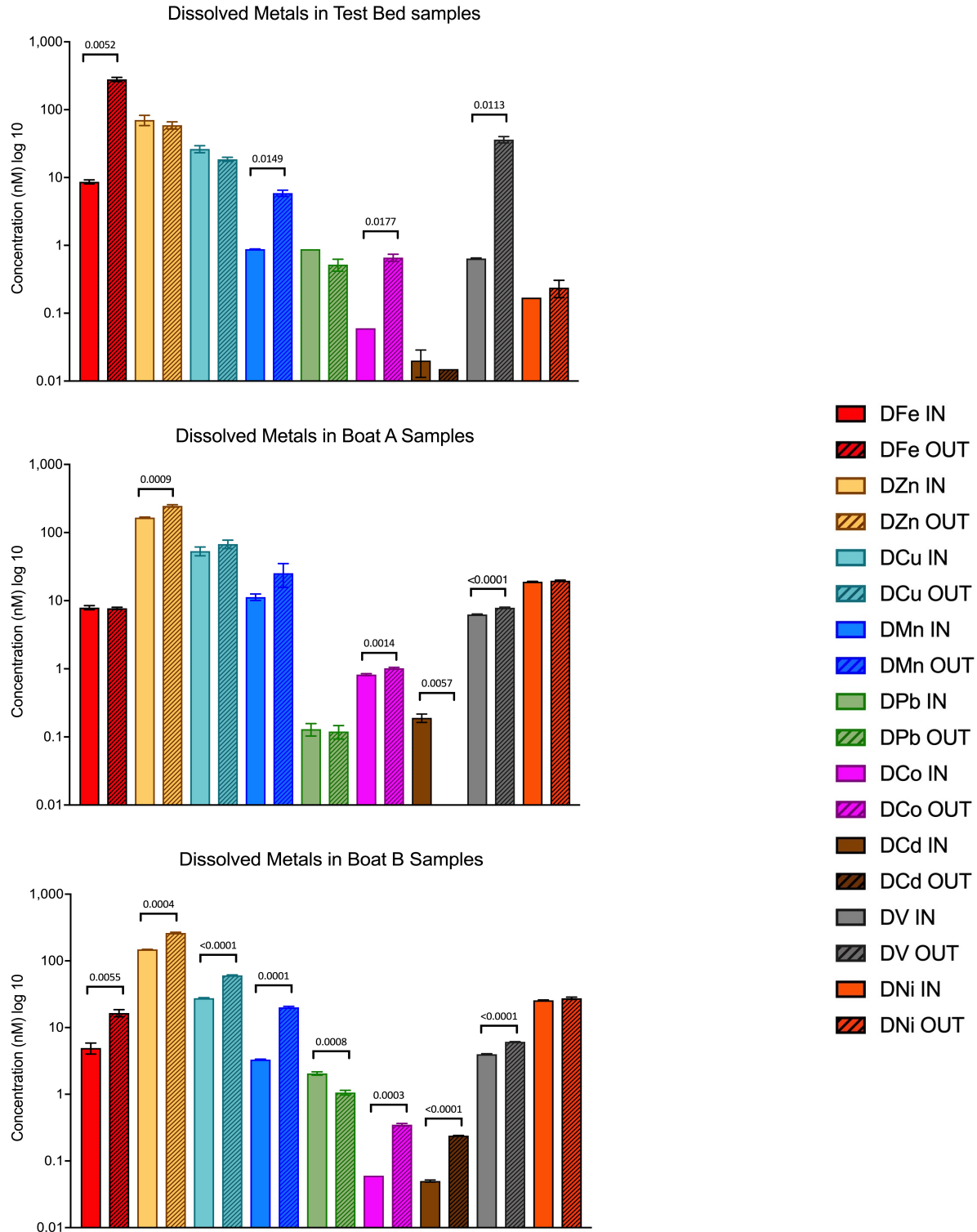


Figure 1.5 a-c. Concentration of dissolved metals in inlet and outlet samples from scrubbers in small engines combusting distilled fuels (in nM and plotted on a log<sub>10</sub> scale). Error bars show standard error and numbers above brackets show p values for significant differences between inlet and outlet values calculated by unpaired t-tests with Welch's correction.



Overall, metal enrichment in the small engines combusting distilled fuels included in this study ranged from 11.6 to 271.0 nM for dFe, 90.7 to 113.4 nM for dZn, 0-33.14 nM for dCu, 5.0 to 16.6 nM for dMn, 0 for dPb, 0.2 to 0.6 nM for dCo, 0 to 0.19 for dCd, 1.6 to 35.6 nM for dNi, and 0 nM for dV.

### **Literature Review and Comparative Analysis for Dissolved Metals**

To the best of our knowledge, only four publicly available studies have quantified the suite of dissolved metals identified here as of interest to phytoplankton ecology in scrubber washwater samples: Ytreberg et al, 2019, Schmolke et al, 2020, The ImpEx report by Marin-Enriquez et al, 2023, and the EMERGE report by Petrovic et al. 2023 (which include the values reported by Picone et al 2023). A summary of relevant aspects of each of these studies is presented in Table 2. Note that four out of the twelve entries reported in the references that were found during this literature review measured the concentration of metals in one single inlet sample and one outlet sample collected (rather than in replicates).

Nitrogen enrichment was reported as being negligible in all three references that investigated scrubbing by large ships using HFO. For that reason, we focus our comparative analysis on metal enrichment, with a special emphasis on dFe. It is important to notice, however, that the nitrogen measurements presented in those reports were conducted for the purpose of evaluating the risk of eutrophication from scrubber wash water discharges, and thus measured with methods with high LOQs (>0.8 mg/ L for nitrate). If one wants to quantify and model the potential role that scrubber washwater discharges may play as a source of N for marine phytoplankton, they should conduct measurements using LOQs in the micromolar ( $\mu\text{M}$ ) range.

Table 1.2. Summary of relevant aspects from literature review. SW= scrubber wash water. NA= not available. Dissolved iron (dFe) values from literature review used as model inputs. Asterisk indicates the ship with the highest dFe discharge rate, which was used to simulate the “maximum dFe discharge rate scenario”. All dFe discharge rate values from large ships were used to calculate the “average dFe discharge rate scenario.”

Reference	Ship Types	Fuel Type and Sulphur Content (m/m)	Engine Load (%)	# of samples (inlet, outlet)	Used in comparative analysis?	~DFe OUT-IN (nM)
This study	Sm. engine	HGO, 1%	30	3 and 3	Yes	280
	Sm. Boat A	CARB diesel, 0.1%	NA	3 and 3	Yes	9
	Sm boat B	CARB diesel, 0.1%	NA	3 and 3	Yes	17
Ytreberg et al, 2019	Sm. engine test bed)	MGO, 1.0%	30	1 and 1	Yes	1,593
Marin et al, 2023	Ferry RoPax (S1)	HFO, 2.1%	75	0 and 1	No	NA
	Ferry RoPax (S2)	HFO, 2.1%	86	1 and 1	Yes	14,916
	Vehicles carrier (S3)*	HFO, 3.2%	63	1 and 1	Yes	1,116
	Cruise ship (S4)	HFO, 2.2%	79	1 and 1	Yes	2,504
Schmolke et al, 2019	Vehicles carrier (S1)	HFO, 3.2%	84	2 and 2	Yes	319
	Cruise ship (S2)	HFO, 2.5%	58	2 and 2	Yes	496
	Cruise ship (S3)	HFO, 2.7%	74	2 and 2	Yes	734
	Cruise ship (S4)	HFO, 0.7%	78	2 and 2	Yes	173
	RoRo (S5_1)	HFO, 2.0%	53	2 and 2	Yes	860
	RoRo (S5_2)	HFO, 2.0%	60	2 and 2	Yes	478
Petrovic et al, 2023	Container ship	HFO, 2.4%	50	2 and 2	Yes	1,970

## Discharge rates for selected dissolved metals

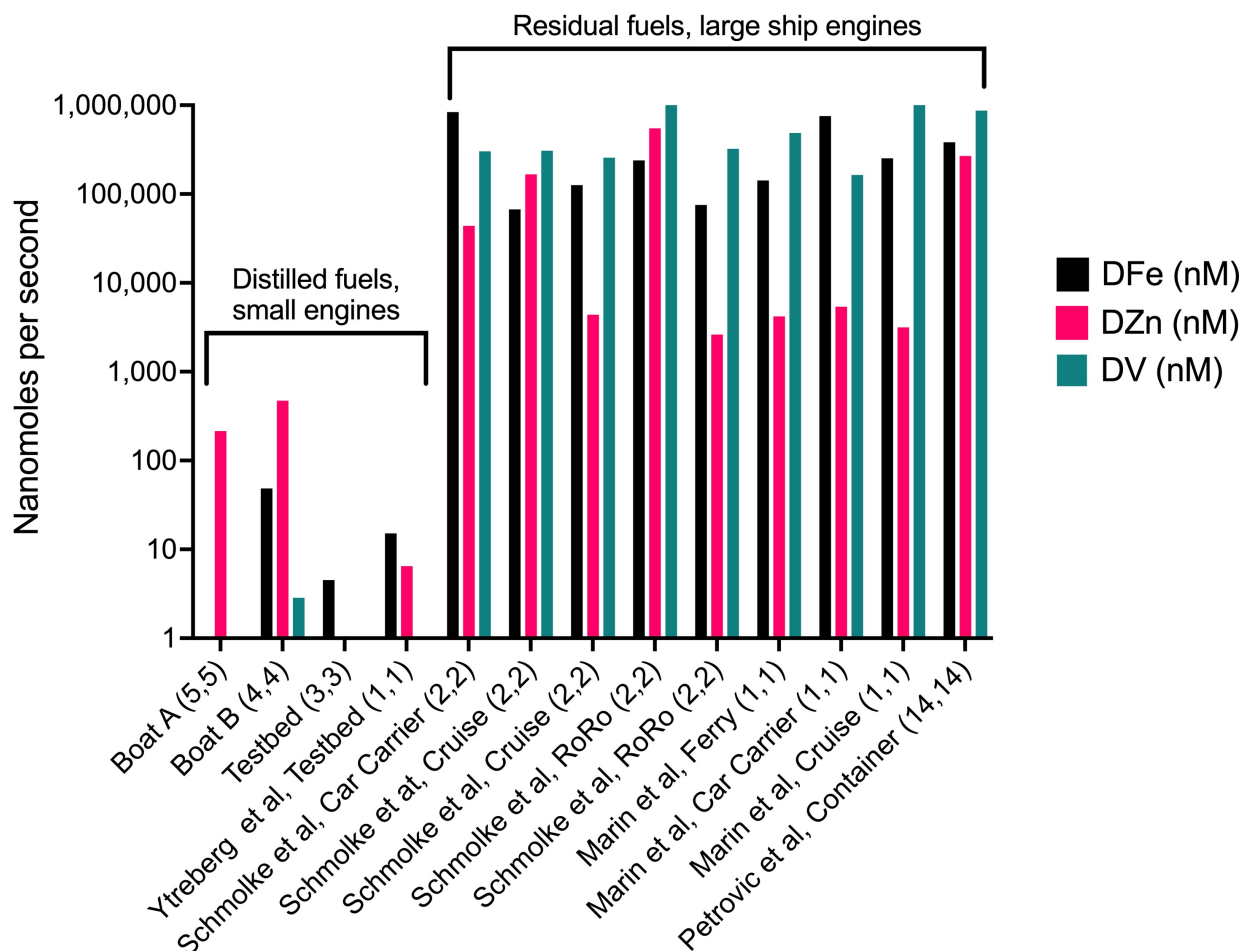


Figure 1.6. Net amounts of selected metals discharged by all open-loop engine and scrubber systems that were included in the comparative analysis. Values shown in these graphs (nanomoles. s<sup>-1</sup>) result from the standardization of net concentration values (i.e., nM in outlet samples minus nM in inlet samples) by their respective scrubber system's washwater discharge rates (L. s<sup>-1</sup>). The number of inlet and outlet samples that were available per engine and scrubber system is shown in parentheses.

The comparison of metal enrichment across various ship types combusting HFO against small engines shows that the concentration of metals varies greatly for all metals. Looking at dFe enrichment from scrubbing in particular (Table 2), we see that it ranged from <10 nM in one of the small boats combusting CARB diesel to ~15,000 nM in the vehicles carrier (Marin S3). Once we consider the discharge rates from each ship (Fig. 1.6), we notice

that the contribution of metals dFe, dZn, dV from scrubber washwater discharges from ships considerably outweighs those from small vessels, and varies greatly within that latter group, ranging from  $6.7 \times 10^4$  to  $8.4 \times 10^5$  nanomoles per sec. for dFe,  $7 \times 10^4$  to  $8 \times 10^5$ ,  $3 \times 10^3$  to  $6 \times 10^5$  for dZ, 41 to  $6 \times 10^4$  for dCu and  $2 \times 10^5$  to  $2 \times 10^6$  nanomoles per second.

### **Simulations of post-discharge dilution of nitrogen and dissolved iron (dFe) in wet exhaust from Boats A and B**

Boats A and B are similar in size, engine type, age, maintenance, and were combusting the same type of fuel. Therefore, we posit that the differences observed between N enrichment in wash water from Boat B vs Boat A were caused mainly by the higher engine load that Boat B was operating at (i.e. 1,300 rpm at 10 knots) as compared to Boat A (800 rpm at 5 knots). That consistent with observations in the literature regarding the production of NO<sub>x</sub>, which is directly proportional to combustion temperature, which is a function of engine load (Cooper & Andreasson, 1999; Hebbar, 2014).

Our results for the rate of nitrogen discharges from engines and scrubbers in Campaigns 1 and 2 (Fig. 1.4) allow us to assess the likely range of concentrations that phytoplankton organisms would experience after scrubber washwater and wet exhaust washwater is discharged and diluted in the receiving seawater parcel underneath the boat or ship's path. For example, taking the results obtained from the analysis of nitrogen enrichment in samples from Boats A and B, we can estimate the maximum plausible N+N input into the coastal waters of Southern California from the combustion of CARB diesel in small boats equipped with wet exhaust systems. To be clear, the state of California prohibits the discharge of scrubber water from vessels combusting fuels with sulfur content > 0.1 %

within its contiguous zone (24 NM from the shore), but allows the use of wet exhaust systems in combination with distilled fuels to reduce fumes and odors on deck, such as the systems installed in Boats A and B. Here, we consider two scenarios that simulate the typical dilution conditions associated with the discharge of wet exhaust washwater from these boats.

In the first scenario, we look at what happens to the dissolved inorganic nitrogen and dFe concentrations when wet exhaust washwater is discharged by Boat A as it moves inside the shallow and semi-enclosed waters of the Newport Bay harbor at 5 knots. In the second scenario, we look at the fate of dissolved inorganic nitrogen and dFe when washwater is discharged by Boat B as it cruises near the coast, in a region known as the Southern California Bight.

**Scenario 1A: Small boats with wet exhaust systems travelling at low speed and discharging washwater inside a semi-enclosed body of water (Newport Harbor, CA, USA).**

The Newport Harbor is a 4 km<sup>2</sup> recreational harbor located in Southern California, USA (33° 36' 7.3794" N, 117° 53' 16.3752" W). If we include the Upper Newport Bay area, which is connected to the harbor, the total area is ~6 km<sup>2</sup> (Fig. 1.7). Once the land areas of the two islands located inside of the Newport Harbor (Balboa and Lido Islands, which are ~0.5 km<sup>2</sup> each) are subtracted from the harbor's total area, we find that the harbor's surface water area is ~5 km<sup>2</sup>. According to the city of Newport Beach, the approximate depth in the center of the channel is 20 feet, while the controlling depth on the outside of the channel is approximately 8 feet (Newportbeachca.gov, 2023). For simplicity, we can assume here that this harbor's depth is uniform and that it is equivalent to the average between the typical depth at the center and the depth outside of the channel or (20 ft+8 ft)/2, which equals to 14 ft or ~4 m. Using this approach, the volume of seawater in this harbor would be

approximately 20,000 m<sup>3</sup>. As shown in Fig. 1.4, on a per hour basis, a boat with a wet exhaust system such as Boat A, which was sampled while moving inside of the Newport Harbor at 5 knots, would be discharging 5.0x10<sup>4</sup> μmoles of N+N per hour. In this case, considering that this amount of nitrogen is being discharged into ~2x 10<sup>7</sup> L, that would mean an addition of ~2.6x10<sup>-3</sup> μM of dissolved inorganic nitrogen per boat, per hour. For context, if 10 boats of similar size, engine, and wet exhaust system as those of Boat A are cruising at the maximum allowed speed of 5 knots inside the Newport Harbor at all hours of daylight (e.g. 12 hours, between 6 am and 6 pm), which could be plausible, particularly in the summer, the discharge of emissions from these boats could add up to ~0.3 μM of N+N per day into these waters, a value that could represent a significant input of nitrogen into this semi-enclosed ecosystem in which the concentration of N+N is normally low (<4 μM of NO<sub>3</sub><sup>-</sup>) during most of the year, except after rainfall events, which usually occur in winters and cause nitrogen pulses in this system (Fong et al., 2021). It is important to highlight that this concentration would likely be somewhat abated by the influence of tidal flushing, which the Newport Harbor experiences twice a day.

Our results from trace metal measurements in Boat A samples (Fig. 1.5b) indicate that these boats will not be releasing significant amounts of dFe or other metals of interest when operating at low speed (i.e., at low engine load, low combustion temperature, and low washwater discharge rate).

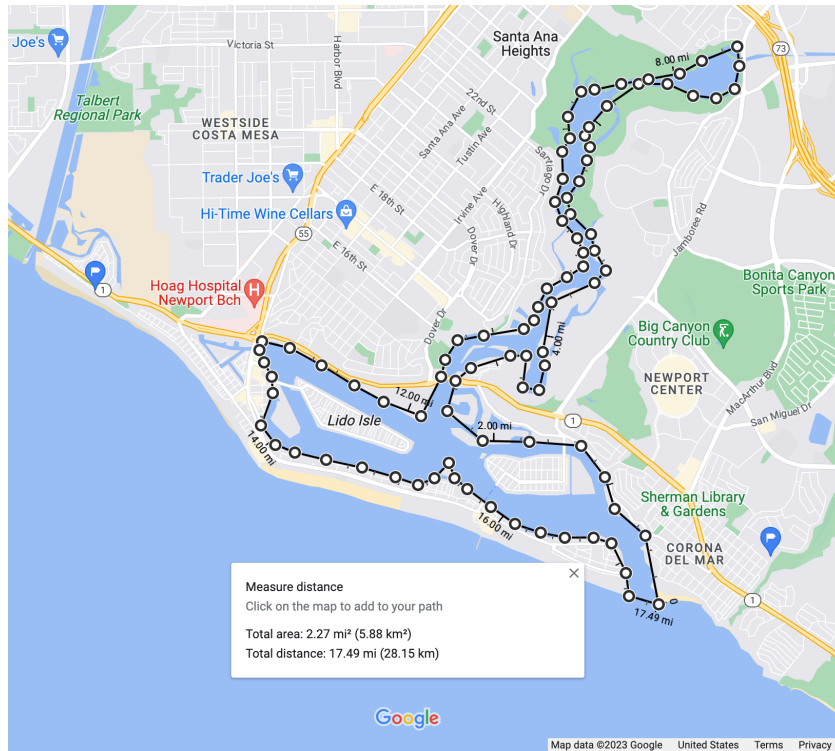


Figure 1.7. Map of the Newport Bay Harbor (California, USA), depicting its total area, which includes two islands: Balboa Island, and Lido Isle. Image and area calculation from Google Maps.

**Scenario 1B: Small boats with wet exhaust systems travelling at cruising speed and discharging along a boat lane in the Southern California Bight, CA, USA.**

In the second scenario, we consider the concentration of dissolved inorganic nitrogen that the phytoplankton community would experience due to nitrogen enrichment from wet exhaust scrubbing in a water parcel underneath the path of a boat like Boat B. Fig. 1.8 shows the schematic description of this scenario, in which the width of the discharge plume into the water is assumed to be the width of the boat’s beam, and the speed of the boat is used to estimate the length of the water parcel. Boat B has a beam of 6.7 m and was sampled while cruising at 10 knots ( $\sim 5$  m/s), which gives us a surface area for this boat lane of

approximately  $33.5 \text{ m}^2$  (per second). This scenario assumes that there is no horizontal mixing.

According to results, Boat B discharges  $\sim 74 \text{ } \mu\text{moles}$  of N+N per second. That means that the post-discharge concentration would be  $\sim 2.2 \times 10^{-3} \text{ } \mu\text{M}$  if all the dissolved inorganic nitrogen that was being discharged by Boat B remained completely entrained in the first 1 meter of depth (i.e.  $\sim 3.3 \times 10^4 \text{ L}$ ), and one order of magnitude lower if that nitrogen were to be entrapped in the top 10 meters. If, instead, we assume that mixing occurs all the way down to 50 m, the resulting concentration from the discharge of dissolved inorganic nitrogen from a boat like Boat B into water parcels underneath its “boat lane” would be of approximately  $4.4 \times 10^{-5} \text{ } \mu\text{M}$ , which is very small concentration compared to typical dissolved inorganic concentration in waters of the Southern California Bight (McLaughlin et al., 2021).

The same calculation can be used to estimate the concentration of dFe caused by the discharge of wet exhaust by Boat B near the coast. According to our estimate, Boat B discharges  $\sim 50 \text{ nM}$  of dFe per second. That means that the post-discharge concentration would be  $\sim 1.5 \times 10^{-3} \text{ nM}$  if all the dFe that was being discharged by Boat B remained completely entrained in the first 1 meter of depth, or  $\sim 3.0 \times 10^{-5} \text{ nM}$  if mixed down to 50 m. Dissolved iron concentrations in the southern California Current System range from  $<0.5 \text{ nM}$  to  $8 \text{ nM}$  during coastal upwelling (King & Barbeau, 2011). Thus, our results suggest that the relevance of dFe added by an individual boat like Boat B is minimal.



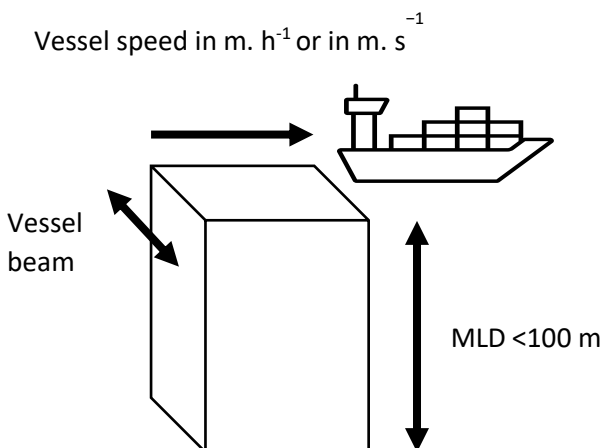


Figure 1.8. Schematics depicting the basic assumptions used to compose scenarios that simulate the range of DIN and trace metal concentrations that marine phytoplankton in a hypothetical water parcel would experience after scrubber washwater is discharged and diluted in the receiving seawater. MLD = mixed layer depth.

### **Simulations of post-discharge dilution of dissolved iron by ships scrubbing HFO emissions (from literature review and comparative analysis)**

The results from our comparative analysis (Fig. 1.6) allow us to assess the likely range of trace metals concentrations that the phytoplankton in a water parcel would be exposed to after scrubber water is discharged into the ocean by large ships combusting residual fuels and operating open-loop scrubbers. Here, we use the results obtained from the comparison of the net discharge rates for dFe for various ships and scrubbers to simulate several scenarios.

#### **Scenario 2A: Maximum net discharge rate of dFe in inventory from literature review**

First, we estimate what the resulting concentration of dFe in a hypothetical shipping lane would be if the ship with the highest net discharge rate in our inventory (car carrier ship sampled by Marin- Enriquez et al 2023, S3 in their report) were to discharge scrubber washwater from its open-loop scrubber at the concentration and discharge rate reported by those authors (~15,000 nM and 50 L/ sec, respectively). For that, we would assume that the

ship's beam is approximately 50 m wide, and that this ship is moving at the slowest end of the usual speed for ships in cruising mode (i.e., ~8 knots or 4 m/s). We also assume no horizontal mixing.

These assumptions establish the volume of the water column in the water parcel underneath the shipping lane over which this ship would be cruising, as shown in Fig. 1.8 and would compose the "Maximum dFe discharge rate" scenario. In this scenario (orange line in Fig. 1.9), phytoplankton in the first meter of seawater would be experiencing a resulting enrichment of ~4.0 nM, if all the dFe being discharged remained entrapped in the top 1 m layer of water. However, we expect that the dFe will get thoroughly mixed to at least the depth of the ship's draft (i.e., vertical distance between the waterline and the bottom of the hull), which usually ranges from 10- 15 m. This in line with what authors have found from *in situ* observations of turbulent ship wakes and their spatiotemporal extent in busy shipping lanes in the Baltic Sea. Using a bottom-mounted acoustic Doppler current profiler (ADCP) that was placed at 32 m depth below the shipping lane outside Gothenburg harbor these researchers documented a median wake depth of 13 m and several occasions of wakes reaching depths >18m (Nylund et al., 2021). The post-discharge concentration of dFe added by the scrubber water drops to 0.4 nM when considering the dilution within the first 10 m of the mixed layer. That decline in concentration continues such that at 50 m, that value is approximately 0.08 nM and by 100m, it is equal to 0.04 nM (Fig. 1.9).

### **Scenario 2B: Average net discharge rate of dFe in inventory**

We repeated these calculations using the averaged values for net dFe concentration measured in open-loop scrubber wash water samples (~2,300 nM) and the average flow rate

of discharge (~200 L/ sec) for all large ships and scrubber units included in our comparative analysis (Fig. 1.6, Table 1.2) and assumed that these ships would be travelling at the average speed for ships cruising in high seas of 20 knots, or ~10 m/s (blue line in Fig. 1.9). In this “Average DFe discharge rate” scenario, the post-discharge concentration of dFe added by the scrubber water would be ~ 0.9 nM if all dFe remained entrapped in the top 1 m layer, ~0.1 nM if dFe remained entrapped in the top 10 m layer and ~ 0.02 nM if we assume mixing down to 50m.

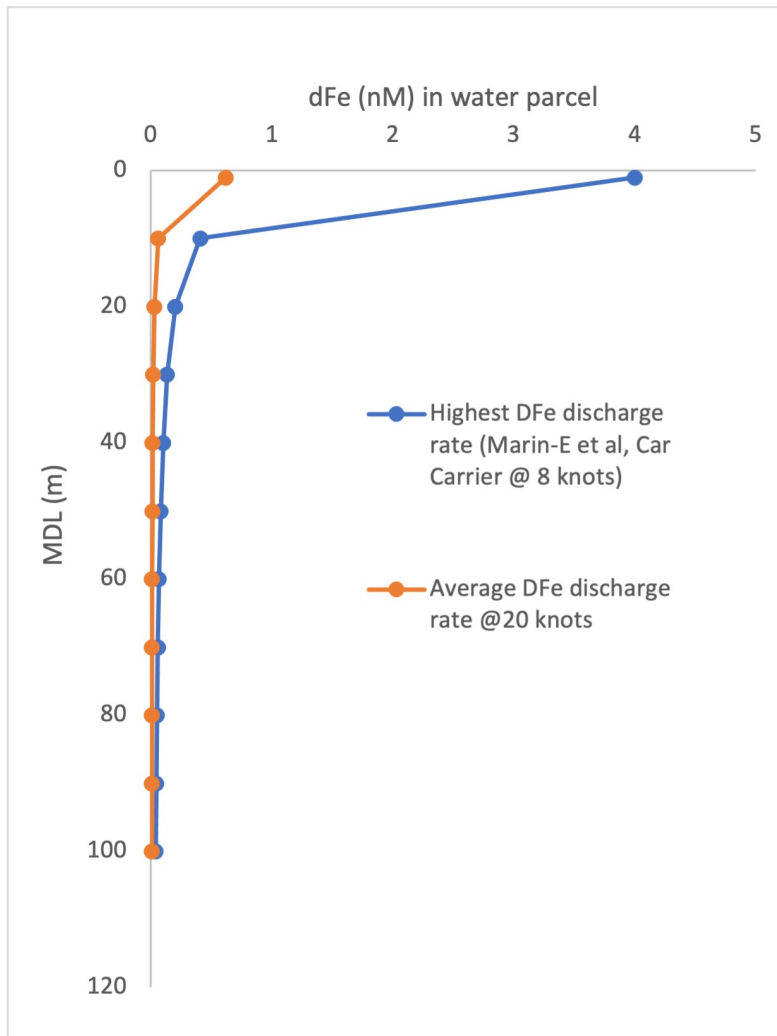


Figure 1.9. Simulated post-dilution dFe concentration in open-ocean seawater receiving scrubber water discharges. MLD= mixed layer depth

The calculations from both maximum and average net discharge rate of dFe in inventory scenarios suggest that in high seas, where vertical mixing is expected to reach down to 50-100 m, the amount of dFe added by open-loop scrubber water discharged by an individual vessel is small compared to other sources, such as wind-driven desert dust deposition (T. D. Jickells et al., 2005; N. Mahowald et al., 2014; N. M. Mahowald et al., 2010). However, in highly stratified, semi-enclosed areas of intensive ship traffic, such as the Baltic Sea, where there is approximately one ship passage every 10 min (Nylund et al., 2021), accumulation of metals from scrubber washwater discharges water could occur. The relative importance of those discharges to the phytoplankton in these various systems would need to be assessed on a region-by-region and season-by-season basis and would need to take into consideration many factors including the system's flushing times, bathymetry, oceanographic conditions, and other natural and anthropogenic sources that bring dissolved metals into those coastal areas.

Bioavailable iron is a requirement for many physiological processes in primary production thus limiting marine phytoplankton growth in much of the world ocean, including oligotrophic gyres and high-nutrient low-chlorophyll (HNLC) areas (Boyd et al., 2007; Coale, 2004; Geider & La Roche, 1994; Martin, 1992; Martin et al., 1991). In other ocean areas, iron may co-limit primary production (Browning & Moore, 2023; Mills et al., 2004a, 2004b; J. K. Moore et al., 2002; Pausch et al., 2019; Saito et al., 2008). Our results suggest that primary production in areas that experience high ship traffic and that are prone to iron limitation or co-limitation, such as in busy shipping lanes that go over HNLC areas or

oligotrophic gyres, could be influenced by scrubber water discharge, particularly during summer, when the water column is more stratified.

Subtropical gyres are known for their oligotrophic nature, where limited input of “new nutrients” can constrain phytoplankton growth. In those gyres, primary production per unit of surface is relatively low, but their massive size makes their total contribution to ocean productivity significant (Jackson, 1980; Jena et al., 2012, 2013; Jones et al., 1996; C. M. Moore et al., 2008; Morel et al., 2010; Regaudie-de-Gioux et al., 2019; Signorini et al., 2015). An important component of the productivity in subtropical gyres is nitrogen fixation by diazotrophs. Diazotrophs are bacteria and archaea capable of fixing atmospheric nitrogen into biologically useful forms, such as ammonia. Several factors contribute to the limitation of diazotrophs in subtropical gyres, including bioavailable iron. Iron serves as a critical cofactor in the structure of nitrogenase, the enzyme responsible for nitrogen fixation in diazotrophs, facilitating the electron transfer reactions essential for the conversion of atmospheric nitrogen into biologically usable forms (Moisander et al., 2012; Ratten et al., 2015; Shiozaki et al., 2014). More modeling studies should be conducted to examine impacts from scrubber washwater discharges to net primary production, nitrogen fixation, community composition, patterns of nutrient limitation and of particulate organic carbon export near subtropical gyres.

Furthermore, it is important to acknowledge the great variability in composition and abundance of metals measured in the twelve scrubber water samples that have been analyzed for dissolved metal content to date (Table 1.2 and Fig. 1.6). In the case of dFe, the enrichment and rate of discharge varied greatly: from zero in the sample from Boat A

combusting a distilled fuel (this study), to  $\sim 8 \times 10^5$  nM per second in the sample from a car carrier combusting a residual fuel (Marine-Enriquez, et al 2019). Even when considering only the large ships combusting HFO, the variability in dFe is still remarkable: the maximum dFe rate of discharge from that car carrier was almost double the average dFe rate of discharge. While this variability matters little on an individual ship basis, it likely becomes important when considering fleet-wide aggregate impacts.

Very little is known about the origins, relative concentrations, physical characteristics, chemical transformations, and solubility of trace metals discharged into the ocean as scrubber water or deposited over the ocean in aerosols emitted by marine engines. The concentration of some metal contaminants found in ship emissions, namely vanadium (V) and nickel (Ni), are believed to be related to the quality of the fuel being combusted. These metals are found in higher concentration in emissions from residual fuels, in lower concentration in emission from blends, and are virtually absent in emissions from distilled fuels (Agrawal et al., 2008; Corbin et al., 2018; Streibel et al., 2017; Tao et al., 2013). The origins of other metals found in emissions produced by marine engines are more difficult to determine. That is particularly true in the case of metals of interest to phytoplankton physiology, which seem to come from various concurrent sources and have not been quantified in emissions as often as other metals have (Lunde Hermansson et al., 2021). Some authors posit that at least a fraction of these metals of interest to phytoplankton physiology that are found in marine engine emissions originate from the pyrolysis of lubricants that seep into the combustion chamber (Eichler et al., 2017; Winnes et al., 2020) or from engine wear (M. Anderson, Salo, & Fridell, 2015; Stone, 2012), while the use of sacrificial anodes, corrosion of various parts of the vessels and fuel additives may also contribute to some metal

contaminants being produced by marine engines and released into the air, as aerosols or directly into the ocean as scrubber water discharge (Jang & Choi, 2016; Ntziachristos et al., 2016).

In summary, scrubbing of emissions produced by small and large engines combusting distilled and refined fuels enriched seawater with nitrogen and metals of interest to phytoplankton ecophysiology. The enrichment of metals measured in scrubber samples from small engines combusting distilled fuels was significantly smaller than what was documented in the literature for scrubber water samples produced from the scrubbing of emissions by large ship engines combusting residual fuels. Once the rates of scrubber water volume discharged by each scrubbing system and the post-discharge dilution are considered, it becomes evident that the input of potentially fertilizing components such as nitrogen and metals from scrubber water discharges in most coastal and open-ocean areas is small compared to typical nutrient levels determined by other sources, such as upwelling, turbulent mixing, land runoff, and atmospheric deposition. Exceptions may occur in coastal estuaries, harbors, and semi-enclosed areas in which heavy ship traffic occurs and scrubber water discharges are permitted. Phytoplankton in those areas may experience cumulative concentrations of nitrogen and metals which may be particularly high in summer, due to stratification and associated shoaling of the MLD.

Other metals that were found in scrubber washwater samples, such as Zn, Mn, Co could also cause fertilization in areas of nitrogen and metal colimitation (Browning & Moore, 2023; C. M. Moore et al., 2013b), but we didn't simulate that, nor the possible toxic effects of Cu, Pb and V, and more research is needed. Increased upper ocean stratification due to climate change may amplify the regional relevance of scrubber washwater discharges as a

source of nutrients to marine phytoplankton in tropical and subtropical gyres, where this effect seems to be more pronounced (Li et al., 2020; Roch et al., 2023; Sallée et al., 2021; Yamaguchi & Suga, 2019).

The maritime industry plays a central role in global trade, as well as in local economies as a means of transportation, recreation, and as a part of fishing and other operations aimed at utilizing ocean resources. Many projections indicate the continued and exponential growth of the sector around the world in the next decade (Müller-Casseres et al., 2021; Noble, 2019; Sardain et al., 2019). Ships and boats are also responsible for a considerable amount of pollution globally experienced by people and marine life along coastlines (Corbett, 2003; Jonson et al., 2020; Tsimplis, 2020; Viana et al., 2020; X. Wang et al., 2019), and there is mounting pressure for the maritime industry to improve the sustainability of their operations by addressing pollution issues, and by transitioning to lower greenhouse gas emissions to meet climate targets (Oloruntobi et al., 2023; Simon Bullock & Larkin, 2022; Walker et al., 2019). As several authors have pointed out (Chu Van et al., 2019; Comer et al., 2020; Lunde Hermansson et al., 2021; Osipova et al., 2021), scrubbers represent an obstacle to these goals – a sidestep that is being used by ship operators to meet current air quality standards while still combusting relatively cheap residual fossil fuels that emit greenhouse gasses and that can alter marine ecosystems. It is also necessary to highlight that other studies investigated the negative effects of scrubber water discharges to marine life and ecosystems (Lunde Hermansson et al., 2021; B. H. Othman et al., 2018; Picone et al., 2023b; Thor et al., 2021), and some found high levels of contaminants that we did not set out to measure in the present study, such as PAHs. The toxic



effects from these scrubber water components for marine microbes should be further investigated.

## **CONCLUSIONS**

The goals of this study were 1) to elucidate any differences in nitrogen and/or trace metal enrichment levels when comparing scrubber washwater produced by various small engines combusting different distilled fuels to large ship engines combusting heavy fuel oil (HFO), and 2) determine if the discharge of scrubber washwater into the ocean represent a significant source of nitrogen and/or trace metals of interest for phytoplankton ecophysiology. We found that scrubber water produced with residual fuels in large ship engines contained more metals than scrubber water produced from the combustion of distillates in small engines. The reasons for that discrepancy remain obscure, but may be related to combustion temperature, and other factors, and not solely to the chemical composition of the original fuel. The type and concentration of trace metals in scrubber washwater varied across engine and fuel types. Our study shows how complex and nuanced marine biogeochemical and ecological responses to anthropogenic activities can be. As the shipping industry adjusts to meet new and future requirements, operators may turn to other increasingly popular alternative fuels, such as liquified natural gas, ammonia, and biofuels (Al-Aboosi et al., 2021; M. Anderson, Salo, & Fridell, 2015; Coufalík et al., 2019; Fun-sang Cepeda et al., 2019; Grönholm et al., 2021; Machaj et al., 2022). We recommend more studies to be conducted to examine the effects of air and water pollution associated with the combustion of these alternative fuels by large ship engines.

## CHAPTER 2

### MARINE PHYTOPLANKTON RESPONSES TO SCRUBBER WASHWATER ADDITIONS IN COASTAL INCUBATION EXPERIMENTS

#### ABSTRACT

The combustion of fuels in the engines of ships releases inorganic compounds and metals that can promote phytoplankton growth (e.g. N, Fe, Mn, Zn) or decrease productivity (e.g. Cu). Many ship operators comply with air quality regulations by installing scrubber systems that clean emissions going into the air, but discharge washwater containing nutrients and contaminants directly into ocean water. This has the potential to change primary production rates and the structure of phytoplankton populations. This mesocosm study documented the responses of coastal phytoplankton communities (comprising dinoflagellate, diatom, picoeukaryote and *Synechococcus*) to high concentrations (1%, 5% and 10%) of scrubber washwater produced by marine engines combusting distilled and residual fuels. The high washwater concentrations and short (48h) incubation periods were intended to simulate acute exposure of phytoplankton to scrubber washwater discharges that could occur in coastal regions with heavy ship traffic such as the Kattegat, Sweden, and the Southern California Bight, USA, where our experiments were conducted. We observed different growth responses across different phytoplankton taxa, as well as to different fuel types.

#### INTRODUCTION

***Maritime Scrubber Washwater Systems.*** The maritime industry plays a central role in global trade, commercial fishing, and transportation and is a significant source of air emissions that cause environmental and human health impacts around the world (Brandt et al., 2013; Corbett, 1997, 2003; Corbett et al., 1999b; Eyring et al., 2010b; Hassellöv et al., 2013; Jägerbrand et al., 2019; Lack et al., 2009b; Y. Zhang et al., 2017). Global emissions from shipping are expected to more than triple between 2020 and 2050 (Gössling et al., 2021). In response, regulations have been enacted to control air pollution from marine engines. The International Maritime Organization's (IMO) global fuel sulfur limit that began on January 1,

2020, reduced the maximum sulfur content for marine fuels from 3.5% (in mass per mass) to 0.50%, except for ships that have an exhaust gas cleaning systems, also known as scrubbers. A growing number of shipping companies have adopted scrubbers, which serve as a relatively cheap air pollution abatement strategy (Osipova et al., 2021; Zis et al., 2022). However, the most popular type of scrubbers used by ships (i.e., open-loop scrubbers) generates residual liquid waste, or scrubber washwater, that is discharged directly into seawater.

The discharge of scrubber washwater into the ocean introduces a novel source of chemical constituents, including nutrients, trace metals, and other compounds (Lunde Hermansson et al., 2021; Marin-Enriquez et al., 2023; Schmolke et al., 2020; Ytreberg et al., 2022a) that could potentially influence phytoplankton growth, species composition, and overall ecosystem dynamics. Phytoplankton are primary producers that form the base of marine food webs and are essential contributors to carbon fixation, oxygen production, and nutrient cycling, and influence biodiversity and climate on a global scale (Barton et al., 2010; P. Falkowski et al., 2000; C. M. Moore et al., 2013b; Sarmiento & Gruber, 2006). Given that perturbations to phytoplankton communities have the potential to cascade throughout marine ecosystems, the importance of measuring emerging anthropogenic disturbances, such as scrubber wash water discharge, on their growth is becoming increasingly important.

Overall, interactions between scrubber washwater constituents and phytoplankton remain poorly understood. To this date, only four studies have been published reporting on experiments conducted to measure the impacts of phytoplankton populations to scrubber washwater exposure, all conducted with natural assemblages of phytoplankton in the Baltic

Sea (Ytreberg et al., 2019, 2021), or monospecific phytoplankton cultures (Marin-Enriquez et al., 2023; Picone et al., 2023a). The results from those studies varied greatly, from artificial fertilization of some phytoplankton groups to complex shifts in abundance, species composition, and size distributions for certain taxa. Some experiments have also evaluated the impacts of scrubber washwater on zooplankton (Koski et al., 2017; Marin-Enriquez et al., 2023; Picone et al., 2023a; Thor et al., 2021) and variable deleterious effects were observed for these phytoplankton grazers.

The chemical composition of scrubber washwater varies greatly based on the type of scrubber technology employed, quality and type of the fuel, type of ship, size of engine, and other operational factors (Lunde Hermansson et al., 2021; Ytreberg et al., 2022a). Air emissions from marine fuel combustion, which are partially captured in scrubber washwater, yield many possible chemical compositions as byproducts, including formulas that may contain potential fertilizers like nitrogen compounds ( $\text{NO}_3$ ,  $\text{NH}_4$ ), iron (Fe), and zinc (Zn) (Coufalík et al., 2019; Eyring et al., 2005, 2010b; Hardaway et al., 2004; Lack et al., 2009a; Moldanová et al., 2009a; Popovicheva et al., 2012; Raudsepp et al., 2019b; Viana et al., 2009). Concurrently, toxic combustion byproducts, such as polycyclic aromatic hydrocarbons (PAHs), and metals such as copper (Cu) and lead (Pb), have the potential to hinder phytoplankton growth in otherwise productive regions (Jordi et al., 2012; Lopez et al., 2019; B. H. Othman et al., 2018; Paytan et al., 2009a). The net effects experienced by marine phytoplankton exposed to scrubber washwater ultimately depends on the intricate interplay between the relative concentration of specific chemical components in the scrubber washwater discharge, the sensitivity of the microbial taxa present in the receiving waters, the background levels of nutrients that might be limiting the growth of

phytoplankton groups in that region, and the possible influences of the scrubber washwater on phytoplankton grazers that exert “top-down” control on phytoplankton populations and communities.

Here, we advance the knowledge in this field by investigating the responses of various coastal phytoplankton populations to acute (48h) exposure to highly concentrated (1, 5 and 10%) scrubber washwater. By employing a combination of mesocosm experiments using natural seawater from two coastal locations where marine traffic is relatively intense, we sought to assess the effects of different scrubber washwater formulations on phytoplankton growth, nutrient uptake, and community composition. Furthermore, we explored potential mechanisms underlying observed responses, including the role of trace metals, and nutrient availability. This work is an important early step to help inform scientists, managers, policy makers and the public at large about possible environmental effects of discharging scrubber washwater directly into marine ecosystems and could assist in the adjustment of regulations and management practices that can reduce aquatic pollution and improve environmental quality in coastal areas exposed to high shipping traffic.

***Site Characteristics.*** We conducted experiments at two sites – the Kattegat Strait (KS) and the Southern California Bight (SCB)– both coastal regions with heavy shipping traffic. The KS is a semi-enclosed marine basin situated between the North Sea and the Baltic Sea, characterized by complex hydrographic and biogeochemical features that are influenced by inflows from the Baltic Sea and the Atlantic Ocean. Surface salinity gradually changes from 18 in the southern part of the KS to 30–32 in the northern transition area into the Skagerrak strait. In this area, known as the Kattegat-Skagerrak front, surface salinities can rapidly

change by 5–10 (Jakobsen, 1997), and primary production is relatively high (Carstensen et al., 2004). High density ship traffic is common in the KS due to its position along major North European trade routes, with container carriers, bulk carriers, fishing boats, tankers, and passenger ferries transiting withing the region year-round. Approximately 70,000 ships pass through the KS annually (Baltic Marine Environment Protection Commission, 2017; Danish Maritime Authority, n.d.). Ships are allowed to discharge untreated open-loop scrubber wash water directly into the KS, as in most of the Baltic Sea

The SCB is the curved coastal region that extends for ~700 km from Point Conception (34.45 N) to northern Baja California (32.44 N). It is an eastern boundary upwelling system located in the U.S. Pacific Coast, with complex circulation patterns that are affected by the southward California Current, the northward California Countercurrent and California Undercurrent. Seasonally changing winds that blow north-to-south alongshore and occasionally onshore-to-offshore, along with the location of the Channel Islands that serve as physical barriers to currents, lead to the formation of eddies and fronts (Bray et al., 1999; Dong et al., 2009; Oram et al., 2008; Sutton et al., 2017). In general, the California Current ecosystem can be divided into a productive nearshore region and an oligotrophic offshore region (Chavez et al., 1991; Hayward & Venrick, 1998). Southern California has two of the largest ports in the world: the Ports of Los Angeles and Long Beach. Maritime traffic in this area is characterized by a diverse array of vessels, including container ships, oil tankers, cruise liners, and fishing boats. Notably, ship traffic intensity surpasses global averages due to its role as a major trade gateway and recreational hub (T. J. Moore et al., 2018). In California, the restrictions for marine vessels' emissions within the contiguous zone (i.e., 24 nm from the shore's baseline) are some of the most stringent in the world. Here, vessels must

comply with regulations that require fuels to meet low sulfur content standards (less than 0.1% S by mass) with additional quality specifications for distillate grades. Ocean-going vessels are not allowed to use scrubbers to meet these requirements in California.

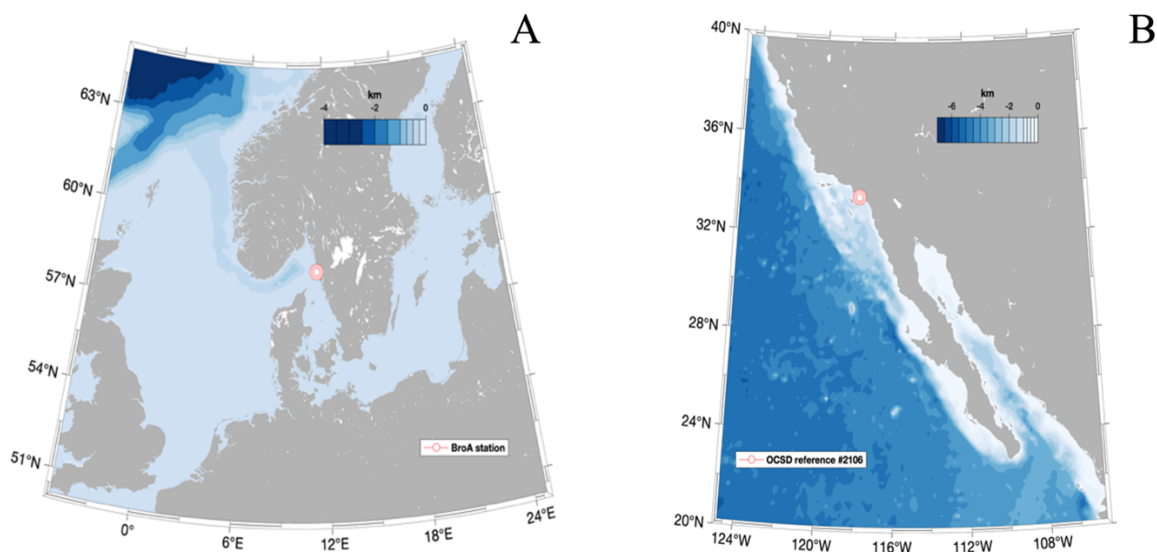


Figure 2.1. Study Areas: sampling stations where incubation water was collected from. (A) BroA Station in the Kattegat Strait (KS) located off the west coast of Sweden, and (B) the OCSD reference station in the Southern California Bight (SCB) located off the west coast of the USA (near Orange County, California).

## METHODS

### Production, collection, and analysis of scrubber washwater spikes

Four types of open-loop scrubber washwater spikes were used in this study (Table 1). Three of these scrubber washwater spikes were produced by small marine engines following the procedures described in detail in the first chapter of this dissertation. These spikes are the liquid residue produced by the scrubbing of exhaust gas from the combustion of two types of distilled fuels, heavy gas oil, or HGO, and a type of marine diesel approved by the California by the California Air Resources Board (CARB) that is popularly known as CARB diesel. Both fuel types are used by relatively small recreational boats and fishing vessels.

HGO is a distilled fuel blend that contains 1% sulfur (in mass per mass), and thus not suitable for use without scrubbing under the IMO regulations that came into effect January 1, 2020. The HGO scrubber washwater was produced at a testbed facility at Chalmers University, Sweden, in June 2019. Two CARB diesel scrubber washwater spikes were produced by the combustion of CARB diesel fuel. CARB diesel is a marine diesel oil with a maximum sulfur content of 0.1% and is chemically comparable to the USA-federally approved ultralow sulfur diesel (ULSD) fuel. The CARB scrubber washwater spikes (CARB-A and CARB-B) were collected from two different small (~70-ft long) recreational boats (boat A and boat B, respectively) cruising in Newport Beach Harbor, CA (2020) and off the Newport Beach coast, CA (2021). Samples of the seawater loaded into these three scrubbing systems (i.e. inlet samples) were collected, processed, and stored in the same way as the scrubber washwater spikes and were used as scrubber washwater (SW) controls in all experiments conducted in this study, as described in Section 2.2., below.

The fourth spike was acquired by collaborators conducting a study on the Environmental Impacts of Discharge Water from Exhaust Gas Cleaning Systems on Ships (i.e., Project ImpEx) on behalf of the German Environmental Agency, in March 2021. Pre-dilution, open-loop scrubber washwater samples were collected from a 4-stroke roll-on/roll-off passenger ferry combusting heavy fuel oil (HFO) and operating in the Baltic Sea (Bay of Pomerania) as described in (Marin-Enriquez et al., 2023). HFO is a residual fuel, popularly known as bunker fuel, and is known to contain variable amounts of contaminants, such as aromatics, sulfur, nitrogen, and metals (Ali & Abbas, 2006; Fridell, 2018; Fun-sang Cepeda et al., 2019; Streibel et al., 2017). The HFO combusted by the ferry operating the open-loop



scrubber used in this study contained 2.1% S, in addition to metals (Fe, Ni, V, Zn) and PAHs (Marin-Enriquez et al., 2023).

All scrubber washwater samples used as spikes were kept frozen from the time they were collected until 24 hours before incubation experiments were conducted, when they were defrosted at 2-4°C. scrubber washwater spikes were analyzed for nutrients and water-soluble trace metals, following the procedures described below (detailed in Chapter 1 of this dissertation). Salinity and pH were recorded using a handheld multiparameter digital probe (YSI Incorporated).

Table 2.1. Fuel and engine types used to generate scrubber washwater (SW) spikes in each of the three experiments in this study.

<b>Experiment location</b>	<b>Month, Year</b>	<b>Fuel and engine type used to produce SW spikes</b>	<b>Treatments (other than controls, SW controls)</b>
Kattegat Strait (KS)	August, 2019	Heavy gas oil (HGO), small testbed engine	5%, 10% HGO N addition = NO <sub>3</sub> <sup>-</sup> (1 μM) + NH <sub>4</sub> <sup>+</sup> (1 μM) Fe (10 nM) Cu (1 μM)
Southern California Bight (SCB)	October, 2020	CARB-A California Air Resources Board (CARB) diesel; small boat engine	5%, 10% CARB-A NO <sub>3</sub> <sup>-</sup> (10 μM) NH <sub>4</sub> <sup>+</sup> (1 μM) Fe (10 nM) Cu (0.5 μM)
Southern California Bight (SCB)	July, 2021	CARB-B California Air Resources Board (CARB) diesel; small boat engine	5%, 10% CARB-B 1%, 5%, 10% HFO NO <sub>3</sub> <sup>-</sup> (15 μM) NH <sub>4</sub> <sup>+</sup> (1.5 μM) Fe (10 nM) Cu (0.5 μM)
		Heavy fuel oil (HFO); large ship engine (4-stroke ro-ro ferry)	

## **Incubation experiments**

Three incubation experiments were conducted in this study (Table 2.1). The first occurred in Sweden with coastal seawater collected from the northern part of the Kattegat Strait (KS, BroA station, 58°15'49.9"N 11°19'30.2"E, Fig.2.1 a), between August 29<sup>th</sup> and 31<sup>st</sup> of 2019. The experiments were conducted at the Kristineberg Center for Marine Research, Sweden. Two additional experiments were conducted in the United States with coastal seawater collected from the Southern California Bight (SCB), in the nearfield subregion of the Orange County Sanitation District (OCSD) Quality Monitoring area (Reference Station #2106, 33°32'24.2"N 117°58'53.7"W, Fig. 2.1 b) in October of 2020, and July of 2021. The latter two incubations were conducted at the Back Bay Science Center in Newport Beach, CA, USA. These regions were selected for the intense ship traffic they experience and for the markedly differences in their oceanographic and biogeochemical regimes.

Mesocosm incubation experiments were conducted following the methods described in Mackey et al. (2017) and references therein. All materials used for collection, filtering, and storage of samples, as well as all materials used later in the incubation experiments were rendered trace metal clean prior to use following the GEOTRACES protocols (Cutter et al., 2017). Surface (0-10 m) seawater was collected from the above-mentioned offshore sites (Fig. 2.1), by boat, transferred into trace metal-clean carboys that were pre-rinsed with sample seawater and transported in the dark to the incubation sites where the experiments were conducted. At the incubation sites, seawater was homogenized, filtered through a 100 µm mesh to remove grazers, and dispensed into acid cleaned, sample rinsed, transparent 250 mL polycarbonate bottles. To characterize initial conditions, three baseline aliquots (i.e.,

unaltered seawater at time zero of the incubation experiment) were immediately collected and processed for chemical and biological analyses, as described below. Treatments were set up as follows: 1) control, which consisted of unamended surface seawater used in all treatments; 2) scrubber washwater (SW) controls, which consisted of the same unamended seawater from #1 mixed with samples of seawater that was loaded into scrubbers to produce the scrubber washwater spikes used in each experiment, and that were kept and transported in the exact same way that the scrubber washwater spikes were, at 10% final concentration in the incubation bottle; 3) various types of scrubber washwater spikes added at 1%, 5% or 10% of final concentration in the incubation bottle; and nutrient additions of known amounts of 4) nitrate, 5) ammonium, 6) iron, and 7) copper, which varies in concentration depending on the experiment. In the KS 2019 experiment, nitrate and ammonium were mixed into one nutrient addition treatment hereinafter referred to as the “N addition treatment” which consisted of using a spike that added  $1 \mu\text{M NO}_3^- + 1\mu\text{M NH}_4^+$  to the incubation bottles; the iron addition treatment consisted of 10 nM Fe, and the copper treatment consisted of  $1 \mu\text{M Cu}$ . In the SCB 2020 experiment, the nitrate addition treatment consisted of adding  $10 \mu\text{M NO}_3^-$ ; for the ammonium treatment we added  $1 \mu\text{M NH}_4^+$ ; for the iron treatment we added 10 nM Fe; for the copper treatment we added  $0.5 \mu\text{M Cu}$ . In the SCB 2021 experiment, the addition treatments consisted of  $15 \mu\text{M NO}_3^-$ ,  $1.5 \mu\text{M NH}_4^+$ , 10 nM Fe, and  $0.5 \mu\text{M Cu}$  (Table 1).

The response of the phytoplankton in nutrient addition treatments makes it possible to identify limitation and tolerance ranges in phytoplankton communities and to identify cause-effect relationships between specific scrubber washwater spike chemical components and observed phytoplankton responses. All treatments were conducted in triplicates or

quadruplicates. The bottles were placed in flow-thru tanks that permit the microorganisms being incubated to experience the typical daily variations in light and surface ocean temperature for the region. A shade cloth was placed over the incubators to decrease the irradiance by half to prevent phytoplankton photoinhibition without altering the spectral quality of the light. The bottles were left undisturbed for 48 hours, after which period they were removed from the incubator and gently shaken so that homogenous aliquots could be collected and processed for chlorophyll *a* (chl *a*), taxonomic composition of marine phytoplankton communities, and dissolved nutrients and water-soluble trace metals.

### **Inorganic nutrients analysis**

Changes in the concentration of macronutrients during the incubation experiments were determined by filtering 30-40 mL of sample water through GF/F filters using a peristaltic pump into 50 mL polypropylene centrifuge tubes (Corning™ Falcon). Samples were stored frozen at  $-20\text{ }^{\circ}\text{C}$  until analysis. Samples from the KS 2019 experiment were analyzed at the Kristineberg Center for Marine Research and Innovation, University of Gothenburg, using a QuAAtro, XY-3 Sampler, Seal Analytical 2015. The method limit of quantification (LOQ) was determined to be  $0.05\text{ }\mu\text{M}$  for  $\text{NO}_3^-$ ,  $0.02\text{ }\mu\text{M}$  for  $\text{NO}_2^-$ ,  $0.20\text{ }\mu\text{M}$  for  $\text{NH}_4^+$ , and  $0.02\text{ }\mu\text{M}$  for  $\text{PO}_4^{3-}$ .

Samples from the SCB 2020 and 2021 experiments were analyzed using a flow injection autoanalyzer (FIA, Lachat Instruments, Zellweger Analytics, Inc., QuikChem 8500 Series 2) at the Marine Science Institute's Analytical Laboratory at the University of California, Santa Barbara, using standards prepared in Milli-Q water and blanks that were prepared in aged, low nutrient seawater. To determine the LOQ, at least seven replicates of

standard solutions (i.e., seawater blanks and spiked samples) that are one- to five-times the estimated detection limit were analyzed, and the appropriate  $t$  value for a 99% confidence interval ( $n - 1$ ) for the number of replicates analyzed was used. The limit of quantification (LOQ) based on three-times the standard deviation of the blanks was determined to be 0.2  $\mu\text{M}$  for  $\text{NO}_3^-$  and  $\text{NH}_4^+$ , and 0.1  $\mu\text{M}$  for  $\text{PO}_4^{3-}$ . Nitrate ( $\text{NO}_3^-$ ) and nitrite ( $\text{NO}_2^-$ ) were measured separately in the KS 2019 experiment, and in combination in the SCB 2020 and SCB 2021 experiments. For the sake of consistency, we added  $\text{NO}_3^-$  and  $\text{NO}_2^-$  values from the KS 2019 experiment, so that they match the measurements from SCB experiments and we identify all those values as N+N. Concentrations of  $\text{NO}_2^-$  in N+N are expected to be minimal, and for that reason we sometimes refer to those measurements as nitrate or  $\text{NO}_3^-$  values. N+N and ammonium ( $\text{NH}_4^+$ ), were measured for all treatments and time steps of all experiments, while phosphate ( $\text{PO}_4^{3-}$ ) was measured in selected samples.

### **Water-Soluble Trace Metals Analysis**

For the analysis of water-soluble dissolved trace metals, 30 mL aliquots of samples were filtered through acid rinsed VWR 0.2  $\mu\text{m}$  PES sterile syringe filter cartridges in a laminar flow hood and stored in acid cleaned high-density polyethylene (HDPE) bottles until analysis. These aliquots were acidified using distilled HCl at sample to acid volume ratio of 1000:1 under a laminar flow hood. Acidified samples were allowed to sit for two weeks to allow labile particulate metals and dissolved metals that may have been adsorbed onto the walls of the vials to be recovered.

Acidified samples were transported to a trace metal-clean room at the University of Southern California (John Lab) where they were preconcentrated using ten parallel PERIFIX

resin columns and prepared according to the following steps: 1) resin was cleaned by filling up columns twice with 3N HNO<sub>3</sub> and conditioned using 3x 0.5 mL MilliQ water; 2) 15 mL aliquots from samples were transferred from HDPE bottles into acid cleaned VWR 15 mL tubes; 3) samples were analyzed in batches of 10, including two method blanks (i.e. 200  $\mu$ L of spike and buffer only); 4) each VWR tube was spiked with 50  $\mu$ L of a multi element spike and 150  $\mu$ L of a buffer (6N ammonium acetate at pH 6, clean); 5) contents were transferred from tubes into columns and when all the liquid had passed thru the columns, 2x 0.5 mL were used to wash away salts; 6) samples were eluted into clean VWR tubes using 5 x 200  $\mu$ L 3NHNO<sub>3</sub>. All these activities were carried out under a laminar flow hood, following the guidelines established by GEOTRACES (Cutter et al., 2017) to reduce metal contamination of samples.

The concentrations of water-soluble trace metals in preconcentrated scrubber washwater inlet and outlet samples were measured with a Thermo Element 2 ICPMS using a 100  $\mu$ L min<sup>-1</sup> Teflon nebulizer, glass cyclonic spray chamber with a PC<sup>3</sup> Peltier cooled inlet system (ESI), standard Ni sampler and Ni 'H-type' skimmer cones at the Department of Earth Sciences of University of Southern California. The sensitivity and stability of the instrument was tuned to optimal conditions before analyses, which were conducted at sensitivity around 10<sup>6</sup> counts s<sup>-1</sup> for 1 ppb In. Both the standard and samples were treated with 1 ppb Indium addition to correct for shifts in instrumental sensitivity and matrix. Elemental concentrations in samples were determined by their signal intensity compared to a 10 ppb multi-element standard, which was diluted from a certified standard (Santa Clarita method). The method's LOQs were the following: dAl= 0.30 nM, dCd= 0.03 nM, dCo= 0.12 nM, dCu=

0.82 nM, dFe= 3.35 nM, dMn= 0.08 nM, dNi= 0.23 nM, dPb= 0.03 nM, dV= 0.34 nM, dZn= 1.39 nM.

### **Chlorophyll analysis**

Changes in chlorophyll *a* (Chl-*a*) were measured by filtering 50- or 100-mL aliquots from each incubation bottle through 25 mm glass fiber filters (GF/F, Whatman) using a peristaltic pump or a manifold system. The GF/F filters were stored frozen at -20 °C until analysis. Chl-*a* was extracted in 90% acetone for 24h and determined fluorometrically on a Turner Trilogy fluorometer (TurnerDesigns). Raw fluorescence units were converted into Chl-*a* concentration ( $\mu\text{g Chl-}a/\text{L}$ ) using a calibration curve prepared with Chl *a* standard solutions from *Anacystis nidulans* (Sigma—Aldrich).

### **Flow cytometry**

Changes in the taxonomic composition of the picophytoplankton ( $\leq 3 \mu\text{m}$ ) community were measured using flow cytometry in all treatments of all experiments. Unfiltered aliquots (1.5  $\mu\text{L}$ ) of sample water were collected in cryogenic vials pre-charged with formaldehyde for a final concentration of 1-4% and stored frozen (-70 °C) until subsequent analysis using an ACEA Biosciences, Inc. Novocyte flow cytometer. *Synechococcus* and other picoeukaryotic populations were distinguished based on their autofluorescence and optical scattering characteristics.

### **Microscopy**

Nano- and microplankton (i.e. cells  $>3 \mu\text{m}$ ), hereinafter referred to as microplankton, were identified and counted via microscopy in baseline, control, and scrubber washwater- spiked samples from the 2019 KS and 2021 SCB experiments. Unfiltered 100 mL water samples were preserved in clear glass bottles with Lugol's Iodine

Solution (1% final concentration) and stored at room temperature and in the dark until microscopy analysis. Aliquots (25- 50 mL) were concentrated using the Utermöhl settling chamber method (Utermöhl, 1931). Phytoplankton taxa were identified to the lowest taxonomic level possible, photographed, and counted using optical inverted microscopes (i.e., Nikon Diaphot, and Nikon Eclipse, 400x maximum magnification). Final phytoplankton concentrations ( $\text{cells.L}^{-1}$ ), and counting error were calculated according to standard microscopic methods for quantitative phytoplankton analysis (Karlson et al., 2010; Lund et al., 1958).

### **Statistical Methods**

Statistical analyses were conducted using GraphPad Prism Version 10.1. Significant differences ( $P \leq 0.05$ ) were determined using ordinary one-way analysis of variance (ANOVA) followed by either Šídák post-hoc tests, when comparing independent pairs of means (i.e. samples from time 0 vs. time 48h in N drawdown analyses) and Dunnett post-hoc tests, when comparing means from baselines and from various treatments to unamended seawater samples used as controls (i.e. all other variables measured at time zero and at 48h). Asterisks used in all figures correspond to the following levels of significance: one asterisk (\*) means  $P \leq 0.05$ , two (\*\*) mean  $P \leq 0.01$ , three (\*\*\*) mean  $P \leq 0.001$ , and four (\*\*\*\*) mean  $P \leq 0.0001$ . Values below the limit of quantification (LOQ) were substituted by  $\frac{1}{2}$  of the LOQ in all analyses and for all parameters.



## RESULTS

### **Inorganic nutrient and trace metal chemistry of experimental seawater and scrubber washwater spikes**

The background concentrations of dissolved inorganic nutrients and trace metals in the incubation seawater and in undiluted (100% concentration) scrubber washwater spikes are given in Table 2. Directly measured N+N and  $\text{NH}_4^+$  concentrations in the spiked incubation bottles at time zero and after 48h are also shown below for each experiment in the following sections. Background  $\text{PO}_4^{3-}$  levels were near or below detection in all three experiments (0.09 – 0.15  $\mu\text{M}$ ). Background N+N concentrations were higher in the KS 2019 experiment ( $1.35 \pm 0.54 \mu\text{M}$ ) than in either the SCB 2020 or 2021 experiments ( $0.15 \pm 0.06 \mu\text{M}$  and  $0.16 \pm 0.10 \mu\text{M}$  respectively). Similarly, background  $\text{NH}_4^+$  levels were higher in the KS ( $2.48 \pm 1.38 \mu\text{M}$ ) than in either of the SCB experiments ( $0.38 \pm 0.48 \mu\text{M}$  and  $0.21 \pm 0.20 \mu\text{M}$  in the 2020 and 2021 experiments, respectively).

Based on measurements of the background incubation waters and scrubber washwater spikes, certain nutrients and trace metals would have been enriched above background levels in the experimental treatments following additions of the scrubber washwater spikes in each of the three experiments. In the 2019 KS experiment, dFe, dCo, dCu, dNi, N+N, and  $\text{NH}_4^+$  were all higher in the HGO spike than in the background incubation water and would have elevated these constituents in the spiked bottles. In the 2020 SCB experiment, the CARB-A spike was enriched in dCd, dCo, dFe, dMn, dNi, dPb, dV, dZn, N+N, and  $\text{NH}_4^+$  relative to the background incubation seawater. The 2021 SCB incubation included two types of spikes: relative to the background seawater, the CARB-B spike was enriched in

dAl, dCd, dCo, dCu, dFe, dMn, dNi, dV, dZn, PO<sub>4</sub><sup>3-</sup>, N+N, and NH<sub>4</sub><sup>+</sup>, whereas the HFO spike was enriched in dAl, dCd, dCo, dCu, dFe, dMn, dNi, dV, PO<sub>4</sub><sup>3-</sup>, N+N and NH<sub>4</sub><sup>+</sup>.

Table 2.2. Water chemistry of incubation seawater and corresponding scrubber washwater spikes. Values correspond to means of at least 3 replicates and standard error of the mean is shown in parenthesis. NM indicates that those parameters were not measured. Values below the LOQ are indicated with an asterisk.

Dissolved components	Kattegat 2019		SCB 2020		SCB 2021		
	Incubation seawater	HGO spike	Incubation seawater	CARB-A spike	Incubation seawater	CARB-B spike	HFO spike
Al (nM)	NM	NM	NM	2.05 (±0.36)	1.05 (±0.58)	77.52 (±6.74)	73.53 (±21.31)
Cd (nM)	1.29 (±0.47)	*<0.03	0.19 (±0.07)	0.38 (±0.01)	0.05 (±0.00)	0.24 (±0.00)	0.09 (±0.02)
Co (nM)	0.41 (±0.46)	0.66 (±0.14)	0.83 (±0.07)	1.30 (±0.06)	0.09 (±0.01)	0.35 (±0.03)	2.86 (±0.31)
Cu (nM)	14.26 (±7.51)	18.61 (±2.22)	57.10 (±18.08)	55.67 (±2.89)	27.55 (±1.09)	60.69 (±1.85)	62.62 (±3.75)
Fe (nM)	72.60 (±46.21)	279.65 (±34.10)	7.97 (±1.42)	9.07 (±2.02)	4.93 (±1.84)	16.54 (±4.03)	1,058.74 (±103.71)
Mn (nM)	16.68 (±0.86)	5.89 (±1.07)	11.16 (±3.20)	107.30 (±0.87)	3.31 (±0.10)	20.13 (±1.34)	51.68 (±2.59)
Ni (nM)	13.31 (±2.14)	36.29 (±6.63)	6.31 (±0.24)	7.85 (±0.09)	3.98 (±0.15)	6.11 (±0.10)	930.60 (±43.32)
Pb (nM)	1.26 (±0.26)	0.52 (±0.18)	0.13 (±0.06)	0.20 (±0.02)	2.05 (±0.244)	1.06 (±0.17)	0.91 (±0.06)
V (nM)	NM	0.29 (±0.07)	18.87 (±0.64)	32.60 (±1.53)	25.6 (±0.70)	27.51 (±2.21)	4,117.77 (±136.57)
Zn (nM)	196.16 (±9.91)	59.07 (±12.56)	164.42 (±5.94)	330.91 (±41.66)	148.38 (±1.33)	261.74 (±13.47)	144.78 (±30.85)
PO <sub>4</sub> (μM)	0.09 (±0.04)	0.14 (±0.01)	0.15 (±0.06)	NM	<0.1*	0.15 (±0.01)	0.67 (±0.06)
N+N (μM)	1.35 (±0.54)	19.69 (±1.10)	0.20 (±0.17)	5.57 (±0.79)	0.16 (±0.10)	17.7 (±0.15)	14.6 (±0.53)
NH <sub>4</sub> (μM)	2.48 (±1.38)	5.83 (±1.34)	0.38 (±0.48)	0.64 (±0.08)	0.21 (±0.20)	0.58 (±0.12)	3.04 (±0.56)
~ pH	<b>8.5</b>	<b>3.5</b>	<b>8.2</b>	<b>6.3</b>	<b>8.0</b>	<b>7.0</b>	<b>3.2</b>
~ Salinity	<b>23.0</b>	<b>13.5</b>	<b>34.5</b>	<b>33.2</b>	<b>34.3</b>	<b>34.1</b>	<b>8.0</b>

## The 2019 KS Experiment

The concentrations of N+N and  $\text{NH}_4^+$  were measured at time 0 and 48h for the control, 5% HGO, 10% HGO, and N addition treatments, and statistical analyses were conducted by comparing concentrations at times 0 and 48h for each treatment using ordinary one-way ANOVA followed by Šídák post-hoc tests (Fig 2.2). At time 0, the mean concentration of N+N in the unamended seawater control was  $1.35 \mu\text{M}$  ( $SEM=0.3 \mu\text{M}$ ) and declined to  $0.56 \mu\text{M}$  ( $SEM= 0.18 \mu\text{M}$ ) by 48h. However, this decrease was not significant at  $p<0.05$ . The mean concentration of N+N in the other treatments at time 0 were  $1.82 \mu\text{M}$  ( $SEM= 0.29 \mu\text{M}$ ) for the 5% HGO,  $5.02 \mu\text{M}$  ( $SEM= 0.41 \mu\text{M}$ ) for the 10% HGO, and  $2.32 \mu\text{M}$  ( $SEM= 0.61 \mu\text{M}$ ) for the added N treatment. By the 48h timepoint, N+N drawdown was significantly different in two treatments: the 10% HGO, in which the mean N+N concentration declined to almost one third of its original value ( $M=1.82 \mu\text{M}$ ,  $SEM= 0.66 \mu\text{M}$ ,  $p=0.0002$ ) and the N addition treatment, in which the N+N concentration declined more than sevenfold between 0 and 48h ( $M=0.32 \mu\text{M}$ ,  $SEM= 0.13 \mu\text{M}$ ,  $p=0.017$ ) (Fig 2.2a).  $\text{NH}_4^+$  concentrations at time 0 were measured for the control ( $M= 2.48 \mu\text{M}$ ,  $SEM=0.80 \mu\text{M}$ ), 5% HGO ( $M= 2.23 \mu\text{M}$ ,  $SEM=0.83 \mu\text{M}$ ,  $SD=1.43 \mu\text{M}$ ), 10% HGO ( $M=3.61 \mu\text{M}$   $SEM=1.18 \mu\text{M}$ ) and added N treatment ( $M=3.45 \mu\text{M}$ ,  $SEM=2.28 \mu\text{M}$ ) treatments. No statistically significant  $\text{NH}_4^+$  drawdown occurred in any of the treatments (Fig 2.2b).

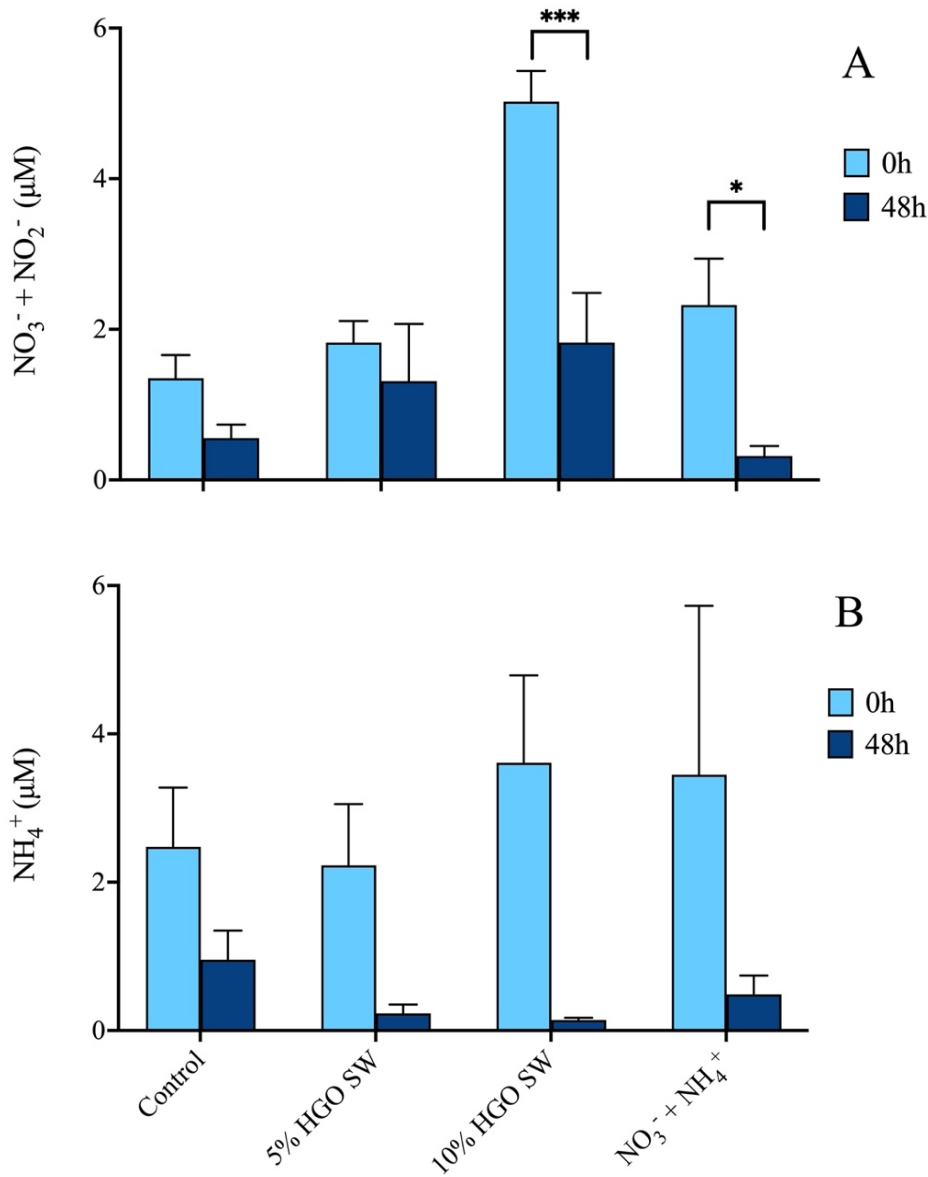


Figure 2.2. Concentration plots for (A) nitrate and nitrite ( $\text{NO}_3^- + \text{NO}_2^-$ ) and (B) ammonium ( $\text{NH}_4^+$ ) for treatments in the 2019 KS experiment at time zero (0h) and following 48h of incubation. Error bars show standard error of the mean. Asterisks indicate that there was a statistically significant difference between concentrations measured at 0h and 48h for each treatment based on results of ANOVA followed by a Šídák test at  $P \leq 0.05$ . One asterisk (\*) means  $P \leq 0.05$ , two (\*\*) mean  $P \leq 0.01$ , three (\*\*\*) mean  $P \leq 0.001$ , and four (\*\*\*\*) mean  $P \leq 0.0001$ .

Chl *a* was measured to track changes in the bulk phytoplankton community abundance in response to incubation treatments. In the KS, the mean chl *a* concentration in the unamended experimental seawater at time 0 was 4.82 mg/L (*SEM*= 0.27 mg/L; Fig. 2.3).

Following 48h of incubation, the chl *a* concentration in the unamended control treatment decreased significantly from time 0, reaching 3.15 mg/L (*SEM*= 0.24 mg/L, *p*=0.029). An ANOVA followed by Dunnett post-hoc tests performed on the day 2 comparing chl *a* concentrations in all treatments to that in the control showed that only the 10% HGO scrubber washwater treatment increased significantly (to *M*= 8.57 mg/L, *SEM*= 0.37 mg/L), while chl *a* in the Cu treatment decreased significantly (*M*=1.24 mg/L, *SEM*= 0.06 mg/L). All other treatments were not significantly different from the control at *p* <0.05 (Fig. 2.3).

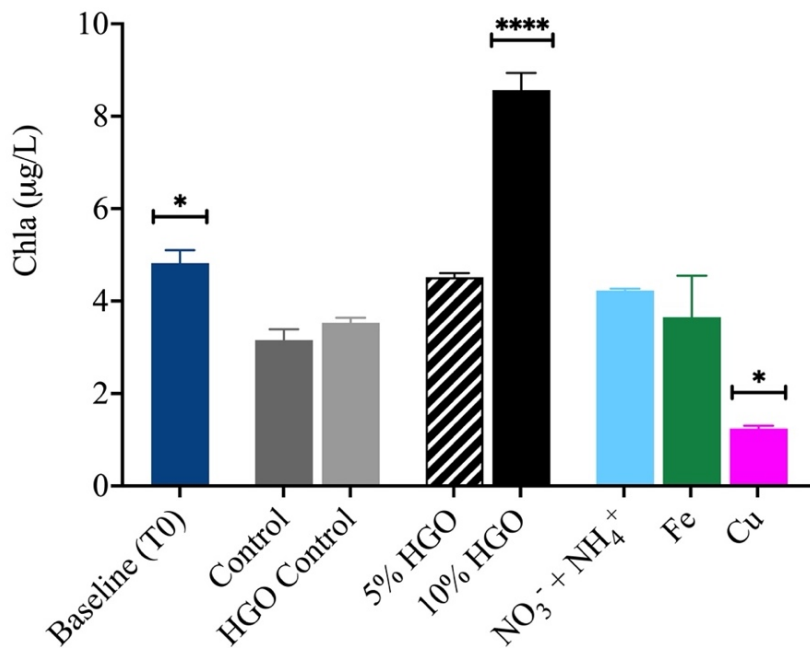


Figure 2.3. Chlorophyll *a* concentrations for treatments in the 2019 KS experiment following 48h of incubation. Error bars show standard error of the mean. Asterisks indicate that there was a statistically significant difference between the treatments and the control based on results of ANOVA followed by Dunnett test at *P* ≤ 0.05. One asterisk (\*) means *P* ≤ 0.05, two (\*\*) mean *P* ≤ 0.01, three (\*\*\*) mean *P* ≤ 0.001, and four (\*\*\*\*) mean *P* ≤ 0.0001.

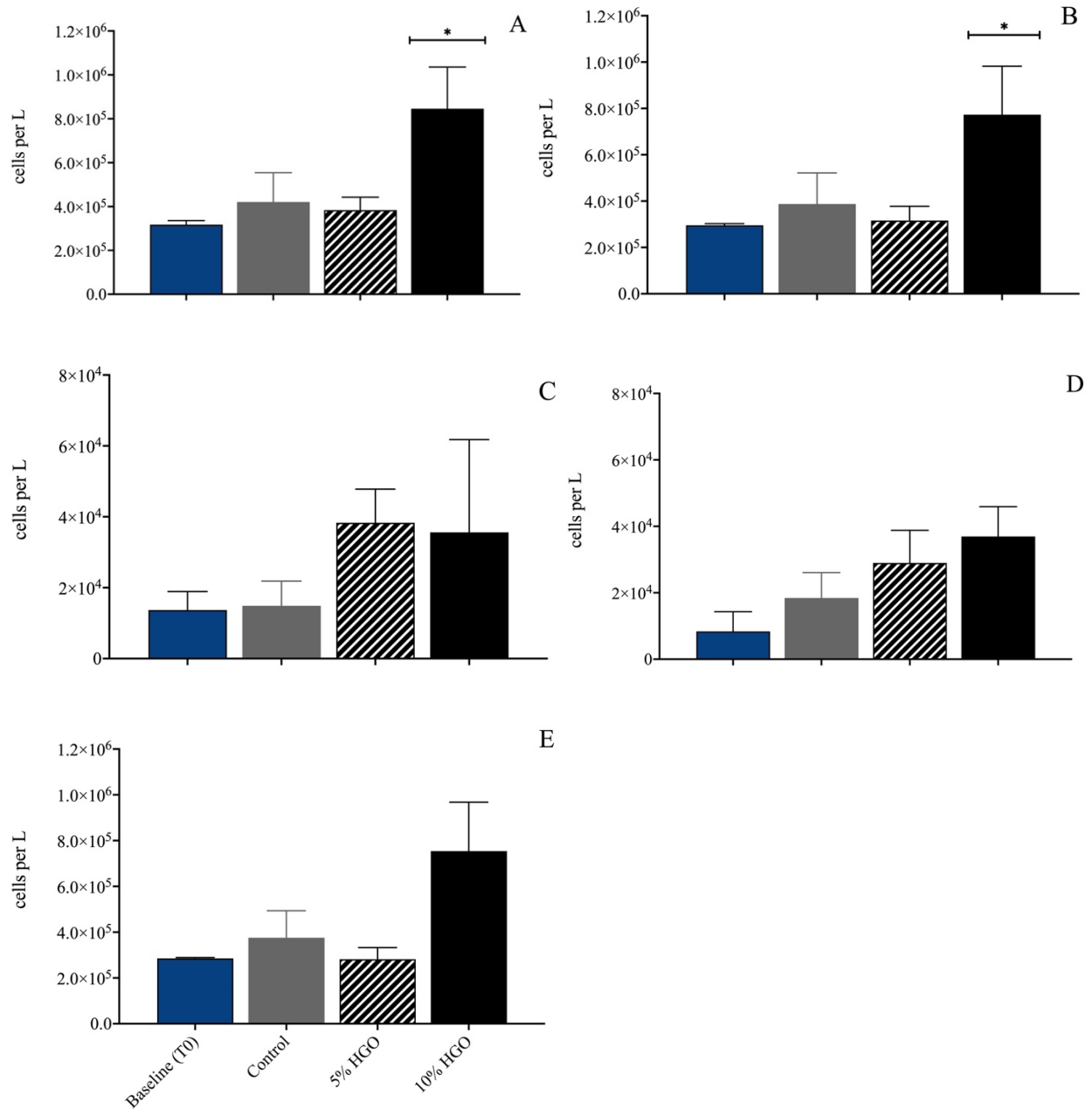


Figure 2.4. Concentrations (cells/L) of microplankton (cells > 3  $\mu\text{m}$ ) at time 0 and day 2 of the 2019 KS experiment, showing (A) total microplankton, (B) dinoflagellates, (C) centric diatoms, and (D) pennate diatoms. Error bars show standard deviation of the mean. Asterisks indicate that there was a statistically significant difference between the treatments and the control based on results of ANOVA followed by Dunnett test at  $p \leq 0.05$ . One asterisk (\*) means  $P \leq 0.05$ , two (\*\*) mean  $P \leq 0.01$ , three (\*\*\*) mean  $P \leq 0.001$ , and four (\*\*\*\*) mean  $P \leq 0.0001$ .



Figure 2.5: Micrographs of representative microplankton observed in the 2019 KS experiment cell counts. (A-C) dinoflagellates in the AAH complex, (B) *Tripos furca* (above, left) and a radiolarian *Dictyocha* sp. (below, right), (C) cf. *Heterocapsa* spp, (E) *Dinophysis rotundata*, (F) *Prorocentrum micans*, and (G) *Tripos macroceros*.

In the KS 2019 experiment, microplankton were identified and counted in baseline samples from time 0, and in the control, 5% and 10% CARB-A treatments at 48h (Fig. 12). All treatments samples were counted in triplicates except for the following, which were counted in fewer than three replicates due to sample losses: baseline (counted in duplicate), and control at 48h (counted in duplicate). Microplankton ( $> 3 \mu\text{m}$ ) were identified to the lowest taxonomic level possible and counted via light microscopy. Statistical analyses were conducted on total community counts, as well as separately for dinoflagellates, centric

diatoms, and pennate diatoms (Fig. 2. 4). Representative examples of cell types are shown in Fig. 5. Statistical analysis using ANOVA followed by a Dunnett post-hoc test comparing the baseline at time 0 and the scrubber wash water addition treatments at 48h to the unamended control at 48h showed that there was no significant difference between concentrations of total microplankton cells at time 0 ( $M=3.17 \times 10^5$ ,  $SD=1.84 \times 10^4$  cells.  $L^{-1}$ ) and the control treatment ( $M= 4.21 \times 10^5$ ,  $SD= 1.33 \times 10^5$  cells.  $L^{-1}$ ), nor between the control and the 5% HGO treatment ( $M= 3.83 \times 10^5$ ,  $SD= 5.88 \times 10^4$  cells.  $L^{-1}$ ) at 48h for  $p<0.05$ . A significant increase in total cell counts was observed in the 10% HGO treatment ( $M= 8.45 \times 10^5$ ,  $SD= 1.90 \times 10^5$  cells.  $L^{-1}$ ,  $p=0.02$ ). Total cell abundance in the 10% HGO treatment approximately doubled in 48h relative to the control. Likewise, there was no significant difference between dinoflagellate cell concentrations at time 0 ( $M= 2.95 \times 10^5$ ,  $SD= 7.29 \times 10^3$  cells.  $L^{-1}$ ) and the control ( $M= 3.87 \times 10^5$ ,  $SD= 1.34 \times 10^5$  cells.  $L^{-1}$ ) or between the control and the 5% HGO treatments at 48h ( $M=3.16 \times 10^5$ ,  $SD= 6.13 \times 10^4$  cells.  $L^{-1}$ ), but there was a significant increase in dinoflagellates in the 10% HGO treatment ( $M= 7.73 \times 10^5$ ,  $SD= 2.09 \times 10^5$  cells.  $L^{-1}$ ,  $p= 0.05$ ), representing a doubling of cell concentration over 48h (Fig. 2.4 a-b).

Collectively, dinoflagellates represented ~93% of the total microplankton at time 0, and after 48h of incubation, they accounted for ~92% of the total count in the control, ~82% in the 5% HGO, and ~91% in the 10% HGO. The mean concentration of centric diatoms at time 0 was  $1.37 \times 10^4$  cells.  $L^{-1}$  ( $SD= 5.24 \times 10^3$  cells.  $L^{-1}$ ), and in the control at 48h it was  $1.49 \times 10^4$  cells.  $L^{-1}$  ( $SD= 6.95 \times 10^3$ ), while in the 5% HGO the mean was  $3.83 \times 10^4$  cells.  $L^{-1}$  ( $SD= 9.50 \times 10^3$ ) and  $3.56 \times 10^4$  cells.  $L^{-1}$  ( $SD= 2.62 \times 10^4$ ) in the 10% HGO treatment. The mean concentration of pennate diatoms at time 0 was  $8.37 \times 10^3$  cells.  $L^{-1}$  ( $SD= 5.92 \times 10^3$ ),  $1.84 \times 10^4$  cells.  $L^{-1}$  ( $SD=7.63 \times 10^3$ ) in the control at time 48h,  $2.89 \times 10^4$  cells.  $L^{-1}$  ( $SD=9.81 \times 10^3$ ) in the



5% HGO, and  $3.69 \times 10^4$  cells.  $L^{-1}$  ( $SD= 8.99 \times 10^3$ ) in the 10% HGO. Although the two scrubber washwater addition treatments appeared to have higher mean diatom cell concentrations than the control, the relatively large uncertainty rendered these comparisons not statistically significant, and overall comparison of diatom concentrations at time 0 versus 48h revealed no significant differences for any of the comparisons for either pennate or centric diatoms at  $p<0.05$  (Fig. 2.4 c-d).

Unequivocal identification of microplankton at genus or species level was beyond the scope of the present study. Nevertheless, we were able to determine that at time 0, the microplankton community in the KS was dominated by a mixed bloom composed of various genera of pennate and centric diatoms of various sizes (e.g. *Chaetoceros*; *Leptocylindrus*; *Guinardia*; *Pseudo-nitzschia*; *Cylindrotheca*; *Rhizosolenia*) and of relatively large dinoflagellates (e.g. *Tripos*, formerly known as *Ceratium*; *Protoperidinium*, *Dinophysis*, *Gyrodinium*) in addition to small dinoflagellates that resembled the *Azadinium*, *Amphidoma*, and *Heterocapsa* genera. Organisms in the last three genera are very small (10-30  $\mu m$  in diameter), and practically impossible to distinguish from each other using light microscopy, thus we counted them as a group that we refer to as the *AAH* complex. The *AAH* complex dominated the dinoflagellates population (97% at time 0, and 89-98% at time 48h) and consequently the microplankton community in all treatments (90% at time 0, and 73-89% at 48h). Mean *AAH* complex cell abundance ranged from  $2.81 \times 10^5$  cells.  $L^{-1}$  ( $SD=5.10 \times 10^4$ ) to  $7.54 \times 10^5$  cells.  $L^{-1}$  ( $SD=2.13 \times 10^5$ ). Although the 10% HGO scrubber washwater addition treatment appeared to have higher mean *AAH* complex count than other treatments, the relatively large uncertainty rendered all comparisons not statistically significant  $p<0.05$  (Fig. 2.4 e).

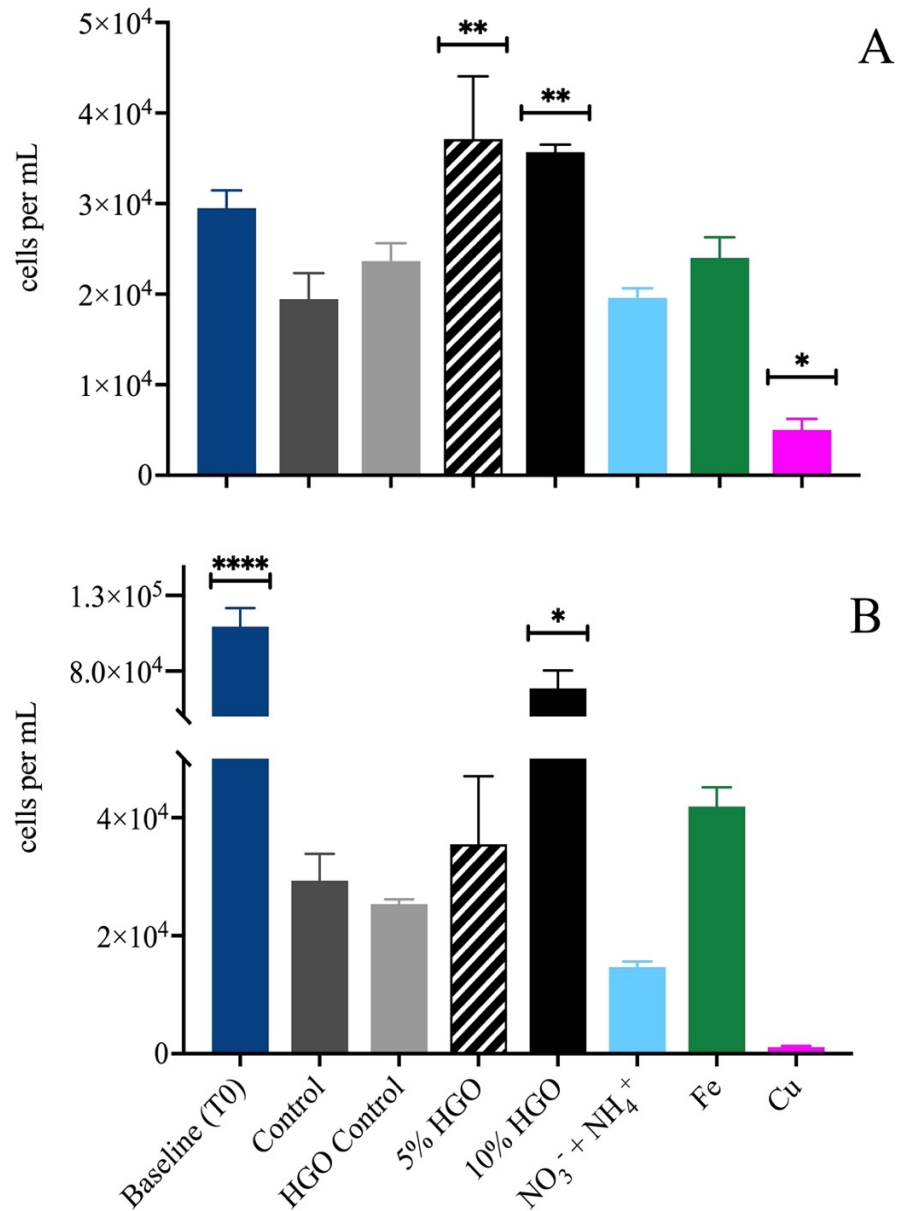


Figure 2.6. Cell concentrations of (A) picoeukaryotes and (B) *Synechococcus* sp. at 48h in the 2019 KS experiment. Error bars show standard error of the mean. Asterisks indicate that there was a statistically significant difference between the treatments and the control based on results of ANOVA followed by Dunnett test at  $P \leq 0.05$ . One asterisk (\*) means  $P \leq 0.05$ , two (\*\*) mean  $P \leq 0.01$ , three (\*\*\*) mean  $P \leq 0.001$ , and four (\*\*\*\*) mean  $P \leq 0.0001$ .

The abundance of picoplankton, including picoeukaryotes and *Synechococcus spp.* were enumerated by flow cytometry. The concentration of picoeukaryotes at time 0 ( $M= 2.9 \times 10^4$ ,  $SEM= 2.0 \times 10^3$  cells.  $mL^{-1}$ ) was not significantly different from either the control ( $M=1.9 \times 10^4$ ,  $SEM= 2.9 \times 10^3$  cells.  $mL^{-1}$ ) or the HGO scrubber washwater control ( $M= 2.4 \times 10^4$ ,  $SEM= 2.0 \times 10^3$  cells.  $mL^{-1}$ ) treatments at 48h. However, significant increases were observed in the 5% HGO ( $M= 3.7 \times 10^4$ ,  $SEM= 6.9 \times 10^3$  cells.  $mL^{-1}$ ,  $p=0.01$ ) and 10% HGO ( $M=3.6 \times 10^4$ ,  $SEM= 8.3 \times 10^2$  cells.  $mL^{-1}$ ,  $p=0.01$ ) treatments. A significantly lower picoeukaryote abundance was observed in the Cu treatment ( $M=5.4 \times 10^3$ ,  $SEM= 1.2 \times 10^3$  cells.  $mL^{-1}$ ,  $p=0.02$ ).

The *Synechococcus* abundance at time 0 ( $M=1.1 \times 10^5$ ,  $SEM=1.2 \times 10^4$  cells.  $mL^{-1}$ ) was significantly higher than in all other treatments at 48h (ranging from  $1.1 \times 10^3$  to  $6.8 \times 10^4$  cells.  $mL^{-1}$ ). Relative to the control at 48h ( $M=2.9 \times 10^4$ ,  $SEM=4.5 \times 10^3$  cells.  $mL^{-1}$ ), the 10% HGO treatment was the only treatment that was significantly higher ( $M=6.8 \times 10^4$ ,  $SEM= 1.2 \times 10^4$  cells.  $mL^{-1}$ ,  $p=0.01$ ), while the Cu treatment was the only one that was significantly lower ( $M= 1.1 \times 10^3$ ,  $SEM= 2.0 \times 10^2$  cells.  $mL^{-1}$ ,  $p=0.04$ ).

## The 2020 SCB Experiment

Initial  $\text{NH}_4^+$  concentrations at time 0 were above the LOQ of  $0.2 \mu\text{M}$  for the unamended seawater control ( $M= 0.38$ ,  $SEM=0.28 \mu\text{M}$ ), the  $\text{NO}_3^-$  addition ( $M= 0.24$ ,  $SEM= 0.14 \mu\text{M}$ ), and  $\text{NH}_4^+$  addition ( $M=1.05$ ,  $SEM=0.01 \mu\text{M}$ ) treatments, and below the LOQ for 5% CARB-A ( $0.10 \mu\text{M}$ ), the 10% CARB-A ( $M= 0.17$ ,  $SEM= 0.07 \mu\text{M}$ ) treatments. Statistical analyses were complicated by the fact that so many  $\text{NH}_4^+$  measurements were at or below the LOQ, but a statistically significant decrease in  $\text{NH}_4^+$  was observed after 48h in the  $\text{NH}_4^+$  addition treatment ( $M= 0.30$ ,  $SEM=0.03 \mu\text{M}$ ) (Fig. 2.7. b).

In the 2020 SCB experiment, the chl-*a* concentration in the unamended experimental seawater at time 0 was  $M=0.39$ ,  $SEM= 0.01 \text{ mg. L}^{-1}$  (Fig. 2.8). Following 48h of incubation, the chl *a* concentration in the unamended control treatment increased significantly from time 0, reaching  $M= 0.72 \text{ mg. L}^{-1}$  ( $SEM=0.13$ ,  $p=0.012$ ). Significant increases in Chl-*a* concentration between the control and other treatments on day 2 were identified for the 10% CARB-A scrubber washwater treatment ( $M=1.34$ ,  $SEM=0.04 \text{ mg. L}^{-1}$ ,  $p<0.0001$ ), as well as the treatments that received added  $\text{NO}_3^-$  ( $M=1.45$ ,  $SEM=0.06 \text{ mg. L}^{-1}$ ,  $p<0.0001$ ) and  $\text{NH}_4^+$  ( $M=1.81$ ,  $SEM=0.02 \text{ mg. L}^{-1}$ ,  $p<0.0001$ ). The apparent increase in the 5% CARB-A scrubber wash water treatment, along with the chl *a* concentrations in the CARB-A scrubber washwater control and the Fe addition treatment, were not significantly different from the control at  $p<0.05$ . Chl *a* concentrations in the Cu treatment declined significantly to  $M=0.09$ ,  $SEM=0.00 \text{ mg. L}^{-1}$  ( $p<0.0001$ ) at 48h.

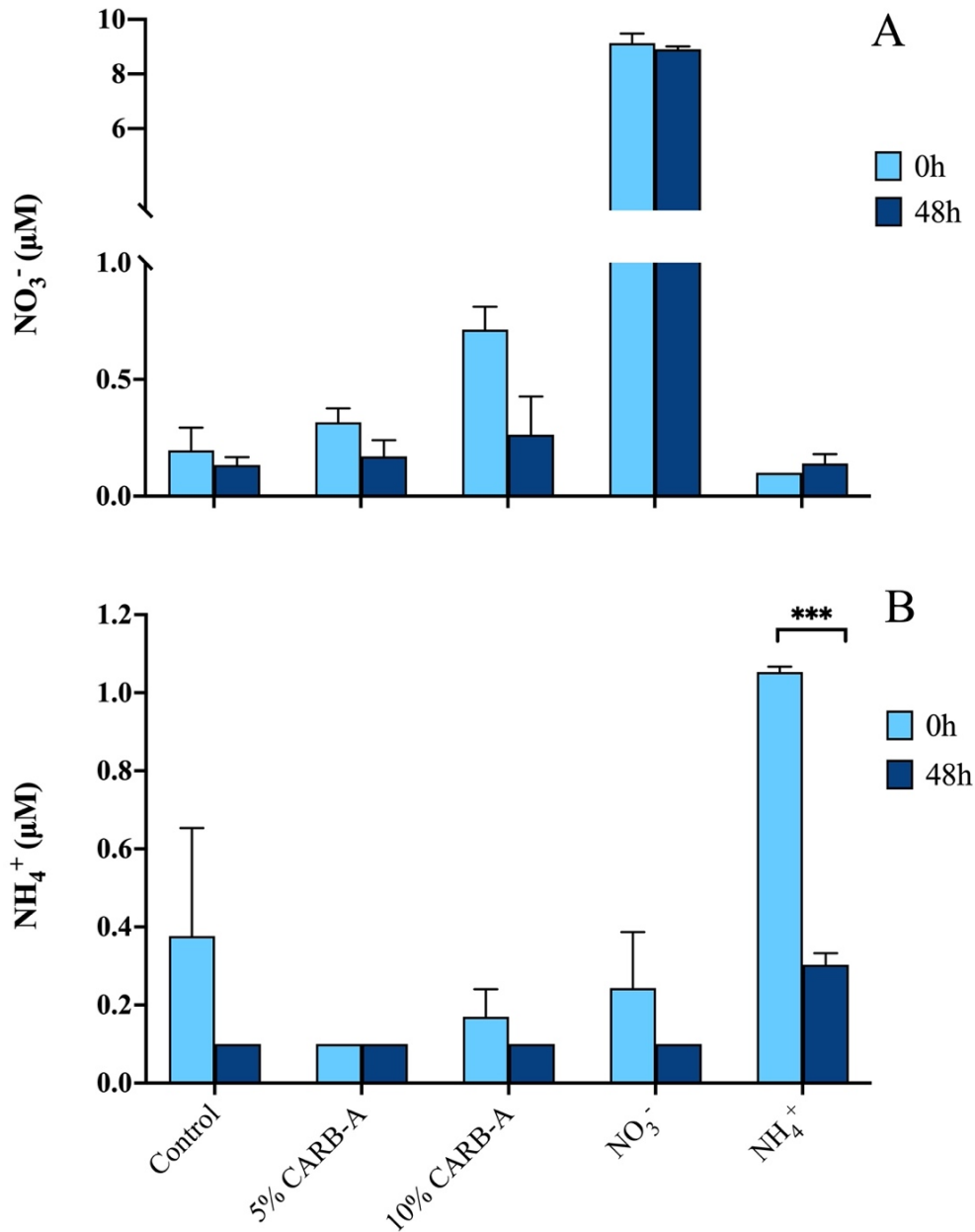


Figure 2.7. Concentration plots for A, Nitrate ( $\text{NO}_3^-$ ) and B, ammonium ( $\text{NH}_4^+$ ) for treatments in the 2020 SCB experiment at time zero (0h) and following 48h of incubation. Error bars show standard error of the mean. Asterisks indicate that there was a statistically significant difference between concentrations measured at 0h and 48h for each treatment based on results of ANOVA followed by a Šídák test at  $P \leq 0.05$ . One asterisk (\*) means  $P \leq 0.05$ , two (\*\*) mean  $P \leq 0.01$ , three (\*\*\*) mean  $P \leq 0.001$ , and four (\*\*\*\*) mean  $P \leq 0.0001$ .

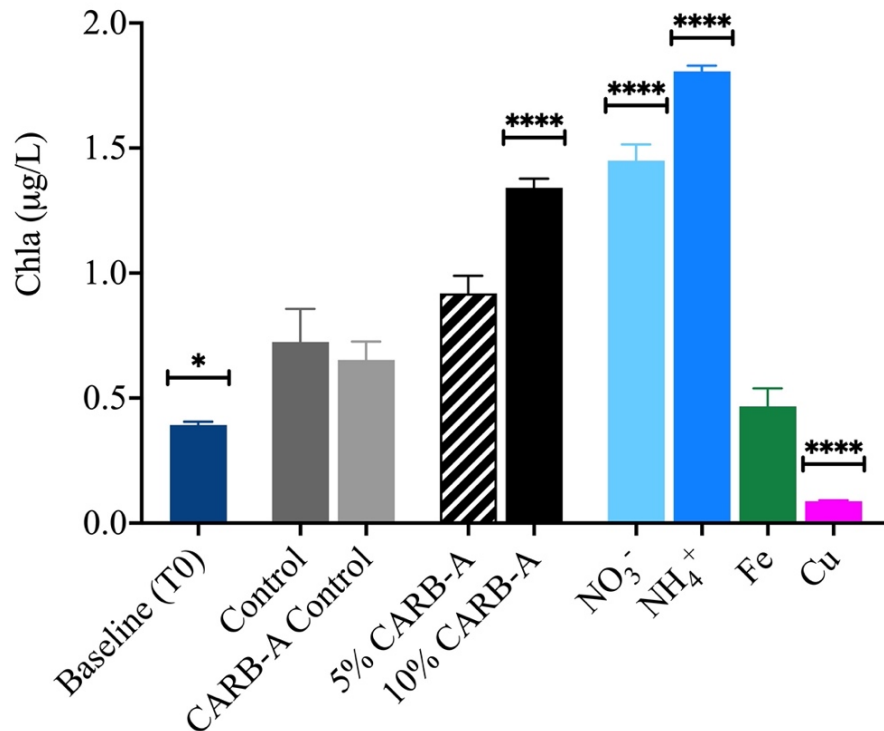


Figure 2.8. Chlorophyll a concentrations for treatments in the 2020 SCB experiment following 48h of incubation. Error bars show standard error of the mean. Asterisks indicate that there was a statistically significant difference between the treatments and the control based on results of ANOVA followed by Dunnett test at  $P \leq 0.05$ . One asterisk (\*) means  $P \leq 0.05$ , two (\*\*) mean  $P \leq 0.01$ , three (\*\*\*) mean  $P \leq 0.001$ , and four (\*\*\*\*) mean  $P \leq 0.0001$ .

Flow cytometry was used to enumerate picoeukaryote and *Synechococcus* abundance in the 2020 SCB samples (Fig. 2.9). The concentration of picoeukaryotes at the time 0 baseline ( $M=2.6 \times 10^4$ ,  $SEM= 6.3 \times 10^2$  cells.  $mL^{-1}$ ) was significantly higher than in all treatments at 48h, which ranged from  $M= 6.2 \times 10^2$  ( $SEM= 5.8 \times 10^1$ ) cells.  $mL^{-1}$ , in the Cu treatment, to  $M= 2.0 \times 10^4$  ( $SEM=1.4 \times 10^3$ ) cells.  $mL^{-1}$  in the 10% CARB-A control treatment. A one-way ANOVA followed by Dunnett multiple comparisons post-hoc test used to compare all treatments at 48h against the control  $M= 1.8 \times 10^4$  ( $SEM=1.4 \times 10^3$ ) cells.  $mL^{-1}$  revealed that the concentration of picoeukariotes in all treatments were significantly lower than in the control, except for the CARB-A Control.

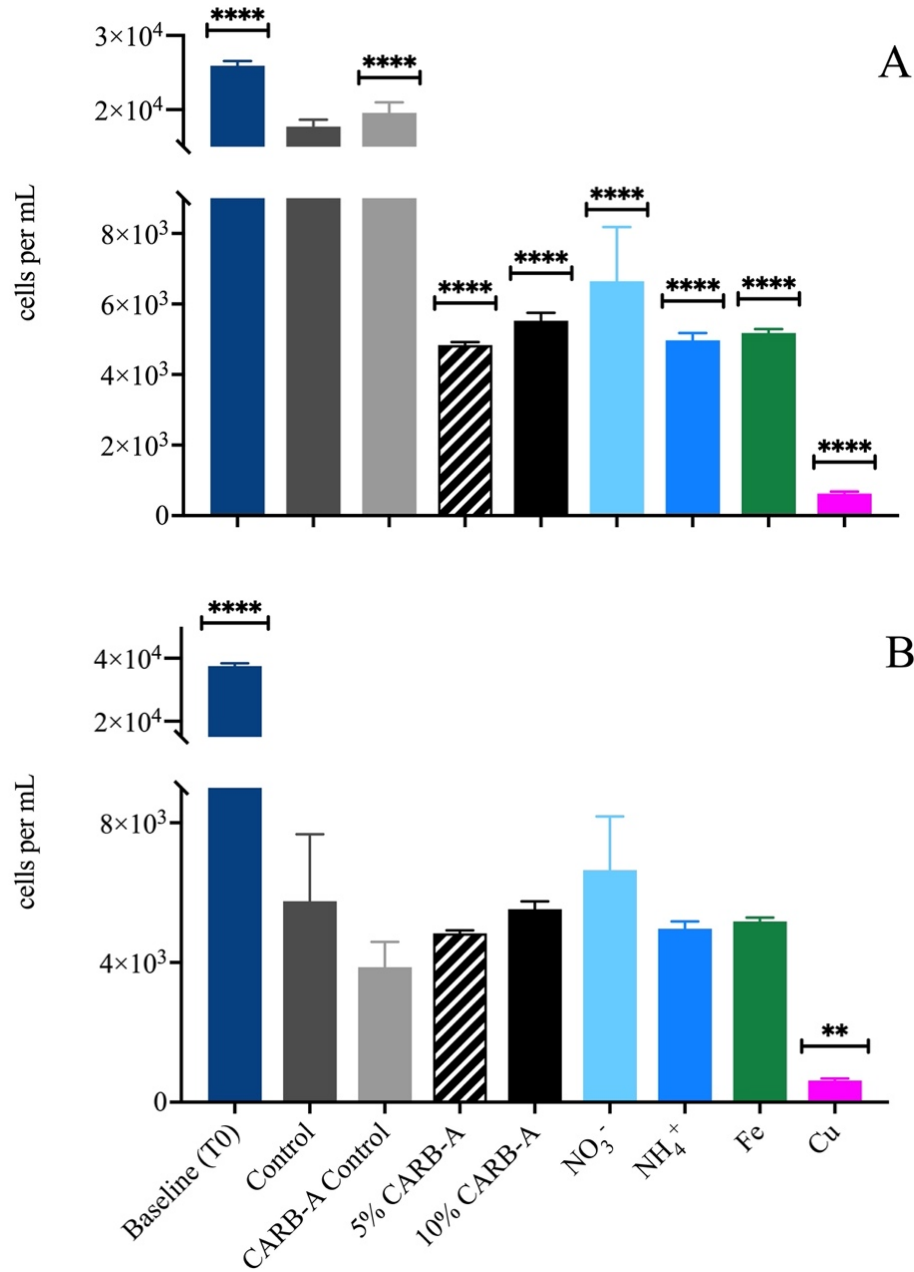


Figure 2.9. Cell concentrations of (A) picoeukaryotes and (B) *Synechococcus* at 48h in the 2020 SCB experiment. Error bars show standard error of the mean. Asterisks indicate that there was a statistically significant difference between the treatments and the control based on results of ANOVA followed by Dunnett test at  $P \leq 0.05$ . One asterisk (\*) means  $P \leq 0.05$ , two (\*\*) mean  $P \leq 0.01$ , three (\*\*\*) mean  $P \leq 0.001$ , and four (\*\*\*\*) mean  $P \leq 0.0001$ .

The *Synechococcus* abundance at the time 0 baseline ( $M= 3.7 \times 10^4$ ,  $SEM=8.6 \times 10^2$  cells.  $mL^{-1}$ ) was significantly higher than in all other treatments at 48h, which ranged from  $M= 6.2 \times 10^2$  ( $SEM= 5.8 \times 10^1$  cells.  $mL^{-1}$ ) in the Cu treatment, to  $M= 6.6 \times 10^3$  ( $SEM=1.5 \times 10^3$  cells.  $mL^{-1}$ ) in the  $NO_3^-$  treatment. A one-way ANOVA followed by Dunnett multiple comparisons post-hoc test used to compare all treatments at 48h against the control ( $M= 5.7 \times 10^3$ ,  $SEM= 1.9 \times 10^3$  cells.  $mL^{-1}$ ), revealed that none of the treatments were significantly different except for the Cu treatment, which was significantly lower ( $p=0.008$ ).

### **The 2021 SCB Experiment**

The concentrations of N+N and  $NH_4^+$  were measured at time 0 and 48h for all treatments in the 2021 SCB experiment and separate statistical analyses using one-way ANOVA and Šídák test were made by comparing the initial and final concentrations for each treatment (Fig. 2.10). N+N was much more abundant than  $NH_4^+$  in these waters, and many of the concentration values measured in replicate samples were below the method limit of quantification (LOQ) of 0.2  $\mu M$ . These values were substituted by  $\frac{1}{2}$  LOQ (0.1  $\mu M$ ) in the calculation of the means used to prepare plots and conduct statistical analysis. The mean initial N+N concentration at time 0 in the unamended control was  $M= 0.16$  ( $SEM= 0.06$ )  $\mu M$ ; for the 5% CARB-B it was  $M= 0.78$  ( $SEM= 0.08$ )  $\mu M$ ; for the 10% CARB-B it was  $M=1.13$  ( $SEM= 0.15$ )  $\mu M$ ; for the 1% HFO it was  $M=0.36$  ( $SEM=0.03$ )  $\mu M$ ; for the 5% HFO it was  $M= 0.78$  ( $SEM= 0.18$ )  $\mu M$ ; for the 10% HFO it was  $M= 1.76$  ( $SEM=0.05$ )  $\mu M$ ; for the  $NO_3^-$  addition it was  $M=14.53$  ( $SEM= 0.29$ )  $\mu M$ ; for the  $NH_4^+$  addition, it was  $M= 0.16$  ( $SEM= 0.06$ )  $\mu M$ . The only statistically significant change in  $NO_3^-$  concentration between time 0 and 48h was a decrease in the added  $NO_3^-$  treatment to  $M=13.57$  ( $SEM=0.43$ )  $\mu M$  ( $p=0.003$ , Fig.2.10).



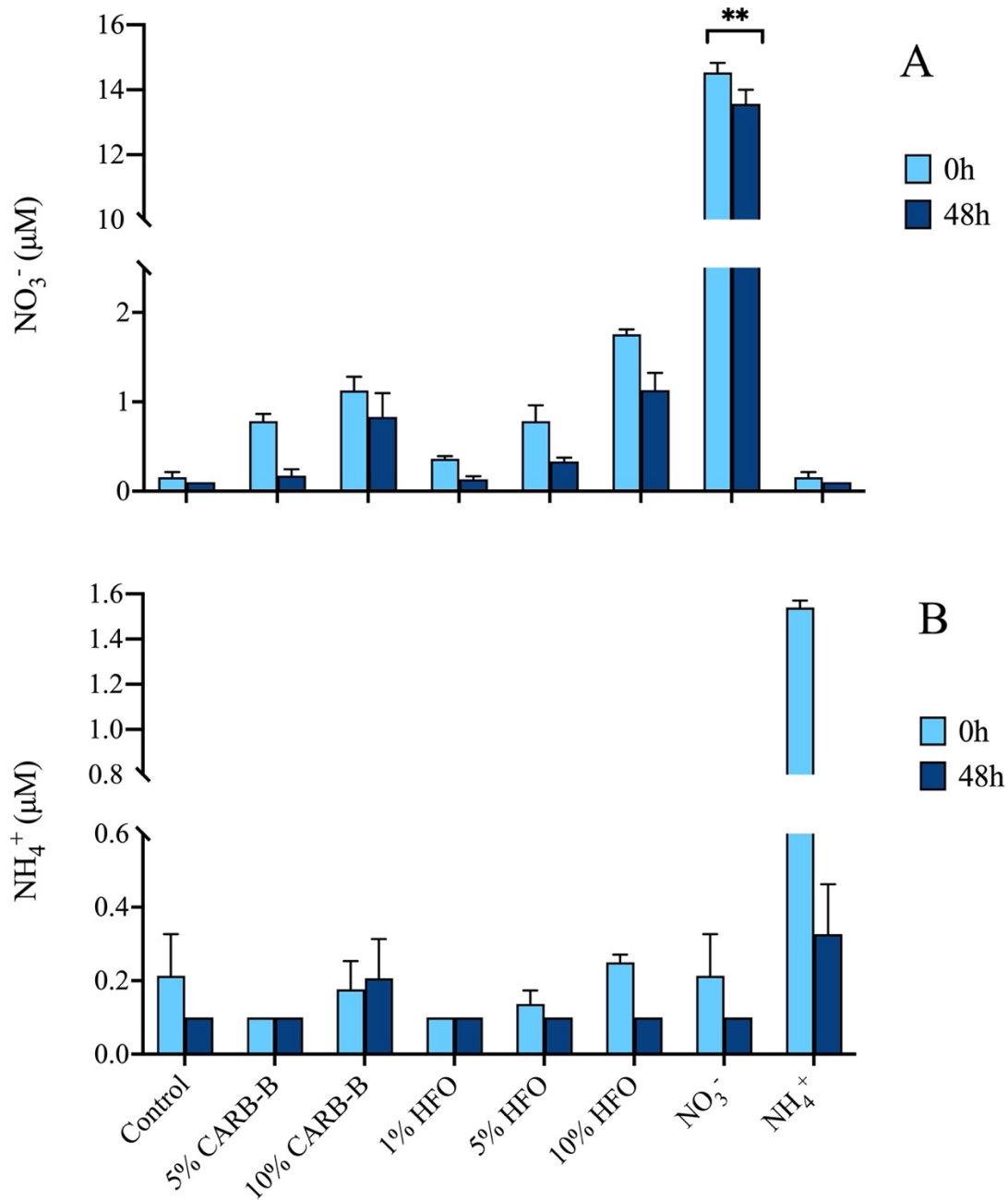


Figure 2.10. Concentration plots for A, Nitrate (NO<sub>3</sub><sup>-</sup>) and B, ammonium (NH<sub>4</sub><sup>+</sup>) for treatments in the 2021 SCB experiment at time zero (0h) and following 48h of incubation. Error bars show standard error of the mean. Asterisks indicate that there was a statistically significant difference between concentrations measured at 0h and 48h for each treatment based on results of ANOVA followed by a Šídák test at P ≤ 0.05. One asterisk (\*) means P ≤ 0.05, two (\*\*) mean P ≤ 0.01, three (\*\*\*) mean P ≤ 0.001, and four (\*\*\*\*) mean P ≤ 0.0001.

The mean initial  $\text{NH}_4^+$  concentration at time 0 in the unamended control was  $M=0.21$  ( $SEM= 0.11$ )  $\mu\text{M}$ , and the rest as follows: below the LOQ of  $0.20 \mu\text{M}$  in 5% CARB-B, 10% CARB-B, 1% HFO, 5% HFO, and above the LOQ in 10% HFO ( $M= 0.25$ ,  $SEM= 0.02 \mu\text{M}$ ),  $\text{NO}_3^-$  addition ( $M=0.21$ ,  $SEM= 0.11 \mu\text{M}$ ), and  $\text{NH}_4^+$  addition ( $M=1.54$ ,  $SEM= 0.03 \mu\text{M}$ ). The only statistically significant decrease in  $\text{NH}_4^+$  concentration between time 0 and 48h occurred in the added  $\text{NH}_4$  treatment ( $M=0.33$ ,  $SEM=0.14 \mu\text{M}$ ,  $p<0.0001$ ).

In the 2021 SCB experiment, the mean chl *a* concentration in the unamended experimental seawater at time 0 (baseline) was  $2.12$  ( $SEM= 0.07$ )  $\text{mg}\cdot\text{L}^{-1}$  (Fig. 2.11). Following 48h of incubation, the chl *a* concentration in the unamended control treatment decreased significantly from time 0, reaching  $M= 0.81$  ( $SEM= 0.05$ )  $\text{mg}\cdot\text{L}^{-1}$  ( $p<0.0001$ ).

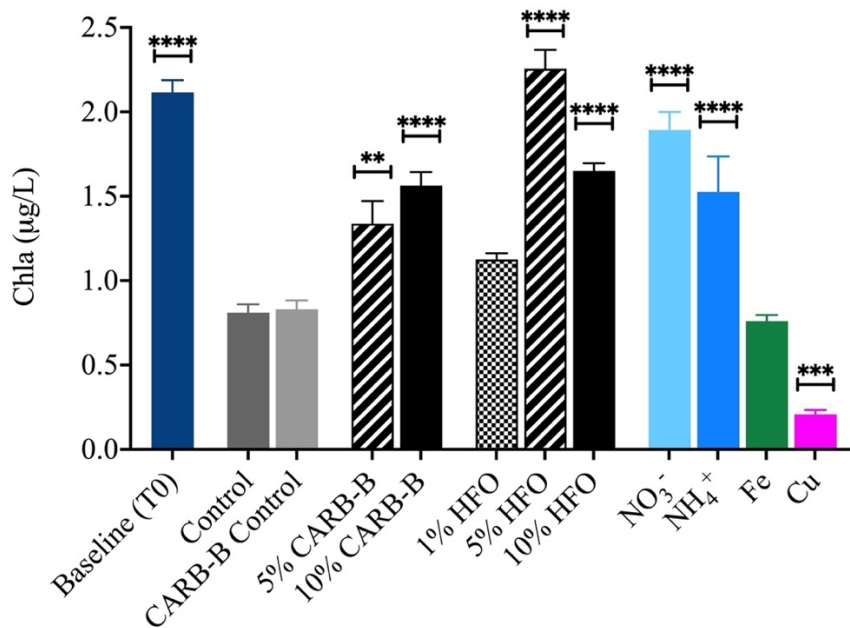


Figure 2.11. Chlorophyll *a* concentrations for treatments in the 2021 SCB experiment following 48h of incubation. Error bars show standard error of the mean. Asterisks indicate that there was a statistically significant difference between the treatments and the control based on results of ANOVA followed by Dunnett test at  $P \leq 0.05$ . One asterisk (\*) means  $P \leq 0.05$ , two (\*\*) mean  $P \leq 0.01$ , three (\*\*\*) mean  $P \leq 0.001$ , and four (\*\*\*\*) mean  $P \leq 0.0001$ .

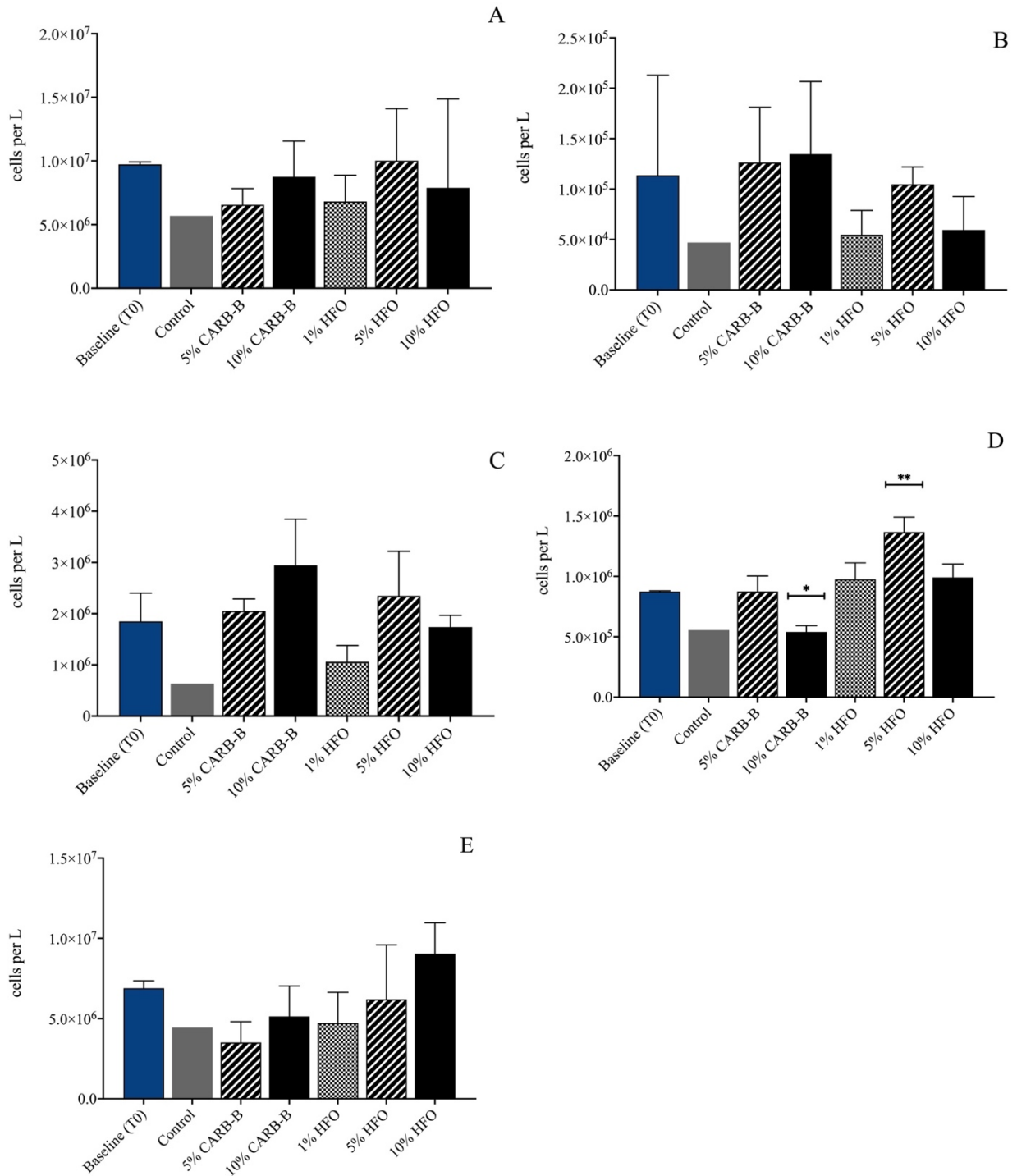


Figure 2.12. Concentrations (cells/L) of microplankton ( $> 5 \mu\text{m}$ ) at time 0 and day 2 of the 2021 SCB experiment, showing (A) total microplankton, (B) dinoflagellates, (C) centric diatoms, (D) pennate diatoms, and (E) flagellates. Error bars show standard deviation. Bars for the control treatment represent the counts from one replicate due to loss of other replicates. Asterisks indicate that there was a statistically significant difference between the treatments and the baseline based on results of ANOVA followed by Dunnett test at  $P \leq 0.05$ .

Compared to the 48h control, significantly higher concentrations were identified for treatments of 5% CARB-B ( $M= 1.34, SEM=0.13 \text{ mg.L}^{-1}, p<0.004$ ), 10% CARB-B ( $M= 1.56, SEM= 0.08 \text{ mg.L}^{-1}, p<0.0001$ ), 5% HFO ( $M= 2.26, SEM= 0.11 \text{ mg.L}^{-1}, p<0.0001$ ), 10% HFO ( $M= 1.65, SEM= 0.05 \text{ mg.L}^{-1}, p <0.0001$ ),  $\text{NO}_3^-$  ( $M= 1.89, SEM= 0.11 \text{ mg.L}^{-1}, p<0.0001$ ), and  $\text{NH}_4^+$  ( $M= 1.53, SEM=0.21 \text{ mg.L}^{-1}, p<0.0001$ ). The chl *a* concentrations in the CARB-B scrubber washwater control, 1% HFO, and the Fe addition treatments were not significantly different from the 48h control at  $p<0.05$ . The Cu treatment chl *a* was significantly lower than the control by 48h ( $M= 0.21, SEM= 0.03 \text{ mg.L}^{-1}, p=0.001$ ).

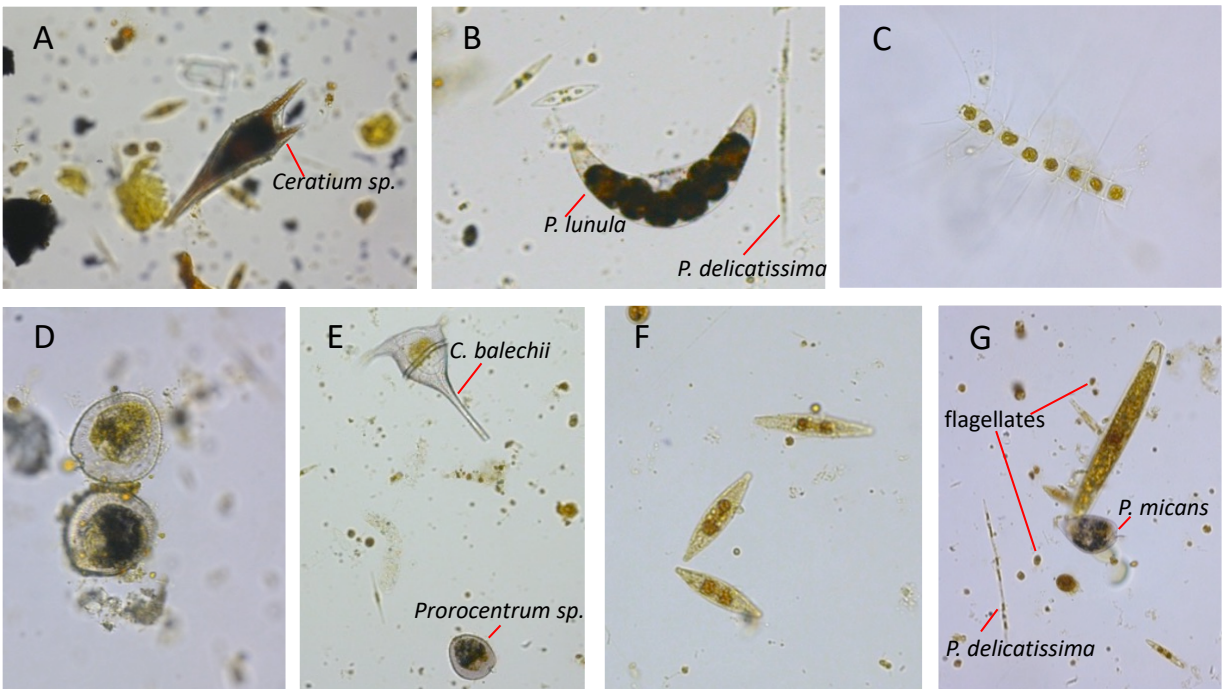


Figure 2.13. Micrographs of representative microplankton observed in the 2021 SCB experiment cell counts. (A) *Tripos sp.*, (B) *Pyrocystis lunula* with *Pseudo-nitzschia* cf. and other diatoms and flagellates surrounding it, (C) *Chaetoceros sp.*, (D) *Prorocentrum sp.*, (E) *Ceratium balechii* (above) and *Prorocentrum sp.* (below) with diatoms surrounding it, (F) *Navicula sp.* (G) *Pseudo-nitzschia* cf. *delicatissima* (left), *Pleurosigma* sp. (above, right), *Prorocentrum micans* (below, right), and flagellates surrounding.

In the 2021 SCB experiment, microplankton were identified and counted in baseline samples from time 0, and in the control, 5% and 10% CARB-B, and 1%, 5%, and 10% HFO treatments at 48h (Fig. 2.12). All treatments samples were counted in triplicates except for the following, which were counted in fewer than three replicates due to sample losses: baseline (counted in duplicate), control at 48h (one sample only), 10% HFO (counted in duplicate). Representative examples of cell types are shown in Fig. 13. Statistical analyses were conducted on total community counts, as well as separately for dinoflagellates, centric diatoms, pennate diatoms, and flagellates (> 3 mm). Statistical comparisons between the control and other treatments at 48h was complicated by the unfortunate loss of control replicates. Accordingly, here we describe the changes among treatments relative to the baseline at T0 using one-way ANOVA followed by Dunnett tests, while comparisons to the control are stated semi-quantitatively.

Mean abundance for the total microplankton for all treatments at 48h ranged from  $M= 6.56 \times 10^6$  ( $SD=1.26 \times 10^6$ ) cells.L<sup>-1</sup> in the 5% CARB-B treatment to  $M= 1.18 \times 10^7$  ( $SD= 2.07 \times 10^6$ ) cells.L<sup>-1</sup> in the 10% HFO and were not significantly different from the time 0 baseline ( $M=9.73 \times 10^6$ ,  $SD=1.91 \times 10^5$  cells.L<sup>-1</sup>). The single sample counted for the 48h control had a notably smaller abundance of total cells ( $5.68 \times 10^6$  cells.L<sup>-1</sup>) compared to the other treatments (Fig. 2.12 a). The only significant differences observed across all microplankton groups at T48 h and their corresponding baseline samples at T0 occurred for pennate diatoms, which significantly decreased from  $M=8.74 \times 10^5$  ( $SD=6.36 \times 10^3$ ) cells.L<sup>-1</sup> to  $M=5.40 \times 10^5$  ( $SD= 5.20 \times 10^4$ ) cells.L<sup>-1</sup> in the 10% CARB-B ( $p=0.02$ ) and significantly increased to  $M=1.37 \times 10^6$  ( $SD=1.23 \times 10^5$ ) cells.L<sup>-1</sup> in the 5% HFO treatment (Fig. 2.12 d). Flagellates were the dominant group at time 0 (71% of the total abundance), and remained so after 48h of

incubation, ranging from 53% of the total abundance in the 5% CARB-B treatment to 76% of the total in the 10% HFO treatment. The next most numerous microplankton group was that of centric diatoms (Fig. 2.12 c), followed by the pennate diatoms (Fig. 2.12 d), including genera common to coastal California such as *Thalassiosira*, *Navicula*, *Pseudo-nitzschia*, among others (Fig. 2.13). Dinoflagellates had the smallest relative abundance of all taxa groups, and their mean abundance ranged from  $5.48 \times 10^4$  ( $SD=2.42 \times 10^4$ ) cells.L<sup>-1</sup> in the 1% HFO treatment and  $1.35 \times 10^5$  ( $SD=7.21 \times 10^4$ ) cells.L<sup>-1</sup> in the 10% CARB-B (Fig. 2.12 b), including genera common to coastal California such as *Tripos* (previously known as *Ceratium*), *Prorocentrum*, *Dynophysis*, and *Pyrocystis* (Fig. 2.13).

The picophytoplankton community in the 2021 SCB experiment included picoeukaryote and *Synechococcus* populations. The mean concentration of picoeukaryotes in the initial unamended seawater at time 0 was  $5.3 \times 10^4$  ( $SEM=5.1 \times 10^3$ ) cells. mL<sup>-1</sup>. After 48h, all treatments declined in abundance relative to the baseline. Compared to the unamended control ( $M=1.4 \times 10^4$ ,  $SEM=1.2 \times 10^3$  cells.mL<sup>-1</sup>), and to the scrubber washwater control ( $M=1.4 \times 10^4$ ,  $SEM=4.1 \times 10^2$  cells. mL<sup>-1</sup>), at 48 h, picoeukaryotes abundance significantly increased ( $p<0.05$ ) in three treatments: the 5% CARB-B ( $M= 2.1 \times 10^4$ ,  $SEM= 1.9 \times 10^3$ ) cells. mL<sup>-1</sup>, the 10% CARB-B ( $M=2.1 \times 10^4$ ,  $SEM=3.3 \times 10^3$ ) and the NO<sub>3</sub><sup>-</sup> addition ( $M= 2.4 \times 10^4$ ,  $SEM= 3.5 \times 10^3$  cells. mL<sup>-1</sup>) treatments. Picoeukaryotes abundance decreased in the Cu addition relative to the control at 48h ( $M=3.8 \times 10^3$ ,  $SEM= 2.1 \times 10^2$ ). None of the other treatments were significantly different from the control.

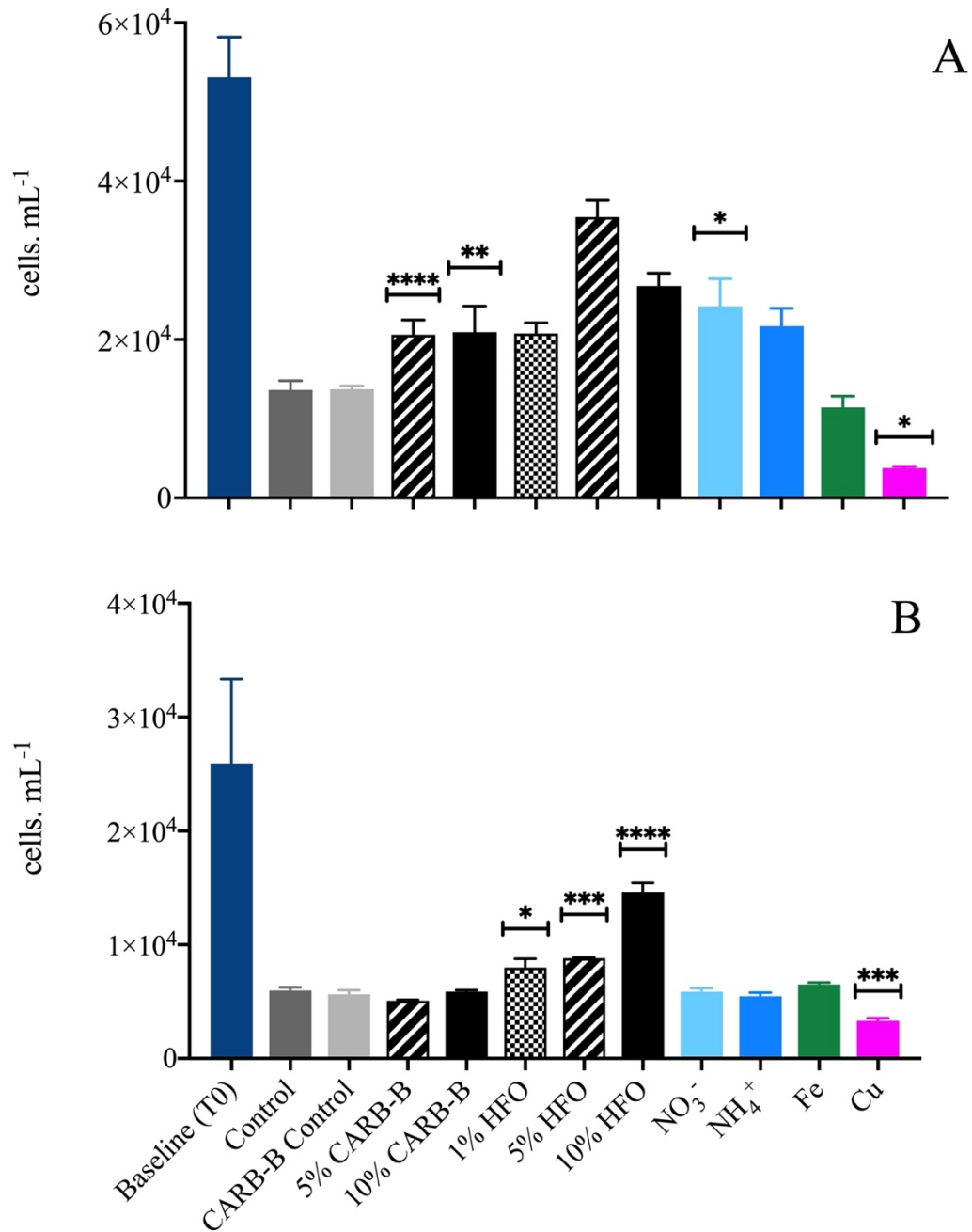


Figure 2.14. Cell concentrations of (A) picoeukaryotes and (B) *Synechococcus* at 48h in the 2021 SCB experiment. Error bars show standard error of the mean. Asterisks indicate that there was a statistically significant difference between the treatments and the control based on results of ANOVA followed by Dunnett test at  $P \leq 0.05$ . One asterisk (\*) means  $P \leq 0.05$ , two (\*\*) mean  $P \leq 0.01$ , three (\*\*\*) mean  $P \leq 0.001$ , and four (\*\*\*\*) mean  $P \leq 0.0001$ .

Likewise, there was considerable decline in *Synechococcus* abundance in all treatments at 48h compared to the concentration in the time 0 baseline ( $M=2.6 \times 10^4$ ,  $SEM= 7.4 \times 10^3$  cells. mL<sup>-1</sup>). Compared to the control ( $M= 6.0 \times 10^3$ ,  $SEM= 3.0 \times 10^2$  cells. mL<sup>-1</sup>) and to the scrubber washwater control ( $M=5.6 \times 10^3$ ,  $SEM= 3.6 \times 10^2$  cells. mL<sup>-1</sup>), the following treatments were significantly higher: 1% HFO ( $M= 8.0 \times 10^3$ ,  $SEM= 790$  cells/mL 5% HFO,  $M=8.8 \times 10^3$ ,  $SEM=68$ ), 10% HFO ( $M=1.5 \times 10^4$ ,  $SEM=8.2 \times 10^2$  cells.mL<sup>-1</sup>). *Synechococcus* abundance decreased in the Cu addition treatment relative to the control at 48h ( $M=3.3 \times 10^3$ ,  $SEM= 2.1 \times 10^2$  cells. mL<sup>-1</sup>). None of the other treatments were significantly different from the control.

## DISCUSSION

Coastal waters differ from the open ocean in that they tend to have higher nutrient and metal concentrations due to proximity to land-based sources and diverse phytoplankton communities comprising multiple taxonomic groups with different nutrient requirements and toxicity thresholds ((Bristow et al., 2017; Chavez et al., 1991; Herbert, 1999; K. R. M. Mackey et al., 2010b; Richardson & Ledrew, 2006; Sunda & Huntsman, 1995b; Voss et al., 2011). In certain coastal regions, especially those along major trade routes, the density of shipping traffic may also be elevated relative to the open ocean (Comer et al., 2020; T. J. Moore et al., 2018; Osipova et al., 2021). Emissions from ships in these regions is therefore high, and the longer residence times in some coastal ports and embayments may concentrate chemical outputs from ships (Jalkanen et al., 2021, 2009; Jutterström et al., 2021; Manner et al., 2009; Merico et al., 2016; Raudsepp et al., 2019b, 2013). The experiments conducted in this study were intended to gauge the acute effects of ship emissions discharges in scrubber water on coastal phytoplankton communities. Together they show that different members of the phytoplankton community respond uniquely to scrubber inputs. The growth and



community composition responses were related to the amount of scrubber water added and the type of fuel that was combusted, the coastal species that were present, and the antecedent conditions of the experiment sites at the start of each experiment. In two of the experiments (KS 2019 and SCB 2021) significant declines in chl<sub>a</sub> and cell counts were observed between the baseline at time zero and all treatments at 48h, including the controls. These shifts in baselines were likely caused by the unusually high values for these parameters at time zero and could also be related to methodological (“bottle”) effects. For this reason, the analyses presented here focus on comparisons between the control and the addition treatments at 48h (and not to baseline values).

### **The KS 2019 Experiment**

Primary production in the KS varies seasonally as follows: production rates are low in winter (November to February) due to light limitation, followed by major spring blooms (March to April) that quickly deplete nutrients in surface waters. Production in the summer (June to September) is relatively low and constant, but wind-induced entrainment of nutrient rich bottom water to the surface layer can induce episodic blooms. Autumn blooms usually begin in September because of degradation of the thermocline (Carstensen et al., 2004; Henriksen, 2009; Murray et al., 2019). Overlaid on this natural cycle, phytoplankton production in the area is driven by large anthropogenic nutrient inputs from land runoff. Eutrophication is a considerable environmental problem in the Baltic Sea that affects the KS (Nehring, 1992; Rosenberg et al., 1990), but bioassay studies have shown that summer primary production in the KS is usually nitrogen limited (Granéli et al., 1990; Wasmund & Uhlig, 2003).

The initial (time 0 baseline) concentration values of N+N and NH<sub>4</sub><sup>+</sup> measured in the unamended seawater that was used in the KS 2019 experiment ( $M= 1.35 \pm 0.31 \mu\text{M}$  and  $M= 2.48 \pm 0.80 \mu\text{M}$ , respectively) were well above the usual summertime range for these parameters in the KS. For context, values measured by Kristineberg Center for Marine Research Station staff near our collection site in July, August, and September of 2018, and in early July of 2019 were all below 0.12  $\mu\text{M}$  N+N and 0.2  $\mu\text{M}$  NH<sub>4</sub><sup>+</sup> (Lars Ljungqvist, personal communication, August 29, 2019). We attribute the high N values that we encountered to the wind-induced mixing caused by a storm that occurred on August 28, 2019, i.e. the day before the seawater was collected. That explains the mesotrophic levels of Chl-*a* ( $M= 4.82 \text{ mg/L}$ ,  $SEM= 0.27 \text{ mg/L}$ ), and relatively high abundances of microplankton, which was dominated by dinoflagellates ( $M= 2.95 \times 10^5 \text{ cells/L}$ ,  $SEM= 7.29 \times 10^3 \text{ cells/L}$ ), and of *Synechococcus* sp. ( $M= 1.1 \times 10^5 \text{ cells/ml}$ ,  $SEM= 1.2 \times 10^4 \text{ cells/ml}$ ) that we observed in baseline samples at time 0.

After 2 days of incubation, Chl-*a* concentration and *Synechococcus* sp. abundance significantly declined in all treatments, except for the 10% HGO treatment, in which those parameters were found to be significantly higher than in the controls. In all treatments, the abundance of microplankton groups, including dinoflagellates, and the abundance of picoeukaryotes remained the same from the time 0 baseline to the 48h time point, except for the 5% HGO treatment, in which the abundance of picoeukaryotes significantly increased, and for the 10% HGO treatment, in which the abundance of both picoeukaryotes and dinoflagellates significantly increased. Meanwhile, a significant N+N drawdown was observed in the 10% HGO treatment (and in the added N treatment). These trends suggest that the components added by the HGO scrubber washwater spikes caused an overall

fertilization effect on the micro- and picoplankton communities at 10% final concentration and that they fertilized picoeukaryotes at 5% concentration. We infer that the nitrogen enrichment caused by the addition of HGO scrubber washwater into natural seawater played a major role in this experiment's outcomes. At the time of collection, the phytoplankton community was responding to a N:P ratio of 1.35 N: 0.09 P or ~15:1, which is just below the canonical Redfield optimal of 16N:1P (Redfield, 1934). The addition of the HGO scrubber washwater spike at 10% final concentration subjected the entrapped phytoplankton to a concentration of N+N that was ~3.7 times higher than what the phytoplankton in the control bottles experienced. At the same time, the HGO scrubber washwater spike added relatively little  $\text{PO}_4^{+}$  (~0.02  $\mu\text{M}$  added to the background 0.09  $\mu\text{M}$   $\text{PO}_4^{+}$  concentration). Thus, in 10% HGO treatment, the N:P ratio was approximately 3 times higher (i.e. 5.03N: 0.11 P or ~ 46:1) than in the control at time 0, and that likely supported the noticeable increase in dinoflagellate abundance, which was almost double the dinoflagellate abundance observed in the control at 48h. The fertilizing effect caused by the addition of 10% HGO scrubber washwater was also reflected in the Chl-*a* concentration for that treatment, which was almost triple of that in the control.

Our results are in line with findings from other authors that conducted a similar study. Ytreberg et al (2019) documented that, relative to the control, microplankton from natural Baltic Sea experienced a significant increase in Chl-*a* following exposure to 10% open-loop scrubber washwater after a 13 day- mesocosm incubation experiment. The scrubber washwater these authors used in their experiment was produced using the same testbed engine and scrubber unit used to produce the HGO scrubber washwater spikes for the present study, but they used Marine Gas Oil (MGO) with 1% sulfur content which, like

HGO, is a distillate fuel that is sometimes used by ships as an alternative to HFO. Like us, these authors inferred that the results were a consequence of nitrate enrichment. These authors also conducted laboratory experiment with this scrubber washwater and two monocultures: one with the filamentous cyanobacteria *Nodularia spumigena* and the other with the diatom *Melosira cf. arctica*. They observed negative responses in photosynthetic activity for *N. spumigena* but increased primary productivity for *M. cf. arctica*, implying species-specific responses to scrubber washwater exposure (Ytreberg et al., 2019). In another experiment (Ytreberg et al., 2021) authors tested the effects of 1%, 3% and 10% open-loop MGO scrubber washwater (also produced at the Chalmers testbed facility's small engine and scrubber) on a natural community of Baltic Sea pelagic microplankton, during a 14-day laboratory experiment. They observed significant increases in total biovolume of microplankton in the 3% and the 10% scrubber treatments. Group-specific impacts were recorded: diatoms, flagellates *incertae sedis*, chlorophytes and ciliates increased in biovolume with increasing concentrations of scrubber washwater while no effect was recorded for cyanobacteria. Changes in biovolume were not observed in the present study, but once again, these authors identified nitrogen enrichment as a likely driver of the observed changes in microplankton abundance and community composition.

Here, it is possible that P limitation in the 10% HGO gave an advantage to the dinoflagellates that were already dominating the community at time 0. Dinoflagellates are known to survive phosphate depletion by activating certain enzymes, such as alkaline phosphatases (AP), to use dissolved organic phosphorus instead of phosphate (Girault et al., 2021; Lin et al., 2016; K. Mackey et al., 2012). The capacity to use AP varies greatly across

taxa with possible consequences for microbial community composition (Labry et al., 2008; Shen et al., 2022).

The availability of certain dissolved metals is also known to affect microbial community composition (Browning & Moore, 2023; Sunda & Huntsman, 1995a; Twining & Baines, 2013; Viljoen et al., 2019). The HGO spike used in this experiment contained high amounts of dissolved Fe and somewhat high amounts of Co, Cu, Ni. However, the background concentrations of these metals were relatively high, which may have annulled major effects these metals could have on phytoplankton physiology. Dissolved Fe (dFe) concentration measured in the baseline sample was  $\sim 70$  nM. Bioavailable dFe limits primary production in over 30% of the ocean surface, where its concentration normally ranges from 0 to 0.2 nM, depending on complex chemical and biological factors, such as water temperature, pH, and the presence of ligands (Arnone et al., 2022; Hutchins & Bruland, 1998; K. S. Johnson et al., 1997; Sarmiento & Gruber, 2006; Sunda & Huntsman, 1995b; Trapp et al., 2010). In contrast, dFe is abundant and rarely limits production in most coastal and semi-enclosed ocean areas. In parts of the Baltic Sea, dFe is known to occasionally reach values higher than 100 nM (Gelting et al., 2010; Magnusson & Westerlund, 1983; Pohl & Fernández-Otero, 2012). In the KS 2019 experiment, the Fe addition treatment (10 nM) probably resulted in an oversaturation of dFe (80nM) and lead to no significant changes in Chl-a concentration, or in picoplankton abundances, which corroborates the notion that dFe was not limiting phytoplankton growth in this experiment. Based on measurements made with the 100% HGO scrubber washwater spike, we estimate that the 5% HGO treatment represented an enrichment of  $\sim 15$ nM dFe and the 10% HGO treatment added  $\sim 30$  nM dFe, thus resulting in even higher final concentrations than in the Fe addition treatment.

Dissolved copper enrichment in the 5% and 10% HGO treatments were estimated to be ~1 and 2nM, respectively. These values were relatively small compared to the background dCu concentration in the baseline sample (~14 nM) and very small compared to the Cu addition treatment of 1  $\mu$ M, which caused significant declines in Chl-a concentration, picoeukaryotes, and *Synechococcus* sp. abundances. The toxic effects of Cu leading to declines in phytoplankton abundance and Chl-a are well documented in the literature (Jordi et al., 2012; Lopez et al., 2019; Mann et al., 2002; Paytan et al., 2009a). Other authors have measured dCu concentrations in the KS (Magnusson & Westerlund, 1983) and those values are comparable the ones we documented in the present study. Relatively high concentrations of Cu, and other metals such as Co and Ni occur in several parts of the Baltic Sea, including the KS, and are associated to natural sources, such as leaching from forest and other land areas, or anthropogenic sources, such as antifouling paint and industries (Magnusson and Westerlund, 1980; Sonesten et al., 2021; Ytreberg et al., 2022). It is plausible to assume that microplankton communities in this region are adapted to high metal concentration conditions (i.e. chronic exposure), and to eventual pulses from intermitted inputs (i.e. acute exposure). While we don't suppose the amounts of dissolved Fe, Cu, Co, and Ni that were added by the scrubber washwater spikes used in this experiment were high enough to affect the overall productivity levels in this region, we highlight the fact that many of these metals can play synergistic roles in the production of certain enzymes and other metabolic functions, thus possibly affecting community composition in ways that the methods used in this study are not suitable to detect. Precise taxonomical identification of microplankton was not a goal in this study and was beyond our methodological capacity, which relied on the use of light microscopy. Nevertheless, we were able to determine that

the high abundance of dinoflagellates consisted of a mixed bloom dominated by organisms that resembled those in the *Azadinium*, *Amphidoma*, and *Heterocapsa* genera (AAH complex). AAH complex dinoflagellates are alike in size and morphology, and impossible to distinguish without the use of molecular methods (Karlson et al., 2010, 2021). All three genera are cosmopolitan and known to occur in the KS (Hällfors, 2004; Infrastructure, 2023; Wietkamp et al., 2019). Some species in the *Azadinium* and *Amphidoma* genera can be toxic and cause Azaspiracid Shellfish Poisoning (AZP) in humans after consumption of contaminated seafood. In the Baltic Sea and KS, AZA-producing microalgae and their respective toxins have been documented in low abundance but are widely present in the area (Wietkamp et al., 2019). Some *Heterocapsa* species are known to produce toxins (D. Kim et al., 2000; Wu et al., 2022), while others may form non-toxic harmful algal blooms (HABs). *H. triquetra* for example, causes extensive blooms in low salinity temperate coastal waters during the summer that can lead to water discoloration and hypoxia at cell densities above  $5 \times 10^3$  cells  $L^{-1}$  (Olli, 2004), which is two orders of magnitude lower than the values documents in the present study. To be clear, due to methodological limitations, our results do not unequivocally show that the HGO scrubber washwater addition affected the HAB-forming species. However, HABs are a recurrent issue in this region that causes losses for the aquaculture industry and other negative environmental and socioeconomic impacts (Karlson et al., 2021). Coastal summer blooms of *H. triquetra* have been associated to eutrophication and local artificial mixing caused by large passenger ferries in the Baltic Sea near Finland (Lindholm & Nummelin, 1999). Therefore, we recommend further studies to be conducted to further investigate what effects scrubber washwater discharges, and that metal inputs in general, may have on specific HAB-forming species.

## The SCB 2020 Experiment

Primary production in the SCB is largely limited by nitrogen availability in the euphotic zone (Cullen & Eppley, 1981; Thomas et al., 1974), but great spatial and temporal variability exists (Kilpatrick et al., 2018; Legaard & Thomas, 2006; Mantyla et al., 2008; Venrick, 2012). Near the coast, seasonal mixing and upwelling of nutrient-rich deep water maintains high rates of biological productivity in the winter and spring. During most of the year, coastal CA is N limited, but the upwelling of deep water with high N:Fe ratios can at times lead to Fe (co)limitation (King and Barbeau 2011), particularly in coastal regions with narrow continental shelves that limit entrainment of sediment-derived Fe (Bruland et al. 2001). Anthropogenic nutrient inputs can be significant in some areas of the SCB that receive discharge from water treatment facilities in the region (Howard et al., 2014), and winter runoff from three highly channelized, human-impacted rivers (Santa Ana, Los Angeles, and San Gabriel Rivers).

In the SCB 2020 experiment, which occurred in October, the time 0 baseline concentration values of chl a ( $M=0.39 \text{ mg}\cdot\text{L}^{-1}$ ), N+N ( $M= 0.2 \text{ }\mu\text{M}$ ) and  $\text{NH}_4^+$  ( $M= 0.38 \text{ }\mu\text{M}$ ) measured in the unamended seawater used as controls were within the ranges expected for the SCB region in fall (Bograd et al., 2015; Howard et al., 2014; McLaughlin et al., 2021). The N:P ratio at time 0 was 0.2N:0.15P, or  $\sim 1.3$ . This low N:P ratio is considered normal for this area of the SCB, which corresponds to the southern section of the California Current ecosystem (A. C. Martiny et al., 2016; Schnetzer et al., 2013). The low N:P ratio at time 0 help explain the phytoplankton responses observed due to the nitrogen enrichment that happened in all treatments of this experiment, except for the 5% CARB-A. The phytoplankton in the 10% CARB-A treatment were exposed to a N+N concentration that was  $\sim 3.5$  times



higher than what was experienced by the microorganisms in the baseline samples, and that likely promoted the observed increase in chl *a*, which almost doubled in that treatment compared to the control at 48h. The addition of CARB-A SW did not cause NH<sub>4</sub><sup>+</sup> enrichment. The ~10 μM of NO<sub>3</sub><sup>-</sup> added in the NO<sub>3</sub><sup>-</sup> treatment, corresponded to a 45-fold increase in N+N relative to the baseline values and it was the likely cause for the doubling in Chl-*a* concentration observed in that treatment compared to the control at 48h. Finally, the added ~1 μM NH<sub>4</sub> in that treatment corresponded to a 2.6-fold increase in NH<sub>4</sub><sup>+</sup> concentration and was associated to a 2.5-fold increase on chl *a* concentration relative to control at 48h. We were unable to monitor changes in microplankton groups in this experiment, but we speculate that taxa in that size range (i.e. 3-100 μm) probably increased in the treatments in which chl *a* increased (i.e. 10% CARB-A, NO<sub>3</sub><sup>-</sup>, NH<sub>4</sub><sup>+</sup>), since picoeukaryotes and *Synechococcus* abundances either decreased or remained the same in all treatments compared the baseline at time 0 and the controls at 48h.

Primary production in coastal waters is rarely limited by trace metals (Martin, 1990), but experiments have demonstrated that growth limitation by iron can occur in certain coastal upwelling regions, including in sections of coastal California (Hutchins et al., 1998; Hutchins & Bruland, 1998). In the SCB 2020 experiment, the added 10 nM Fe treatment did not stimulate changes in chl *a*. Based on metals measured in the 100% CARB-A spike, we deduce that the enrichment of dFe, dCu, and other dissolved metals in the 5% and 10% CARB-A treatments was negligible, except for dMn, which according to our estimate, increased from an already high background value of 11 nM to 22 nM. For context, a study that measured dMn along surface transects in the North Coast of CA (38.4–39.3°N) in August of 2011, documented onshore dMn concentrations ranging from 2.1 to 11.3 nM, where the highest

dMn concentrations were sampled in the freshly upwelled plume on the southern portion of the transect (D. V Biller & Bruland, 2013). Like Fe, Mn is required for the maintenance of photosynthetic machinery, and Mn is known to co-limit phytoplankton in parts of the Southern Ocean, where dMn availability is very low (Browning & Moore, 2023; Pausch et al., 2019). Considering that the dMn background concentrations observed in our study were relatively high, we conclude that the influence of the dMn added by SW spikes was likely negligible.

### **The SCB 2021 Experiment**

The SCB 2021 experiment was conducted on July 27, 2021. The mean Chl-*a* concentration ( $M=2.12$ ,  $SEM=0.07$  mg/L) was within the expected ranges for this region but slightly elevated for this time of the year (Eppley, 1992; H.-J. Kim et al., 2009; Legaard & Thomas, 2006). Cell counts for pico-, nano- and microplankton were also relatively high. We posit that the microbial community that we captured at time 0 was at the peak of a bloom which was likely triggered by nutrient enrichment caused by vertical mixing, runoff, and nutrient enrichment associated with an unusual storm system that moved into Southern California bringing record-setting rainfall, two days before our collection (Cappucci, 2021). By the time we collected the water, nutrients were very low (all measurements of N+N,  $NH_4^+$  and  $PO_4^{3-}$  in baseline samples values were below or at the LOQ). Thus, we posit that by the time we collected the baseline samples, nutrients that were elevated by the storm, had already been depleted by the abundant microbes, which would explain the abrupt decline we observed in chl *a* and cell counts between the control at time 0 and at 48h.

Comparing the chl *a* concentration across all treatments at 48 h (Fig. 2. 11), we notice that all addition treatments ended up at higher values than the control, which suggests that

components in all spikes used in this experiment fertilized the entrapped phytoplankton. As in the two previous experiments conducted in this study, nitrogen played an important fertilizing role as evidenced by the positive chl *a* response in the two N addition treatments. However, in this experiment, we notice something different: the treatment that ended up with the highest chl *a* values at 48h was not an N addition one, but the 5% HFO SW treatment. That happened even though the N addition treatments added ~20 times more N+N and 15 times more NH<sub>4</sub><sup>+</sup> than the 5% HFO treatment (Fig. 2.10). That, combined to the observation that the chl *a* value for the 10% HFO treatment was lower than in the 5% HFO, suggests that besides nitrogen there were other components in the HFO spike (possibly metals) that fertilized at least certain phytoplankton at 5% HFO concentration, but that suppressed net growth at the 10% concentration. At 1% concentration, the HFO addition had no measurable effect on chl *a*. As in the KS 2019 and SCB 2020 experiments, the addition of relatively high (10 nM) concentration of dFe alone, did not affect any of the metrics we used to monitor the microbial community, while the addition of (0.5 μM) dCu caused toxicity. Looking at the responses by different microplankton groups (Fig. 2.12), we see that pennate diatoms increased in the 5% HFO treatment, decreased in the 10% CARB-B, and did not significantly change in other treatments relative to the baseline and control. As with the chlorophyll *a* trends, it is impossible to determine the exact causes of this increase in pennate diatoms abundance observed in the 5% HFO treatment; it could be connected to the variety of metals present in high concentration in the HFO scrubber washwater formulation (Table 2). Compared to the initial water used in the incubation (baseline samples), the 10% HFO spike contained relatively high concentrations of dAl, dCo, dCu, dFe, dMn, dNi, and dV. While some of these metals are well-known to fertilize phytoplankton (Fe, Co, Mn), others may be

toxic to certain groups when in high concentrations. Cu, for instance, has been shown to both stimulate and suppress phytoplankton growth depending on several complex factors, including chelation, interactions with other chemical components, and taxa-specific sensitivity (Kong, 2022; Lopez et al., 2019). In the present study, the 10% HFO treatment is estimated to have exposed marine phytoplankton to an additional 6 nM of dCu, which is a relatively high concentration. Bottle experiments conducted in the Sargasso Sea showed that additions of 2 and 5 nM Cu decreased the growth rates of *Prochlorococcus*, while *Synechococcus* net growth rates only decreased in their 5 nM Cu (Mann et al., 2002). Cu toxicity to marine diatoms has also been documented but usually at much higher concentration exposures than 6 nM (Anu et al., 2016; Cid et al., 1995; Florence & Stauber, 1986; Neethu et al., 2021; Stelmakh et al., 2022). Ni and dV were also estimated to be high in the 10% HFO treatment (~93 and 412 nM, respectively). The effects of these two metals on marine phytoplankton have been studied by many. While Ni seems to have limited toxic impact on most phytoplankton in temperate regions, even at concentrations several orders of magnitude higher than the ones we observed (J. A. Guo et al., 2022), V has been found to be toxic to microorganisms (Gustafsson, 2019; Nalewajko et al., 1995; Rehder, 2022; Ünsal, 1982; Watt et al., 2018). More research to investigate taxa-specific sensitivities to these metals would be needed to elucidate the impacts of the 10% HFO additions to coastal phytoplankton communities.

The CARB-B addition treatments behaved somewhat similarly to what was observed in the SCB 2020 experiment with CARB-A spikes. Here, we saw an increase in chl *a* in the 10% CARB-B treatment relative to control at 48h. However, in the 2021 experiment, we saw a lower but significantly positive effect produced by the 5% CARB-B treatment, which was

not observed in the SCB 2020 5% CARB-A treatment. We did not observe any significant changes in microplankton groups in response to CARB-B addition, but picoeukaryotes abundance significantly increased in both the 5% and the 10% CARB-B relative to all other treatments at 48h. Note that the CARB-B spike contained a much higher amount of dFe (and dPb) than the CARB-A spike (Table 1), whereas other metals concentrations were either comparable to, or lower in the CARB-B formulation. CARB-A and CARB-B spikes were generated using the same fuel type combusted in similar small boat engines, and we conjecture that chemical composition differences in these spikes were caused mainly by the combustion temperature, which was higher in the CARB-B case, because boat B was cruising at a higher speed and rpm than boat A at the time the SW was produced and collected. Although we cannot unequivocally explain the effects that N, metals, and other possible chemical constituents had on the microbial abundance and composition in these treatments, these results suggest that components added by scrubber washwater discharges can influence phytoplankton communities after acute exposure in ways that vary depending on factors such as the fuel type, temperature of combustion, and initial condition of the receiving seawater. Polyaromatic hydrocarbons (PAHs), for example, could be playing a role in the selective impacts of scrubber washwater additions observed here. PAHs have been measured in scrubber washwater samples (Lunde Hermansson et al., 2021; Tronczynski et al., 2022; Ytreberg et al., 2022b), and have been found to cause lethal and sublethal effects on marine phytoplankton (Bopp & Lettieri, 2007; Cerezo & Agustí, 2015; Echeveste et al., 2016; Kottuparambil & Agusti, 2018, 2020; H. Ben Othman et al., 2012). Also, the influence of other processes that we did not investigate here, such as complex inter-specific competition for nutrients, metal chelation dynamics (Hirose, 2006; Hutchins et al., 1999;

Raspor et al., 1980; Sunda, 2012), and co-limitations (C. M. Moore et al., 2013b; Saito et al., 2008) cannot be ruled out.

In summary, our results match what has been found in previous experiments conducted to measure scrubber washwater impacts of coastal phytoplankton (Marin-Enriquez et al., 2023; Picone et al., 2023b; Ytreberg et al., 2019, 2021). As these other authors, we found that coastal phytoplankton response varied greatly, and included fertilization effects of some phytoplankton groups and complex shifts in abundance and composition. variable deleterious effects were observed for these phytoplankton grazers. The variability in responses documented in all these studies is likely due to the wide range of sensitivity of various microbial taxa to the many possible combinations of components present in the different types of scrubber washwater used in the experiments.

It is important to acknowledge that, although the exposure concentrations used in this study (1%, 5% and 10%) were comparable to what has been used in similar experiments by other authors, these values are well above the expected range of concentration that phytoplankton communities would experience in most ocean areas upon the discharge of scrubber washwater by any individual vessel. As explained in chapter 1 of this dissertation, the dilution of scrubber washwater discharges will vary greatly depending on the depth of the mixed layer, which in turn varies with geography and season. If we consider that the volume of water that is influenced by a ship's discharge water is a function of the ship's beam (typically, 10-50 m), speed (typically, 8-20 knots), and the thickness of the layer of water in which the scrubber wash water discharge will dissolve we can deduce that the typical exposure concentrations caused by the passage of an individual vessel will necessarily be

<0.1%. It is safe to assume that exposure to scrubber washwater concentrations higher than 5% would be extremely unlikely, even in the case of shallow, stratified, and heavily trafficked areas.

## **CONCLUSIONS**

The goal of the present study was to evaluate the effects of different scrubber washwater formulations on phytoplankton growth, nutrient uptake, and community composition, and to investigate potential mechanisms underlying observed responses, including the role of trace metals, and nutrient availability. Acute (48 h) exposure to extremely high (5% and 10%) concentrations of various formulations of scrubber water caused the artificial fertilization of certain groups of coastal phytoplankton populations. Here, this effect seems to be driven mostly by nitrogen enrichment caused by the scrubber washwater additions, which is in line with what has been documented in previous studies. However, in at least one of the experiments we conducted (SCB 2021), the 5% HFO scrubber washwater exposure treatment resulted in a greater increase in chl *a*, and in picoeukaryotes abundance than exposure to the 10% HFO SW treatment, even though the latter added double the amount of nitrogen to the incubation bottles. That suggests that other components in the HFO scrubber washwater formulation used in this study, likely trace metals and possibly PAHs, which we did not measure, may have impaired the growth of certain phytoplankton groups at 10% but not at 5% concentration exposure. This disproportionate impairment in growth at high exposure particularly affected eukaryotes and picoeukaryotes.

## CHAPTER 3

### PHYTOPLANKTON RESPONSES TO SCRUBBER WASHWATER ADDITIONS IN THE COASTAL AND OPEN-OCEAN SARGASSO SEA.

#### ABSTRACT

This research evaluated the impact of ship scrubber washwater discharges on natural phytoplankton communities in both the open and coastal regions of the Sargasso Sea. The goal was to ascertain whether the washwater generated from burning two different fuels had a fertilizing, inhibiting, or neutral effect in this oligotrophic system, where picophytoplankton are prevalent. Both the conventional heavy fuel oil combusted in a large ship engine (HFO) and the alternative distilled fuel from a small testbed engine (HGO) exhibited a mild fertilizing effect on oceanic phytoplankton at a 2% concentration. The HGO formulation specifically had a fertilizing impact on *Synechococcus* and potentially enhanced *Prochlorococcus* fluorescence. The results indicate that microbial populations in the Sargasso Sea were not solely restricted by nitrogen (N) or iron (Fe), but likely experienced co-limitation by multiple nutrients, which were adequately supplied by scrubber washwater discharges at a 2% concentration, but not at 0.1% or lower.

#### INTRODUCTION

Marine phytoplankton do half of all photosynthesis on Earth and influence global biogeochemical cycles, food webs, biodiversity, and climate. To grow, phytoplankton need dissolved macronutrients, such as nitrogen and phosphorus, and relatively smaller amounts of micronutrients, such as trace metals and vitamins (Antoine et al., 1996; Bunt, 1975; P. G. Falkowski et al., 1998; P. Falkowski & Knoll, 2011; Field et al., 1998; Martin, 1992; Martin & Fitzwater, 1988).

Early models of marine primary production were based on Liebig's law of the minimum and assumed primary production to be limited by the nutrient in shortest supply relative to microbial requirements in any given marine community (Baird et al., 2022). Recent studies have described a more complex picture in which chemical, physical,



physiological, and ecological interactions can lead to nutrient co-limitation in many ocean regions (Browning et al., 2017; Browning & Moore, 2023; C. M. Moore et al., 2013b; Saito et al., 2008, 2015).

Browning and Moore (2023) provided a comprehensive review of nutrient limitation patterns in the ocean and showed that nitrogen serves as the primary limitation in stratified subtropical gyres and in summertime Arctic Ocean, while bioavailable iron commonly limits primary production in upwelling regions. Co-limitation of both nitrogen and iron occurs frequently in boundary regions between the nitrogen and iron limited systems. In parts of the Southern Ocean, manganese can be co-limiting with iron, and in certain settings, phosphate and cobalt can be either co-limiting or serially limiting. The review's key conclusion is that surface seawaters often approach nutrient co-limitation of some kind. Thus, increases in the supply of various nutrients at once can significantly enhance phytoplankton net growth, irrespective of latitude, temperature, or trophic status. It is therefore clear that understanding nutrient sources and their influence on phytoplankton abundance and activity is a vital quest for comprehending and forecasting how environmental shifts can affect marine ecosystem responses. Central to this quest, are the roles that natural and anthropogenic sources of nutrients play in coastal and open-ocean areas.

Nutrient availability in the euphotic zone results from the regeneration of organic matter, or from the influx of “new” nutrients from external sources (Dugdale & Goering, 1967). Two main physical processes control most new nitrogen input into the ocean: turbulent vertical mixing, and upwelling (Sarmiento & Gruber, 2006; Sverdrup, 1953; Voss

et al., 2011, 2013). Vertical mixing occurs throughout the world's oceans and is particularly important in higher latitudes, where eddies and strong winds can overcome stratification and bring nutrients from deeper layers to the surface (Bendtsen & Richardson, 2018; Henson et al., 2013; Tesdal et al., 2022; Tsutsumi et al., 2020; Williams et al., 2013). Upwelling is important in certain coastal regions and divergence zones (Chavez & Messié, 2009; Romera-Castillo et al., 2016). Additional sources of new nitrogen include nitrogen fixation (Canfield et al., 2010; Gruber & Sarmiento, 1997; Mills & Arrigo, 2010; Monteiro et al., 2011), groundwater (Slomp & Van Cappellen, 2004), rivers (Meybeck, 1993; S. V Smith et al., 2003), runoff from land (Beman et al., 2005; Carpenter et al., 1998; V. H. Smith & Schindler, 2009) and atmospheric deposition (Duce et al., 2008; Ito et al., 2014; T. D. Jickells et al., 2017; Kanakidou et al., 2016).

The deposition of atmospheric aerosols to the ocean's surface is a major source of new nitrogen and trace metals to the open ocean (Altieri et al., 2021; T. D. Jickells et al., 2017; X. Zhang et al., 2020) and a smaller source in coastal regions (K. R. M. Mackey et al., 2010b). Atmospheric aerosols are solids or liquids suspended in air of diverse origins, and of various sizes and chemical composition. Natural aerosols transported by strong wind events are the most significant source of nutrients to the open ocean by mass. Globally, desert dust provides most of the N, P, and trace metals available to marine phytoplankton in the open ocean, including aluminum (Al), titanium (Ti), manganese (Mn), and iron (Fe). Additionally, anthropogenic emissions from fossil fuel combustion and biomass burning represent important sources of nutrients in some coastal and open-ocean areas (Bowie et al., 2009; Farahat & Abuelgasim, 2019; Fu et al., 2015; Guieu et al., 2005; C. Guo et al., 2022; Hamilton et al., 2022; Meng et al., 2016; Pinedo-González et al., 2020; Y. Wang et al., 2022; Xiao et al.,

2018). Atmospheric deposition of macro- and micronutrients can alleviate nutrient limitation, spur growth, and alter the composition of phytoplankton communities. Under some circumstances, aerosol trace metal inputs have also been shown to cause toxicity to certain phytoplankton populations (T. D. Jickells et al., 2017; Jordi et al., 2012; Paytan et al., 2009a).

Several authors have identified shipping-derived Fe as a potentially significant source of bioavailable Fe in areas where maritime traffic is intense and other sources of Fe are scarce. For instance, shipping may be responsible for up to 50% of the soluble Fe input into remote northern hemisphere and equatorial Pacific HNLC ocean regions (Ito, 2013b; Matthias et al., 2010; Raudsepp et al., 2019c; Salo et al., 2016). Overall, it is estimated that Fe emissions from anthropogenic biomass burning and from the combustion of fossil fuels, including ship emissions, are two orders of magnitude smaller than mineral dust Fe by mass, but may account for up to 50% of the bioavailable Fe deposited in remote HNLC ocean regions due to higher solubility compared to that of mineral dust. Specifically, shipping contributes a relatively small (~2%) source of Fe; however, the solubility of oil combustion-derived Fe is significantly higher (36–81%) even when compared to other fossil fuel sources such as coal (0.2–25%) (N. M. Mahowald et al., 2018). Therefore, given the global geographical distribution of shipping lanes across the world's oceans, ship emissions could be an important source of Fe affecting phytoplankton in certain marine environments.

Ship emissions are known to release significant amounts of nitrogen and sulfur oxides (NO<sub>x</sub> and SO<sub>x</sub>) in addition to other metals, some of which can serve as nutrients that promote (e.g., Fe, Mn, Zn, Co) or inhibit (e.g., Cu) phytoplankton growth. Due to great variability in

the types of ship engines and quality of fuels being used by maritime transport, the chemical composition and particle size distribution of aerosols from ship emissions is expected to vary greatly (M. Anderson, Salo, Hallquist, et al., 2015; Corbin et al., 2018; Eyring et al., 2010a; Moldanová et al., 2009a; Popovicheva et al., 2009, 2012; Salo et al., 2016). To reduce air pollution from shipping activities, the governmental of several nations, and the International Maritime Organization (IMO) passed regulations that limit the concentration sulfur in ships air emissions. To comply with these rules ship operators can do one of two things: they can switch from the highly polluting residual fuels known as heavy fuel oil (HFO) to more expensive alternative fuels or, in some parts of the world, they can use exhaust gas cleaning systems, also known as scrubbers.

Scrubbers are pollution abatement devices that remove pollutants from the exhaust gasses by spraying water on it before it comes out from the ships' smokestacks. Most ships that are equipped with these systems have open-loop scrubbers that discharge the washwater directly into the ocean (Comer et al., 2020; Osipova et al., 2021; Turner et al., 2017; Zis et al., 2022). Scrubber washwater discharges contain variable types and amounts of chemical components (Koski et al., 2017; Lunde Hermansson et al., 2021; Teuchies et al., 2020; Thor et al., 2021) and can affect the growth of marine phytoplankton (Picone et al., 2023; Ytreberg et al., 2021, 2019; Tavares et al in prep.), depending on its chemical composition, which seems to vary with fuel quality, size of the engine, age of the vessel, speed and load, among other factors (Marin-Enriquez et al., 2023; Schmolke et al., 2020).

The effect of nutrients from scrubber washwater discharges on phytoplankton populations is also influenced by the interplay of natural factors such as geographical

location and taxon-specific differences, including nutrient requirements and growth rates. Along the Atlantic Meridional Transect (AMT) for example, the Saharan dust plume over the tropical North Atlantic causes a strong interhemispheric difference in dust loadings, with much lower dust supplies over the tropical South Atlantic. Consequently, higher average concentrations of Fe are found in surface water of the North Atlantic gyre (Ussher et al., 2013). That, in turn, causes an increase in nitrogen fixation by diazotrophs, which require high Fe concentrations to grow, and therefore leads to a decrease in the concentration of P in these waters (Mark Moore et al., 2009). These geographical and biological factors can further influence competition and succession of different phytoplankton functional groups, including picoplankton that thrive in oligotrophic environments. Geography also affects shipping lanes and the interaction between these multiple factors ultimately determines the relative importance of scrubber wash water discharges for marine biogeochemistry and microbial ecology.

Predictions from modelling studies along with the different geographical complexities introduced from the overlay of biogeographical regions and shipping lane locations, suggest that the effects of different scrubber wash water discharge scenarios on marine phytoplankton could be highly variable (Tavares et al, in prep). An important next step in this area of research is therefore to identify and characterize the relationships and patterns of ship emissions and scrubber water discharges as they relate to marine phytoplankton communities. Here, we investigate the effects of ship scrubber water discharge on natural phytoplankton assemblages in the open and coastal North Atlantic Ocean using bottle incubation experiments. In this oligotrophic environment where picophytoplankton such as *Synechococcus*, *Prochlorococcus*, and picoeukaryotes dominate,

we sought to determine if scrubber water discharge causes fertilization, inhibition or neutral/null effects in these oligotrophic open ocean and eutrophic coastal ocean marine biomes, and to determine which nutrients and trace metals, if any, are important in influencing phytoplankton growth and community composition.

More specifically, the goal of this study was to evaluate phytoplankton growth responses to scrubber washwater additions in an oligotrophic open-ocean and compare them to responses in the microbial communities from nutrient-rich coastal waters. Incubation experiments with varying concentrations (0.01%, 0.1% and 2%) of two types of scrubber washwater (HFO and HGO) were conducted in Sargasso Sea in early fall of 2021. Different responses among phytoplankton subpopulations at the two sites (oceanic vs coastal) reveal variations in metal requirements and sensitivity. The study highlights how anthropogenic impacts can alter regional marine biogeochemistry by providing nitrogen and trace metals to phytoplankton communities, offering insights into ecosystem dynamics in marine environments with diverse nutrient inputs.

## **MATERIALS AND METHODS**

### **Study Area**

The Sargasso Sea is an ocean region bounded by the Gulf Stream, the North Atlantic Current, the Canary Current, and the North Atlantic Equatorial Current, which form the North Atlantic Gyre. The island of Bermuda, and the Bermuda Atlantic Time-series Study area (BATS) are located at the northwestern boundary of the Sargasso Sea, in a transition region between relatively eutrophic waters to the north and an oligotrophic subtropical

convergence zone to the south (Siegel et al., 1990; Talley & Raymer, 1982; Woods & Barkmann, 1986). This southern region is characterized by high sea surface temperatures and a geostrophic downwelling zone that provide consistent vertical stratification during most of the year making it a suitable location for the investigation of the impacts of scrubber wastewater discharges on phytoplankton communities from oligotrophic regions.

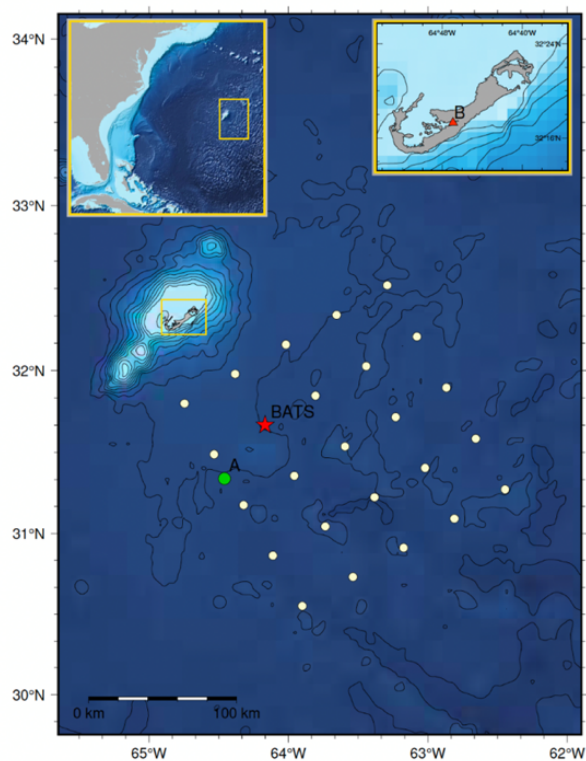


Figure 3.1. Map showing the location of the sampling location for the oceanic experiment (A), the nearby Bermuda Atlantic Time-Series Station (BATS, red star) Rectangle in the upper right corner shows the site where the coastal water was collected in Hamilton Harbor, Bermuda (B). Rectangle in the upper left corner shows the location of Bermuda in the North Atlantic Ocean.

### Initial Conditions

To understand how water column characteristics may have changed due to the passage of Hurricane Larry over this region days before we begun our experiments, on Sept 8., 2021, we compare water column chemistry parameters that were measured at

Hydrostation S during casts on BATS cruise 385 (Sept. 13, 2021, or three days before the incubation water for the oceanic experiment was collected) and the prior cruise 384 (Aug. 20, 2021). Measurements of temperature, salinity, photosynthetically active radiation (PAR), chlorophyll fluorescence, and dissolved oxygen were made using a Sea-bird 9/11 CTD aboard the R/V *Atlantic Explorer*. Samples were taken from the rosette Niskin bottles at discrete depths of 4, 10, 20, 40, 60, 80, 100, 120, 140, 160, 200, and 250m for NO<sub>3</sub><sup>-</sup> (plus negligible NO<sub>2</sub><sup>-</sup>), PO<sub>4</sub><sup>3-</sup>, SiO<sub>4</sub><sup>2-</sup>, chlorophyll a, and flow cytometry. All sample collection and measurements followed the standard procedures for BATS cruises. Weather data for Bermuda was recorded at the L.F. Wade International Airport weather station and was retrieved from weatherspark.com.

### **Incubation Experiments**

Mesocosm incubation experiments were conducted in September of 2021 with seawater collected at open ocean (“oceanic”) and coastal locations in the Sargasso Sea (Figure 3.1). For the oceanic experiment, surface water (10 m) was collected at an offshore site (Station A, 31.3377° N, 64.4585°W) located ~40 km SW of the Bermuda Atlantic Time-series Station (BATS). This collection took place on September 16<sup>th</sup>, a week after the passage of a category 2 hurricane (Hurricane Larry) over this region, which brought winds of 29-46 kt and light rain. The weather remained mostly overcast until the morning of Sept. 16. At the time of the collection (~13:00h), the weather was sunny, wind conditions were mild (4-8 kt), and the mixed layer depth (MLD) was ~50 m. Surface seawater was dispensed from the R/V *Atlantic Explorer*’s rosette of Niskin bottles into clear 10-L polyethylene terephthalate plastic water container bags that had been previously acid-cleaned, following standard procedures to prevent contamination (Cutter et al., 2017). Individual bags were filled with 4



L of seawater and kept in the dark for approximately 4 hours, from collection until arrival at the Bermuda Institute of Ocean Sciences (BIOS).

In the coastal experiment, we used surface water (0-1 m) collected inside Bermuda's Hamilton Harbor (32.2885° N, 64.7821° W), on September 17<sup>th</sup>. At the time of this collection (~10:00h) the weather was sunny and wind conditions were mild (4-8 kt). Ambient seawater was collected by casting an acid-cleaned plastic bucket from the side of a boat. This water was transferred into two acid-cleaned carboys, and the spigots were covered with a mesh (100 µm) to remove grazers as the seawater was dispensed as described above for the oceanic experiment. Bags were filled with 4 L of seawater and kept in the dark for ~2 hours, during transportation to BIOS. Upon arriving at BIOS, untreated samples were immediately processed to establish baseline conditions at time zero (T0), while other bags were spiked with solutions of either scrubber water or nutrients. Two types of scrubber discharge water spikes were used in each of the experiments: heavy gas oil (HGO) scrubber water was produced at a testbed facility operated by Chalmers University, in Gothenburg, Sweden, as described in the methods section in Chapter 1 of this dissertation, and heavy fuel oil (HFO) scrubber water was collected aboard a real ship (ferry RoPax) in a collaboration with German Environmental Agency (Project IMPEX) as described in Chapter 2 of this dissertation. Nutrient and metal solutions used as spikes were prepared using reagent grade chemicals in a laminar flow hood following standard procedures to prevent contamination. Scrubber water treatments used the two types of scrubber wastewater diluted to different concentrations on a vol/vol basis. The final concentrations of treatments were as follows: control (no additions), 0.01% HFO, 0.1% HFO, 2% HFO, 0.1% HGO, 2% HGO, 7.5 µM NO<sub>3</sub><sup>-</sup> (as NaNO<sub>3</sub>), 2 µM NH<sub>4</sub><sup>+</sup> (as NH<sub>4</sub>Cl<sub>2</sub>), and 10 nM Fe.

Once spiked, the bags were incubated under shading material (50% light attenuation) in mesocosm incubation tanks with circulating seawater to maintain surface ocean temperature. The coastal experiment was initiated one day after the oceanic experiment started. Weather conditions during these experiments varied from sunny (during the first 48h of the oceanic experiment and during part of the first 24h of the coastal experiment), to rainy and overcast (from ~24h to 48h of the coastal experiment). To monitor changes in chlorophyll *a* (chl *a*), picophytoplankton cell abundance, as well as the concentration of dissolved macronutrients during the incubation, aliquots of 300-350 mL were dispensed from each of the bags at two time points: day 1 (24 ±3 hours from time zero), and day 2 (48 ±4 hours from time zero). Water soluble trace metals were measured at the beginning (~1 hour from time zero) of each experiment.

### **Macronutrients And Trace Metal Analyses**

For macronutrient analyses of phosphate  $\text{PO}_4^{3-}$  (baseline samples only), ammonium ( $\text{NH}_4^+$ ), and nitrate ( $\text{NO}_3^-$ ) plus nitrite ( $\text{NO}_2^-$ ), reported here as N+N, samples of 40 mL of seawater were filtered through GF/F filters using a peristaltic pump. Samples were stored in acid cleaned 50 mL polypropylene (PP) centrifuge tubes (Corning™ Falcon) and stored frozen at -20 °C until analyses, which were carried out with a flow injection autoanalyzer (FIA, Lachat Instruments, Zellweger Analytix, Inc., QuikChem 8500 Series 2) using standards prepared in Milli-Q water and blanks that were prepared in aged, low nutrient seawater. To determine the detection limit, at least seven replicates of standard solutions (i.e., seawater blanks and spiked samples) that were one- to five-times the estimated detection limit were analyzed and the appropriate *t* value for a 99% confidence interval (*n* - 1) for the number of replicates analyzed was used. The limit of quantification based on three-

times the standard deviation of the blanks was determined to be 0.1  $\mu\text{M}$  for  $\text{PO}_4^{3-}$  and 0.2  $\mu\text{M}$  for N+N and  $\text{NH}_4^+$ .

For the analysis of water-soluble dissolved trace metals, 30 mL aliquots of samples were filtered through acid rinsed VWR 0.2  $\mu\text{m}$  PES sterile syringe filter cartridges in a laminar flow hood and stored in acid cleaned high-density polyethylene (HDPE) bottles until analysis. These aliquots were acidified using distilled HCl at sample to acid volume ratio of 1000:1 under a laminar flow hood. Acidified samples were allowed to sit for two weeks to allow labile and dissolved metals that may have been adsorbed onto the walls of the vials to be recovered. Acidified samples were transported to a trace metal-clean room at the University of Southern California (John Lab).

The analysis of scrubber wash water samples used as spikes (HGO and HFO) were preconcentrated using ten parallel PERIFIX resin columns and prepared according to the following steps detailed in Chapter 2 of this dissertation. The concentrations of water-soluble trace metals in those spikes were measured with a Thermo Element 2 ICPMS using a 100  $\mu\text{L min}^{-1}$  Teflon nebulizer, glass cyclonic spray chamber with a PC<sup>3</sup> Peltier cooled inlet system (ESI), standard Ni sampler and Ni 'H-type' skimmer cones at the Department of Earth Sciences of University of Southern California. The sensitivity and stability of the instrument was tuned to optimal conditions before analyses, which were conducted at sensitivity around  $10^6$  counts  $\text{s}^{-1}$  for 1 ppb In. Both the standard and samples were treated with 1 ppb Indium addition to correct for shifts in instrumental sensitivity and matrix. Elemental concentrations in samples were determined by their signal intensity compared to a 10 ppb multi-element standard, which was diluted from a certified standard (Santa Clarita method).

The method's LOQs were the following: dAl= 0.30 nM, dCd= 0.03 nM, dCo= 0.12 nM, dCu= 0.82 nM, dFe= 3.35 nM, dMn= 0.08 nM, dNi= 0.23 nM, dPb= 0.03 nM, dV= 0.34 nM, dZn= 1.39 nM. Baseline (time zero) samples from the oceanic and coastal experiments were not preconcentrated and were analyzed on an Agilent 8900 triple quadrupole ICP-MS. The method's LOQs were the following: dAl= 0.202 nM, dCd= 0.005 nM, dCo= 0.002 nM, dCu= 0.014 nM, dFe= 0.272 nM, dMn= 0.003 nM, dNi= 0.108 nM, dPb= 0.001 nM, dV= 0.080 nM, dZn= 0.253 nM.

### **Phytoplankton Growth Responses**

For chlorophyll *a* (chl *a*) analysis, 250mL of seawater were filtered through GFF filters (Whatman). Filters were frozen until extraction in 90% acetone and further incubated for 24h at -20 °C in the dark. Chl-*a* concentrations were determined fluorometrically using a Turner Trilogy fluorometer (Turner Designs) calibrated with chl-*a* standard solution derived from *Anacystis nidulans* cyanobacteria (JGOFS, 1994).

Picophytoplankton abundances were determined via flow cytometry. Seawater aliquots (1.5mL) were preserved with 75 µL 10% paraformaldehyde solution, incubated in the dark at room temperature for 10 min, and frozen at -80°C until analysis. Samples were analyzed on a Bio-Rad ZE5 cell analyzer flow cytometer with 405 nm, 488 nm, and 640 nm lasers activated (Center for Aquatic Cytometry, Bigelow Laboratory of Sciences, East Boothbay, ME, USA). Cell abundances were determined for each group. Populations of *Synechococcus* spp., *Prochlorococcus* spp., and picoeukaryotic phytoplankton (cells <3 µm in size containing chlorophyll) were identified in all samples and identified based on their characteristic fluorescence and scattering properties. Two types of detection limits are

relevant for these analyses. The first is a fluorescence intensity threshold (applying mainly to *Prochlorococcus*) that is used to exclude very dim particles on the chlorophyll band. Due to their relatively low cellular chlorophyll quotas and propensity for photobleaching in surface waters, this threshold may exclude *Prochlorococcus* cells with very dim chlorophyll fluorescence. The same gates that were constructed based on the baseline treatments were applied to all treatments including the cases in which populations were dim. In other words, the counts that we do have were made based on a population that was identified in the baseline samples. The second detection limit is a count threshold to ensure accurate statistical conclusions can be drawn when certain populations are rare within a sample. For our measurements, to be considered significant, 100 cells must have been counted in the volume of each sample analyzed (i.e. 300  $\mu\text{L}$  for the oceanic experiment and 100  $\mu\text{L}$  for the coastal experiment). This threshold applied to each of the three groups quantified (*Prochlorococcus*, *Synechococcus*, and picoeukaryotes); populations with counts below this threshold were deemed too rare to accurately quantify.

### **Statistical Methods**

Statistical analyses were conducted using GraphPad Prism Version 10.1. Significant differences ( $P \leq 0.05$ ) were determined using ordinary one-way analysis of variance (ANOVA) followed by either Šídák post-hoc tests, when comparing independent pairs of means (i.e. samples from time 0 vs. time 48h in N drawdown analyses) and Dunnett post-hoc tests, when comparing means from baselines and from various treatments to unamended seawater samples used as controls (i.e. all other variables measured at time zero and at 48h). Asterisks used in all figures correspond to the following levels of significance: one asterisk (\*) means  $P \leq 0.05$ , two (\*\*) mean  $P \leq 0.01$ , three (\*\*\*) mean  $P \leq 0.001$ , and four (\*\*\*\*) mean

$P \leq 0.0001$ . Values below the limit of quantification (LOQ) were substituted by  $\frac{1}{2}$  of the LOQ in all analyses and for all parameters.

## RESULTS

### Initial Conditions

Both the August and September BATS cruises were preceded by weather events that temporarily affected water column characteristics. On Aug. 16-17, a low-pressure system was present, and winds changed from mostly N and E to S. Peak wind speed was  $\sim 17$  mph, gusting up to 30 mph on Aug. 17. The weather was cloudy and overcast with rain showers throughout, and with heavy rain observed on Aug. 17. The weather had changed by Aug. 20 when the depth profile data were taken during cruise 384, the air pressure had increased. South winds remained consistently  $\sim 12$  mph. The weather was mostly clear to partly cloudy. On Aug. 20, 2021, the surface mixed layer extended to 33m, where temperature was  $\sim 28^\circ\text{C}$ , salinity was  $\sim 36.6$  (-), and DO was  $\sim 199$  mmol. kg<sup>-1</sup>. Temperature decreased to  $18.8^\circ\text{C}$  at 250 m. Salinity remained relatively stable throughout the water column, where it slightly increased at 50 and 130 m to 36.7, and then declined back to 36.6 at 250 m. The euphotic depth (taken as 1% of surface irradiance) was 105 m, similar to the depth of the deep chlorophyll maximum (DCM) layer at 107m. DO reached a peak value of 233 mmol/kg at 55m. NO<sub>3</sub><sup>-</sup> and PO<sub>4</sub><sup>3-</sup> were below detection down to 80 m and 100 m, respectively, before increasing to 3.6  $\mu\text{M}$  and 0.16  $\mu\text{M}$  at 250m. Silicate reached a minimum of 0.70  $\mu\text{M}$  at 60 m.

The effects of Hurricane Larry were observed on and around Sept. 9, prior to the September cruise 385, during which the oceanic experiment incubation water was collected. A drop in air pressure was observed, accompanied by N and E winds at 25-30mph that

brought light to moderate rain. Conditions were mostly cloudy to overcast. Four days later, on Sept. 13 when the cast was taken, air pressure had recovered, and east winds below ~10mph were observed. The conditions during the cast were partly cloudy to overcast with episodic light rain in the vicinity.

On Sept. 13, the surface mixed layer had deepened to 50 m, where temperature was ~28 °C, salinity was ~37.1, and DO was ~196 mmol/kg. Below the mixed layer, temperature gradually decreased to 19.0 °C. Salinity showed a secondary peak at 95 m (36.9) before declining to 36.6 at 250m. The euphotic depth was 117 m, and the DCM layer was at 119 m. DO reached a peak value of 235.7 mmol/kg at 75 m. As on the Aug. 20 cast,  $\text{NO}_3^-$  and  $\text{PO}_4^{3-}$  were below detection in the shallow depths down to 100 m and 160 m, respectively.  $\text{NO}_3^-$  increased to 2.81  $\mu\text{M}$  at 250m, and  $\text{PO}_4^{3-}$  increased to 0.11  $\mu\text{M}$  at 250m.  $\text{SiO}_4^{4-}$  was 1.08  $\mu\text{M}$  at the surface and showed a slight decrease within the euphotic zone, reaching 0.801  $\mu\text{M}$  at 60m before increasing to 1.26  $\mu\text{M}$  at 250m.

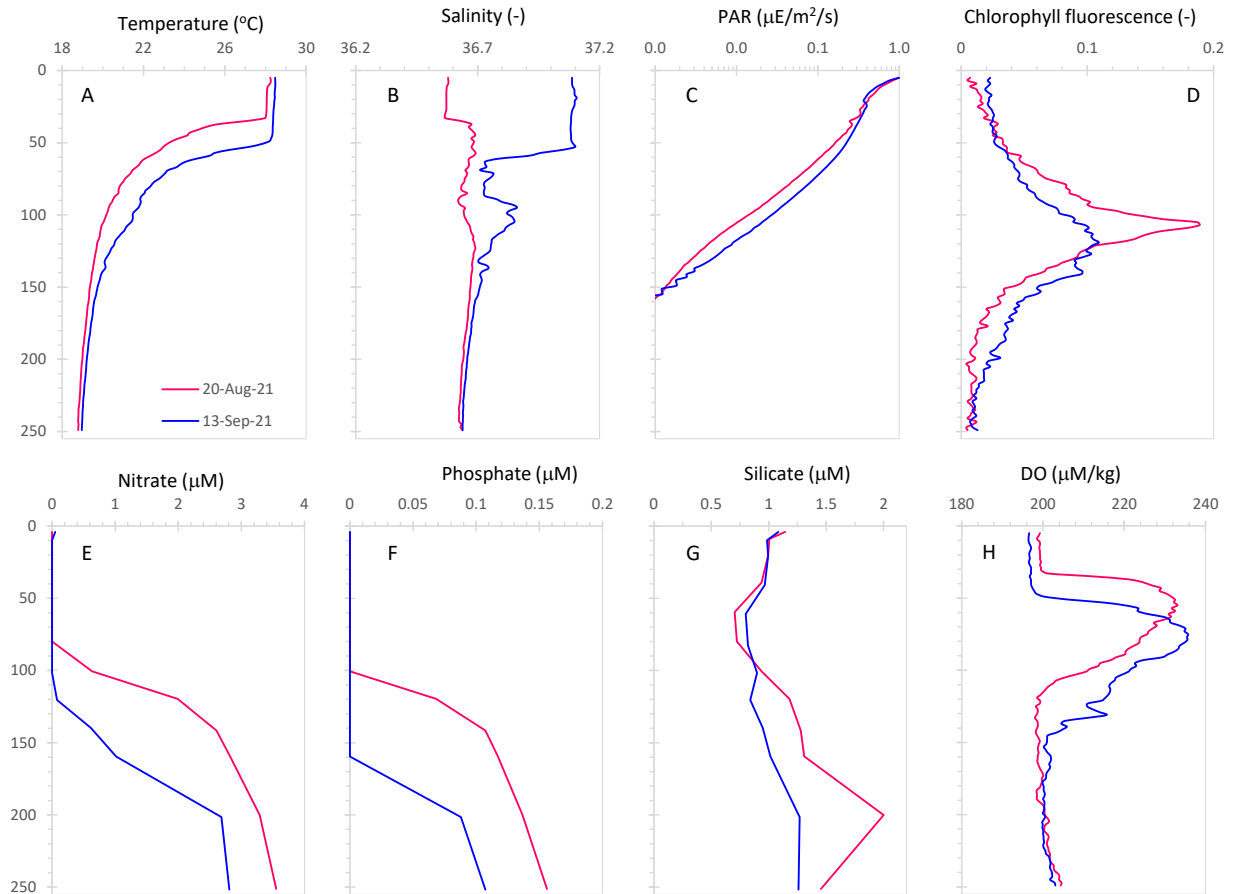


Figure 3.2. Water column conditions at Hydrostation S from casts conducted during BATS cruise 384 on Aug. 20, 2021 (red line) and during BATS cruise 385 on Sept. 13, 2021 (blue line), 3 days before the seawater for the oceanic experiment was collected.

### Macronutrients And Trace Metal Analyses

To assess the consumption of dissolved nitrogen by the phytoplankton exposed to different treatments (i.e., nutrient drawdown), we monitored the concentration of N+N, and  $\text{NH}_4$  during the experiments. In the oceanic experiment, the initial concentrations (baseline values) of  $\text{PO}_4^{3-}$ ,  $\text{NH}_4^+$ , N+N were below the method's detection limits of 0.1, 0.2, and 0.2  $\mu\text{M}$ , respectively. In the coastal experiment, the baselines were 0.23 ( $SEM=0.01$ )  $\mu\text{M}$  for  $\text{PO}_4^{3-}$ , below the method's LOQ of 0.2  $\mu\text{M}$  for  $\text{NH}_4^+$ , and 1.92 ( $SEM=0.13$ )  $\mu\text{M}$  for N+N (Table 1).



The concentrations of N+N in the spikes used for the HFO and HGO treatments (at 100% concentration) were 14.6 (SEM=0.53)  $\mu\text{M}$  in HFO and 19.69 (SEM=1.10)  $\mu\text{M}$  in HGO (Table 2). The initial concentration of N+N in each treatment of both experiments was calculated by adding the baseline values to the diluted values for each treatment. For the oceanic experiment, calculated initial values were as follows: for N+N 0.11  $\mu\text{M}$  for 0.1% HFO, 0.39  $\mu\text{M}$  for the 2% HFO, 0.12  $\mu\text{M}$  for the 0.1% HGO, 0.49  $\mu\text{M}$  for the 2% HGO, and 7.60  $\mu\text{M}$  for the  $\text{NO}_3^-$  addition treatment. For  $\text{NH}_4^+$ , concentration values upon dilution to treatment levels (0.1 and 2%) associated to the HFO and HGO spikes used in all treatments were negligible ( $<0.12 \mu\text{M}$ ). Drawdown of  $\text{NH}_4^+$  was not observed in any treatment of either experiment. In the oceanic experiment N+N drawdown was observed in the 2% HGO treatment (Fig. 3.3 a), and in the coastal experiment, it occurred in all treatments, except for the  $\text{NO}_3^-$  and  $\text{NH}_4^+$  addition treatments (Fig. 3.3 b).

The concentration of dissolved trace metals in the oceanic experiment baseline samples was significantly lower than the values in the coastal experiment baseline samples and are shown in table 1.

Table 3.1. Water chemistry of incubation seawater and corresponding scrubber washwater spikes. Values correspond to means of at least 3 replicates and standard error of the mean is shown in parenthesis. NM indicates that those parameters were not measured. Values below the LOQ are indicated with(\*).Scrubber washwater spike data are reproduced from chapter 1 of this dissertation.

<b>Dissolved components</b>	<b>OCEANIC Baseline</b>	<b>COASTAL Baseline</b>	<b>100% HFO spike</b>	<b>100% HGO spike</b>
Al (nM)	9.07 ( $\pm$ 3.62)	27.55 ( $\pm$ 0.73)	73.53 ( $\pm$ 21.31)	NM
Cd (nM)	0.01 ( $\pm$ 0.00)	0.03 ( $\pm$ 0.00)	0.09 ( $\pm$ 0.02)	*<0.03
Co (nM)	0.07 ( $\pm$ 0.02)	0.24 ( $\pm$ 0.02)	2.86 ( $\pm$ 0.31)	0.66 ( $\pm$ 0.14)
Cu (nM)	1.20 ( $\pm$ 0.14)	23.37 ( $\pm$ 1.15)	62.62 ( $\pm$ 3.75)	18.61 ( $\pm$ 2.22)
Fe (nM)	4.37 ( $\pm$ 1.54)	7.28 ( $\pm$ 0.45)	1,058.74 ( $\pm$ 103.71)	279.65 ( $\pm$ 34.10)
Mn (nM)	2.90 ( $\pm$ 0.15)	4.38 ( $\pm$ 0.29)	51.68 ( $\pm$ 2.59)	5.89 ( $\pm$ 1.07)
Ni (nM)	2.20 ( $\pm$ 0.22)	2.46 ( $\pm$ 0.18)	930.60 ( $\pm$ 43.32)	36.29 ( $\pm$ 6.63)
Pb (nM)	0.03 ( $\pm$ 0.00)	1.27 ( $\pm$ 0.03)	0.91 ( $\pm$ 0.06)	0.52 ( $\pm$ 0.18)
V (nM)	39.30 ( $\pm$ 2.23)	39.21 ( $\pm$ 2.46)	4,117.77 ( $\pm$ 136.57)	0.29 ( $\pm$ 0.07)
Zn (nM)	4.19 ( $\pm$ 1.03)	48.35 ( $\pm$ 2.50)	144.78 ( $\pm$ 30.85)	59.07 ( $\pm$ 12.56)
PO <sub>4</sub> ( $\mu$ M)	*<0.1	0.23 ( $\pm$ 0.01)	0.67 ( $\pm$ 0.06)	0.14 ( $\pm$ 0.01)
N+N ( $\mu$ M)	*<0.2	1.92 ( $\pm$ 0.13)	14.6 ( $\pm$ 0.53)	19.69 ( $\pm$ 1.10)
NH <sub>4</sub> ( $\mu$ M)	*<0.2	*<0.2	3.04 ( $\pm$ 0.56)	5.83 ( $\pm$ 1.34)

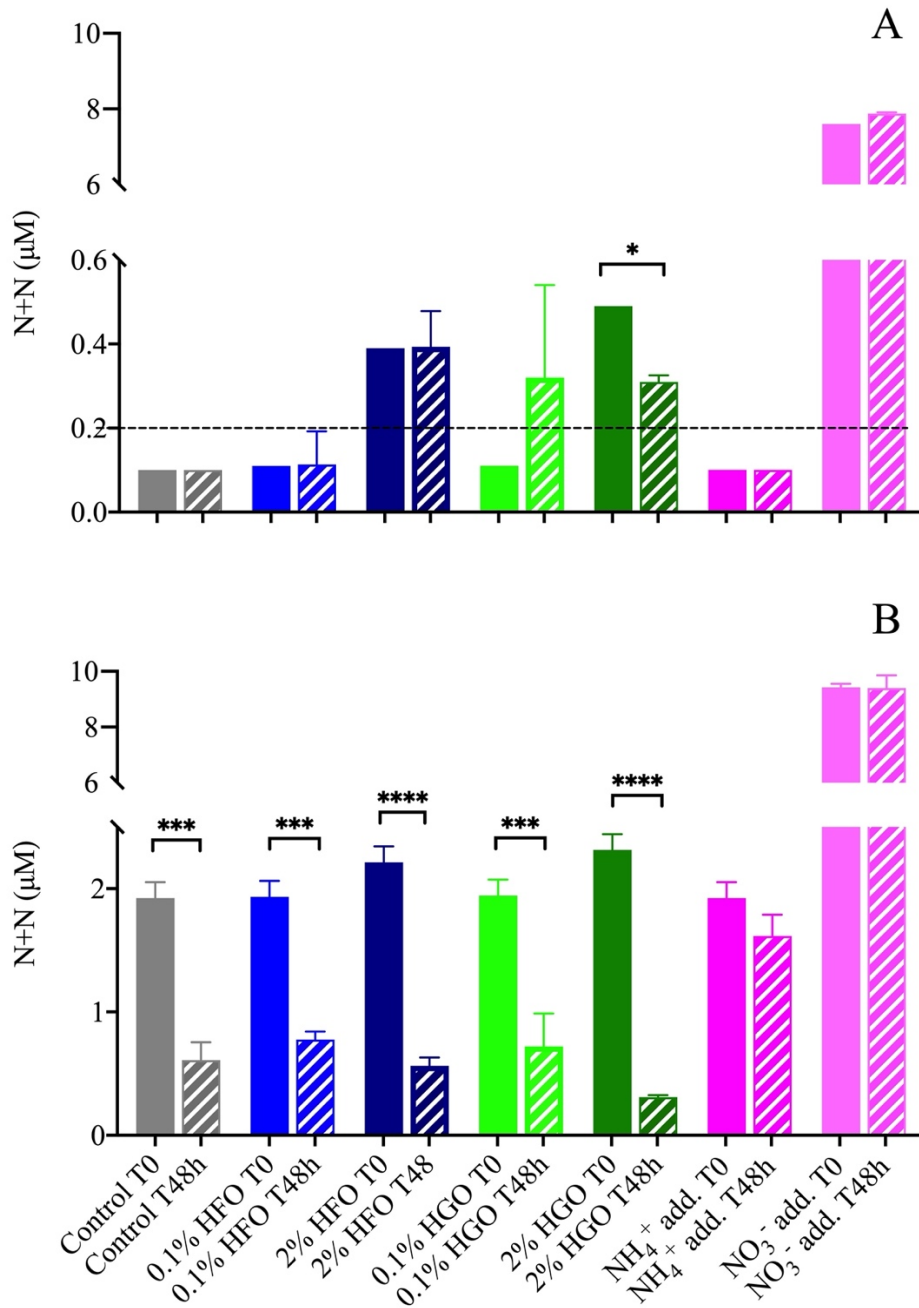


Figure 3.3. Initial and final N+N concentrations in the (A) oceanic experiment, and (B) coastal experiment. Error bars show standard error of mean for triplicate bags. Dashed line in panel A shows the method's LOQ. Asterisks indicate that there was a statistically significant difference between concentrations measured at 0h and 48h for each treatment based on results of ANOVA followed by a Šídák test at  $P \leq 0.05$ . One asterisk (\*) means  $P \leq 0.05$ , two (\*\*) mean  $P \leq 0.01$ , three (\*\*\*) mean  $P \leq 0.001$ , and four (\*\*\*\*) mean  $P \leq 0.0001$ .

## Phytoplankton Growth

### Changes in chlorophyll a concentration

Acute effects of scrubber water additions on total phytoplankton abundance were estimated using chl *a* as a proxy for phytoplankton biomass. Changes in chl *a* concentration were measured after 1 day and 2 days of incubation for all treatments in the oceanic (Fig. 3.4a) and the coastal (Fig. 3.4 b) experiments.

The mean baseline chl *a* concentration in the open-ocean experiment was 0.06 ( $SEM=0.004$ )  $\mu\text{g.L}^{-1}$ . An ordinary one-way ANOVA followed by Dunnett's post hoc test used to compare the scrubber washwater addition treatments to the control ( $M= 0.04 \mu\text{g.L}^{-1}$ ,  $p=0.05$ ) revealed that, after one day, the only significant difference ( $p < 0.05$ ) observed was the higher chl *a* observed in the 2% HGO treatment ( $M= 0.06 \mu\text{g.L}^{-1}$ ). After two days, the chl *a* concentration values in the 2% HFO ( $M= 0.05 \mu\text{g.L}^{-1}$ ) and 2% HGO ( $M= 0.05 \mu\text{g.L}^{-1}$ ) treatments were significantly higher ( $p < 0.001$ ) than in the control at that time point ( $M= 0.03 \mu\text{g.L}^{-1}$ ). There were no other statistically significant differences between the chl *a* in any other treatments relative to the control at these two time points.

In the coastal experiment, the mean initial chl *a* concentration was 2.29 ( $SEM=0.073$ )  $\mu\text{g.L}^{-1}$ . After one day, we observed a significant lower chl *a* concentration in both 0.01 % HFO and 0.1% HFO treatments ( $M= 1.28 \mu\text{g.L}^{-1}$ ,  $p=0.0003$  and  $M= 1.35 \mu\text{g.L}^{-1}$ ,  $p= 0.0008$ , respectively) relative to the control ( $M= 2.00 \mu\text{g.L}^{-1}$ ). On day 1, there were no other statistically significant differences between scrubber water addition treatments and the control. After two days, none of the treatment were significantly different from the control.

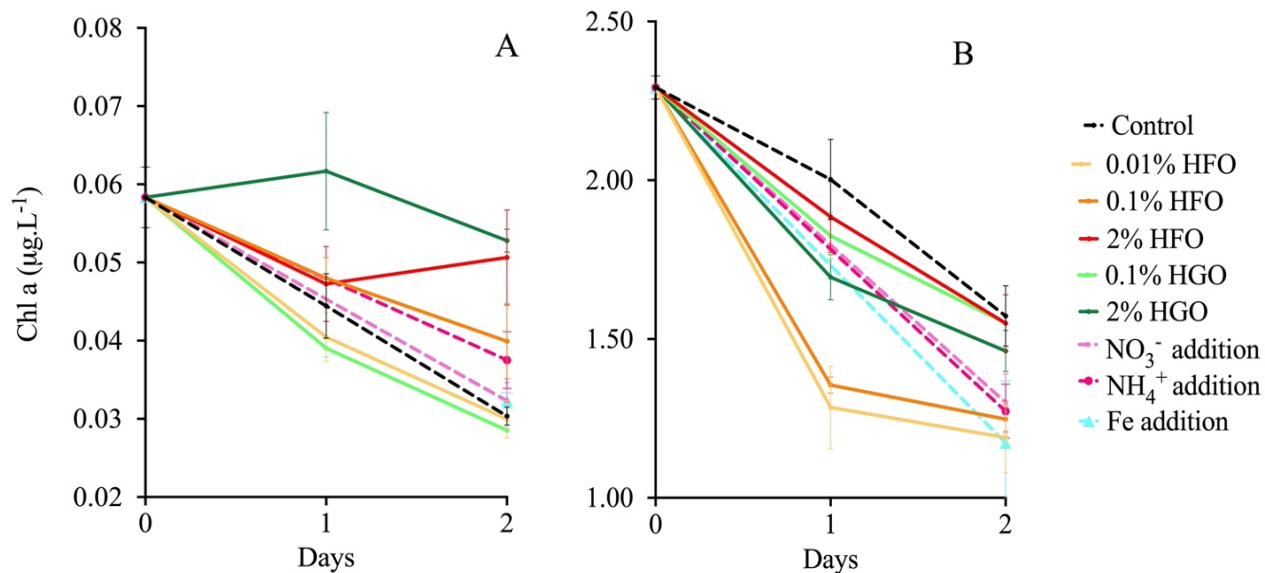


Figure 3.4. Changes in mean chlorophyll a for (a) oceanic experiment and (b) coastal experiment. Error bars show standard error of the mean for quadruplicates.

### Flowcytometry

To quantify the acute effects of scrubber water additions on picoplankton groups, changes in the abundance of *Synechococcus*, *Prochlorococcus*, and picoeukaryotes, were measured at the start of each experiment (baseline) and after two days of incubation for all treatments except the 0.01% HFO treatment. The mean concentration of *Synechococcus* in baseline samples from the open-ocean experiment (Fig. 3.5 a) was  $6.5 \times 10^3$  ( $SEM= 9.8 \times 10^2$ ) cells. mL<sup>-1</sup>. An ordinary one-way ANOVA followed by Dunnett's multiple comparisons test revealed that, after two days, the concentration of *Synechococcus* in the control treatment ( $M= 9.2 \times 10^3$ ,  $SEM= 4.62 \times 10^2$  cells.mL<sup>-1</sup>) was not significantly different from the baseline ( $p= 0.15$ ) and that the only significant difference observed between the control (and the baseline), and any of the treatments was the increase in *Synechococcus* abundance in the 2% HGO ( $M= 1.8 \times 10^4$ ,  $SEM= 7.5 \times 10^2$  cells.mL<sup>-1</sup>). No other significant differences were observed between the control and other treatments on day 2.

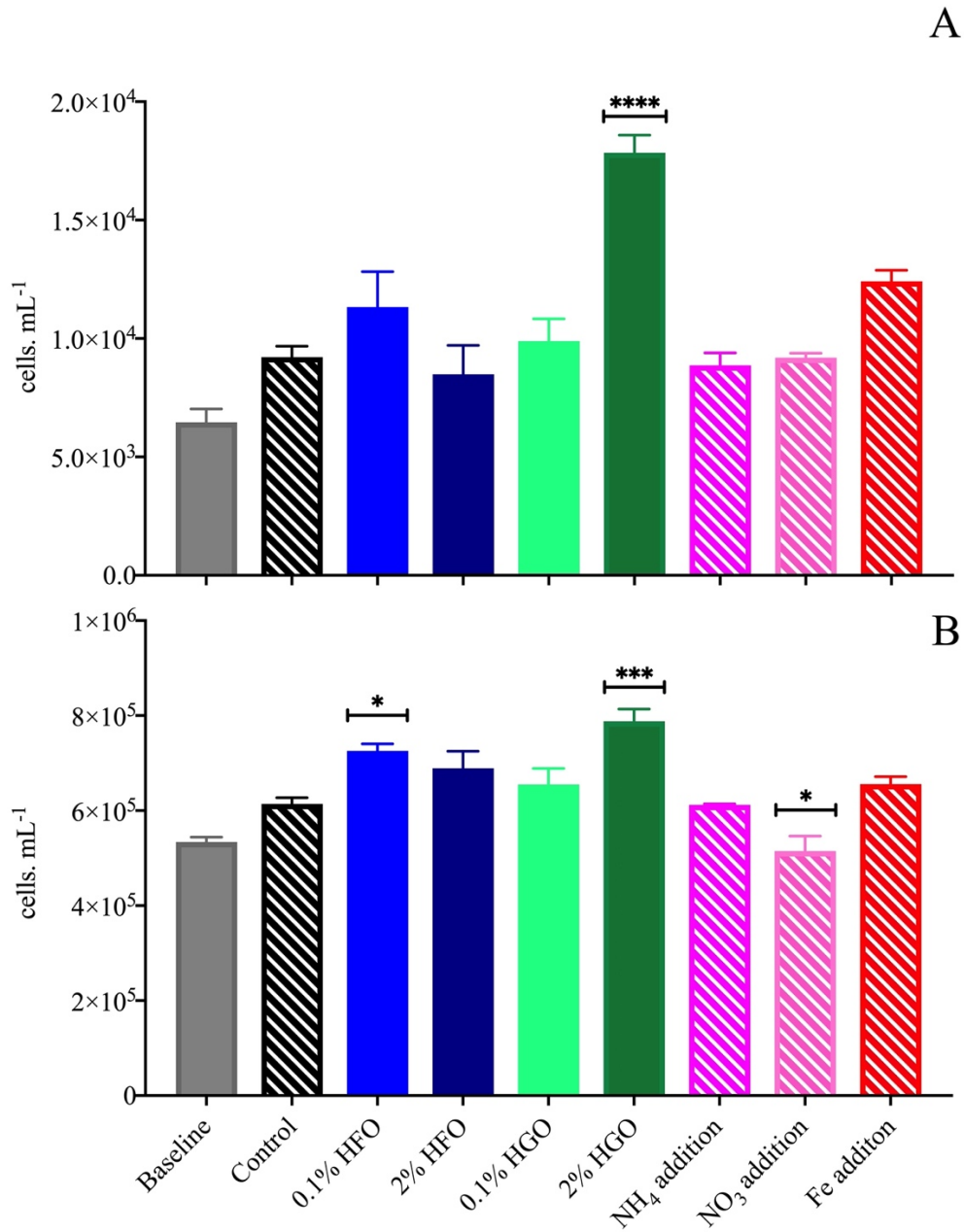


Figure 3.5. Mean *Synechococcus* abundance in (A) oceanic and (B) coastal experiments. Error bars show standard error of the mean for triplicate bags. Asterisks indicate that there was a statistically significant difference between the treatments and the control based on results of ANOVA followed by Dunnett test at  $P \leq 0.05$ . one asterisk (\*) means  $P \leq 0.05$ , two (\*\*) mean  $P \leq 0.01$ , three (\*\*\*) mean  $P \leq 0.001$ , and four (\*\*\*\*) mean  $P \leq 0.0001$ .

In the coastal experiment, the mean concentration of *Synechococcus* in the baseline was  $5.3 \times 10^5$  ( $SEM=1.0 \times 10^4$ ) cells.mL<sup>-1</sup> (Fig. 3.4 b). An ordinary one-way ANOVA followed by Dunnett's multiple comparisons test revealed that, after two days, the concentration of *Synechococcus* in the control treatment ( $M= 6.1 \times 10^5$ ,  $SEM= 1.3 \times 10^4$  cells.mL<sup>-1</sup>), was not significantly different from the baseline and that, relative to the baseline and control, there were significant increases in *Synechococcus* abundance in the 0.1% HFO ( $M= 7.3 \times 10^5$ ,  $SEM= 1.5 \times 10^4$  cells.mL<sup>-1</sup>), and in the 2% HGO ( $M= 7.8 \times 10^5$ ,  $SEM= 2.6 \times 10^4$  cells.mL<sup>-1</sup>) treatments. *Synechococcus* concentration in the NO<sub>3</sub><sup>-</sup> addition treatment significantly decreased relative to the control ( $M= 5.1 \times 10^5$ ,  $SEM= 3.2 \times 10^4$  cells.mL<sup>-1</sup>). No other significant differences were observed between the control and other treatments on day 2.

Analyses of the *Prochlorococcus* populations in both the open-ocean and coastal experiments were hampered by low abundances and the dimness of the cells in several treatments. As discussed in the methods section above, these two measurement issues precluded meaningful statistics from being performed. In the oceanic experiment (Fig. 3.6), *Prochlorococcus* cells were bright enough to be quantified in the following: baseline ( $M= 6.1 \times 10^3$ ,  $SEM= 9.54 \times 10^2$  cells.mL<sup>-1</sup>, Fig. 3.6 and 3.7a), 0.1% HGO ( $M=5.3 \times 10^3$ ,  $SEM= 77.7$  cells.mL<sup>-1</sup>, Figs. 3.6 and 3.7b), 2% HGO ( $M=7.29 \times 10^2$ ,  $SEM= 1.0 \times 10^2$  cells.mL<sup>-1</sup>, Figs. 3.6 and 3.7c), and Fe addition ( $M= 1.4 \times 10^3$ ,  $SEM=2.2 \times 10^2$  cells.mL<sup>-1</sup>, Figs. 3.6 and 3.7d) treatments, while *Prochlorococcus* in all other treatments were too dim to be counted, including in the control (Fig. 3.6, and 3.7e). In the coastal experiment, *Prochlorococcus* cells in all treatments were too dim to be properly quantified, including in the baseline (Fig. 3.6 and Fig. 3.7 f).

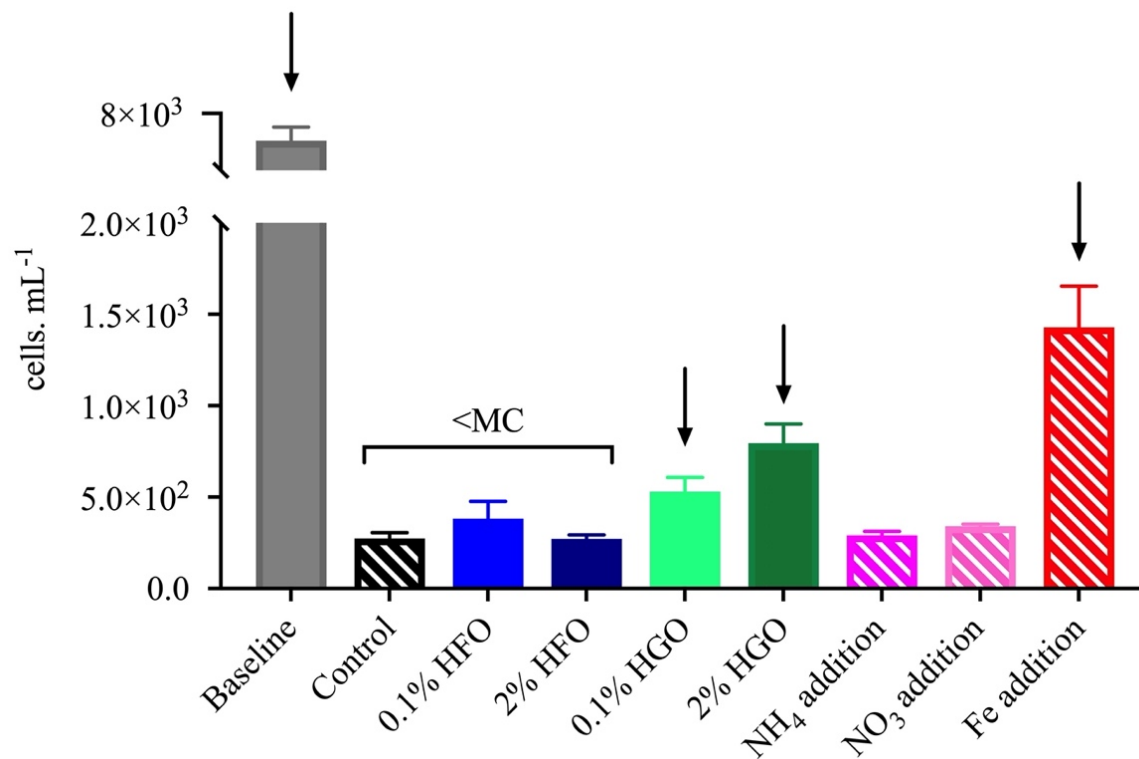


Figure 3.6. Mean *Prochlorococcus* abundance in oceanic experiment. Error bars show standard error of the mean for triplicate bags. Arrows indicate that *Prochlorococcus* in those treatments were bright enough to be quantified. <MC indicates that *Prochlorococcus* in those treatments were below the minimum count threshold of 100 cells in at least two of the triplicate bags.



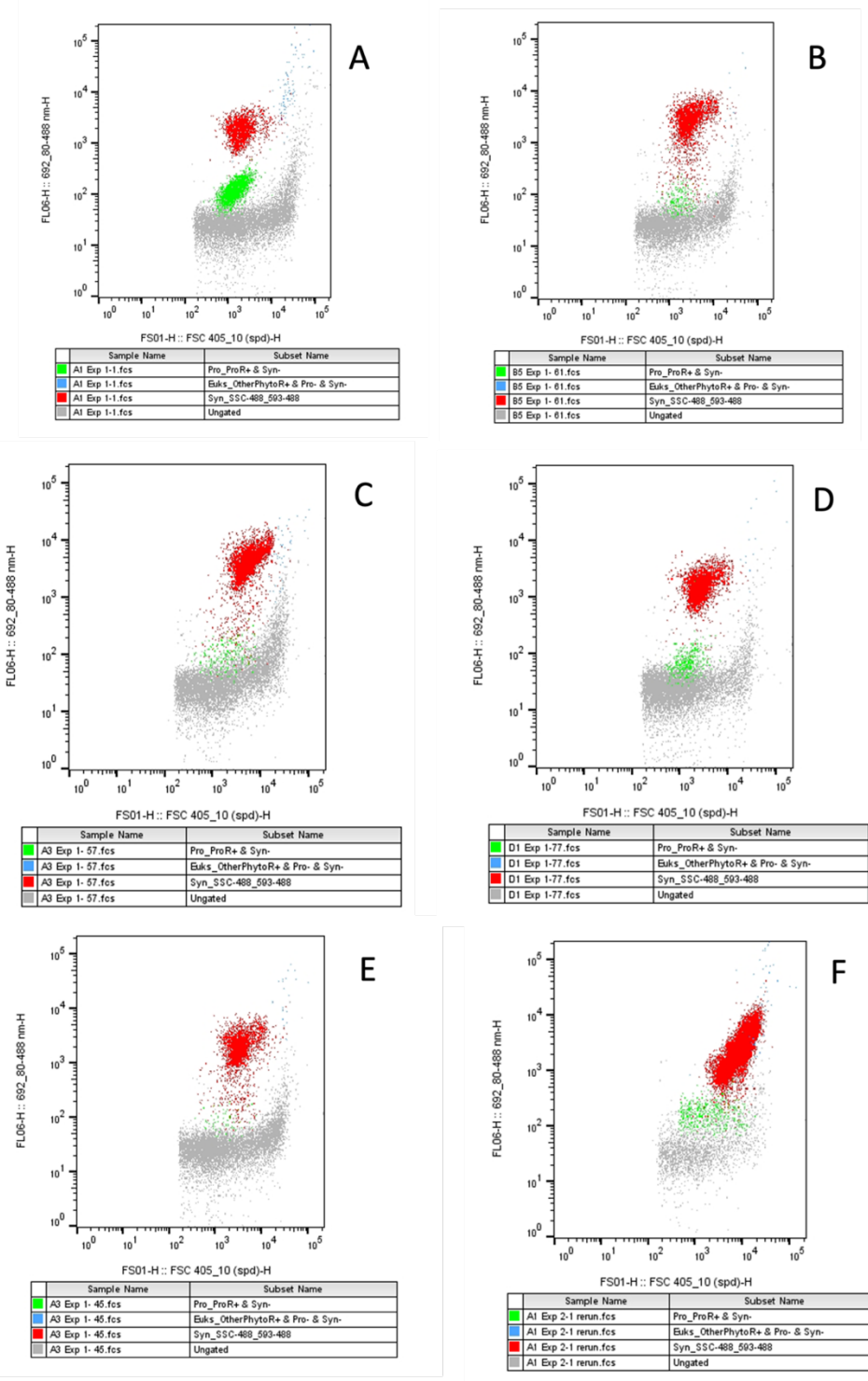


Figure 3.7. Cytograms from pico- and nanophytoplankton analysis. Prochlorococcus is shown in green, Synechococcus in red, and picoeukaryotes in blue, where (A) is the baseline in oceanic exp., (B) is the 0.1% HGO in oceanic exp., (C) 2% HGO in oceanic exp., (D) Fe addition in oceanic exp., (E) control in oceanic exp., (F) is the baseline in coastal experiment.

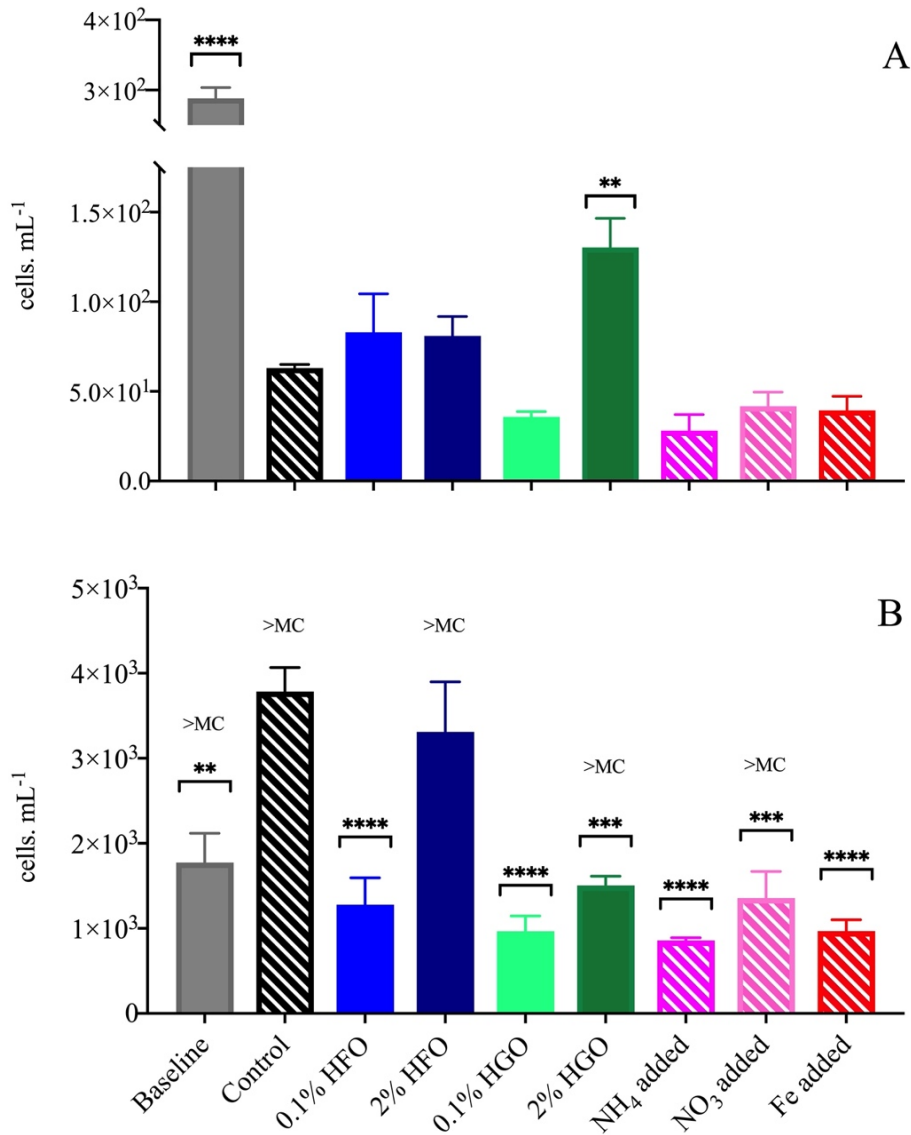


Figure 3.8. Mean abundance of picoeukaryotes in (a) oceanic experiment and (b) coastal experiment. Error bars show standard error of the mean for triplicate bags. Asterisks indicate that there was a statistically significant difference between the treatments and the control based on results of ANOVA followed by Dunnett test at  $P \leq 0.05$ . >MC indicates that the number of cells counted for those treatments were above the minimum count threshold of 100 cells in at least two of the triplicate bags. All others were below the minimum count threshold. one asterisk (\*) means  $P \leq 0.05$ , two (\*\*) mean  $P \leq 0.01$ , three (\*\*\*) mean  $P \leq 0.001$ , and four (\*\*\*\*) mean  $P \leq 0.0001$ .

The mean concentration of picoeukaryotes in all triplicates from all treatments in open-ocean experiment (Fig. 3.8 a) were below the minimum count threshold of 100 cells.

For this reason, the results in this section are presented for semi-quantitative interpretation purposes. The mean concentration of picoeukaryotes in baseline samples from the open-ocean experiment (Fig. 3.8 a) was 288 ( $SEM= 15.2$ ) cells. mL<sup>-1</sup>. An ordinary one-way ANOVA followed by Dunnett's multiple comparisons test revealed that, after two days, the concentration of picoeukaryotes in the control treatment ( $M= 63$ ,  $SEM= 2$  cells.mL<sup>-1</sup>) was significantly different from the baseline ( $p < 0.01$ ) and that the only significant difference observed between the baseline and any of the treatments and the control and any of the treatments was the increase in picoeukaryotes abundance in the 2% HGO ( $M= 130$ ,  $SEM= 16.2$  cells.mL<sup>-1</sup>). No other significant differences were observed between the control and other treatments on day 2.

In contrast to the oceanic experiment, most of the picoeukaryotes cell counts in the coastal experiment were above the minimum count threshold. The mean concentration of picoeukaryotes in the baseline was  $1.7 \times 10^3$  ( $SEM=343$ ) cells.mL<sup>-1</sup> (Fig. 3.8 b). An ordinary one-way ANOVA followed by Dunnett's multiple comparisons test revealed that, after two days, the concentration of picoeukaryotes in the control treatment ( $M= 3.8 \times 10^3$ ,  $SEM= 282$  cells.mL<sup>-1</sup>), was significantly higher than in all other treatments, except for the 2% HFO ( $M= 3.3 \times 10^3$ ,  $SEM= 589$  cells.mL<sup>-1</sup>) treatment.

## **DISCUSSION**

Previous research has demonstrated that the discharge of ships scrubber washwater can cause the artificial fertilization of marine phytoplankton via selective fertilization (Ytreberg et al., 2019, 2021), and toxicity (Picone et al., 2023b). The results from a global coupled ecosystem-biogeochemical modeling exercise suggest that oceanic oligotrophic

areas, such as tropical and subtropical gyres, may be particularly sensitive to those discharges (Tavares et al., in prep). The goal of the present study was to evaluate the responses of a phytoplankton community following the simulated discharge of scrubber washwater in an oligotrophic open-ocean region (oceanic experiment) and contrast those responses to those observed in an area where phytoplankton community is adapted to eutrophic conditions (coastal experiment).

In the Sargasso Sea, the dominant sources of nitrogen to phytoplankton are “new N” advected to the surface waters by mixing, and “regenerated N” in the form of ammonium and other labile organic N compounds that are recycled by microbes in the euphotic zone (Menzel and Ryther 1960; Dugdale and Goering 1967; Lipschultz 2001). N<sub>2</sub> fixation by diazotrophs and atmospheric N deposition are relatively smaller sources of “new N” (Altabet 1988; Michaels et al. 1993; Knapp et al. 2005). Wet deposition also represents a small source of N, but could be important under specific circumstances, such as after large rain events that are followed by calm conditions (Michaels et al., 1993). Primary production in this region is co-limited by macronutrients and trace metals (Lomas et al., 2013; Mills et al., 2004a; C. M. Moore et al., 2008), and their concentrations vary seasonally. From late fall to early spring, the Sargasso Sea is subject to deep convective mixing (150- 300 m), when nutrient enrichment in the euphotic zone and biological production peak. As temperature rises during spring, the upper water column stratifies and forms a shallow (<50 m), oligotrophic surface mixed layer that usually persists until the end of summer (Lomas et al., 2013; Steinberg et al., 2001; Tin et al., 2016). Tropical storms in summer and early fall alter the thermal and physical structure and ecosystem dynamics, which sometimes enriches surface waters with nutrients (Bates et al., 1998; Dickey et al., 1998; Nelson et al., 2001).

The experiments conducted in the present study were preceded by a category 2 hurricane, which could have significantly enriched the euphotic zone via turbulent mixing. However, the comparative analysis of CTD cast data from a cruise before the one in which we collected the water used in the oceanic experiment, to cast data from 3 days before the collection, indicates that the initial conditions of our oceanic experiment were not significantly affected by this early weather event. In the oceanic experiment, the initial chl *a* concentration, and the concentrations for *Synechococcus*, *Prochlorococcus* and picoeukaryotes were all low, and comparable to chl *a* values and cell abundances classified as low by other researchers that quantified cyanobacteria in surface water from this region (Durand et al., 2001; Mackey et al., 2012; Martiny et al., 2020).

Small ( $0.02 \mu\text{g.L}^{-1}$ ) but significant increases in chl *a* concentration in the oceanic experiment (Fig. 3.4 a) relative to the control were observed in both treatments that exposed microorganisms to the higher concentrations of scrubber washwater (2% HGO and 2% HFO), but not in any of the other treatments, including the controlled additions of N and Fe. Furthermore, the 2% HGO treatment was the only one that caused *Synechococcus* abundance to significantly increase, with a concurrent drawdown in N+N (Fig. 3.3 a). *Prochlorococcus* cells were very dim in most samples analyzed in both experiments, except in the baseline of the oceanic experiment. This issue is discussed in more detail, below. Picoeukaryotes abundance was below the minimum counts for statistically significant analysis in all samples from the oceanic experiment, but it is interesting to note that there was an apparent increase in their concentration in the 2% HGO treatment relative to the control.

These results suggest that the microbial population in the oceanic experiment was not limited by N or Fe alone, but likely co-limited by multiple nutrients. At 2% concentration, the two types of scrubber washwater additions (HGO and HFO) added relatively small amounts of N, but considerable amounts of metals, including dFe, dZn, and dCu (Table 1). It is impossible to determine the exact reason for why the 2% HGO caused a fertilizing effect on *Synechococcus*, while the 2% HFO didn't, but it is noteworthy that compared to the 2% HGO treatment, the 2% HFO spike added higher amounts of all metals, and particularly high amounts of dV (~80 nM) and dNi (~20 nM). The amount of dCu added by the 2% HFO spike (1.2 nM) was more than 3 times the amount added by the 2% HGO. In high concentrations, Cu can be toxic to phytoplankton (Jordi et al., 2012; Levy et al., 2008; Lopez et al., 2019; Moffett et al., 1990), but previous Cu addition experiments in the Sargasso Sea found no decrease in the growth of *Synechococcus* following 2nM Cu additions (Mann et al., 2002).

The influence of other components and processes that we did not investigate here, such as complex inter-specific competition for nutrients, metal chelation dynamics (Hirose, 2006; Hutchins et al., 1999; Raspor et al., 1980; Sunda, 2012), and co-limitations (C. M. Moore et al., 2013b; Saito et al., 2008) cannot be ruled out. Polyaromatic hydrocarbons (PAHs), may also be playing a role in the selective impacts of scrubber washwater additions observed here. PAHs have been measured in scrubber washwater samples (Lunde Hermansson et al., 2021; Tronczynski et al., 2022; Ytreberg et al., 2022b), and have been found to cause lethal and sublethal effects on marine phytoplankton (Bopp & Lettieri, 2007; Cerezo & Agustí, 2015; Echeveste et al., 2016; Kottuparambil & Agusti, 2018, 2020; H. Ben Othman et al., 2012).

The results from the oceanic experiment were noticeably different from what we observed in the coastal experiments. The coastal experiments were conducted with washwater collected from the Hamilton Harbour, which is a shallow semi-enclosed body of water that continuously receives significant inputs of nitrogen, metals, and other contaminants from urban runoff (T. D. Jickells et al., 1986; Slabbing et al., 1990). Those components accumulate in the water and in sediments (Burns et al., 1990), and on occasion, eutrophication and harmful algal blooms occur inside the harbor (Gov. of Bermuda, 2020). As expected, the initial nutrients concentration in the coastal experiment were considerably higher than in the oceanic experiment, and the N to P ratio (8:1) suggests that phytoplankton growth in the coastal experiment was limited by N. Initial chl *a* in the coastal experiment was also higher than in the oceanic experiment and declined in all treatments. We posit that this decline was due to a co-limitation of N and other factor(s) that could not be alleviated in any of the treatments. As in the oceanic experiment, the abundance of *Synechococcus* increased in the 2% HGO treatment relative to the baseline and to the control. Differently from the oceanic experiment, here *Synechococcus* also increased in the 0.1% HFO treatment. We can't explain why. Picoeukaryotes abundance declined in all treatments relative to control, except for those in the 10% HFO treatment, while *Prochlorococcus* cells were too dim to be separated from the noise and quantified in any sample from the coastal experiment.

*Prochlorococcus* is quantified via flow cytometry based on its autofluorescence, particularly its chlorophyll fluorescence (Chisholm et al., 1988; G erikas Ribeiro et al., 2016; van den Engh et al., 2017). In the present study, *Prochlorococcus* populations in many treatments of both the open-ocean and coastal experiments were too dim to be quantified via flow cytometry. The autofluorescence or "brightness" of *Prochlorococcus* cells

is influenced by several factors such as stage in their life cycle, nutrient availability, and other environmental conditions, including light regimes (Bibby et al., 2003; S. J. Biller et al., 2015; J. B. H. Martiny et al., 2015; Partensky et al., 1999; Partensky & Garczarek, 2010; Ulloa et al., 2021). It is not uncommon for *Prochlorococcus* from surface samples to be too dim for flow cytometry quantification (Laura Llubelczyk, personal communication, June 20, 2023). But here, we documented some noteworthy differences amongst treatments: in the oceanic experiment, *Prochlorococcus* were bright enough to be quantified in the baseline and in three treatments at 48h (0.1% HGO, 2% HGO, and Fe addition treatments), whereas in the coastal experiment, *Prochlorococcus* cells were dim in all treatments. We posit that this discrepancy between experiments has to do with the fact that we sampled the incubation water for the oceanic experiment after several days of overcast weather and that the microorganisms in this water were likely acclimated to low-light conditions, thus bright enough to be distinguished and quantified in time 0 (baseline) samples. However, once these *Prochlorococcus* cells were placed in bags and in the incubator, the *Prochlorococcus* were abruptly exposed to more light than what they had been acclimated to (even though we used a light attenuation sheet).

*Prochlorococcus* has evolved to adapt to a wide range of light conditions in the ocean, from well-lit surface waters to deeper, dimly lit regions. In response to changes in light availability, *Prochlorococcus* can undergo several physiological and molecular adjustments to optimize its photosynthetic efficiency. In dimmer light conditions, *Prochlorococcus* may increase the size of its light-harvesting antennae complexes, which allows the cells to capture more available light, enhancing their photosynthetic efficiency in low-light environments. Increasing the size of the antennae complexes often involves a higher concentration of



pigments, including chlorophyll, which increases their autofluorescence (Bibby et al., 2003; Garczarek et al., 2000, 2001). When exposed to sudden increases in light intensity, *Prochlorococcus* can respond in several ways that may reduce their autofluorescence. For example, they may undergo dynamic reconfiguration of its antennae complexes or activate non-photochemical quenching (NPQ), which helps dissipate excess absorbed light energy as heat, preventing potential damage to the photosynthetic apparatus (Bailey et al., 2005; Bailey & Grossman, 2008; Kulk et al., 2013). As a result, the fluorescence emitted by chlorophyll is temporarily reduced and in flow cytometry, this reduction may be interpreted as a decrease in brightness.

Our results for the oceanic experiment showed that this decrease in brightness that was likely induced by the sudden increase in light exposure, happened in several treatments, but not equally in all. *Prochlorococcus* fared better in the 10 nM Fe addition treatment, where, after 48h, the cells were bright enough to be quantified via flow cytometry and their concentration ended up being 5 times higher than those in the control. Fe is known to play crucial roles in important physiological processes for *Prochlorococcus*, including acclimation to changes in light (J. B. H. Martiny et al., 2015; L. R. Moore & Chisholm, 1999; Partensky & Garczarek, 2010). In general, Fe requirements for phytoplankton growth, are expected to be higher for organisms in low light requirements (Hogle et al., 2018; Raven, 1990; Sunda & Huntsman, 1995b, 2015). However, at least one recent study has shown that variations to this canonical model are possible and that, in some cases, large photosynthetic Fe demand may not be downregulated at higher light (Hawco et al., 2021). In the present study, the other treatments in which *Prochlorococcus* autofluorescence was bright enough for quantification via flow cytometry were the HGO ones. These are the same treatments in which we

observed increase in chl *a* and *Synechococcus* abundance and were characterized by high dFe content associated to the HGO spike (Table 1). The other scrubber washwater treatments (2% HFO), also corresponded to considerable amounts of added dFe but did not result in bright enough *Prochlorococcus* for flow cytometry quantification. We conjecture that this may be related to toxic effects by other components in the HFO formulation, such as what we discussed in relation to the selective fertilization effect of *Synechococcus*, above.

Finally, our results reveal a possible difference in the response of oceanic picoplankton to these two types of scrubber washwater. The addition of scrubber washwater generated by the distilled fuel (HGO), in a small testbed engine had a noticeable fertilizing effect on oceanic chl *a* and *Synechococcus* populations, and possibly boosted *Prochlorococcus* fluorescence. The scrubber water from the residual fuel (HFO) combusted by a real ship caused an increase in chl *a* in the oceanic experiment, but the specific group that responded positively to this addition could not be identified. Comparing the results from both the oceanic and coastal experiments conducted here, to those from coastal incubation experiments we conducted the Kattegat Strait (2019 KS) with the same HGO spike and in the Southern California Bight (SCB 2021) with the same HFO spike (Tavares et al in prep and Chapter 2 of this dissertation), we notice the importance of the concentration of exposure. In the 2019 KS experiment we documented significant increases in chl *a*, and cell counts for microplankton (which was dominated by dinoflagellates) and for *Synechococcus*, with concurrent N drawdown, but these effects were only present in the 10% HGO concentration, and not in the 5% HGO treatment. In the 2021 SCB experiment, we saw an increase in chl *a* in the 5% and 10% HFO treatments, but not in the 1% HFO, while all three concentrations of HFO fertilized *Synechococcus* in the 2021 SCB coastal experiment. Here only the 2% HGO

caused the above-described fertilizing effects, but the 0.1% HGO didn't. Considering what we know about the post-discharge dilution (Tavares et al in prep and Chapter 1 of this dissertation), it is important to acknowledge that in most open-ocean conditions, the phytoplankton underneath an individual ship discharging scrubber washwater along its route will be experiencing scrubber water concentrations that are <0.1%. As explained in chapter 1, higher concentration exposures may occur in heavily trafficked shipping routes and/or in highly stratified regions.

## **CONCLUSIONS**

This study investigated the effects of ship scrubber washwater discharges on natural phytoplankton assemblages in the open and coastal Sargasso Sea. We sought to determine if scrubber washwater produced from the combustion of two fuels causes fertilization, inhibition, or neutral/null effects in this oligotrophic environment where picophytoplankton such as *Synechococcus*, *Prochlorococcus*, and picoeukaryotes dominate. For comparative purposes, we conducted a parallel coastal experiment in a nutrient-rich harbor area. We found that both the traditional heavy fuel oil combusted in a large ship engine (HFO) and the alternative distilled fuel combusted in a small testbed engine (HGO) caused a mild fertilization on oceanic phytoplankton at 2% concentration, but the HGO formulation had a particular fertilizing effect on *Synechococcus*, and possibly a positive effect on *Prochlorococcus* fluorescence. Our results suggest that the microbial populations in the Sargasso Sea were not limited by N or Fe alone, but likely co-limited by multiple nutrients that were supplied in enough quantity by the scrubber washwater discharges at 2% concentration but not at 0.1% or lower.

## REFERENCES

- Agrawal, H., Eden, R., Zhang, X., Fine, P. M., Katzenstein, A., Miller, J. W., Ospital, J., Teffera, S., & Cocker, D. R. (2009). Primary particulate matter from ocean-going engines in the Southern California Air Basin. *Environmental Science and Technology*, 43(14), 5398–5402. <https://doi.org/10.1021/es8035016>
- Agrawal, H., Malloy, Q. G. J., Welch, W. A., Wayne Miller, J., & Cocker, D. R. (2008). In-use gaseous and particulate matter emissions from a modern ocean going container vessel. *Atmospheric Environment*, 42(21), 5504–5510. <https://doi.org/https://doi.org/10.1016/j.atmosenv.2008.02.053>
- Al-Aboosi, F. Y., El-Halwagi, M. M., Moore, M., & Nielsen, R. B. (2021). Renewable ammonia as an alternative fuel for the shipping industry. *Current Opinion in Chemical Engineering*, 31, 100670. <https://doi.org/https://doi.org/10.1016/j.coche.2021.100670>
- Ali, M. F., & Abbas, S. (2006). A review of methods for the demetallization of residual fuel oils. In *Fuel Processing Technology* (Vol. 87, Issue 7, pp. 573–584). <https://doi.org/10.1016/j.fuproc.2006.03.001>
- Altieri, K. E., Fawcett, S. E., & Hastings, M. G. (2021). Reactive Nitrogen Cycling in the Atmosphere and Ocean. *Annual Review of Earth and Planetary Sciences*, 49(1), 523–550. <https://doi.org/10.1146/annurev-earth-083120-052147>
- Anderson, J. O., Thundiyil, J. G., & Stolbach, A. (2012). Clearing the Air: A Review of the Effects of Particulate Matter Air Pollution on Human Health. In *Journal of Medical Toxicology* (Vol. 8, Issue 2, pp. 166–175). <https://doi.org/10.1007/s13181-011-0203-1>
- Anderson, M., Salo, K., & Fridell, E. (2015). Particle- and Gaseous Emissions from an LNG Powered Ship. *Environmental Science and Technology*, 49(20), 12568–12575. <https://doi.org/10.1021/acs.est.5b02678>
- Anderson, M., Salo, K., Hallquist, Å. M., & Fridell, E. (2015). Characterization of particles from a marine engine operating at low loads. *Atmospheric Environment*, 101, 65–71. <https://doi.org/10.1016/j.atmosenv.2014.11.009>
- Andersson, K., Baldi, F., Brynolf, S., Lindgren, J. F., Granhag, L., & Svensson, E. (2016). *Shipping and the Environment BT - Shipping and the Environment : Improving Environmental Performance in Marine Transportation* (K. Andersson, S. Brynolf, J. F. Lindgren, & M. Wilewska-Bien, Eds.; pp. 3–27). Springer Berlin Heidelberg. [https://doi.org/10.1007/978-3-662-49045-7\\_1](https://doi.org/10.1007/978-3-662-49045-7_1)

- Antoine, D., Andrt, J. M., & Morel, A. (1996). Oceanic primary production: 2. Estimation at global scale from satellite (Coastal Zone Color Scanner) chlorophyll. *Global Biogeochemical Cycles*, *10*(1), 57–69. <https://doi.org/10.1029/95GB02832>
- Anu, P. R., Nandan, S. B., Jayachandran, P. R., & Xavier, N. D. D. (2016). Toxicity effects of copper on the marine diatom, *Chaetoceros calcitrans*. *Regional Studies in Marine Science*, *8*, 498–504.
- Arnone, V., González-Santana, D., González-Dávila, M., González, A. G., & Santana-Casiano, J. M. (2022). Iron and copper complexation in Macaronesian coastal waters. *Marine Chemistry*, *240*, 104087. <https://doi.org/https://doi.org/10.1016/j.marchem.2022.104087>
- Arrigo, K. R. (2005). Marine microorganisms and global nutrient cycles. In *Nature* (Vol. 437, Issue 7057, pp. 349–355). Nature Publishing Group. <https://doi.org/10.1038/nature04159>
- Arrigo, K. R., DiTullio, G. R., Dunbar, R. B., Robinson, D. H., VanWoert, M., Worthen, D. L., & Lizotte, M. P. (2000). Phytoplankton taxonomic variability in nutrient utilization and primary production in the Ross Sea. *Journal of Geophysical Research: Oceans*, *105*(C4), 8827–8846. <https://doi.org/10.1029/1998JC000289>
- Avakian, M. D., Dellinger, B., Fiedler, H., Gullet, B., Koshland, C., Marklund, S., Oberdörster, G., Safe, S., Sarofim, A., Smith, K. R., Schwartz, D., & Suk, W. A. (2002). The origin, fate, and health effects of combustion by-products: A research framework. *Environmental Health Perspectives*, *110*(11), 1155–1162. <https://doi.org/10.1289/EHP.021101155>
- Bailey, S., & Grossman, A. (2008). Photoprotection in Cyanobacteria: Regulation of Light Harvesting†. *Photochemistry and Photobiology*, *84*(6), 1410–1420. <https://doi.org/https://doi.org/10.1111/j.1751-1097.2008.00453.x>
- Bailey, S., Mann, N. H., Robinson, C., & Scanlan, D. J. (2005). The occurrence of rapidly reversible non-photochemical quenching of chlorophyll a fluorescence in cyanobacteria. *FEBS Letters*, *579*(1), 275–280. <https://doi.org/https://doi.org/10.1016/j.febslet.2004.11.091>
- Baird, M., Dutkiewicz, S., Hickman, A., Mongin, M., Soja-Wozniak, M., Skerratt, J., & Wild-Allen, K. (2022). Chapter 8 - Modeling phytoplankton processes in multiple functional types. In L. A. Clementson, R. S. Eriksen, & A. Willis (Eds.), *Advances in Phytoplankton Ecology* (pp. 245–264). Elsevier. <https://doi.org/https://doi.org/10.1016/B978-0-12-822861-6.00016-9>
- Baltic Marine Environment Protection Commission. (2017). Information on new Traffic Separation Schemes and other adjacent routing measures for ship traffic in Kattegat and Skagerrak. *Group of Experts on Safety of Navigation Stockholm-Arlanda, Sweden, 28 September 2017, September 2017*, 3–5.

- Barton, A. D., Dutkiewicz, S., Flierl, G., Bragg, J., & Follows, M. J. (2010). Patterns of Diversity in Marine Phytoplankton. *Science*, 327(5972), 1509–1511. <https://doi.org/10.1126/science.1184961>
- Barwise, A. J. G. (1990). Role of Nickel and Vanadium in Petroleum Classification. *Energy and Fuels*, 4(6), 647–652. <https://doi.org/10.1021/ef00024a005>
- Basu, S., Mackey, K. R. M., Basu, S., & Mackey, K. R. M. (2018). Phytoplankton as Key Mediators of the Biological Carbon Pump: Their Responses to a Changing Climate. *Sustainability*, 10(3), 869. <https://doi.org/10.3390/su10030869>
- Bates, N. R., Knap, A. H., & Michaels, A. F. (1998). Contribution of hurricanes to local and global estimates of air–sea exchange of CO<sub>2</sub>. *Nature*, 395(6697), 58–61.
- Beman, J. M., Arrigo, K. R., & Matson, P. A. (2005). Agricultural runoff fuels large phytoplankton blooms in vulnerable areas of the ocean. *Nature*, 434(7030), 211–214. <https://doi.org/10.1038/nature03370>
- Bendtsen, J., & Richardson, K. (2018). Turbulence measurements suggest high rates of new production over the shelf edge in the northeastern North Sea during summer. *Biogeosciences*, 15(23), 7315–7332. <https://doi.org/10.5194/bg-15-7315-2018>
- Bibby, T. S., Mary, I., Nield, J., Partensky, F., & Barber, J. (2003). Low-light-adapted Prochlorococcus species possess specific antennae for each photosystem. *Nature*, 424(6952), 1051–1054. <https://doi.org/10.1038/nature01933>
- Biller, S. J., Berube, P. M., Lindell, D., & Chisholm, S. W. (2015). Prochlorococcus: the structure and function of collective diversity. *Nature Reviews Microbiology*, 13(1), 13–27.
- Biller, D. V., & Bruland, K. W. (2013). Sources and distributions of Mn, Fe, Co, Ni, Cu, Zn, and Cd relative to macronutrients along the central California coast during the spring and summer upwelling season. *Marine Chemistry*, 155, 50–70. <https://doi.org/https://doi.org/10.1016/j.marchem.2013.06.003>
- Bograd, S. J., Buil, M. P., Lorenzo, E. Di, Castro, C. G., Schroeder, I. D., Goericke, R., Anderson, C. R., Benitez-Nelson, C., & Whitney, F. A. (2015). Changes in source waters to the Southern California Bight. *Deep Sea Research Part II: Topical Studies in Oceanography*, 112, 42–52. <https://doi.org/https://doi.org/10.1016/j.dsr2.2014.04.009>
- Bopp, S. K., & Lettieri, T. (2007). Gene regulation in the marine diatom *Thalassiosira pseudonana* upon exposure to polycyclic aromatic hydrocarbons (PAHs). *Gene*, 396(2), 293–302.
- Bowie, A. R., Lannuzel, D., Remenyi, T. A., Wagener, T., Lam, P. J., Boyd, P. W., Guieu, C., Townsend, A. T., & Trull, T. W. (2009). Biogeochemical iron budgets of the Southern Ocean south of Australia: Decoupling of iron and nutrient cycles in the subantarctic

zone by the summertime supply. *Global Biogeochemical Cycles*, 23(4), n/a-n/a.  
<https://doi.org/10.1029/2009GB003500>

- Boyd, P. W., Jickells, T., Law, C. S., Blain, S., Boyle, E. A., Buesseler, K. O., Coale, K. H., Cullen, J. J., de Baar, H. J. W., Follows, M., Harvey, M., Lancelot, C., Levasseur, M., Owens, N. P. J., Pollard, R., Rivkin, R. B., Sarmiento, J., Schoemann, V., Smetacek, V., ... Watson, A. J. (2007). Mesoscale Iron Enrichment Experiments 1993-2005: Synthesis and Future Directions. *Science*, 315(5812), 612–617. <https://doi.org/10.1126/science.1131669>
- Brandt, J., Silver, J. D., Christensen, J. H., Andersen, M. S., Bønløkke, J. H., Sigsgaard, T., Geels, C., Gross, A., Hansen, A. B., Hansen, K. M., Hedegaard, G. B., Kaas, E., & Frohn, L. M. (2013). Assessment of past, present and future health-cost externalities of air pollution in Europe and the contribution from international ship traffic using the EVA model system. *Atmospheric Chemistry and Physics*, 13(15), 7747–7764.  
<https://doi.org/10.5194/acp-13-7747-2013>
- Bray, N. A., Keyes, A., & Morawitz, W. M. L. (1999). The California current system in the Southern California bight and the Santa Barbara Channel. *Journal of Geophysical Research: Oceans*, 104(C4), 7695–7714.
- Bristow, L. A., Mohr, W., Ahmerkamp, S., & Kuypers, M. M. M. (2017). Nutrients that limit growth in the ocean. *Current Biology*, 27(11), R474–R478.  
<https://doi.org/10.1016/J.CUB.2017.03.030>
- Brook, R. D., Rajagopalan, S., Pope, C. A., Brook, J. R., Bhatnagar, A., Diez-Roux, A. V., Holguin, F., Hong, Y., Luepker, R. V., Mittleman, M. A., Peters, A., Siscovick, D., Smith, S. C., Whitsel, L., & Kaufman, J. D. (2010). Particulate matter air pollution and cardiovascular disease: An update to the scientific statement from the american heart association. In *Circulation* (Vol. 121, Issue 21, pp. 2331–2378).  
<https://doi.org/10.1161/CIR.0b013e3181d8e1>
- Browning, T. J., Achterberg, E. P., Rapp, I., Engel, A., Bertrand, E. M., Tagliabue, A., & Moore, C. M. (2017). Nutrient co-limitation at the boundary of an oceanic gyre. *Nature*, 551(7679), 242. <https://doi.org/10.1038/nature24063>
- Browning, T. J., & Moore, C. M. (2023). Global analysis of ocean phytoplankton nutrient limitation reveals high prevalence of co-limitation. *Nature Communications*, 14(1), 5014. <https://doi.org/10.1038/s41467-023-40774-0>
- Buck, C. S., Landing, W. M., & Resing, J. (2013). Pacific Ocean aerosols: Deposition and solubility of iron, aluminum, and other trace elements. *Marine Chemistry*, 157, 117–130. <https://doi.org/10.1016/J.MARCHEM.2013.09.005>
- Bunt, J. S. (1975). *Primary productivity of marine ecosystems*. Springer.
- Burns, K. A., Ehrhardt, M. G., MacPherson, J., Tierney, J. A., Kananen, G., & Connelly, D. (1990). Organic and trace metal contaminants in sediments, seawater and organisms

- from two Bermudan harbours. *Journal of Experimental Marine Biology and Ecology*, 138(1), 9–34. [https://doi.org/https://doi.org/10.1016/0022-0981\(90\)90174-B](https://doi.org/https://doi.org/10.1016/0022-0981(90)90174-B)
- Canfield, D. E., Glazer, A. N., & Falkowski, P. G. (2010). The Evolution and Future of Earth's Nitrogen Cycle. *Science*, 330(6001), 192–196. <https://doi.org/10.1126/science.1186120>
- Cao, Y., Liang, S., Sun, L., Liu, J., Cheng, X., Wang, D., Chen, Y., Yu, M., & Feng, K. (2022). Trans-Arctic shipping routes expanding faster than the model projections. *Global Environmental Change*, 73, 102488. <https://doi.org/https://doi.org/10.1016/j.gloenvcha.2022.102488>
- Cappucci, M. (2021, August 27). Desert downpours: Rare summer rains soaked Death Valley and parts of California on Monday. *The Washington Post*, online.
- Fuel Sulfur and Other Operational Requirements for Ocean-Going Vessels within California Waters and 24 Nautical Miles of the California Baseline. Title 13, California Code of Regulations (CCR) §2299.2 and title 17, CCR §93118.2., (2008). <https://ww3.arb.ca.gov/regact/2008/fuelogv08/22992.pdf>
- Carpenter, S. R., Caraco, N. F., Correll, D. L., Howarth, R. W., Sharpley, A. N., & Smith, V. H. (1998). Nonpoint pollution of surface waters with phosphorus and nitrogen. *Ecological Applications*, 8(3), 559–568.
- Carstensen, J., Conley, D. J., & Henriksen, P. (2004). Frequency, composition, and causes of summer phytoplankton blooms in a shallow coastal ecosystem, the Kattegat. *Limnology and Oceanography*, 49(1), 191–201. <https://doi.org/https://doi.org/10.4319/lo.2004.49.1.0191>
- Celo, V., Dabek-Zlotorzynska, E., & McCurdy, M. (2015). Chemical characterization of exhaust emissions from selected Canadian marine vessels: The case of trace metals and lanthanoids. *Environmental Science and Technology*, 49(8), 5220–5226. <https://doi.org/10.1021/acs.est.5b00127>
- Cerezo, M. I., & Agustí, S. (2015). PAHs reduce DNA synthesis and delay cell division in the widespread primary producer *Prochlorococcus*. *Environmental Pollution*, 196, 147–155.
- Chavez, F. P., Barber, R. T., Kosro, P. M., Huyer, A., Ramp, S. R., Stanton, T. P., & Rojas de Mendiola, B. (1991). Horizontal transport and the distribution of nutrients in the coastal transition zone off northern California: effects on primary production, phytoplankton biomass and species composition. *Journal of Geophysical Research: Oceans*, 96(C8), 14833–14848.
- Chavez, F. P., & Messié, M. (2009). A comparison of Eastern Boundary Upwelling Ecosystems. *Progress in Oceanography*, 83(1), 80–96. <https://doi.org/https://doi.org/10.1016/j.pocean.2009.07.032>



- Cheng, C.-W., Hua, J., & Hwang, D.-S. (2017). NO<sub>x</sub> emission calculations for bulk carriers by using engine power probabilities as weighting factors. *Journal of the Air & Waste Management Association*, 67(10), 1146–1157.  
<https://doi.org/10.1080/10962247.2017.1356763>
- Chisholm, S. W., Olson, R. J., Zettler, E. R., Goericke, R., Waterbury, J. B., & Welschmeyer, N. A. (1988). A novel free-living prochlorophyte abundant in the oceanic euphotic zone. *Nature*, 334(6180), 340–343.
- Christodoulou, A., Gonzalez-Aregall, M., Linde, T., Vierth, I., & Cullinane, K. (2019). Targeting the reduction of shipping emissions to air. *Maritime Business Review*, 4(1), 16–30.  
<https://doi.org/10.1108/MABR-08-2018-0030>
- Chu Van, T., Ramirez, J., Rainey, T., Ristovski, Z., & Brown, R. J. (2019). Global impacts of recent IMO regulations on marine fuel oil refining processes and ship emissions. *Transportation Research Part D: Transport and Environment*, 70, 123–134.  
<https://doi.org/10.1016/J.TRD.2019.04.001>
- Chu Van, T., Ristovski, Z., Surawski, N., Bodisco, T. A., Rahman, S. M. A., Alroe, J., Miljevic, B., Hossain, F. M., Suara, K., Rainey, T., & Brown, R. J. (2018). Effect of sulphur and vanadium spiked fuels on particle characteristics and engine performance of auxiliary diesel engines. *Environmental Pollution*, 243, 1943–1951.  
<https://doi.org/10.1016/J.ENVPOL.2018.08.055>
- Cid, A., Herrero, C., Torres, E., & Abalde, J. (1995). Copper toxicity on the marine microalga *Phaeodactylum tricornutum*: effects on photosynthesis and related parameters. *Aquatic Toxicology*, 31(2), 165–174. [https://doi.org/https://doi.org/10.1016/0166-445X\(94\)00071-W](https://doi.org/https://doi.org/10.1016/0166-445X(94)00071-W)
- Coale, K. H. (2004). Southern Ocean Iron Enrichment Experiment: Carbon Cycling in High- and Low-Si Waters. *Science*, 304(5669), 408–414.  
<https://doi.org/10.1126/science.1089778>
- Comer, B., Georgeff, E., & Osipova, L. (2020). *Air emissions and water pollution discharges from ships with scrubbers*. [www.theicct.org](http://www.theicct.org)
- Cooper, D. A., & Andreasson, K. (1999). Predictive NO<sub>x</sub> emission monitoring on board a passenger ferry. *Atmospheric Environment*, 33(28), 4637–4650.  
[https://doi.org/10.1016/S1352-2310\(99\)00239-3](https://doi.org/10.1016/S1352-2310(99)00239-3)
- Corbett, J. J. (1997). Emissions from Ships. *Science*, 278(5339), 823–824.  
<https://doi.org/10.1126/science.278.5339.823>
- Corbett, J. J. (2003). Updated emissions from ocean shipping. *Journal of Geophysical Research*, 108(D20), 4650. <https://doi.org/10.1029/2003JD003751>

- Corbett, J. J., Fischbeck, P. S., & Pandis, S. N. (1999a). Global nitrogen and sulfur inventories for oceangoing ships. *Journal of Geophysical Research: Atmospheres*, *104*(D3), 3457–3470. <https://doi.org/10.1029/1998JD100040>
- Corbett, J. J., Fischbeck, P. S., & Pandis, S. N. (1999b). Global nitrogen and sulfur inventories for oceangoing ships. *Journal of Geophysical Research: Atmospheres*, *104*(D3), 3457–3470. <https://doi.org/10.1029/1998JD100040>
- Corbett, J. J., Winebrake, J. J., Green, E. H., Kasibhatla, P., Eyring, V., & Lauer, A. (2007). Mortality from ship emissions: A global assessment. *Environmental Science and Technology*, *41*(24), 8512–8518. <https://doi.org/10.1021/es071686z>
- Corbin, J. C., Mensah, A. A., Pieber, S. M., Orasche, J., Michalke, B., Zanatta, M., Czech, H., Massabò, D., Buatier De Mongeot, F., Mennucci, C., El Haddad, I., Kumar, N. K., Stengel, B., Huang, Y., Zimmermann, R., Prévôt, A. S. H., & Gysel, M. (2018). Trace Metals in Soot and PM<sub>2.5</sub> from Heavy-Fuel-Oil Combustion in a Marine Engine. *Environmental Science and Technology*, *52*(11), 6714–6722. <https://doi.org/10.1021/acs.est.8b01764>
- Coufalík, P., Matoušek, T., Křůmal, K., Vojtíšek-Lom, M., Beránek, V., & Mikuška, P. (2019). Content of metals in emissions from gasoline, diesel, and alternative mixed biofuels. *Environmental Science and Pollution Research*, *26*(28), 29012–29019. <https://doi.org/10.1007/s11356-019-06144-4>
- Cullen, J. J., & Eppley, R. W. (1981). Chlorophyll maximum layers of the Southern-California Bight and possible mechanisms of their formation and maintenance. *Oceanologica Acta*, *4*(1), 23–32.
- Cutter, G., Casciotti, K., Croot, P., Geibert, W., Geochemistry, M., Heimbürger, L.-E., & Lohan, M. (2017). *Sampling and Sample-handling Protocols for GEOTRACES Cruises*.
- Danish Maritime Authority. (n.d.). *New shipping routes in Kattegat and Skagerrak (Press Release)*. Retrieved August 7, 2023, from <https://dma.dk/safety-at-sea/navigational-information/new-shipping-routes-in-kattegat-and-skagerrak>
- Dickey, T., Frye, D., Jannasch, H., Boyle, E., Manov, D., Sigurdson, D., McNeil, J., Stramska, M., Michaels, A., & Nelson, N. (1998). Initial results from the Bermuda Testbed Mooring program. *Deep Sea Research Part I: Oceanographic Research Papers*, *45*(4–5), 771–794.
- Dong, C., Idica, E. Y., & McWilliams, J. C. (2009). Circulation and multiple-scale variability in the Southern California Bight. *Progress in Oceanography*, *82*(3), 168–190.
- Duce, R. A., LaRoche, J., Altieri, K., Arrigo, K. R., Baker, A. R., Capone, D. G., Cornell, S., Dentener, F., Galloway, J., Ganeshram, R. S., Geider, R. J., Jickells, T., Kuypers, M. M., Langlois, R., Liss, P. S., Liu, S. M., Middelburg, J. J., Moore, C. M., Nickovic, S., ... Zamora, L. (2008). Impacts of atmospheric anthropogenic nitrogen on the open ocean. In *Science* (Vol. 320, Issue 5878, pp. 893–897). <https://doi.org/10.1126/science.1150369>

- Duce, R. A., & Tindale, N. W. (1991). Atmospheric Transport of Iron and its Desposition in the Ocean. *Limnology Oceanography*, 36(8), 1715–1726.  
<https://aslopubs.onlinelibrary.wiley.com/doi/pdf/10.4319/lo.1991.36.8.1715>
- Dugdale, R. C., & Goering, J. J. (1967). UPTAKE OF NEW AND REGENERATED FORMS OF NITROGEN IN PRIMARY PRODUCTIVITY1. *Limnology and Oceanography*, 12(2), 196–206. <https://doi.org/https://doi.org/10.4319/lo.1967.12.2.0196>
- Durand, M. D., Olson, R. J., & Chisholm, S. W. (2001). Phytoplankton population dynamics at the Bermuda Atlantic Time-series station in the Sargasso Sea. *Deep-Sea Research Part II: Topical Studies in Oceanography*, 48(8–9), 1983–2003.  
[https://doi.org/10.1016/S0967-0645\(00\)00166-1](https://doi.org/10.1016/S0967-0645(00)00166-1)
- Echeveste, P., Galbán-Malagón, C., Dachs, J., Berrojalbiz, N., & Agustí, S. (2016). Toxicity of natural mixtures of organic pollutants in temperate and polar marine phytoplankton. *Science of the Total Environment*, 571, 34–41.
- Eichler, P., Müller, M., Rohmann, C., Stengel, B., Orasche, J., Zimmermann, R., & Wisthaler, A. (2017). Lubricating Oil as a Major Constituent of Ship Exhaust Particles. *Environmental Science & Technology Letters*, 4(2), 54–58.  
<https://doi.org/10.1021/acs.estlett.6b00488>
- Eppley, R. W. (1992). Chlorophyll, photosynthesis and new production in the Southern California Bight. *Progress in Oceanography*, 30(1–4), 117–150.
- Eyring, V., Isaksen, I. S. A., Berntsen, T., Collins, W. J., Corbett, J. J., Endresen, O., Grainger, R. G., Moldanova, J., Schlager, H., & Stevenson, D. S. (2010a). Transport impacts on atmosphere and climate: Shipping. *Atmospheric Environment*, 44(37), 4735–4771.  
<https://doi.org/10.1016/J.ATMOSENV.2009.04.059>
- Eyring, V., Isaksen, I. S. A., Berntsen, T., Collins, W. J., Corbett, J. J., Endresen, O., Grainger, R. G., Moldanova, J., Schlager, H., & Stevenson, D. S. (2010b). Transport impacts on atmosphere and climate: Shipping. *Atmospheric Environment*, 44(37), 4735–4771.  
<https://doi.org/10.1016/j.atmosenv.2009.04.059>
- Eyring, V., Köhler, H. W., van Aardenne, J., & Lauer, A. (2005). Emissions from international shipping: 1. The last 50 years. In *Journal of Geophysical Research D: Atmospheres* (Vol. 110, Issue 17, pp. 171–182). <https://doi.org/10.1029/2004JD005619>
- Falkowski, P. G., Barber, R. T., & Smetacek, V. (1998). Biogeochemical Controls and Feedbacks on Ocean Primary Production. *Science (New York, N.Y.)*, 281(5374), 200–207. <https://doi.org/10.1126/SCIENCE.281.5374.200>
- Falkowski, P., & Knoll, A. H. (2011). *Evolution of primary producers in the sea*. Academic Press.

- Falkowski, P., Scholes, R. J., Boyle, E., Canadell, J., Canfield, D., Elser, J., Gruber, N., Hibbard, K., Hogberg, P., Linder, S., Mackenzie, F. T., Moore, B., Pedersen, T., Rosental, Y., Seitzinger, S., Smetacek, V., & Steffen, W. (2000). The global carbon cycle: A test of our knowledge of earth as a system. In *Science* (Vol. 290, Issue 5490, pp. 291–296).  
<https://doi.org/10.1126/science.290.5490.291>
- Farahat, A., & Abuelgasim, A. (2019). Role of atmospheric nutrient pollution in stimulating phytoplankton growth in small area and shallow depth water bodies: Arabian Gulf and the sea of Oman. *Atmospheric Environment*, *219*, 117045.  
<https://doi.org/https://doi.org/10.1016/j.atmosenv.2019.117045>
- Field, C. B., Behrenfeld, M. J., Randerson, J. T., & Falkowski, P. (1998). Primary production of the biosphere: integrating terrestrial and oceanic components. *Science*, *281*(5374), 237–240.
- Florence, T. M., & Stauber, J. L. (1986). Toxicity of copper complexes to the marine diatom *Nitzschia closterium*. *Aquatic Toxicology*, *8*(1), 11–26.
- Fong, C. R., Kennison, R. L., & Fong, P. (2021). Nutrient Subsidies to Southern California Estuaries Can Be Characterized as Pulse-Interpulse Regimes that May Be Dampened with Extreme Eutrophy. *Estuaries and Coasts*, *44*(3), 867–874.  
<https://doi.org/10.1007/s12237-020-00810-4>
- Fridell, E. (2018). Emissions and Fuel Use in the Shipping Sector. In *Green Ports: Inland and Seaside Sustainable Transportation Strategies* (pp. 19–33). Elsevier.  
<https://doi.org/10.1016/B978-0-12-814054-3.00002-5>
- Fridell, E. (2019). *Chapter 2 - Emissions and Fuel Use in the Shipping Sector* (R. Bergqvist & J. B. T.-G. P. Monios, Eds.; pp. 19–33). Elsevier.  
<https://doi.org/https://doi.org/10.1016/B978-0-12-814054-3.00002-5>
- Fu, H., Zheng, M., Yan, C., Li, X., Gao, H., Yao, X., Guo, Z., & Zhang, Y. (2015). Sources and characteristics of fine particles over the Yellow Sea and Bohai Sea using online single particle aerosol mass spectrometer. *Journal of Environmental Sciences*, *29*, 62–70.
- Fun-sang Cepeda, M. A., Pereira, N. N., Kahn, S., & Caprace, J.-D. (2019). A review of the use of LNG versus HFO in maritime industry. *Marine Systems & Ocean Technology*, *14*(2), 75–84. <https://doi.org/10.1007/s40868-019-00059-y>
- Gangwar, J. N., Gupta, T., & Agarwal, A. K. (2012). Composition and comparative toxicity of particulate matter emitted from a diesel and biodiesel fuelled CRDI engine. *Atmospheric Environment*, *46*, 472–481.  
<https://doi.org/10.1016/j.atmosenv.2011.09.007>
- Garczarek, L., Hess, W. R., Holtzendorff, J., van der Staay, G. W. M., & Partensky, F. (2000). Multiplication of antenna genes as a major adaptation to low light in a marine prokaryote. *Proceedings of the National Academy of Sciences*, *97*(8), 4098–4101.

- Garczarek, L., van der Staay, G. W. M., Hess, W. R., Le Gall, F., & Partensky, F. (2001). Expression and phylogeny of the multiple antenna genes of the low-light-adapted strain *Prochlorococcus marinus* SS120 (Oxyphotobacteria). *Plant Molecular Biology*, *46*, 683–693.
- Geider, R. J., & La Roche, J. (1994). The role of iron in phytoplankton photosynthesis, and the potential for iron-limitation of primary productivity in the sea. In *Photosynthesis Research* (Vol. 39, Issue 3, pp. 275–301). Kluwer Academic Publishers. <https://doi.org/10.1007/BF00014588>
- Gelting, J., Breitbarth, E., Stolpe, B., Hassellöv, M., & Ingri, J. (2010). Fractionation of iron species and iron isotopes in the Baltic Sea euphotic zone. *Biogeosciences*, *7*(8), 2489–2508. <https://doi.org/10.5194/bg-7-2489-2010>
- Gérikas Ribeiro, C., Marie, D., Lopes dos Santos, A., Pereira Brandini, F., & Vault, D. (2016). Estimating microbial populations by flow cytometry: Comparison between instruments. *Limnology and Oceanography: Methods*, *14*(11), 750–758. <https://doi.org/https://doi.org/10.1002/lom3.10135>
- Girault, M., Siano, R., Labry, C., Latimier, M., Jauzein, C., Beneyton, T., Buisson, L., Del Amo, Y., & Baret, J.-C. (2021). Variable inter and intraspecies alkaline phosphatase activity within single cells of revived dinoflagellates. *The ISME Journal*, *15*(7), 2057–2069. <https://doi.org/10.1038/s41396-021-00904-2>
- Gössling, S., Meyer-Habighorst, C., & Humpe, A. (2021). A global review of marine air pollution policies, their scope and effectiveness. *Ocean & Coastal Management*, *212*, 105824. <https://doi.org/https://doi.org/10.1016/j.ocecoaman.2021.105824>
- Gov. of Bermuda, . (2020). *Degrading Plankton Bloom Produces Brown Surface Layer in Areas of Hamilton Harbour*. 04 August, 2020. <https://www.gov.bm/articles/degrading-plankton-bloom-produces-brown-surface-layer-areas-hamilton-harbour>
- Granéli, E., Wallström, K., Larsson, U., Granéli, W., & Elmgren, R. (1990). Nutrient Limitation of Primary Production in the Baltic Sea Area. *Ambio*, *19*(3), 142–151. <http://www.jstor.org/stable/4313680>
- Griffiths, S. J. (2011). Implications of individual particulate matter component toxicity for population exposure. *Air Quality, Atmosphere and Health*, *4*(3), 189–197. <https://doi.org/10.1007/s11869-010-0077-4>
- Grönholm, T., Mäkelä, T., Hatakka, J., Jalkanen, J.-P., Kuula, J., Laurila, T., Laakso, L., & Kukkonen, J. (2021). Evaluation of Methane Emissions Originating from LNG Ships Based on the Measurements at a Remote Marine Station. *Environmental Science & Technology*, *55*(20), 13677–13686. <https://doi.org/10.1021/acs.est.1c03293>

- Gruber, N., & Sarmiento, J. L. (1997). Global patterns of marine nitrogen fixation and denitrification. *Global Biogeochemical Cycles*, *11*(2), 235–266. <https://doi.org/10.1029/97GB00077>
- Guieu, C., Bonnet, S., Wagener, T., & Lojze-Pilot, M. D. (2005). Biomass burning as a source of dissolved iron to the open ocean? *Geophysical Research Letters*, *32*(19), 1–5. <https://doi.org/10.1029/2005GL022962>
- Guo, C., Zhou, Y., Zhou, H., Su, C., & Kong, L. (2022). Aerosol Nutrients and Their Biological Influence on the Northwest Pacific Ocean (NWPO) and Its Marginal Seas. *Biology*, *11*(6). <https://doi.org/10.3390/biology11060842>
- Guo, J. A., Strzpek, R., Willis, A., Ferderer, A., & Bach, L. T. (2022). Investigating the effect of nickel concentration on phytoplankton growth to assess potential side-effects of ocean alkalinity enhancement. *Biogeosciences*, *19*(15), 3683–3697. <https://doi.org/10.5194/bg-19-3683-2022>
- Gustafsson, J. P. (2019). Vanadium geochemistry in the biogeosphere –speciation, solid-solution interactions, and ecotoxicity. *Applied Geochemistry*, *102*, 1–25. <https://doi.org/10.1016/J.APGEOCHEM.2018.12.027>
- Hällfors, G. (2004). *Checklist of Baltic Sea phytoplankton species (including some heterotrophic protistan groups)*. *Baltic Sea Environment Proceedings 95: [1]-208*.
- Hamilton, D. S., Moore, J. K., Arneeth, A., Bond, T. C., Carslaw, K. S., Hantson, S., Ito, A., Kaplan, J. O., Lindsay, K., Nieradzik, L., Rathod, S. D., Scanza, R. A., & Mahowald, N. M. (2020). Impact of Changes to the Atmospheric Soluble Iron Deposition Flux on Ocean Biogeochemical Cycles in the Anthropocene. *Global Biogeochemical Cycles*, *34*(3). <https://doi.org/10.1029/2019GB006448>
- Hamilton, D. S., Perron, M. M. G., Bond, T. C., Bowie, A. R., Buchholz, R. R., Guieu, C., Ito, A., Maenhaut, W., Myriokefalitakis, S., Olgun, N., Rathod, S. D., Schepanski, K., Tagliabue, A., Wagner, R., & Mahowald, N. M. (2022). Earth, Wind, Fire, and Pollution: Aerosol Nutrient Sources and Impacts on Ocean Biogeochemistry. *Annual Review of Marine Science*, *14*(1), 303–330. <https://doi.org/10.1146/annurev-marine-031921-013612>
- Hamilton, D. S., Scanza, R. A., Rathod, S. D., Bond, T. C., Kok, J. F., Li, L., Matsui, H., & Mahowald, N. M. (2020). Recent (1980 to 2015) Trends and Variability in Daily-to-Interannual Soluble Iron Deposition from Dust, Fire, and Anthropogenic Sources. *Geophysical Research Letters*, *47*(17), e2020GL089688. <https://doi.org/10.1029/2020GL089688>
- Hansen, J. E., Sato, M., Simons, L., Nazarenko, L. S., Sangha, I., Kharecha, P., Zachos, J. C., von Schuckmann, K., Loeb, N. G., Osman, M. B., Jin, Q., Tselioudis, G., Jeong, E., Lacic, A., Ruedy, R., Russell, G., Cao, J., & Li, J. (2023). Global warming in the pipeline. *Oxford Open Climate Change*, *3*(1), kgad008. <https://doi.org/10.1093/oxfclm/kgad008>

- Hardaway, C., Sneddon, J., & Beck, J. N. (2004). Determination of metals in crude oil by atomic spectroscopy. In *Analytical Letters* (Vol. 37, Issue 14, pp. 2881–2899). Marcel Dekker Inc. <https://doi.org/10.1081/AL-200035776>
- Hassellöv, I.-M., Turner, D. R., Lauer, A., & Corbett, J. J. (2013). Shipping contributes to ocean acidification. *Geophysical Research Letters*, *40*(11), 2731–2736. <https://doi.org/10.1002/grl.50521>
- Hawco, N. J., Fu, F., Yang, N., Hutchins, D. A., & John, S. G. (2021). Independent iron and light limitation in a low-light-adapted *Prochlorococcus* from the deep chlorophyll maximum. *The ISME Journal*, *15*(1), 359–362. <https://doi.org/10.1038/s41396-020-00776-y>
- Hayward, T. L., & Venrick, E. L. (1998). Nearsurface pattern in the California Current: coupling between physical and biological structure. *Deep Sea Research Part II: Topical Studies in Oceanography*, *45*(8–9), 1617–1638.
- Hebbar, G. S. (2014). NOx from diesel engine emission and control strategies-a review. *International Journal of Mechanical Engineering and Robotics Research*, *3*(4), 471.
- Henson, S. A., Painter, S. C., Penny Holliday, N., Stinchcombe, M. C., & Giering, S. L. C. (2013). Unusual subpolar North Atlantic phytoplankton bloom in 2010: Volcanic fertilization or North Atlantic Oscillation? *Journal of Geophysical Research: Oceans*, *118*(10), 4771–4780. <https://doi.org/https://doi.org/10.1002/jgrc.20363>
- Herbert, R. A. (1999). Nitrogen cycling in coastal marine ecosystems. *FEMS Microbiology Reviews*, *23*(5), 563–590. <https://doi.org/10.1111/j.1574-6976.1999.tb00414.x>
- Hirose, K. (2006). Chemical Speciation of Trace Metals in Seawater: a Review. *Analytical Sciences*, *22*(8), 1055–1063. <https://doi.org/10.2116/analsci.22.1055>
- Hogle, S. L., Dupont, C. L., Hopkinson, B. M., King, A. L., Buck, K. N., Roe, K. L., Stuart, R. K., Allen, A. E., Mann, E. L., & Johnson, Z. I. (2018). Pervasive iron limitation at subsurface chlorophyll maxima of the California Current. *Proceedings of the National Academy of Sciences*, *115*(52), 13300–13305.
- Howard, M. D. A., Sutula, M., Caron, D. A., Chao, Y., Farrara, J. D., Frenzel, H., Jones, B., Robertson, G., McLaughlin, K., & Sengupta, A. (2014). Anthropogenic nutrient sources rival natural sources on small scales in the coastal waters of the Southern California Bight. *Limnology and Oceanography*, *59*(1), 285–297.
- Hutchins, D. A., & Bruland, K. W. (1998). Iron-limited diatom growth and Si:N uptake ratios in a coastal upwelling regime. *Nature*, *393*(6685), 561–564. <https://doi.org/10.1038/31203>

- Hutchins, D. A., DiTullio, G. R., Zhang, Y., & Bruland, K. W. (1998). An iron limitation mosaic in the California upwelling regime. *Limnology and Oceanography*, *43*(6), 1037–1054. <https://doi.org/https://doi.org/10.4319/lo.1998.43.6.1037>
- Hutchins, D. A., Witter, A. E., Butler, A., & Luther, G. W. (1999). Competition among marine phytoplankton for different chelated iron species. *Nature*, *400*(6747), 858–861. <https://doi.org/10.1038/23680>
- ICCT. (2023). *Global update on scrubber bans and restrictions - International Council on Clean Transportation*. June. <https://theicct.org/publication/marine-scrubber-bans-and-restrictions-jun23/>
- Infrastructure, S. B. D. (2023). *The Nordic Microalgae and Aquatic Protozoa Website*. Funded by SMHI and the Swedish Research Council through Grant No 2019-00242. <http://nordicmicroalgae.org/galleries/skagerrak-kattegat?page=4>
- International Chamber of Shipping, I. (2023). *Shipping and World Trade: Global Supply and Demand for Seafarers*. Shipping Fact. <https://www.ics-shipping.org/shipping-fact/shipping-and-world-trade-global-supply-and-demand-for-seafarers/>
- Ito, A. (2013a). Global modeling study of potentially bioavailable iron input from shipboard aerosol sources to the ocean. *Global Biogeochemical Cycles*, *27*(1), 1–10. <https://doi.org/10.1029/2012GB004378>
- Ito, A. (2013b). Global modeling study of potentially bioavailable iron input from shipboard aerosol sources to the ocean. *Global Biogeochemical Cycles*, *27*(1), 1–10. <https://doi.org/10.1029/2012GB004378>
- Ito, A. (2015). Atmospheric Processing of Combustion Aerosols as a Source of Bioavailable Iron. *Environmental Science & Technology Letters*, *2*(3), 70–75. <https://doi.org/10.1021/acs.estlett.5b00007>
- Ito, A., & Feng, Y. (2010). Role of dust alkalinity in acid mobilization of iron. *Atmospheric Chemistry and Physics*, *10*(19), 9237–9250. <https://doi.org/10.5194/acp-10-9237-2010>
- Ito, A., Lin, G., & Penner, J. E. (2014). Reconciling modeled and observed atmospheric deposition of soluble organic nitrogen at coastal locations. *Global Biogeochemical Cycles*, *28*(6), 617–630. <https://doi.org/10.1002/2013GB004721>
- Ito, A., Myriokefalitakis, S., Kanakidou, M., Mahowald, N. M., Scanza, R. A., Hamilton, D. S., Baker, A. R., Jickells, T., Sarin, M., Bikkina, S., Gao, Y., Shelley, R. U., Buck, C. S., Landing, W. M., Bowie, A. R., Perron, M. M. G., Guieu, C., Meskhidze, N., Johnson, M. S., ... Duce, R. A. (2019). Pyrogenic iron: The missing link to high iron solubility in aerosols. *Science Advances*, *5*(5). <https://doi.org/10.1126/sciadv.aau7671>



- Ito, A., & Shi, Z. (2016). Delivery of anthropogenic bioavailable iron from mineral dust and combustion aerosols to the ocean. *Atmospheric Chemistry and Physics*, 16(1), 85–99. <https://doi.org/10.5194/acp-16-85-2016>
- Ito, A., Ye, Y., Baldo, C., & Shi, Z. (2021). Ocean fertilization by pyrogenic aerosol iron. *Npj Climate and Atmospheric Science*, 4(1), 30. <https://doi.org/10.1038/s41612-021-00185-8>
- Jackson, G. A. (1980). Phytoplankton growth and zooplankton grazing in oligotrophic oceans. *Nature*, 284(5755), 439–441.
- Jägerbrand, A. K., Brutemark, A., Barthel Svedén, J., & Gren, I.-M. (2019). A review on the environmental impacts of shipping on aquatic and nearshore ecosystems. *Science of The Total Environment*, 695, 133637. <https://doi.org/https://doi.org/10.1016/j.scitotenv.2019.133637>
- Jakobsen, F. (1997). Hydrographic investigation of the Northern Kattegat front. *Continental Shelf Research*, 17(5), 533–554. [https://doi.org/https://doi.org/10.1016/S0278-4343\(96\)00044-1](https://doi.org/https://doi.org/10.1016/S0278-4343(96)00044-1)
- Jalkanen, J. P., Brink, A., Kalli, J., Pettersson, H., Kukkonen, J., & Stipa, T. (2009). A modelling system for the exhaust emissions of marine traffic and its application in the Baltic Sea area. *Atmospheric Chemistry and Physics*, 9(23), 9209–9223. <https://doi.org/10.5194/acp-9-9209-2009>
- Jalkanen, J. P., Johansson, L., Kukkonen, J., Brink, A., Kalli, J., & Stipa, T. (2012). Extension of an assessment model of ship traffic exhaust emissions for particulate matter and carbon monoxide. *Atmospheric Chemistry and Physics*, 12(5), 2641–2659. <https://doi.org/10.5194/acp-12-2641-2012>
- Jalkanen, J.-P., Johansson, L., Wilewska-Bien, M., Granhag, L., Ytreberg, E., Eriksson, K. M., Yngsell, D., Hassellöv, I.-M., Magnusson, K., Raudsepp, U., Maljutenko, I., Winnes, H., & Moldanova, J. (2021). Modelling of discharges from Baltic Sea shipping. *Ocean Science*, 17(3), 699–728. <https://doi.org/10.5194/os-17-699-2021>
- Jang, S. H., & Choi, J. H. (2016). Comparison of fuel consumption and emission characteristics of various marine heavy fuel additives. *Applied Energy*, 179, 36–44.
- Jena, B., Sahu, S., Avinash, K., & Swain, D. (2013). Observation of oligotrophic gyre variability in the south Indian Ocean: Environmental forcing and biological response. *Deep Sea Research Part I: Oceanographic Research Papers*, 80, 1–10. <https://doi.org/https://doi.org/10.1016/j.dsr.2013.06.002>
- Jena, B., Swain, D., & Avinash, K. (2012). Investigation of the biophysical processes over the oligotrophic waters of South Indian Ocean subtropical gyre, triggered by cyclone Edzani. *International Journal of Applied Earth Observation and Geoinformation*, 18, 49–56.

- Jickells, T. D. (2005). Global Iron Connections Between Desert Dust, Ocean Biogeochemistry, and Climate. *Science*, *308*(5718), 67–71. <https://doi.org/10.1126/science.1105959>
- Jickells, T. D., An, Z. S., Andersen, K. K., Baker, A. R., Bergametti, C., Brooks, N., Cao, J. J., Boyd, P. W., Duce, R. A., Hunter, K. A., Kawahata, H., Kubilay, N., LaRoche, J., Liss, P. S., Mahowald, N., Prospero, J. M., Ridgwell, A. J., Tegen, I., & Torres, R. (2005). Global iron connections between desert dust, ocean biogeochemistry, and climate. In *Science* (Vol. 308, Issue 5718, pp. 67–71). <https://doi.org/10.1126/science.1105959>
- Jickells, T. D., Buitenhuis, E., Altieri, K., Baker, A. R., Capone, D., Duce, R. A., Dentener, F., Fennel, K., Kanakidou, M., LaRoche, J., Lee, K., Liss, P., Middelburg, J. J., Moore, J. K., Okin, G., Oschlies, A., Sarin, M., Seitzinger, S., Sharples, J., ... Zamora, L. M. (2017). A reevaluation of the magnitude and impacts of anthropogenic atmospheric nitrogen inputs on the ocean. *Global Biogeochemical Cycles*, *31*(2), 289–305. <https://doi.org/https://doi.org/10.1002/2016GB005586>
- Jickells, T. D., Knap, A. H., & Smith, S. R. (1986). Trace metal and nutrient fluxes through the Bermuda inshore waters. *Rapports et Procès-Verbaux Des Réunions-Conseil International Pour l'exploration de La Mer*, *186*, 251–262.
- Jickells, T., & Moore, C. M. (2015). The Importance of Atmospheric Deposition for Ocean Productivity. *Annual Review of Ecology, Evolution, and Systematics*, *46*(1), 481–501. <https://doi.org/10.1146/annurev-ecolsys-112414-054118>
- Johnson, K. S., Gordon, R. M., & Coale, K. H. (1997). What controls dissolved iron concentrations in the world ocean? *Marine Chemistry*, *57*(3), 137–161. [https://doi.org/https://doi.org/10.1016/S0304-4203\(97\)00043-1](https://doi.org/https://doi.org/10.1016/S0304-4203(97)00043-1)
- Johnson, M. S., & Meskhidze, N. (2013). Atmospheric dissolved iron deposition to the global oceans: effects of oxalate-promoted Fe dissolution, photochemical redox cycling, and dust mineralogy. *Geoscientific Model Development*, *6*(4), 1137–1155. <https://doi.org/10.5194/gmd-6-1137-2013>
- Jones, D. R., Karl, D. M., & Laws, E. A. (1996). Growth rates and production of heterotrophic bacteria and phytoplankton in the North Pacific subtropical gyre. *Deep Sea Research Part I: Oceanographic Research Papers*, *43*(10), 1567–1580.
- Jonson, J. E., Gauss, M., Schulz, M., Jalkanen, J.-P., & Fagerli, H. (2020). Effects of global ship emissions on European air pollution levels. *Atmospheric Chemistry and Physics*, *20*(19), 11399–11422.
- Jordi, A., Basterretxea, G., Tovar-Sanchez, A., Alastuey, A., & Querol, X. (2012). Copper aerosols inhibit phytoplankton growth in the Mediterranean Sea. *Proceedings of the National Academy of Sciences*, *109*(52), 21246–21249. <https://doi.org/10.1073/pnas.1207567110>

- Jutterström, S., Moldan, F., Moldanová, J., Karl, M., Matthias, V., & Posch, M. (2021). The impact of nitrogen and sulfur emissions from shipping on the exceedance of critical loads in the Baltic Sea region. *Atmospheric Chemistry and Physics*, 21(20), 15827–15845. <https://doi.org/10.5194/acp-21-15827-2021>
- Kanakidou, M., Myriokefalitakis, S., Daskalakis, N., Fanourgakis, G., Nenes, A., Baker, A. R., Tsigaridis, K., & Mihalopoulos, N. (2016). Past, Present, and Future Atmospheric Nitrogen Deposition. *Journal of the Atmospheric Sciences*, 73(5), 2039–2047. <https://doi.org/10.1175/JAS-D-15-0278.1>
- Karlson, B., Andersen, P., Arneborg, L., Cembella, A., Eikrem, W., John, U., West, J. J., Klemm, K., Kobos, J., Lehtinen, S., Lundholm, N., Mazur-Marzec, H., Naustvoll, L., Poelman, M., Provoost, P., De Rijcke, M., & Suikkanen, S. (2021). Harmful algal blooms and their effects in coastal seas of Northern Europe. *Harmful Algae*, 102, 101989. <https://doi.org/https://doi.org/10.1016/j.hal.2021.101989>
- Karlson, B., Cusack, C., & Bresnan, E. (2010). *Microscopic and molecular methods for quantitative phytoplankton analysis*. <https://doi.org/10.25607/OBP-1371>
- Khan, M. Y., Giordano, M., Gutierrez, J., Welch, W. A., Asa-Awuku, A., Miller, J. W., & Cocker, D. R. (2012). Benefits of two mitigation strategies for container vessels: Cleaner engines and cleaner fuels. *Environmental Science and Technology*, 46(9), 5049–5056. <https://doi.org/10.1021/es2043646>
- Kilpatrick, T., Xie, S.-P., Miller, A. J., & Schneider, N. (2018). Satellite Observations of Enhanced Chlorophyll Variability in the Southern California Bight. *Journal of Geophysical Research: Oceans*, 123(10), 7550–7563. <https://doi.org/https://doi.org/10.1029/2018JC014248>
- Kim, D., Sato, Y., Oda, T., Muratamatsu, T., Matsuyama, Y., & Honjo, T. (2000). Specific Toxic Effect of Dinoflagellate *Heterocapsa circularisquama* on the Rotifer *Brachionus plicatilis*. *Bioscience, Biotechnology, and Biochemistry*, 64(12), 2719–2722. <https://doi.org/10.1271/bbb.64.2719>
- Kim, H.-J., Miller, A. J., McGowan, J., & Carter, M. L. (2009). Coastal phytoplankton blooms in the Southern California Bight. *Progress in Oceanography*, 82(2), 137–147. <https://doi.org/https://doi.org/10.1016/j.pocean.2009.05.002>
- King, A. L., & Barbeau, K. A. (2011). Dissolved iron and macronutrient distributions in the southern California Current System. *Journal of Geophysical Research: Oceans*, 116(C3). <https://doi.org/https://doi.org/10.1029/2010JC006324>
- Kong, L. (2022). Copper Requirement and Acquisition by Marine Microalgae. *Microorganisms*, 10(9). <https://doi.org/10.3390/microorganisms10091853>

- Kontovas, C. A. (2020). Integration of air quality and climate change policies in shipping: The case of sulphur emissions regulation. *Marine Policy*, 113, 103815. <https://doi.org/https://doi.org/10.1016/j.marpol.2020.103815>
- Koshland, C. P., & Seeker, W. R. (2007). Combustion By-product Formation: An Overview. *Http://Dx.Doi.Org/10.1080/00102209008951675*, 74(1–6), i–viii. <https://doi.org/10.1080/00102209008951675>
- Koski, M., Stedmon, C., & Trapp, S. (2017). Ecological effects of scrubber water discharge on coastal plankton: Potential synergistic effects of contaminants reduce survival and feeding of the copepod *Acartia tonsa*. *Marine Environmental Research*, 129, 374–385. <https://doi.org/10.1016/j.marenvres.2017.06.006>
- Kottuparambil, S., & Agusti, S. (2018). PAHs sensitivity of picophytoplankton populations in the Red Sea. *Environmental Pollution*, 239, 607–616.
- Kottuparambil, S., & Agusti, S. (2020). Cell-by-cell estimation of PAH sorption and subsequent toxicity in marine phytoplankton. *Chemosphere*, 259, 127487. <https://doi.org/https://doi.org/10.1016/j.chemosphere.2020.127487>
- Kulk, G., de Vries, P., van de Poll, W. H., Visser, R. J. W., & Buma, A. G. J. (2013). *Temperature-dependent photoregulation in oceanic picophytoplankton during excessive irradiance exposure*.
- Labry, C., Erard–Le Denn, E., Chapelle, A., Fauchot, J., Youenou, A., Crassous, M. P., Le Grand, J., & Lorgeoux, B. (2008). Competition for phosphorus between two dinoflagellates: A toxic *Alexandrium minutum* and a non-toxic *Heterocapsa triquetra*. *Journal of Experimental Marine Biology and Ecology*, 358(2), 124–135. <https://doi.org/https://doi.org/10.1016/j.jembe.2008.01.025>
- Lack, D. A., Corbett, J. J., Onasch, T., Lerner, B., Massoli, P., Quinn, P. K., Bates, T. S., Covert, D. S., Coffman, D., Sierau, B., Herndon, S., Allan, J., Baynard, T., Lovejoy, E., Ravishankara, A. R., & Williams, E. (2009a). Particulate emissions from commercial shipping: Chemical, physical, and optical properties. *Journal of Geophysical Research*, 114(D7), D00F04. <https://doi.org/10.1029/2008JD011300>
- Lack, D. A., Corbett, J. J., Onasch, T., Lerner, B., Massoli, P., Quinn, P. K., Bates, T. S., Covert, D. S., Coffman, D., Sierau, B., Herndon, S., Allan, J., Baynard, T., Lovejoy, E., Ravishankara, A. R., & Williams, E. (2009b). Particulate emissions from commercial shipping: Chemical, physical, and optical properties. *Journal of Geophysical Research*, 114(D7), D00F04. <https://doi.org/10.1029/2008JD011300>
- Legaard, K. R., & Thomas, A. C. (2006). Spatial patterns in seasonal and interannual variability of chlorophyll and sea surface temperature in the California Current. *Journal of Geophysical Research: Oceans*, 111(C6). <https://doi.org/https://doi.org/10.1029/2005JC003282>

- Lehtoranta, K., Aakko-Saksa, P., Murtonen, T., Vesala, H., Ntziachristos, L., Rönkkö, T., Karjalainen, P., Kuittinen, N., & Timonen, H. (2019). Particulate Mass and Nonvolatile Particle Number Emissions from Marine Engines Using Low-Sulfur Fuels, Natural Gas, or Scrubbers. *Environmental Science and Technology*, *53*(6), 3315–3322. <https://doi.org/10.1021/acs.est.8b05555>
- Levy, J. L., Angel, B. M., Stauber, J. L., Poon, W. L., Simpson, S. L., Cheng, S. H., & Jolley, D. F. (2008). Uptake and internalisation of copper by three marine microalgae: comparison of copper-sensitive and copper-tolerant species. *Aquatic Toxicology*, *89*(2), 82–93.
- Li, G., Cheng, L., Zhu, J., Trenberth, K. E., Mann, M. E., & Abraham, J. P. (2020). Increasing ocean stratification over the past half-century. *Nature Climate Change*, *10*(12), 1116–1123. <https://doi.org/10.1038/s41558-020-00918-2>
- Lin, S., Litaker, R. W., & Sunda, W. G. (2016). Phosphorus physiological ecology and molecular mechanisms in marine phytoplankton. *Journal of Phycology*, *52*(1), 10–36.
- Lindholm, T., & Nummelin, C. (1999). Red tide of the dinoflagellate *Heterocapsa triquetra* (Dinophyta) in a ferry-mixed coastal inlet. *Hydrobiologia*, *393*(0), 245–251. <https://doi.org/10.1023/A:1003563022422>
- Liu, M., Matsui, H., Hamilton, D. S., Lamb, K. D., Rathod, S. D., Schwarz, J. P., & Mahowald, N. M. (2022). The underappreciated role of anthropogenic sources in atmospheric soluble iron flux to the Southern Ocean. *Npj Climate and Atmospheric Science*, *5*(1). <https://doi.org/10.1038/s41612-022-00250-w>
- Lomas, M. W., Bates, N. R., Johnson, R. J., Knap, A. H., Steinberg, D. K., & Carlson, C. A. (2013). Two decades and counting: 24-years of sustained open ocean biogeochemical measurements in the Sargasso Sea. *Deep Sea Research Part II: Topical Studies in Oceanography*, *93*, 16–32.
- Lopez, J. S., Lee, L., & Mackey, K. R. M. (2019). The toxicity of copper to *Crocospaera watsonii* and other marine phytoplankton: A systematic review. In *Frontiers in Marine Science* (Vol. 6, Issue JAN, p. 511). Frontiers Media S.A. <https://doi.org/10.3389/fmars.2018.00511>
- Lund, J. W. G., Kipling, C., & Le Cren, E. D. (1958). The inverted microscope method of estimating algal numbers and the statistical basis of estimations by counting. *Hydrobiologia*, *11*(2), 143–170. <https://doi.org/10.1007/BF00007865>
- Lunde Hermansson, A., Hassellöv, I. M., Moldanová, J., & Ytreberg, E. (2021). Comparing emissions of polyaromatic hydrocarbons and metals from marine fuels and scrubbers. *Transportation Research Part D: Transport and Environment*, *97*. <https://doi.org/10.1016/j.trd.2021.102912>

- Machaj, K., Kupecki, J., Malecha, Z., Morawski, A. W., Skrzypkiewicz, M., Stanclik, M., & Chorowski, M. (2022). Ammonia as a potential marine fuel: A review. *Energy Strategy Reviews, 44*, 100926. <https://doi.org/https://doi.org/10.1016/j.esr.2022.100926>
- Mackey, K., Mioni, C., Ryan, J., & Paytan, A. (2012). Phosphorus Cycling in the Red Tide Incubator Region of Monterey Bay in Response to Upwelling. *Frontiers in Microbiology, 3*. <https://doi.org/10.3389/fmicb.2012.00033>
- Mackey, K. R. M., Buck, K. N., Casey, J. R., Cid, A., Lomas, M. W., Sohrin, Y., & Paytan, A. (2012). Phytoplankton responses to atmospheric metal deposition in the coastal and open-ocean Sargasso Sea. *Frontiers in Microbiology, 3*(OCT), 359. <https://doi.org/10.3389/FMICB.2012.00359/BIBTEX>
- Mackey, K. R. M., Kavanaugh, M. T., Wang, F., Chen, Y., Liu, F., Glover, D. M., Chien, C.-T., & Paytan, A. (2017). Atmospheric and Fluvial Nutrients Fuel Algal Blooms in the East China Sea. *Frontiers in Marine Science, 4*. <https://doi.org/10.3389/fmars.2017.00002>
- Mackey, K. R. M., Mioni, C. E., Ryan, J. P., Paytan, A., Moore, L., Jenkins, B., & Sylvan, J. B. (2012). *Phosphorus cycling in the red tide incubator region of Monterey Bay in response to upwelling*. <https://doi.org/10.3389/fmicb.2012.00033>
- Mackey, K. R. M., van Dijken, G. L., Mazloom, S., Erhardt, A. M., Ryan, J., Arrigo, K. R., & Paytan, A. (2010a). Influence of atmospheric nutrients on primary productivity in a coastal upwelling region. *Global Biogeochemical Cycles, 24*(4), n/a-n/a. <https://doi.org/10.1029/2009GB003737>
- Mackey, K. R. M., van Dijken, G. L., Mazloom, S., Erhardt, A. M., Ryan, J., Arrigo, K. R., & Paytan, A. (2010b). Influence of atmospheric nutrients on primary productivity in a coastal upwelling region. *Global Biogeochemical Cycles, 24*(4), n/a-n/a. <https://doi.org/10.1029/2009GB003737>
- Magnusson, B., & Westerlund, S. (1980). The determination of Cd, Cu, Fe, Ni, Pb and Zn in Baltic Sea water. *Marine Chemistry, 8*(3), 231–244.
- Magnusson, B., & Westerlund, S. (1983). Trace Metal Levels in Sea Water from the Skagerrak and the Kattegat. In C. S. Wong, E. Boyle, K. W. Bruland, J. D. Burton, & E. D. Goldberg (Eds.), *Trace Metals in Sea Water* (pp. 467–473). Springer US. [https://doi.org/10.1007/978-1-4757-6864-0\\_27](https://doi.org/10.1007/978-1-4757-6864-0_27)
- Mahowald, N., Albani, S., Kok, J. F., Engelstaeder, S., Scanza, R., Ward, D. S., & Flanner, M. G. (2014). The size distribution of desert dust aerosols and its impact on the Earth system. *Aeolian Research, 15*, 53–71. <https://doi.org/10.1016/j.aeolia.2013.09.002>
- Mahowald, N. M., Hamilton, D. S., Mackey, K. R. M., Moore, J. K., Baker, A. R., Scanza, R. A., & Zhang, Y. (2018). Aerosol trace metal leaching and impacts on marine microorganisms. *Nature Communications, 9*(1), 2614. <https://doi.org/10.1038/s41467-018-04970-7>

- Mahowald, N. M., Kloster, S., Engelstaedter, S., Moore, J. K., Mukhopadhyay, S., McConnell, J. R., Albani, S., Doney, S. C., Bhattacharya, A., Curran, M. A. J., Flanner, M. G., Hoffman, F. M., Lawrence, D. M., Lindsay, K., Mayewski, P. A., Neff, J., Rothenberg, D., Thomas, E., Thornton, P. E., & Zender, C. S. (2010). Observed 20th century desert dust variability: Impact on climate and biogeochemistry. *Atmospheric Chemistry and Physics*, *10*(22), 10875–10893. <https://doi.org/10.5194/acp-10-10875-2010>
- Mann, E. L., Ahlgren, N., Moffett, J. W., & Chisholm, S. W. (2002). Copper toxicity and cyanobacteria ecology in the Sargasso Sea. *Limnology and Oceanography*, *47*(4), 976–988. <https://doi.org/10.4319/lo.2002.47.4.0976>
- Manner, E., Dentener, F., V Aardenne, J., Cavalli, F., Vignati, E., Velchev, K., Hjorth, J., Boersma, F., Vinken, G., Mihalopoulos, N., & Raes, F. (2009). What can we learn about ship emission inventories from measurements of air pollutants over the Mediterranean Sea? *Atmospheric Chemistry and Physics*, *9*(18), 6815–6831. <https://doi.org/10.5194/acp-9-6815-2009>
- Mantyla, A. W., Bograd, S. J., & Venrick, E. L. (2008). Patterns and controls of chlorophyll-a and primary productivity cycles in the Southern California Bight. *Journal of Marine Systems*, *73*(1), 48–60. <https://doi.org/10.1016/j.jmarsys.2007.08.001>
- Marin-Enriquez, O., Krutwa, A., Fenske, M., Spira, D., Reifferscheid, G., Lukas, M., & Achten, C. (2023). *Environmental Impacts of Discharge Water from Exhaust Gas Cleaning Systems on Ships Final report of the project ImpEx On behalf of the German Environment Agency*. <http://www.umweltbundesamt.de/publikationen>
- Mark Moore, C., Mills, M. M., Achterberg, E. P., Geider, R. J., Laroche, J., Lucas, M. I., McDonagh, E. L., Pan, X., Poulton, A. J., Rijkenberg, M. J. A., Suggett, D. J., Ussher, S. J., & Woodward, E. M. S. (2009). Large-scale distribution of Atlantic nitrogen fixation controlled by iron availability. *Nature Geoscience*, *2*(12), 867–871. <https://doi.org/10.1038/ngeo667>
- Martin, J. H. (1990). Glacial-interglacial CO<sub>2</sub> change: The Iron Hypothesis. *Paleoceanography*, *5*(1), 1–13. <https://doi.org/10.1029/PA005i001p00001>
- Martin, J. H. (1992). Iron as a Limiting Factor in Oceanic Productivity. *Primary Productivity and Biogeochemical Cycles in the Sea*, *43*, 123–137. [https://doi.org/10.1007/978-1-4899-0762-2\\_8](https://doi.org/10.1007/978-1-4899-0762-2_8)
- Martin, J. H., & Fitzwater, S. E. (1988). Iron deficiency limits phytoplankton growth in the north-east pacific subarctic. *Nature*, *331*(6154), 341–343. <https://doi.org/10.1038/331341a0>
- Martin, J. H., Gordon, M., & Fitzwater, S. E. (1991). The case for iron. *Limnology and Oceanography*, *36*(8), 1793–1802. <https://doi.org/10.4319/lo.1991.36.8.1793>

- Martiny, A. C., Talarmin, A., Mouginot, C., Lee, J. A., Huang, J. S., Gellene, A. G., & Caron, D. A. (2016). Biogeochemical interactions control a temporal succession in the elemental composition of marine communities. *Limnology and Oceanography*, *61*(2), 531–542. <https://doi.org/https://doi.org/10.1002/lno.10233>
- Martiny, A. C., Ustick, L., A. Garcia, C., & Lomas, M. W. (2020). Genomic adaptation of marine phytoplankton populations regulates phosphate uptake. *Limnology and Oceanography*, *65*(S1), S340–S350. <https://doi.org/https://doi.org/10.1002/lno.11252>
- Martiny, J. B. H., Jones, S. E., Lennon, J. T., & Martiny, A. C. (2015). Microbiomes in light of traits: a phylogenetic perspective. *Science*, *350*(6261), aac9323.
- Matthias, V., Bewersdorff, I., Aulinger, A., & Quante, M. (2010). The contribution of ship emissions to air pollution in the North Sea regions. *Environmental Pollution*, *158*(6), 2241–2250. <https://doi.org/10.1016/J.ENVPOL.2010.02.013>
- McLaughlin, K., Howard, M. D. A., Robertson, G., Beck, C. D. A., Ho, M., Kessouri, F., Nezlin, N. P., Sutula, M., & Weisberg, S. B. (2021). Influence of anthropogenic nutrient inputs on rates of coastal ocean nitrogen and carbon cycling in the Southern California Bight, United States. *Elementa: Science of the Anthropocene*, *9*(1), 145. <https://doi.org/10.1525/elementa.2020.00145>
- Meng, X., Chen, Y., Wang, B., Ma, Q. W., & Wang, F. J. (2016). Responses of phytoplankton community to the input of different aerosols in the East China Sea. *Geophysical Research Letters*, *43*(13), 7081–7088.
- Merico, E., Donato, A., Gambaro, A., Cesari, D., Gregoris, E., Barbaro, E., Dinoi, A., Giovanelli, G., Masieri, S., & Contini, D. (2016). Influence of in-port ships emissions to gaseous atmospheric pollutants and to particulate matter of different sizes in a Mediterranean harbour in Italy. *Atmospheric Environment*, *139*, 1–10. <https://doi.org/10.1016/j.atmosenv.2016.05.024>
- Meybeck, M. (1993). *C, N, P and S in Rivers: From Sources to Global Inputs BT - Interactions of C, N, P and S Biogeochemical Cycles and Global Change* (R. Wollast, F. T. Mackenzie, & L. Chou, Eds.; pp. 163–193). Springer Berlin Heidelberg.
- Michaels, A. F., Siegel, D. A., Johnson, R. J., Knap, A. H., & Galloway, J. N. (1993). Episodic inputs of atmospheric nitrogen to the Sargasso Sea: Contributions to new production and phytoplankton blooms. *Global Biogeochemical Cycles*, *7*(2), 339–351. <https://doi.org/https://doi.org/10.1029/93GB00178>
- Mills, M. M., & Arrigo, K. R. (2010). Magnitude of oceanic nitrogen fixation influenced by the nutrient uptake ratio of phytoplankton. *Nature Geoscience*, *3*(6), 412–416. <https://doi.org/10.1038/ngeo856>



- Mills, M. M., Ridame, C., Davey, M., La Roche, J., & Geider, R. J. (2004a). Iron and phosphorus co-limit nitrogen fixation in the eastern tropical North Atlantic. *Nature*, *429*(6989), 292–294. <https://doi.org/10.1038/nature02550>
- Mills, M. M., Ridame, C., Davey, M., La Roche, J., & Geider, R. J. (2004b). Iron and phosphorus co-limit nitrogen fixation in the eastern tropical North Atlantic. *Nature*, *429*(6989), 292–294. <https://doi.org/10.1038/nature02550>
- Moffett, J. W., Zika, R. G., & Brand, L. E. (1990). Distribution and potential sources and sinks of copper chelators in the Sargasso Sea. *Deep Sea Research Part A. Oceanographic Research Papers*, *37*(1), 27–36.
- Moisander, P. H., Zhang, R., Boyle, E. A., Hewson, I., Montoya, J. P., & Zehr, J. P. (2012). Analogous nutrient limitations in unicellular diazotrophs and *Prochlorococcus* in the South Pacific Ocean. *The ISME Journal*, *6*(4), 733–744. <https://doi.org/10.1038/ismej.2011.152>
- Moldanová, J., Fridell, E., Popovicheva, O., Demirdjian, B., Tishkova, V., Faccinnetto, A., & Focsa, C. (2009a). Characterisation of particulate matter and gaseous emissions from a large ship diesel engine. *Atmospheric Environment*, *43*(16), 2632–2641. <https://doi.org/10.1016/j.atmosenv.2009.02.008>
- Moldanová, J., Fridell, E., Popovicheva, O., Demirdjian, B., Tishkova, V., Faccinnetto, A., & Focsa, C. (2009b). Characterisation of particulate matter and gaseous emissions from a large ship diesel engine. *Atmospheric Environment*, *43*(16), 2632–2641. <https://doi.org/10.1016/J.ATMOSENV.2009.02.008>
- Moldanová, J., Fridell, E., Winnes, H., Holmin-Fridell, S., Boman, J., Jedynska, A., Tishkova, V., Demirdjian, B., Joulie, S., Bladt, H., Ivleva, N. P., & Niessner, R. (2013). Physical and chemical characterisation of PM emissions from two ships operating in European emission control areas. *Atmospheric Measurement Techniques*, *6*(12), 3577–3596. <https://doi.org/10.5194/amt-6-3577-2013>
- Monteiro, F. M., Dutkiewicz, S., & Follows, M. J. (2011). Biogeographical controls on the marine nitrogen fixers. *Global Biogeochemical Cycles*, *25*(2), GB2003. <https://doi.org/10.1029/2010GB003902>
- Moore, C. M., Mills, M. M., Arrigo, K. R., Berman-Frank, I., Bopp, L., Boyd, P. W., Galbraith, E. D., Geider, R. J., Guieu, C., Jaccard, S. L., Jickells, T. D., La Roche, J., Lenton, T. M., Mahowald, N. M., Marañón, E., Marinov, I., Moore, J. K., Nakatsuka, T., Oschlies, A., ... Ulloa, O. (2013a). Processes and patterns of oceanic nutrient limitation. *Nature Geoscience*, *6*(9), 701–710. <https://doi.org/10.1038/ngeo1765>
- Moore, C. M., Mills, M. M., Arrigo, K. R., Berman-Frank, I., Bopp, L., Boyd, P. W., Galbraith, E. D., Geider, R. J., Guieu, C., Jaccard, S. L., Jickells, T. D., La Roche, J., Lenton, T. M., Mahowald, N. M., Marañón, E., Marinov, I., Moore, J. K., Nakatsuka, T., Oschlies, A., ...

- Ulloa, O. (2013b). Processes and patterns of oceanic nutrient limitation. *Nature Geoscience*, 6(9), 701–710. <https://doi.org/10.1038/ngeo1765>
- Moore, C. M., Mills, M. M., Langlois, R., Milne, A., Achterberg, E. P., La Roche, J., & Geider, R. J. (2008). Relative influence of nitrogen and phosphorus availability on phytoplankton physiology and productivity in the oligotrophic sub-tropical North Atlantic Ocean. *Limnology and Oceanography*, 53(1), 291–305. <https://doi.org/10.4319/lo.2008.53.1.0291>
- Moore, J. K., Doney, S. C., Glover, D. M., & Fung, I. Y. (2002). Iron cycling and nutrient-limitation patterns in surface waters of the world ocean. *Deep-Sea Research Part II: Topical Studies in Oceanography*, 49(1–3), 463–507. [https://doi.org/10.1016/S0967-0645\(01\)00109-6](https://doi.org/10.1016/S0967-0645(01)00109-6)
- Moore, L. R., & Chisholm, S. W. (1999). Photophysiology of the marine cyanobacterium *Prochlorococcus*: ecotypic differences among cultured isolates. *Limnology and Oceanography*, 44(3), 628–638.
- Moore, T. J., Redfern, J. V., Carver, M., Hastings, S., Adams, J. D., & Silber, G. K. (2018). Exploring ship traffic variability off California. *Ocean & Coastal Management*, 163, 515–527. <https://doi.org/https://doi.org/10.1016/j.ocecoaman.2018.03.010>
- Morel, A., Claustre, H., & Gentili, B. (2010). The most oligotrophic subtropical zones of the global ocean: similarities and differences in terms of chlorophyll and yellow substance. *Biogeosciences*, 7(10), 3139–3151.
- Müller-Casseres, E., Edelenbosch, O. Y., Szklo, A., Schaeffer, R., & van Vuuren, D. P. (2021). Global futures of trade impacting the challenge to decarbonize the international shipping sector. *Energy*, 237, 121547. <https://doi.org/https://doi.org/10.1016/j.energy.2021.121547>
- Myriokefalitakis, S., Daskalakis, N., Mihalopoulos, N., Baker, A. R., Nenes, A., & Kanakidou, M. (2015). Changes in dissolved iron deposition to the oceans driven by human activity: a 3-D global modelling study. *Biogeosciences*, 12(13), 3973–3992. <https://doi.org/10.5194/bg-12-3973-2015>
- Nalewajko, C., Lee, K., & Jack, T. R. (1995). Effects of vanadium on freshwater phytoplankton photosynthesis. *Water, Air, and Soil Pollution*, 81(1), 93–105. <https://doi.org/10.1007/BF00477258>
- Neethu, K. V., Saranya, K. S., Krishna, N. G. A., Praved, P. H., Aneesh, B. P., Nandan, S. B., & Marigoudar, S. R. (2021). Toxicity of copper on marine diatoms, *Chaetoceros calcitrans* and *Nitzschia closterium* from Cochin estuary, India. *Ecotoxicology*, 30(5), 783–793. <https://doi.org/10.1007/s10646-021-02410-9>

- Nelson, N. B., Bates, N. R., Siegel, D. A., & Michaels, A. F. (2001). Spatial variability of the CO<sub>2</sub> sink in the Sargasso Sea. *Deep Sea Research Part II: Topical Studies in Oceanography*, 48(8–9), 1801–1821.
- Neumann, D., Karl, M., Radtke, H., Matthias, V., Friedland, R., & Neumann, T. (2020). Quantifying the contribution of shipping NO<sub>x</sub> emissions to the marine nitrogen inventory -- a case study for the western Baltic Sea. *Ocean Science*, 16(1), 115–134. <https://doi.org/10.5194/os-16-115-2020>
- Newportbeachca.gov. (2023). *Visiting Vessels- Newport Harbor, City of Newport Beach website*. <https://www.newportbeachca.gov/government/departments/harbor/visiting-vessels>
- Noble, P. (2019). *Growth in the Shipping Industry: Future Projections and Impacts* (pp. 456–461). Brill | Nijhoff. [https://doi.org/https://doi.org/10.1163/9789004380271\\_079](https://doi.org/https://doi.org/10.1163/9789004380271_079)
- Ntziachristos, L., Saukko, E., Lehtoranta, K., Rönkkö, T., Timonen, H., Simonen, P., Karjalainen, P., & Keskinen, J. (2016). Particle emissions characterization from a medium-speed marine diesel engine with two fuels at different sampling conditions. *Fuel*, 186, 456–465. <https://doi.org/10.1016/j.fuel.2016.08.091>
- Nylund, A. T., Arneborg, L., Tengberg, A., Mallast, U., & Hassellöv, I.-M. (2021). In situ observations of turbulent ship wakes and their spatiotemporal extent. *Ocean Science*, 17(5), 1285–1302. <https://doi.org/10.5194/os-17-1285-2021>
- Olli, K. (2004). Temporary cyst formation of *Heterocapsa triquetra* (Dinophyceae) in natural populations. *Marine Biology*, 145, 1–8. <https://doi.org/10.1007/s00227-004-1295-9>
- Oloruntobi, O., Mokhtar, K., Gohari, A., Asif, S., & Chuah, L. F. (2023). Sustainable transition towards greener and cleaner seaborne shipping industry: Challenges and opportunities. *Cleaner Engineering and Technology*, 13, 100628. <https://doi.org/https://doi.org/10.1016/j.clet.2023.100628>
- Oram, J. J., McWilliams, J. C., & Stolzenbach, K. D. (2008). Gradient-based edge detection and feature classification of sea-surface images of the Southern California Bight. *Remote Sensing of Environment*, 112(5), 2397–2415. <https://doi.org/https://doi.org/10.1016/j.rse.2007.11.010>
- Osipova, L., Georgeff, E., & Comer, B. (2021). *Global scrubber washwater discharges under IMO's 2020 fuel sulfur limit*. <https://theicct.org/publications/global->
- Othman, B. H., Lanouguère, É., Got, P., Sakka Hlaili, A., & Leboulanger, C. (2018). Structural and functional responses of coastal marine phytoplankton communities to PAH mixtures. *Chemosphere*, 209, 908–919. <https://doi.org/10.1016/J.CHEMOSPHERE.2018.06.153>

- Othman, H. Ben, Leboulanger, C., Le Floc'h, E., Mabrouk, H. H., & Hlaili, A. S. (2012). Toxicity of benz (a) anthracene and fluoranthene to marine phytoplankton in culture: does cell size really matter? *Journal of Hazardous Materials*, *243*, 204–211.
- Partensky, F., & Garczarek, L. (2010). Prochlorococcus: advantages and limits of minimalism. *Annual Review of Marine Science*, *2*, 305–331.
- Partensky, F., Hess W, R., & Vaultot, D. (1999). Prochlorococcus, a Marine Photosynthetic Prokaryote of Global Significance. *Microbiology and Molecular Biology Reviews*, *63*(1), 106–127. <https://doi.org/10.1128/membr.63.1.106-127.1999>
- Pausch, F., Bischof, K., & Trimborn, S. (2019). Iron and manganese co-limit growth of the Southern Ocean diatom *Chaetoceros debilis*. *PLoS ONE*, *14*(9). <https://doi.org/10.1371/journal.pone.0221959>
- Paytan, A., Mackey, K. R. M., Chen, Y., Lima, I. D., Doney, S. C., Mahowald, N., Labiosa, R., & Post, A. F. (2009a). Toxicity of atmospheric aerosols on marine phytoplankton. *Proceedings of the National Academy of Sciences of the United States of America*, *106*(12), 4601–4605. [https://doi.org/10.1073/PNAS.0811486106/SUPPL\\_FILE/0811486106SI.PDF](https://doi.org/10.1073/PNAS.0811486106/SUPPL_FILE/0811486106SI.PDF)
- Paytan, A., Mackey, K. R. M., Chen, Y., Lima, I. D., Doney, S. C., Mahowald, N., Labiosa, R., & Post, A. F. (2009b). Toxicity of atmospheric aerosols on marine phytoplankton. *Proceedings of the National Academy of Sciences*, *106*(12), 4601–4605. <https://doi.org/10.1073/pnas.0811486106>
- Picone, M., Russo, M., Distefano, G. G., Baccichet, M., Marchetto, D., Volpi Ghirardini, A., Lunde Hermansson, A., Petrovic, M., Gros, M., Garcia, E., Giubilato, E., Calgaro, L., Magnusson, K., Granberg, M., & Marcomini, A. (2023a). Impacts of exhaust gas cleaning systems (EGCS) discharge waters on planktonic biological indicators. *Marine Pollution Bulletin*, *190*, 114846. <https://doi.org/10.1016/J.MARPOLBUL.2023.114846>
- Picone, M., Russo, M., Distefano, G. G., Baccichet, M., Marchetto, D., Volpi Ghirardini, A., Lunde Hermansson, A., Petrovic, M., Gros, M., Garcia, E., Giubilato, E., Calgaro, L., Magnusson, K., Granberg, M., & Marcomini, A. (2023b). Impacts of exhaust gas cleaning systems (EGCS) discharge waters on planktonic biological indicators. *Marine Pollution Bulletin*, *190*, 114846. <https://doi.org/https://doi.org/10.1016/j.marpolbul.2023.114846>
- Pierce, D. W., Barnett, T. P., & Gleckler, P. J. (2011). Ocean Circulations, Heat Budgets, and Future Commitment to Climate Change. *Annual Review of Environment and Resources*, *36*(1), 27–43. <https://doi.org/10.1146/annurev-environ-022610-112928>
- Pinedo-González, P., Hawco, N. J., Bundy, R. M., Armbrust, E. V., Follows, M. J., Cael, B. B., White, A. E., Ferrón, S., Karl, D. M., & John, S. G. (2020). Anthropogenic Asian aerosols provide Fe to the North Pacific Ocean. *Proceedings of the National Academy of Sciences*, *117*(45), 27862–27868.

- Pohl, C., & Fernández-Otero, E. (2012). Iron distribution and speciation in oxic and anoxic waters of the Baltic Sea. *Marine Chemistry*, 145–147, 1–15.  
<https://doi.org/https://doi.org/10.1016/j.marchem.2012.09.001>
- Popovicheva, O., Kireeva, E., Persiantseva, N., Timofeev, M., Bladt, H., Ivleva, N. P., Niessner, R., & Moldanová, J. (2012). Microscopic characterization of individual particles from multicomponent ship exhaust. *Journal of Environmental Monitoring*, 14(12), 3101–3110. <https://doi.org/10.1039/c2em30338h>
- Popovicheva, O., Kireeva, E., Shonija, N., Zubareva, N., Persiantseva, N., Tishkova, V., Demirdjian, B., Moldanová, J., & Mogilnikov, V. (2009). Ship particulate pollutants: Characterization in terms of environmental implication. *Journal of Environmental Monitoring*, 11(11), 2077–2086. <https://doi.org/10.1039/b908180a>
- Raspor, B., Nürnberg, H. W., Valenta, P., & Branica, M. (1980). Kinetics and mechanism of trace metal chelation in sea water. *Journal of Electroanalytical Chemistry and Interfacial Electrochemistry*, 115(2), 293–308.  
[https://doi.org/https://doi.org/10.1016/S0022-0728\(80\)80333-0](https://doi.org/https://doi.org/10.1016/S0022-0728(80)80333-0)
- Rathod, S. D., Hamilton, D. S., Mahowald, N. M., Klimont, Z., Corbett, J. J., & Bond, T. C. (2020a). A Mineralogy-Based Anthropogenic Combustion-Iron Emission Inventory. *Journal of Geophysical Research: Atmospheres*, 125(17), e2019JD032114.  
<https://doi.org/10.1029/2019JD032114>
- Rathod, S. D., Hamilton, D. S., Mahowald, N. M., Klimont, Z., Corbett, J. J., & Bond, T. C. (2020b). A Mineralogy-Based Anthropogenic Combustion-Iron Emission Inventory. *Journal of Geophysical Research: Atmospheres*, 125(17), e2019JD032114.  
<https://doi.org/10.1029/2019JD032114>
- Ratten, J.-M., LaRoche, J., Desai, D. K., Shelley, R. U., Landing, W. M., Boyle, E., & Langlois, R. J. (2015). Sources of iron and phosphate affect the distribution of diazotrophs in the North Atlantic. *Deep Sea Research Part II: Topical Studies in Oceanography*, 116, 332–341. <https://doi.org/10.1016/J.DSR2.2014.11.012>
- Raudsepp, U., Laanemets, J., Maljutenko, I., Hongisto, M., & Jalkanen, J.-P. (2013). Impact of ship-borne nitrogen deposition on the Gulf of Finland ecosystem: an evaluation\*\*The work presented in this study was jointly funded by the European Regional Development Fund, Central Baltic INTERREG IV A Programme within the project SNOOP and th. *Oceanologia*, 55(4), 837–857.  
<https://doi.org/https://doi.org/10.5697/oc.55-4.837>
- Raudsepp, U., Maljutenko, I., Kõuts, M., Granhag, L., Wilewska-Bien, M., Hassellöv, I. M., Eriksson, K. M., Johansson, L., Jalkanen, J. P., Karl, M., Matthias, V., & Moldanova, J. (2019a). Shipborne nutrient dynamics and impact on the eutrophication in the Baltic Sea. *Science of the Total Environment*, 671, 189–207.  
<https://doi.org/10.1016/j.scitotenv.2019.03.264>

- Raudsepp, U., Maljutenko, I., Kõuts, M., Granhag, L., Wilewska-Bien, M., Hassellöv, I.-M., Eriksson, K. M., Johansson, L., Jalkanen, J.-P., Karl, M., Matthias, V., & Moldanova, J. (2019b). Shipborne nutrient dynamics and impact on the eutrophication in the Baltic Sea. *Science of The Total Environment*, *671*, 189–207. <https://doi.org/10.1016/J.SCITOTENV.2019.03.264>
- Raudsepp, U., Maljutenko, I., Kõuts, M., Granhag, L., Wilewska-Bien, M., Hassellöv, I.-M., Eriksson, K. M., Johansson, L., Jalkanen, J.-P., Karl, M., Matthias, V., & Moldanova, J. (2019c). Shipborne nutrient dynamics and impact on the eutrophication in the Baltic Sea. *Science of The Total Environment*, *671*, 189–207. <https://doi.org/10.1016/J.SCITOTENV.2019.03.264>
- Raven, J. A. (1990). Predictions of Mn and Fe use efficiencies of phototrophic growth as a function of light availability for growth and of C assimilation pathway. *New Phytologist*, *116*(1), 1–18.
- Redfield, A. C. (1934). *On the proportions of organic derivatives in sea water and their relation to the composition of plankton* (Vol. 1). university press of liverpool Liverpool.
- Regaudie-de-Gioux, A., Huete-Ortega, M., Sobrino, C., López-Sandoval, D. C., González, N., Fernández-Carrera, A., Vidal, M., Marañón, E., Cermeño, P., Latasa, M., Agustí, S., & Duarte, C. M. (2019). Multi-model remote sensing assessment of primary production in the subtropical gyres. *Journal of Marine Systems*, *196*, 97–106. <https://doi.org/https://doi.org/10.1016/j.jmarsys.2019.03.007>
- Rehder, D. (2022). *Vanadium-Based Transformations Effected by Algae and Microbes*. 563–577. [https://doi.org/10.1007/978-3-030-97185-4\\_18](https://doi.org/10.1007/978-3-030-97185-4_18)
- Richardson, L. L., & Ledrew, E. F. (2006). Remote sensing of aquatic coastal ecosystem processes. In *Libro* (Vol. 9, Issue DECEMBER 2005). <https://doi.org/10.1007/1-4020-3968-9>
- Roch, M., Brandt, P., & Schmidtko, S. (2023). Recent large-scale mixed layer and vertical stratification maxima changes . In *Frontiers in Marine Science* (Vol. 10). <https://www.frontiersin.org/articles/10.3389/fmars.2023.1277316>
- Romera-Castillo, C., Letscher, R. T., & Hansell, D. A. (2016). New nutrients exert fundamental control on dissolved organic carbon accumulation in the surface Atlantic Ocean. *Proceedings of the National Academy of Sciences*, *113*(38), 10497–10502. <https://doi.org/10.1073/pnas.1605344113>
- Saito, M. A., Dorsk, A., Post, A. F., McIlvin, M. R., Rappé, M. S., DiTullio, G. R., & Moran, D. M. (2015). Needles in the blue sea: Sub-species specificity in targeted protein biomarker analyses within the vast oceanic microbial metaproteome. *Proteomics*, *15*(20), 3521–3531.

- Saito, M. A., Goepfert, T. J., & Ritt, J. T. (2008). Some thoughts on the concept of colimitation: Three definitions and the importance of bioavailability. *Limnology and Oceanography*, 53(1), 276–290. <https://doi.org/10.4319/lo.2008.53.1.0276>
- Sallée, J.-B., Pellichero, V., Akhoudas, C., Pauthenet, E., Vignes, L., Schmidtke, S., Garabato, A. N., Sutherland, P., & Kuusela, M. (2021). Summertime increases in upper-ocean stratification and mixed-layer depth. *Nature*, 591(7851), 592–598. <https://doi.org/10.1038/s41586-021-03303-x>
- Salo, K., Zetterdahl, M., Johnson, H., Svensson, E., Magnusson, M., Gabriellii, C., & Brynolf, S. (2016). Emissions to the Air. In *Shipping and the Environment* (pp. 169–227). Springer Berlin Heidelberg. [https://doi.org/10.1007/978-3-662-49045-7\\_5](https://doi.org/10.1007/978-3-662-49045-7_5)
- Santos, L. F. E. d., Salo, K., & Thomson, E. S. (2022). Quantification and physical analysis of nanoparticle emissions from a marine engine using different fuels and a laboratory wet scrubber. *Environmental Science: Processes & Impacts*, 24(10), 1769–1781. <https://doi.org/10.1039/D2EM00054G>
- Sardain, A., Sardain, E., & Leung, B. (2019). Global forecasts of shipping traffic and biological invasions to 2050. *Nature Sustainability*, 2(4), 274–282. <https://doi.org/10.1038/s41893-019-0245-y>
- Sarmiento, J. L., & Gruber, N. (2006). *Ocean biogeochemical dynamics*. Princeton University Press.
- Sarvi, A., Lyyränen, J., Jokiniemi, J., & Zevenhoven, R. (2011). Particulate emissions from large-scale medium-speed diesel engines: 2. Chemical composition. *Fuel Processing Technology*, 92(10), 2116–2122. <https://doi.org/10.1016/j.fuproc.2011.06.021>
- Schmolke, S., Ewert, K., Kaste, M., Schöngaßner, T., Kirchgeorg, T., & Marin-Enriquez, O. (2020). *Environmental Protection in Maritime Traffic-Scrubber Wash Water Survey Final report*.
- Schnetzer, A., Jones, B. H., Schaffner, R. A., Cetinic, I., Fitzpatrick, E., Miller, P. E., Seubert, E. L., & Caron, D. A. (2013). Coastal upwelling linked to toxic Pseudo-nitzschia australis blooms in Los Angeles coastal waters, 2005–2007. *Journal of Plankton Research*, 35(5), 1080–1092.
- Schroth, A. W. (2018). Impacts of Anthropocene Fossil Fuel Combustion on Atmospheric Iron Supply to the Ocean. In *Encyclopedia of the Anthropocene* (pp. 103–113). Elsevier. <https://doi.org/10.1016/B978-0-12-809665-9.09919-5>
- Schroth, A. W., Crusius, J., Sholkovitz, E. R., & Bostick, B. C. (2009). Iron solubility driven by speciation in dust sources to the ocean. *Nature Geoscience*, 2(5), 337–340. <https://doi.org/10.1038/ngeo501>

- Sedwick, P. N., Sholkovitz, E. R., & Church, T. M. (2007). Impact of anthropogenic combustion emissions on the fractional solubility of aerosol iron: Evidence from the Sargasso Sea. *Geochemistry, Geophysics, Geosystems*, 8(10), n/a-n/a. <https://doi.org/10.1029/2007GC001586>
- Shen, A., Liu, H., Xin, Q., Hu, Q., Wang, X., & Chen, J. (2022). Responses of Marine Diatom&ndash;Dinoflagellate Interspecific Competition to Different Phosphorus Sources. *Journal of Marine Science and Engineering*, 10(12). <https://doi.org/10.3390/jmse10121972>
- Shiozaki, T., Ijichi, M., Kodama, T., Takeda, S., & Furuya, K. (2014). Heterotrophic bacteria as major nitrogen fixers in the euphotic zone of the Indian Ocean. *Global Biogeochemical Cycles*, 28(10), 1096–1110. <https://doi.org/https://doi.org/10.1002/2014GB004886>
- Sholkovitz, E. R., Sedwick, P. N., Church, T. M., Baker, A. R., & Powell, C. F. (2012). Fractional solubility of aerosol iron: Synthesis of a global-scale data set. *Geochimica et Cosmochimica Acta*, 89, 173–189. <https://doi.org/10.1016/j.gca.2012.04.022>
- Siegel, D. A., Granata, T. C., Michaels, A. F., & Dickey, T. D. (1990). Mesoscale eddy diffusion, particle sinking, and the interpretation of sediment trap data. *Journal of Geophysical Research: Oceans*, 95(C4), 5305–5311.
- Signorini, S. R., Franz, B. A., & McClain, C. R. (2015). Chlorophyll variability in the oligotrophic gyres: mechanisms, seasonality and trends. *Frontiers in Marine Science*, 2. <https://doi.org/10.3389/fmars.2015.00001>
- Simon Bullock, J. M., & Larkin, A. (2022). The urgent case for stronger climate targets for international shipping. *Climate Policy*, 22(3), 301–309. <https://doi.org/10.1080/14693062.2021.1991876>
- Slabbing, A. R. D., Soria, S., Burt, G. R., & Cleary, J. J. (1990). Water quality bioassays in two Bermudan harbours using the ciliate *Euplotes vannus*, in relation to tributyltin distribution. *Journal of Experimental Marine Biology and Ecology*, 138(1), 159–166. [https://doi.org/https://doi.org/10.1016/0022-0981\(90\)90182-C](https://doi.org/https://doi.org/10.1016/0022-0981(90)90182-C)
- Slomp, C. P., & Van Cappellen, P. (2004). Nutrient inputs to the coastal ocean through submarine groundwater discharge: controls and potential impact. *Journal of Hydrology*, 295(1), 64–86. <https://doi.org/https://doi.org/10.1016/j.jhydrol.2004.02.018>
- Smith, V. H., & Schindler, D. W. (2009). Eutrophication science: where do we go from here? *Trends in Ecology & Evolution*, 24(4), 201–207.
- Smith, S. V., Swaney, D. P., Talaue-Mcmanus, L., Bartley, J. D., Sandhei, P. T., McLaughlin, C. J., Dupra, V. C., Crossland, C. J., Buddemeier, R. W., Maxwell, B. A., & Wulff, F. (2003). Humans, Hydrology, and the Distribution of Inorganic Nutrient Loading to the Ocean.



*BioScience*, 53(3), 235–245. [https://doi.org/10.1641/0006-3568\(2003\)053\[0235:HHATDO\]2.0.CO;2](https://doi.org/10.1641/0006-3568(2003)053[0235:HHATDO]2.0.CO;2)

- Sofiev, M., Winebrake, J. J., Johansson, L., Carr, E. W., Prank, M., Soares, J., Vira, J., Kouznetsov, R., Jalkanen, J. P., & Corbett, J. J. (2018). Cleaner fuels for ships provide public health benefits with climate tradeoffs. *Nature Communications*, 9(1). <https://doi.org/10.1038/s41467-017-02774-9>
- Solmon, F., Chuang, P. Y., Meskhidze, N., & Chen, Y. (2009). Acidic processing of mineral dust iron by anthropogenic compounds over the north Pacific Ocean. *Journal of Geophysical Research*, 114(D2), D02305. <https://doi.org/10.1029/2008JD010417>
- Steinberg, D. K., Carlson, C. A., Bates, N. R., Johnson, R. J., Michaels, A. F., & Knap, A. H. (2001). Overview of the US JGOFS Bermuda Atlantic Time-series Study (BATS): a decade-scale look at ocean biology and biogeochemistry. *Deep Sea Research Part II: Topical Studies in Oceanography*, 48(8), 1405–1447. [https://doi.org/https://doi.org/10.1016/S0967-0645\(00\)00148-X](https://doi.org/https://doi.org/10.1016/S0967-0645(00)00148-X)
- Stelmakh, L. V., Mansurova, I. M., Gorbunova, T. L., & Alatartseva, O. S. (2022). Toxicity effects of copper on two species of marine diatoms microalgae and two species of dinoflagellates. *Ecologica Montenegrina*, 58, 55–68.
- Stone, R. (2012). *Introduction to Internal Combustion Engines 4th edition*. <https://www.bookdepository.com/Introduction-Internal-Combustion-Engines-Richard-Stone/9780230576636>
- Streibel, T., Schnelle-Kreis, J., Czech, H., Harndorf, H., Jakobi, G., Jokiniemi, J., Karg, E., Lintelmann, J., Matuschek, G., Michalke, B., Müller, L., Orasche, J., Passig, J., Radischat, C., Rabe, R., Reda, A., Rüger, C., Schwemer, T., Sippula, O., ... Zimmermann, R. (2017). Aerosol emissions of a ship diesel engine operated with diesel fuel or heavy fuel oil. *Environmental Science and Pollution Research*, 24(12), 10976–10991. <https://doi.org/10.1007/s11356-016-6724-z>
- Sunda, W. G. (2012). Feedback interactions between trace metal nutrients and phytoplankton in the ocean. *Frontiers in Microbiology*, 3, 204.
- Sunda, W. G., & Huntaman, S. A. (1997). Interrelated influence of iron, light and cell size on marine phytoplankton growth. *Nature*, 390(6658), 389–392. <https://doi.org/10.1038/37093>
- Sunda, W. G., & Huntsman, S. A. (1995a). Cobalt and zinc interreplacement in marine phytoplankton: Biological and geochemical implications. *Limnology and Oceanography*, 40(8), 1404–1417. <https://doi.org/10.4319/lo.1995.40.8.1404>
- Sunda, W. G., & Huntsman, S. A. (1995b). Iron uptake and growth limitation in oceanic and coastal phytoplankton. *Marine Chemistry*, 50(1), 189–206. [https://doi.org/https://doi.org/10.1016/0304-4203\(95\)00035-P](https://doi.org/https://doi.org/10.1016/0304-4203(95)00035-P)

- Sunda, W. G., & Huntsman, S. A. (1998). Control of Cd concentrations in a coastal diatom by interactions among free ionic Cd, Zn, and Mn in seawater. *Environmental Science and Technology*, 32(19), 2961–2968. <https://doi.org/10.1021/es980271y>
- Sunda, W. G., & Huntsman, S. A. (2015). High iron requirement for growth, photosynthesis, and low-light acclimation in the coastal cyanobacterium *Synechococcus bacillaris*. *Frontiers in Microbiology*, 6, 561.
- Sutton, A. J., Wanninkhof, R., Sabine, C. L., Feely, R. A., Cronin, M. F., & Weller, R. A. (2017). Variability and trends in surface seawater pCO<sub>2</sub> and CO<sub>2</sub> flux in the Pacific Ocean. *Geophysical Research Letters*, 44(11), 5627–5636. <https://doi.org/https://doi.org/10.1002/2017GL073814>
- Sverdrup, H. U. (1953). On conditions for the vernal blooming of phytoplankton. *J. Cons. Int. Explor. Mer*, 18(3), 287–295.
- Talley, L. D., & Raymer, M. E. (1982). *Eighteen degree water variability*.
- Tao, L., Fairley, D., Kleeman, M. J., & Harley, R. A. (2013). Effects of switching to lower sulfur marine fuel oil on air quality in the San Francisco Bay area. *Environmental Science and Technology*, 47(18), 10171–10178. <https://doi.org/10.1021/es401049x>
- Tesdal, J.-E., Ducklow, H. W., Goes, J. I., & Yashayaev, I. (2022). Recent nutrient enrichment and high biological productivity in the Labrador Sea is tied to enhanced winter convection. *Progress in Oceanography*, 206, 102848. <https://doi.org/https://doi.org/10.1016/j.pocean.2022.102848>
- Teuchies, J., Cox, T. J. S., Van Itterbeeck, K., Meysman, F. J. R., & Blust, R. (2020). The impact of scrubber discharge on the water quality in estuaries and ports. *Environmental Sciences Europe*, 32(1), 1–11. <https://doi.org/10.1186/s12302-020-00380-z>
- Thomas, W. H., Seibert, D. L. R., & Dodson, A. N. (1974). Phytoplankton enrichment experiments and bioassays in natural coastal sea water and in sewage outfall receiving waters off Southern California. *Estuarine and Coastal Marine Science*, 2(3), 191–206.
- Thor, P., Granberg, M. E., Winnes, H., & Magnusson, K. (2021). Severe Toxic Effects on Pelagic Copepods from Maritime Exhaust Gas Scrubber Effluents. *Environmental Science & Technology*, 55(9), 5826–5835. <https://doi.org/10.1021/acs.est.0c07805>
- Tin, H. C., Lomas, M. W., & Ishizaka, J. (2016). Satellite-derived estimates of primary production during the Sargasso Sea winter/spring bloom: Integration of in-situ time-series data and ocean color remote sensing observations. *Regional Studies in Marine Science*, 3, 131–143.
- Trapp, J. M., Millero, F. J., & Prospero, J. M. (2010). Trends in the solubility of iron in dust-dominated aerosols in the equatorial Atlantic trade winds: Importance of iron

- speciation and sources. *Geochemistry, Geophysics, Geosystems*, 11(3), n/a-n/a.  
<https://doi.org/10.1029/2009GC002651>
- Tronczynski, J., Saussey, L., & Ponzevera, E. (2022). *Trace metals and PAHs discharge from ship with exhaust gas cleaning system (EGCS)*. <https://doi.org/10.13155/87494>
- Tsimplis, M. (2020). Marine pollution from shipping activities. In *Maritime law* (pp. 403–464). Informa law from Routledge.
- Tsutsumi, E., Matsuno, T., Itoh, S., Zhang, J., Senjyu, T., Sakai, A., Lee, K., Yanagimoto, D., Yasuda, I., Ogawa, H., & Villanoy, C. (2020). Vertical fluxes of nutrients enhanced by strong turbulence and phytoplankton bloom around the ocean ridge in the Luzon Strait. *Scientific Reports*, 10(1), 17879. <https://doi.org/10.1038/s41598-020-74938-5>
- Turner, D. R., Hassellöv, I.-M., Ytreberg, E., & Rutgersson, A. (2017). Shipping and the environment: Smokestack emissions, scrubbers and unregulated oceanic consequences. *Elementa: Science of the Anthropocene*, 5, 45.  
<https://doi.org/10.1525/elementa.167>
- Twining, B. S., & Baines, S. B. (2013). The Trace Metal Composition of Marine Phytoplankton. *Annual Review of Marine Science*, 5(1), 191–215.  
<https://doi.org/10.1146/annurev-marine-121211-172322>
- Ulloa, O., Henríquez-Castillo, C., Ramírez-Flandes, S., Plominsky, A. M., Murillo, A. A., Morgan-Lang, C., Hallam, S. J., & Stepanauskas, R. (2021). The cyanobacterium *Prochlorococcus* has divergent light-harvesting antennae and may have evolved in a low-oxygen ocean. *Proceedings of the National Academy of Sciences*, 118(11), e2025638118. <https://doi.org/10.1073/pnas.2025638118>
- Ünsal, M. (1982). The accumulation and transfer of vanadium within the food chain. *Marine Pollution Bulletin*, 13(4), 139–141. [https://doi.org/10.1016/0025-326X\(82\)90373-3](https://doi.org/10.1016/0025-326X(82)90373-3)
- Ussher, S. J., Achterberg, E. P., Powell, C., Baker, A. R., Jickells, T. D., Torres, R., & Worsfold, P. J. (2013). Impact of atmospheric deposition on the contrasting iron biogeochemistry of the North and South Atlantic Ocean. *Global Biogeochemical Cycles*, 27(4), 1096–1107.  
<https://doi.org/https://doi.org/10.1002/gbc.20056>
- Utermöhl, H. (1931). Über das umgekehrte Mikroskop. *Arch. Hydrobiol. Plankt*, 22, 643–645.
- Valavanidis, A., Fiotakis, K., & Vlachogianni, T. (2008). Airborne particulate matter and human health: Toxicological assessment and importance of size and composition of particles for oxidative damage and carcinogenic mechanisms. In *Journal of Environmental Science and Health - Part C Environmental Carcinogenesis and Ecotoxicology Reviews* (Vol. 26, Issue 4, pp. 339–362).  
<https://doi.org/10.1080/10590500802494538>

- van den Engh, G. J., Doggett, J. K., Thompson, A. W., Doblin, M. A., Gimpel, C. N. G., & Karl, D. M. (2017). Dynamics of Prochlorococcus and Synechococcus at Station ALOHA Revealed through Flow Cytometry and High-Resolution Vertical Sampling . In *Frontiers in Marine Science* (Vol. 4).  
<https://www.frontiersin.org/articles/10.3389/fmars.2017.00359>
- Venrick, E. L. (2012). Phytoplankton in the California Current system off southern California: Changes in a changing environment. *Progress in Oceanography*, 104, 46–58.  
<https://doi.org/https://doi.org/10.1016/j.pocean.2012.05.005>
- Viana, M., Amato, F., Alastuey, A., Querol, X., Moreno, T., Dos Santos, S. G., Herce, M. D., & Fernández-Patier, R. (2009). Chemical tracers of particulate emissions from commercial shipping. *Environmental Science and Technology*, 43(19), 7472–7477.  
<https://doi.org/10.1021/es901558t>
- Viana, M., Kuhlbusch, T. A. J., Querol, X., Alastuey, A., Harrison, R. M., Hopke, P. K., Winiwarter, W., Vallius, M., Szidat, S., Prévôt, A. S. H., Hueglin, C., Bloemen, H., Wählin, P., Vecchi, R., Miranda, A. I., Kasper-Giebl, A., Maenhaut, W., & Hitzenberger, R. (2008). Source apportionment of particulate matter in Europe: A review of methods and results. In *Journal of Aerosol Science* (Vol. 39, Issue 10, pp. 827–849). Elsevier Ltd.  
<https://doi.org/10.1016/j.jaerosci.2008.05.007>
- Viana, M., Rizza, V., Tobías, A., Carr, E., Corbett, J., Sofiev, M., Karanasiou, A., Buonanno, G., & Fann, N. (2020). Estimated health impacts from maritime transport in the Mediterranean region and benefits from the use of cleaner fuels. *Environment International*, 138, 105670. <https://doi.org/10.1016/j.envint.2020.105670>
- Viljoen, J. J., Weir, I., Fietz, S., Cloete, R., Loock, J., Philibert, R., & Roychoudhury, A. N. (2019). Links between the phytoplankton community composition and trace metal distribution in summer surface waters of the Atlantic southern ocean. *Frontiers in Marine Science*, 6, 295.
- Voss, M., Baker, A., Bange, H. W., Conley, D., Cornell, S., Deutsch, B., Engel, A., Ganeshram, R., Garnier, J., Heiskanen, A.-S., Jickells, T., Lancelot, C., McQuatters-Gollop, A., Middelburg, J., Schiedek, D., Slomp, C. P., & Conley, D. P. (2011). Nitrogen processes in coastal and marine ecosystems. In A. Bleeker, B. Grizzetti, C. M. Howard, G. Billen, H. van Grinsven, J. W. Erisman, M. A. Sutton, & P. Grennfelt (Eds.), *The European Nitrogen Assessment: Sources, Effects and Policy Perspectives* (pp. 147–176). Cambridge University Press.  
<https://doi.org/DOI:10.1017/CBO9780511976988.011>
- Voss, M., Bange, H. W., Dippner, J. W., Middelburg, J. J., Montoya, J. P., & Ward, B. (2013). The marine nitrogen cycle: recent discoveries, uncertainties and the potential relevance of climate change. *Philosophical Transactions of the Royal Society B: Biological Sciences*, 368(1621), 20130121. <https://doi.org/10.1098/rstb.2013.0121>

- Walker, T. R., Adebambo, O., Del Aguila Feijoo, M. C., Elhaimer, E., Hossain, T., Edwards, S. J., Morrison, C. E., Romo, J., Sharma, N., Taylor, S., & Zomorodi, S. (2018). Environmental effects of marine transportation. In *World Seas: An Environmental Evaluation Volume III: Ecological Issues and Environmental Impacts* (pp. 505–530). Elsevier.  
<https://doi.org/10.1016/B978-0-12-805052-1.00030-9>
- Walker, T. R., Adebambo, O., Feijoo, M. C. D. A., Elhaimer, E., Hossain, T., Edwards, S. J., Morrison, C. E., Romo, J., Sharma, N., & Taylor, S. (2019). Environmental effects of marine transportation. In *World seas: an environmental evaluation* (pp. 505–530). Elsevier.
- Wang, X., Shen, Y., Lin, Y., Pan, J., Zhang, Y., Louie, P. K. K., Li, M., & Fu, Q. (2019). Atmospheric pollution from ships and its impact on local air quality at a port site in Shanghai. *Atmospheric Chemistry and Physics*, *19*(9), 6315–6330.
- Wang, Y., Chen, H.-H., Tang, R., He, D., Lee, Z., Xue, H., Wells, M., Boss, E., & Chai, F. (2022). Australian fire nourishes ocean phytoplankton bloom. *Science of The Total Environment*, *807*, 150775.
- Wasmund, N., & Uhlig, S. (2003). Phytoplankton trends in the Baltic Sea. *ICES Journal of Marine Science*, *60*(2), 177–186. [https://doi.org/10.1016/S1054-3139\(02\)00280-1](https://doi.org/10.1016/S1054-3139(02)00280-1)
- Watt, J. A. J., Burke, I. T., Edwards, R. A., Malcolm, H. M., Mayes, W. M., Olszewska, J. P., Pan, G., Graham, M. C., Heal, K. V., Rose, N. L., Turner, S. D., & Spears, B. M. (2018). Vanadium: A Re-Emerging Environmental Hazard. *Environmental Science and Technology*, *52*(21), 11973–11974.  
[https://doi.org/10.1021/ACS.EST.8B05560/ASSET/IMAGES/LARGE/ES-2018-055607\\_0002.JPEG](https://doi.org/10.1021/ACS.EST.8B05560/ASSET/IMAGES/LARGE/ES-2018-055607_0002.JPEG)
- Wietkamp, S., Krock, B., Gu, H., Voß, D., Klemm, K., & Tillmann, U. (2019). Occurrence and distribution of Amphidomataceae (Dinophyceae) in Danish coastal waters of the North Sea, the Limfjord and the Kattegat/Belt area. *Harmful Algae*, *88*, 101637.  
<https://doi.org/https://doi.org/10.1016/j.hal.2019.101637>
- Williams, C., Sharples, J., Mahaffey, C., & Rippeth, T. (2013). Wind-driven nutrient pulses to the subsurface chlorophyll maximum in seasonally stratified shelf seas. *Geophysical Research Letters*, *40*(20), 5467–5472.  
<https://doi.org/https://doi.org/10.1002/2013GL058171>
- Winnes, H., Fridell, E., & Moldanová, J. (2020). Effects of marine exhaust gas scrubbers on gas and particle emissions. *Journal of Marine Science and Engineering*, *8*(4), 299.  
<https://doi.org/10.3390/JMSE8040299>
- Woods, J. D., & Barkmann, W. (1986). A Lagrangian mixed layer model of Atlantic 18 C water formation. *Nature*, *319*(6054), 574–576.

- Wu, X., Liu, Y., Weng, Y., Li, L., & Lin, S. (2022). Isolation, identification and toxicity of three strains of *Heterocapsa* (Dinophyceae) in a harmful event in Fujian, China. *Harmful Algae*, 120, 102355. <https://doi.org/https://doi.org/10.1016/j.hal.2022.102355>
- Xiao, H.-W., Xiao, H.-Y., Shen, C.-Y., Zhang, Z.-Y., & Long, A.-M. (2018). Chemical composition and sources of marine aerosol over the Western North Pacific Ocean in winter. *Atmosphere*, 9(8), 298.
- Yamaguchi, R., & Suga, T. (2019). Trend and Variability in Global Upper-Ocean Stratification Since the 1960s. *Journal of Geophysical Research: Oceans*, 124(12), 8933–8948. <https://doi.org/https://doi.org/10.1029/2019JC015439>
- Ytreberg, E., Hansson, K., Hermansson, A. L., Parsmo, R., Lagerström, M., Jalkanen, J. P., & Hassellöv, I. M. (2022a). Metal and PAH loads from ships and boats, relative other sources, in the Baltic Sea. *Marine Pollution Bulletin*, 182. <https://doi.org/10.1016/j.marpolbul.2022.113904>
- Ytreberg, E., Hansson, K., Hermansson, A. L., Parsmo, R., Lagerström, M., Jalkanen, J.-P., & Hassellöv, I.-M. (2022b). Metal and PAH loads from ships and boats, relative other sources, in the Baltic Sea. *Marine Pollution Bulletin*, 182, 113904. <https://doi.org/https://doi.org/10.1016/j.marpolbul.2022.113904>
- Ytreberg, E., Hassellöv, I. M., Nylund, A. T., Hedblom, M., Al-Handal, A. Y., & Wulff, A. (2019). Effects of scrubber washwater discharge on microplankton in the Baltic Sea. *Marine Pollution Bulletin*, 145, 316–324. <https://doi.org/10.1016/j.marpolbul.2019.05.023>
- Ytreberg, E., Karlberg, M., Hassellöv, I. M., Hedblom, M., Nylund, A. T., Salo, K., Imberg, H., Turner, D., Tripp, L., Yong, J., & Wulff, A. (2021). Effects of seawater scrubbing on a microplanktonic community during a summer-bloom in the Baltic Sea. *Environmental Pollution*, 291. <https://doi.org/10.1016/j.envpol.2021.118251>
- Zehr, J. P., & Kudela, R. M. (2011). Nitrogen Cycle of the Open Ocean: From Genes to Ecosystems. *Annual Review of Marine Science*, 3(1), 197–225. <https://doi.org/10.1146/annurev-marine-120709-142819>
- Zetterdahl, M., Moldanová, J., Pei, X., Pathak, R. K., & Demirdjian, B. (2016). Impact of the 0.1% fuel sulfur content limit in SECA on particle and gaseous emissions from marine vessels. *Atmospheric Environment*, 145, 338–345. <https://doi.org/10.1016/j.atmosenv.2016.09.022>
- Zhang, C., Shi, Z., Zhao, J., Zhang, Y., Yu, Y., Mu, Y., Yao, X., Feng, L., Zhang, F., Chen, Y., Liu, X., Shi, J., & Gao, H. (2021). Impact of air emissions from shipping on marine phytoplankton growth. *Science of the Total Environment*, 769, 145488. <https://doi.org/10.1016/j.scitotenv.2021.145488>

- Zhang, X., Ward, B. B., & Sigman, D. M. (2020). Global Nitrogen Cycle: Critical Enzymes, Organisms, and Processes for Nitrogen Budgets and Dynamics. *Chemical Reviews*, 120(12), 5308–5351. <https://doi.org/10.1021/acs.chemrev.9b00613>
- Zhang, Y., Yang, X., Brown, R., Yang, L., Morawska, L., Ristovski, Z., Fu, Q., & Huang, C. (2017). Shipping emissions and their impacts on air quality in China. In *Science of the Total Environment* (Vols. 581–582, pp. 186–198). Elsevier B.V. <https://doi.org/10.1016/j.scitotenv.2016.12.098>
- Zis, T. P. V., Cullinane, K., & Ricci, S. (2022). Economic and environmental impacts of scrubbers investments in shipping: a multi-sectoral analysis. *Maritime Policy & Management*, 49(8), 1097–1115. <https://doi.org/10.1080/03088839.2021.1937742>